UNIVERSITY OF LONDON

IMPERIAL COLLEGE OF SCIENCE AND TECHNOLOGY

PHYSICS DEPARTMENT

BIOPHYSICS SECTION

SPATIAL FILTER CHARACTERISTICS IN NORMAL AND ABNORMAL HUMAN VISUAL PATHWAYS

BY

ANNETTE ROSALIND GROUNDS

THESIS SUBMITTED FOR THE DEGREE

OF DOCTOR OF PHILOSOPHY OF THE

UNIVERSITY OF LONDON

1984

CONTENTS

ABSTRACT

Spatial and temporal response characteristics have been determined psychophysically for a group of 24 amblyopes and an albino. The experimental data were obtained by measurement of thresholds for detection of a target moving across a modulated background, and by appropriate choice of background, two classes of spatial response and one temporal response characteristic were investigated. With a spatially periodic background (Barbur and Ruddock, 1980a) spatial response characteristics, called the ST1 spatial response, are obtained and it is shown that for amblyopes, this response is coarser than for subjects with normal vision. Further, in subjects who have received patching, coarser ST1 spatial responses are found in the non-amblyopic as well as in the amblyopic eyes. In contrast, a second spatial response, the ST2 spatial response, obtained with a spatio-temporal modulated background is, with certain exceptions, the same in amplyopic as in normal vision. Further, the temporal response characteristics obtained with a flickering spatially uniform background (Barbur and Ruddock, 1980a) are unaffected by amblyopia. The changes in the ST1 spatial response observed in amblyopic subjects is examined in relation to their visual acuity and it is shown that in untreated cases, there is a good correlation between the visual acuity and the ST1 spatial response. The influence of eccentric fixation and age of onset of amblyopia on the ST1 spatial response are also analysed and the results of this study are discussed in relation to changes in X- and Y-type neural responses observed in cats with surgically induced squint (Ikeda, 1980).

Chapter One Anatomy and Physiology of the Eye and Visual Pathways.

Anatomy and Physiology of the Eye and Visual Pathways

1.1 Anatomical Introduction

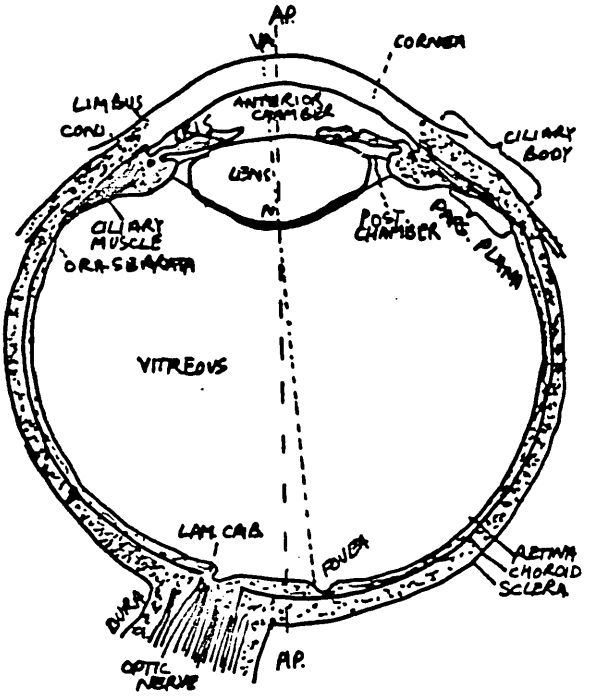

Fig. 1.1 Horizontal section of the eye.
P.P = Posterior Pole
A.P = Anterior Pole
V.A = Visual Axis (Wolff, 1968)

The globe of the eye has three coats which enclose the transparent refractive media. The outermost tunic is made up of the sclera and cornea, the latter being transparent. The middle coat is mainly vascular and comprises the choroid, ciliary body and iris. The innermost layer is the retina, which contains the essential nervous elements responsible for vision.

The refractive elements of the eye are the following transparent structures - the cornea, occupying the anterior sixth of the surface of the globe, the lens which is supported by zonules, and by the aqueous humour which fills the anterior and posterior chambers, and the vitreous body which occupies the large space behind the lens and ciliary body.

The iris works like a diaphram, limiting the amount of light entering the eye, whilst the ciliary body contains muscle fibres which, on contraction, increase the refractive power of the lens (accommodation). The refractive elements form an image on the retina which is largely made up of nervous tissue, and is an outgrowth of the central nervous system. Nerve fibres, which form the optic nerve, carry electrical impulses elicited by light stimulation from the eye. These visual impulses pass from the optic nerve along the optic tract to the lateral geniculate body or to the mid brain. Fibres from the L.G.B. form the optic radiation which leads to the cortex (fig. 1.10). The fibres carrying messages from the medial, or nasal half of the retina decussate in the optic chiasma, so that the L.G.B. of the left side receives fibres from the temporal half of the left retina and the nasal half of the right. The partial decussation may be considered as an essential development for binocular vision. In albinism, more complete decussation occurs so each eye is handled largely by either the right or left hemispheres, hence no binocular vision is possible.

1.2 The Retinal Zones

The retina is divided morphologically into the central and peripheral zones. Region one is the fovea which is a small depression with a concave floor, on the vitreal face of the retina. This depression is formed by the bending away of layers 5-9 and a thickening of the bacillary and outer nuclear layers, see Fig.1.2. The diameter of the depression is about 1,500μ across and subtends about 5° at the nodal point of the eye. The floor of the fovea is about 400μ across and convex in shape

because of lengthening of the cones in the bacillary layer. The rod free area extends some 500-600μ across and contains some 34,000cones. Beyond this limit rods begin to appear, increasing in proportion to the cones with greater eccentricity.

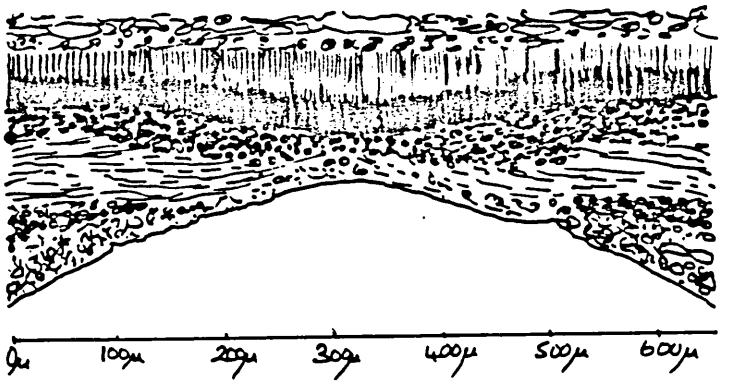

Fig. 1.2 Schematic representation of a microscopic section of the central portion of a human retina. The diagram covers about 2 degrees, or about 2/3 millimetres. (from Polyak, 1941)

The second and third regions are called the para and perifoveal regions respectively, the outer edge of the former being 1,250μ from the foveal centre, the latter 2,750μ. The total diameter of the whole central area is some 5,000-6,000μ. The cone density in the outer two regions is greatly reduced whilst the rod density is increased such that in region three there are some twelve cones per 100μ, compared to some fifty rods per 100μ. The peripheral region is associated with a further decrease in cone density while rods continue to increase in number out to some 16° from the fovea, beyond this eccentricity a gradual fall off in rod density occurs out to the periphery.

1.3 Structure and Function of the Retina

The retina is a complex nervous structure made up of a number of layers (Fig. 1.3). It possesses a layer of receptors, (rods and cones), two layers of cell bodies, the inner nuclear

layer which contains bipolar cells, and the ganglion cell layer. The rods and cones are highly differentiated cells and their orderly arrangement gives rise to a bacillary layer, which consists of the photoreceptor outer segments and an outer plexiform layer consisting of their fibres and synapses with the bipolar cells. The inner plexiform layer is the region of synapses between the bipolar and ganglion cells. Two other types of nerve cell are present in the retina, namely the horizontal and amacrine cells, with their bodies in the inner nuclear layer; the ramifications of their dendritic and axonal processes contribute to the outer and inner plexiform layers respectively. The largely horizontal organisation of these layers allows them to mediate connections between receptors, bipolars and ganglion cells. As well as the nerve cells there are numerous neuroglial cells, an example being those that give rise to the radial fibres of Muller, which act as supporting and insulating structures.

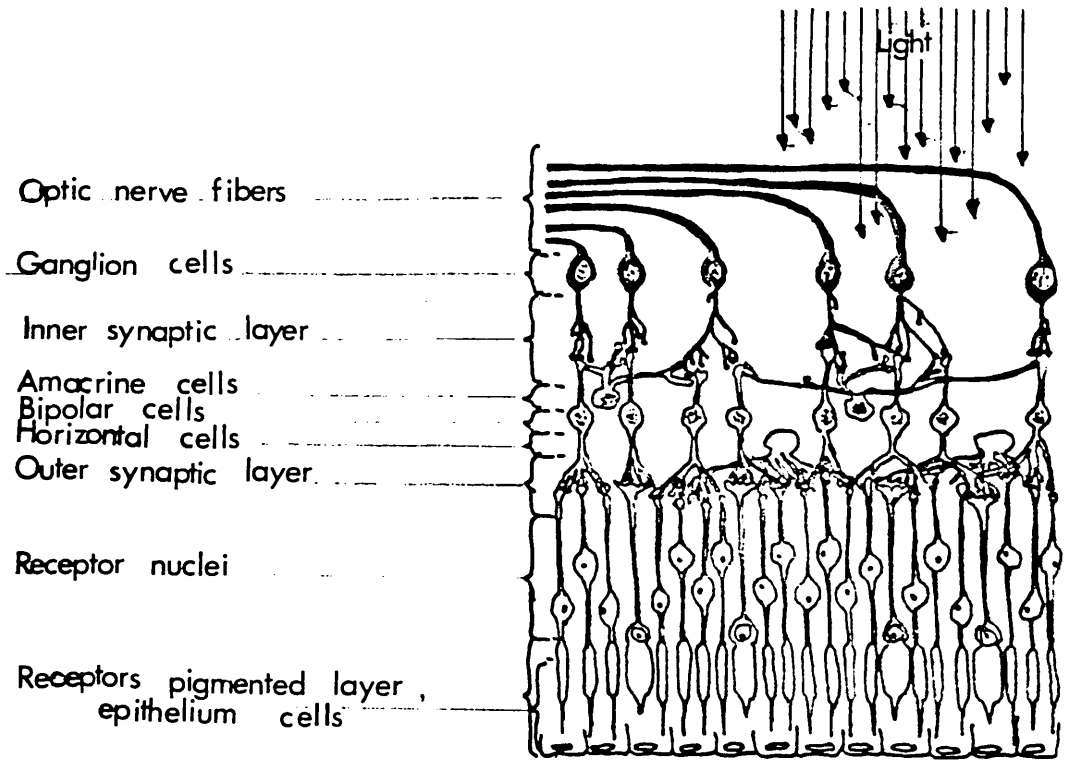

Fig. 1.3 Schematic diagram of the neural interconnections among receptors and bipolars, ganglion, horizontal, and amacrine cells. (from Dowling and Boycott, 1966)

The main organisation of the retina is on a vertical basis, that is activity in the rods and cones is transmitted to the bipolar cells and then to the ganglion cells and out of the eye via the optic nerve to higher neural centres. However, one receptor may activate many bipolar cells, and likewise a single bipolar cell may activate many ganglion cells, so that the effect of a light-stimulus may also spread horizontally as it moves vertically. Also, the connections brought about by the horizontal and amacrine cells further increases the possibilities of horizontal spread and interaction. This leads to a highly complex retinal pathway. A basic picture of retinal organisation in primates was given by Polyak (Fig. 1.4). According

to this, there are two main classes of bipolar cells, namely midget bipolars, h, which connect to one cone only, and the diffuse type, which has synaptic connections with many receptors, d, e and f. The ganglion cells similarly fall into two classes, the midget ganglion cell, connecting to only one midget bipolar cell, and the diffuse ganglion cell which connects with groups of bipolar cells. Based on this, convergence of receptors on to ganglion cells is achieved predominantly by the diffuse types of bipolar and ganglion cells, whilst a virtual one-to-one relationship is achieved by those receptors which connect to a midget ganglion cell via a midget bipolar cell. This, however, is not strictly true since a receptor which connects to a midget bipolar also connects to the diffuse bipolar, so giving a possible lateral spreading effect. Polyak's view has more recently been updated by Boycott and Dowling, 1969, who have largely confirmed the earlier work.

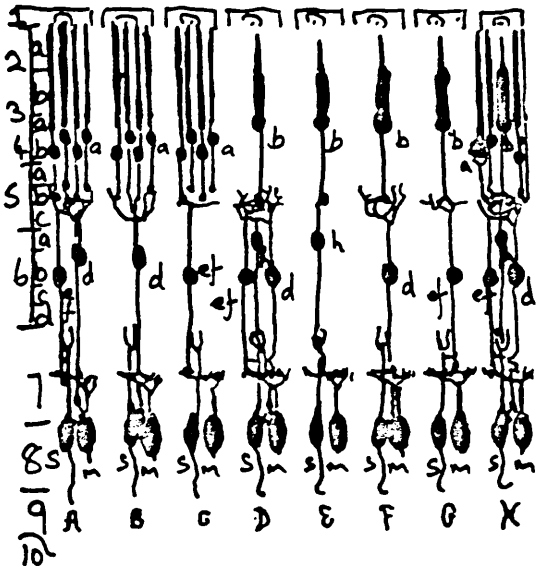

Fig. 1.4. Some receptor-bipolar synapses in the retina a, rod; b, cone; d,e, and f, bipolars; h,midget bipolar; s, midget ganglion cell, m, parasol cell (which makes several synaptic relationships with bipolars) (Polyak 1941)

1.3.1. The Rods and Cones

The rods and cones are the photosensitive cells in the primate and most other vertebrate retinae. The rods are generally much thinner than the cones, but both are similar in overall construction, see Fig. 1.5. The light-sensitive pigment is contained in the outer segment, which rests on the pigment epithelium, the inner end, the synaptic body, is known as the spherule and the pedicle in rods and cones respectively. In humans the rods are some 2μ thick and 60μ long, but the cones vary greatly in size and shape with their retinal location, being thus long and rather rod-like in appearance in the most central part (region one), see Fig. 1.6. There are about 120 million rods and 7 million cones, the distribution of which is illustrated in Fig. 1.7.

Each receptor connects to a bipolar cell via a synapse. The foveal cones are usually connected to a midget bipolar, whereas in the periphery many receptors connect to a diffuse bipolar. This produces convergence of hundreds of rods onto one bipolar at eccentricities greater than 20 degrees, giving a larger receptive field size in the periphery because an individual bipolar will not be able to distinguish which of its many connecting receptors was stimulated.

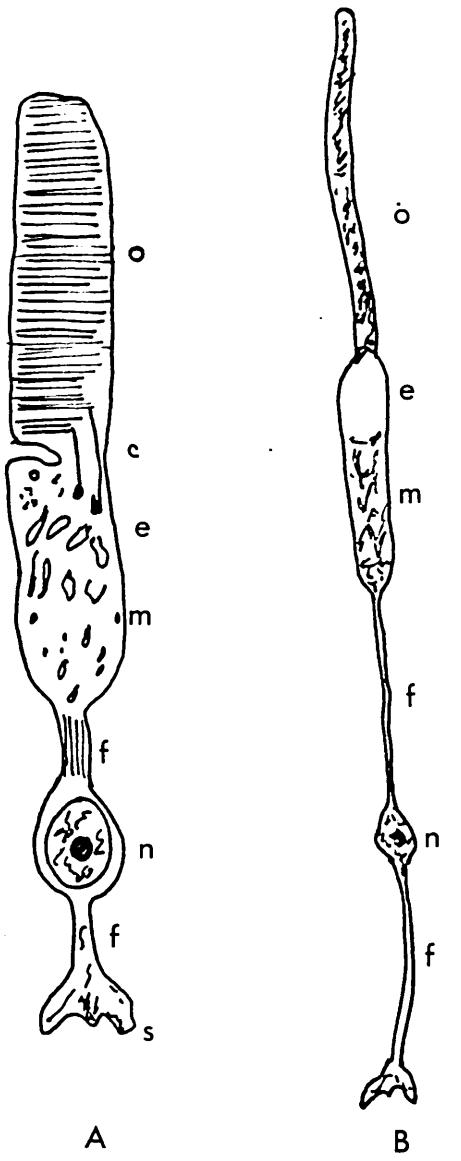

Fig. 1.5 Diagramatic representation of retinal photoreceptor cells. A, is a schematic drawing of a vertebrate photoreceptor, illustrates the compartmentation of organelles as shown by the electron microscope. The following subdivisions of the cell may be distinguished; outer segment o, connecting tissue c, ellipsoid e, and myoid m, which comprise the inner segment fibre f, nucleus n, and synaptic body s. The scleral end of the cell is at the top in this diagram. B, is a rod from the rat retina. (Young, 1967)

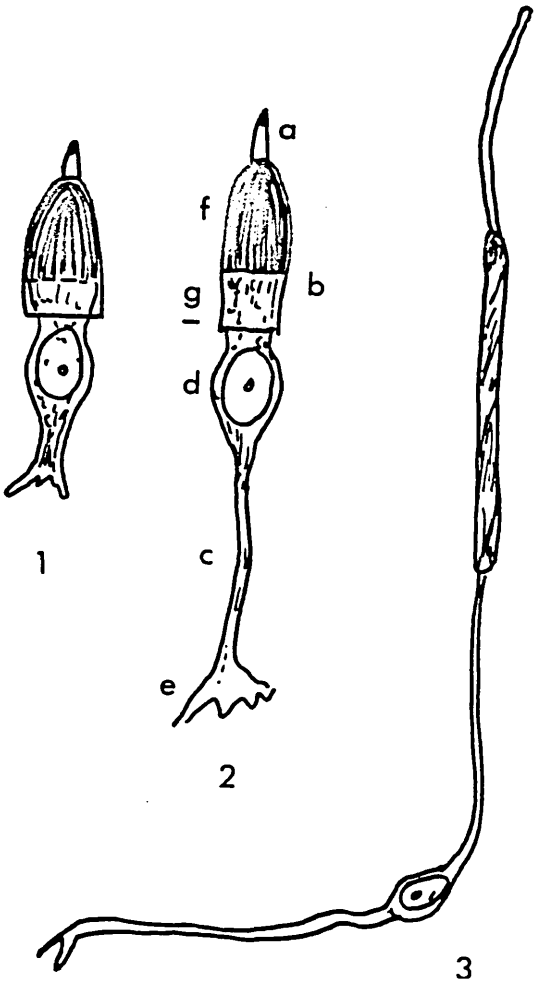

Fig. 1.6 Human cones, 1, near ora serrata; 2, at equator; 3, at macular; a, outer segment; b, inner segment; c, cone fibre; d, cell body and nucleus; e, cone foot; f, ellipsoid; g, myoid. (Duke-Elder, 1949)

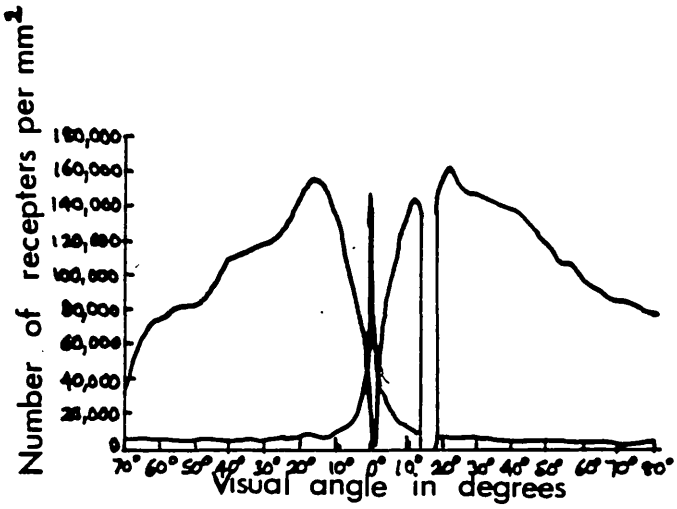

Fig. 1.7 Density distribution of rods and cones receptors across the retinal surface. (from Pirenne, 1967).

1.3.2. Bipolar Cells

Polyak's study showed three different classes of bipolar cells, two of which connect to cones and one to rods. The midget bipolar connects to one cone only, while the flat cone bipolar makes connections with several cones. Their synapses are characteristically different; the dendritic process from the midget bipolar cell penetrates an invagination of the cone pedicle, the flat bipolar makes a simple contact and the diffuse bipolar, connects to up to about fifty rods with an invaginating synaptic contact similar to that of the midget bipolar. Kolb (1970), showed that a single bipolar may make some twenty-five connections with a single cone pedicle, providing single central dendritic processes for the twenty-five invaginations. Since these twenty-five invaginations constituted the total for a cone pedicle, this

shows that the bipolar cell made synapses with just one cone. In the peripheral retina she found some branched midgets, which probably make contact with two cones. Kolb also noticed that there was also a flat bipolar, these only make a superficial contact with the base. Thus a cone pedicle contained twenty-five invaginating contacts and some forty-eight superficial contac ts. Like the invaginating midget, the flat midget makes contact with only a single cone pedicle (see Fig. 1.8).

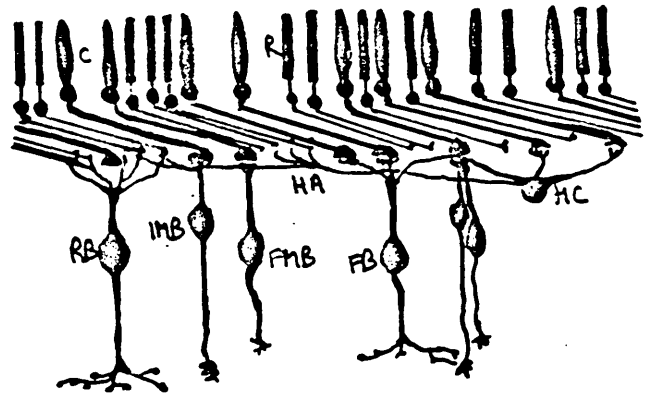

Fig. 1.8 The organisation of the outer plexiform layer of the primate retina; R.B. = Rod Bipolar; I.M.B. = Invaginating Midget Bipolar; F.M.B.= Flat Midget Bipolar; H.A. = Horizontal Axon terminal; F.B. = Flat Bipolar; H.C. = Horizontal Cells; R. = Rod; C. = Cone. (Kolb, 1970).

1.3.3. Horizontal Cells

The dentritic processes of these cells make synaptic contacts with the cone pedicles as lateral processes of the triads. Kolb (1970) has shown that these make dendritic connection only with cones but there are two variations. The differentiation consists in the number of cones with which a single horizontal cell makes contact; the "small-field" contacting about seven cones and the

"large-field" about twelve. The axons of the horizontal cells terminate exclusively in rod spherules, according to Kolb, constituting lateral elements in triads; each rod spherule thereby receives input from two horizontal cells. Horizontal cells, therefore, mix the rod and cone messages.

1.3.4. The Outer Plexiform Layer (see Fig. 1.8)

Kolb (1970) has shown the appearance of the outer plexiform layer. The structure of the cone triad, see Fig. 1.9, is much more complex than previously thought. It contains in addition to the invaginating midget bipolar process (I.M.B.) and the lateral horizontal processes ($H.C._1$ and $H.C._2$), more superficially placed processes from flat midget bipolars (F.M.B.) and from flat cone bipolars (F.B.). Consequently there is a considerable capacity for the spread of information.

Fig. 1.9 Illustrating synaptic arrangements in rod spherule (left) and cone pedicle (right) as deduced from electron-microscopy.
Left:The lobed lateral elements are horizontal cell axon terminals, each from a different horizontal cell (HA_1 and HA_2). The central elements are rod bipolar dendrites from different rod bipolars RB_1 and RB_2).
Right:The horizontal cell dendrites, usually form different horizontal cells (HC_1 and HC_2) from the lateral elements of the invagination. The invaginating midget bipolar (I.M.B.) pushes up into the invagination to lie between the two lateral elements. The synaptic ribbon and synaptic vesicles point into the junction of the three processes. The flat midget bipolar (F.M.B.) dendrites lie alongside the invaginating midget bipolar dendrite and push part of the way up into the triad, but are in contact with the cone pedicle base. The flat bipolar (F.B.) terminals are also clustered around the invaginating bipolar dendrite and make superficial contact on the cone pedicle base. (Kolb, 1970).

1.3.5. Inner Plexiform Layer

The process of vertical and horizontal connections is repeated in the inner plexiform layer, which consists of axons and terminals of bipolar cells, processes of amacrine cells, and dendrites of ganglion cells. Ganglion cells fall into two main types, the midget ganglion cell which in turn connects with a midget bipolar and one cone, thus providing an exclusive pathway as far as the inner plexiform layer; the other type of ganglion

cell is the diffuse, which connects with many bipolar cells; this type falls into many categories dependent on the manner of their dendritic branching. Physiological evidence shows that some ganglion cell may respond to both rod and cone stimulation, whilst others may respond exclusively to cone stimulation (the latter is probably a midget ganglion cell). Certain ganglion cells have extremely wide receptive fields, (in the peripheral retina) in the sense that they may respond to light falling on diverse retinal points, hence information is collected from a wide area of rods and cones.

1.3.6. The Amacrine Cells

The amacrine cells are classified into several types regarding the nature and extent of their ramification. These cells receive influences from bipolar cells as well as other amacrine cells, whilst they transmit influences to other bipolar terminals and to ganglion cells. The convergence, mentioned in the previous section, of the retinal messages are also assisted by the diffuse type of bipolar and ganglion cells. It is therefore not surprising that there are a total of 1 million nerve fibres leaving the eye via the optic nerve, which is far less than the total number of receptors (7 million cones and $\simeq$ 120 million rods). It should be noted, however, that in the central retina, there are three times as many bipolar cells as cones.

1.3.7. Centrifugal Pathways

There is no evidence of centrifugal pathways in cats or primates. (Dowling and Boycott, 1966 and Brindley and Hamasaki, 1966).

1.4. The Visual Pathways to the Brain (see Fig. 1.10)

There are about 1 million fibres in the optic nerve and these are separated anatomically according to the area of the retina from which they originate. All the ganglion cells connected to receptors from the temporal side of each retina pass to the L.G.N. on the same side as that eye, whilst the nasal fibres pass to the L.G.N. on the opposite side, hence, on viewing an object which falls to the left, the nasal receptors of the left eye and the temporal receptors of the right will receive the image. The output from both sets of receptors will then pass to the right L.G.N. and hence to the right hemisphere only. If the object is viewed centrally, then the image will fall on both sides of each retina, and consequently will be projected into both brain hemispheres, but still in two halves. The optical radiation leaves the L.G.N. and passes to the striate cortex, known as area 17, which is the primary visual cortex. Despite decussation of optic nerve fibres there is still an approximate point-to-point representation between the retinal ganglion cells, the L.G.N. and the striate cortex.

Both the L.G.N. and the striate cortex have their cells arranged in layers and columns. The striate cortex projects to the association cortex, areas 18 and 19. The two hemispheres are also interconnected via the corpus callosum.

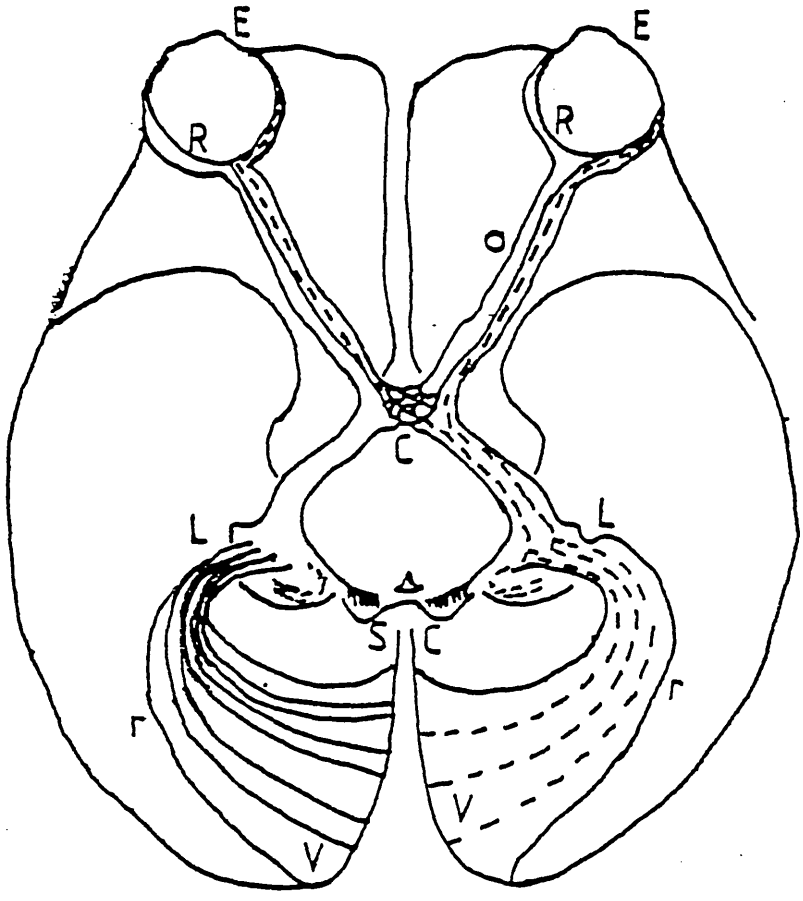

THE HUMAN VISUAL SYSTEM

E - Eye
R - Retina
O - Optic nerve
C - Chiasma
L - Lateral geniculate nucleus
SC - SUperior Colliculi
r - Optic Radiation
V - Visual Cortex

Fig. 1.10 Diagram of the visual pathways (as seen from below the brain) (from Polyak, 1957)

1.4.1. The Optic Nerve and Tract

Retinal ganglion cells are the second order neurones in the transmission of retinal impulses to the cerebral cortex and their axons form the optic nerves and tracts, passing predominantly to the L.G.N.. The other fibres pass to the pretectal centre of the midbrain. A visual impulse, arising from the right half field, is conveyed in the left optic nerve and tract to the left cerebral hermisphere.

Binocular vision requires hemi-decussation of the afferent optic nerve fibres at the optic chiasma. As a result, nerve fibres from corresponding retinal areas in the two eyes associate with one another in the visual cortex. Fibres from the temporal half of the retina, including the temporal half of the fovea, pass through the optic chiasma without any decussation and enter the ipsilateral optic tract (see Fig. 1.10). The fibres arising from the nasal half of the retina decussate in the chiasma and pass to the contralateral optic tract. From this it follows that corresponding retinal points travel in the same optic tract to the lateral geniculate body from there they relay in the optic radiations to the striate area of the visual cortex. If the optic tract is severed then a homonymous hemianopia or half-field blindness results. The degree of decussation varies from species to species and is a function of binocular vision; in man and primate approximately half the fibres are crossed, the others uncrossed.

The fibres are grouped in three bundles according to the retinal fields from which they originate as follows:-

a) Macular fibres

b) Uncrossed temporal fibres

c) Crossed nasal fibres

The macular fibres decussate in the chiasma so that half pass to each optic tract. The relative positions of the bundles in the optic nerve and tract are shown in Fig. 1.11. There are two different thicknesses, coarse and fine; the speed of conduction increases with increasing diameter, thus impulses carried by the coarse fibres arrive before those carried by the fine fibres. So great is the difference in conduction speed, that a visual impulse can be transmitted to the L.G.B., relayed to the cortex, and the cortical response may pass to the mid-brain before the impulse in the fine fibres has arrived. It is therefore possible for the mid-brain's reflex activities to be anticipated and modified by cortical influences induced by the same stimulus. Doty (1961) showed that the evoked potential recorded from the mid-brain, in response to a light stimulus, comes some 12mSec. after that recorded at the cerebral cortex of the cat.

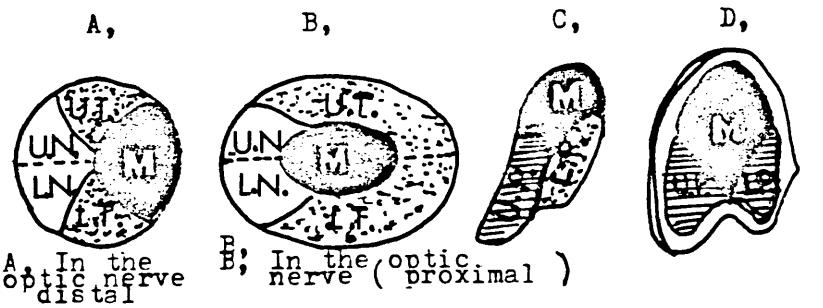

Fig. 1.11 Distribution of the fibres in the optic nerve, optic tract and lateral geniculate body. A, in the optic nerve (distal); B, in the optic nerve (proximal); C, in the optic tract; D, in the lateral geniculate body; U.T., upper temporal; U.N., upper nasal; L.N., lower nasal; L.T., lower temporal; U.P., upper peripheral. (Wolff, 1968)

1.4.2. Non-Geniculate Pathways

The fibres within the optic tract travel via two different roots. The small mesencephalic root goes to the superior colliculus, while the large, diencephalic root runs to the lateral geniculate body. Dependent on the animal's position in the phylogenetic scale, the proportion of optic fibres travelling to the midbrain station changes; in birds there is very little cortical representation of retinal impulses, most fibres running to the superior colliculus whereas in higher animals the number of fibres to the superior colliculus declines, and in Man is estimated at 20% of the total, (Dawson, 1972).

1.4.3. The Lateral Geniculate Body (L.G.B.)

In Man the cells of the dorsal nucleus of the L.G.B. are arranged in six laminae. The optic tract fibres synapse with these cells such that the crossed optic fibres relay in layers 1, 4 and 6 while the uncrossed fibres relay in layers 2, 3 and 5 (Glees and Le Gros-Clark 1941). Thus, there is a rigid separation of the fibres arriving from the two eyes, and binocular fusion does not take place in the L.G.B.. The L.G.B. acts as a sorting centre which rearranges the crossed and uncrossed fibres which have been mixed in the optic tract. In degeneration studies Penman (1934) found a virtual point-to-point representation of the retina in the L.G.B.. Each optic tract fibre entering a lamina splits into a number of terminals. These terminals end in "boutons" connecting to up to 30 L.G.B. cells but there is no overlap from different retinal receptors. The function of the L.G.B. is mainly to relay messages to the

cortex, but there is evidence of centrifugal control of geniculate neurones (Guillary, 1967). By this feedback arrangement, the cortex is able to modify and control messages it receives. According to Vastola, (1960) the principal cell (this refers to the cell which is receiving the main stimulation), is activated by an optic tract fibre sending its messages to the cortex and also via a collateral fibre which activates a short axon neurone in the L.G.B.. This then inhibits the activity of surrounding geniculate cells (see Fig. 1.12). Vastola (1960) found that the most strongly inhibited cells were those which received a weak stimulation to the initial excitation. This type of response causes a "sharpening" of the retinal image.

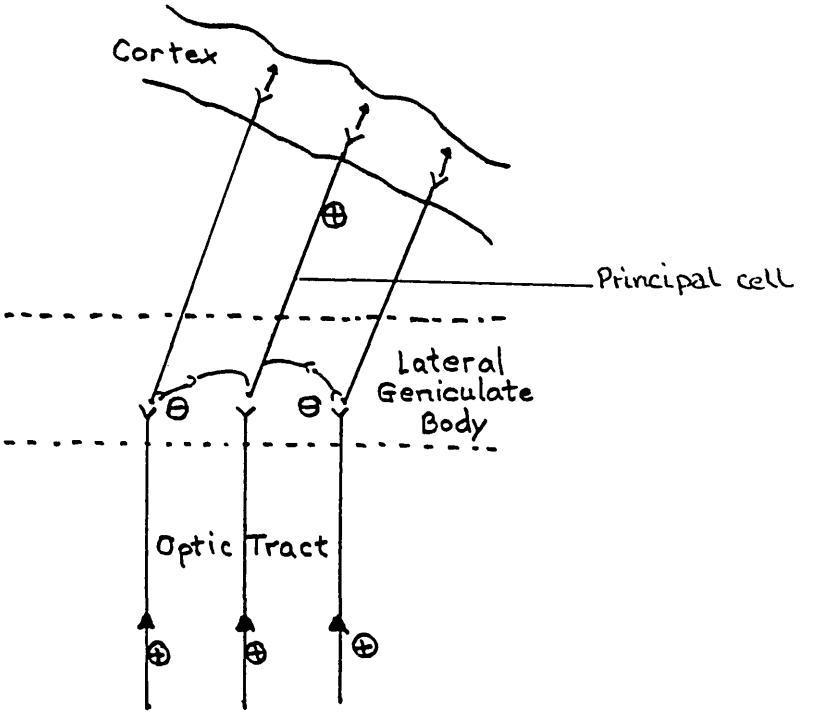

Fig. 1.12 Illustrates the inhibition within the L.G.B. The middle one of the three geniculate cells relays an excitatory influence to the cerebral cortex and also to short-axon inhibitory cells which, as a result of this activation, inhibit the neighbouring geniculate cells. (from Davson, 1972, after Vastola, 1960).

1.4.4. The Visual Cortex

From the L.G.N. (Lateral Geniculate Nucleus), the third order neurones pass as the optic radiations to the surface of the occipital pole, relaying with the cortical neurones in Brodmann's Area 17, or the striate area, so called because the axons of the optic radiations form a well defined white line on their way to their synapses in Layer IV.

When small lesions are made in the striate cortex loss of vision occurs in a small well-defined area of the visual fields. A detailed study of people with gun-shot wounds has been made and this has helped to map out the projections from the retina on the visual cortex. (Holmes, 1945 See Fig. 1.13)

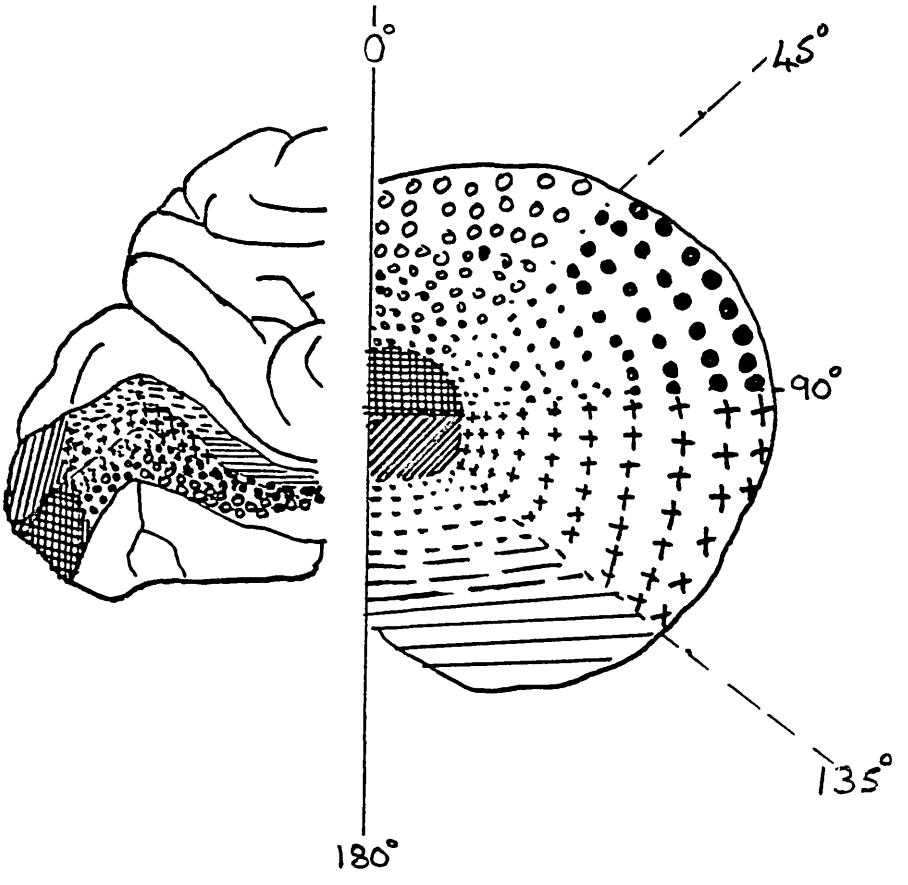

Fig. 1.13 Diagram of the probable representation of the different portions of the visual fields in the calcarine cortex. (Holmes, 1945).

Anatomical and physiological investigation has confirmed this general plan of retinal projection and shows the existence of a virtual "point-to-point" relationship between retinal stimulus and cortical representation. This relationship is only true for the central foveal region and even here it is only functional owing to the lateral connections. Under deep anaesthesia this "point-to-point" relationship between light-stimulus and cortical evoked response can be elicited. When implanted electrodes are used in different areas of the cortex, the evoked response is found to be highly localised.

The effects of discreet lesions in specific layers of the L.G.B. are revealed in degeneration of geniculate fibres and their terminal boutons in the striate cortex. This was discovered in studies of Hubel and Wiesel (1961).

When lesions in the cortex or optic radiations occur the macula function is frequently unimpaired. This "macula sparing" was thought to arise because some macula fibres crossed at the corpus callosum, or by mesencephalic connections, giving a bilateral cortical representation. Studies have shown, however, that complete destruction of one occipital lobe is followed by complete cellular atrophy of the homolateral geniculate body, proving that projection is exclusively to the occipital cortex of the same side. Such damage also leads to loss of half the retinal fields including

half the macula. Macula sparing is probably the result of its large cortical representation and of the location of this representation in the margins of the distribution of the middle and posterior cerebral arteries. Thus, if one artery or part of an artery is occluded, sufficient blood may still reach this region to allow function to continue.

1.4.5. The Lower Visual Centres

There is considerable projection of the optic tract on to the superior colliculus & Apter (1945), showed that this was essentially "point-to-point". Garey (1965) showed that the projection of the visual cortex on the superior colliculus has the same topological features as the retina, every point on the retina being related to a specific part of the colliculus, both directly and indirectly via the L.G.B. and cortex. Following studies of lesions in the colliculus Sprague and Meikle (1965) argue that it should be regarded as an integrating centre as opposed to a simple relay station for cortically directed eye movements. Damage to one side of the superior colliculus in cats, caused an obvious defect in the contralateral field of visual guided activity. The receptive fields of single collicular neurones were studied by Mohler and Wurtz (1977) and were found to be similar to those observed in ganglion cells. As the colliculus is layered, he suggested that there might be a columnar ordering of cells with receptive fields analogous to the cortical arrangement described by Hubel and Wiesel, (1962) see sect. 1.5.4. Sprague (1966), working on cats, found that large cortical

lesions on one side cause a permanent loss of visually guided activity in the contralateral field. If, however, the superior-colliculus was removed on the opposite side, the visually directed responses returned. He decided that the opposite colliculus was inhibiting the other colliculus on the same side as the cortical lesion.

It is thought that the S.C. is responsible for guided ballistic eye movements. Also, in more recent investigations evidence has shown that a fair degree of residual vision may be associated with the S.C. (Pasik and Pasik, 1971; Weiskrantz et al, 1974, Barbur et al, (1980).

1.4.6. The Corpus Callosum

This is an interhemispherical tract that connects between a given point on one hemisphere with a symmetrical point on the other. Studies by Myers (1962) and Ebner and Myers (1965) show that the great majority of the posterior callosal fibres project to the junction of Areas 18 and 17. Choudhury, Whitteridge and Wilson (1965) found that the receptive fields of cortical units in the medial edge of Area 18, just adjacent to Area 17, were within a few degrees of the vertical meridian. These responses were recorded when the ipsilateral optic tract was severed, so a callosal route from the opposite hemisphere was probably involved, and this was confirmed by complete section of the callosum.

When a pattern stimulus was presented close to the vertical meridian, callosal units were excited and could be detected by electrodes inserted in the posterior callosum of cats. Three out of seventeen units were found to be driven by both eyes by stimuli located in the same part of the visual field. Of the remainder, nine were driven by one eye, five with the other (Berlucchi et al, 1967).

1.5. Electrophysiology of the Visual Pathways

Extra-cellular and intra-cellular electrical recordings have been obtained from many classes of visual neurone and the principal results are now summarised. No data are available for pre-ganglionic neurones of the primate retina.

1.5.1. The Ganglion Cells

The basic receptive field organisation of these cells is circular, with central and surrounding regions responding in opponent fashions, Kuffler, (1953). Some cells respond with an excitatory response when the centre is stimulated by light and this is inhibited or suppressed when the surrounding annular area of the receptive field is stimulated. Conversely, some cells respond with an excitatory response when the annular surround is stimulated by light, but have a central inhibitory response. Such cells can be regarded as selectively sensitive to either light or dark spots, a maximum response being achieved when the size of the excitatory spot matches the size and contrast polarity of the central area of the receptive field.

Enroth-Cugell and Robson (1966) identified two classes of ganglion cells, in the cat retina, those which responded with continuous firing for as long as the stimulus was present called X-type neurones, and those which only responded by firing momentarily when the stimulus was either first presented or just withdrawn, called the Y-type neurones. For the X-type cell, a position of the grating can be found such that it can be exchanged for a uniform field of the same mean luminance without evoking a response, whereas for Y-type cells, no such position can be found. (This technique is known as the "null" test of Enroth-Cugell and Robson, 1966). These experiments show that the X-type cells sum the signals about illumination over the receptive field, and that these signals are proportional to the illumination of the retinal region in which they arise (see Fig. 1.14). Since then, many researchers have reported finding these X- and Y- type neurones. Cleland et al (1971) classified cat retinal ganglion cells on the basis of their temporal properties as "sustained" or "transient" which correspond to X- and Y- cells, and they also demonstrated a difference in the response of these two types of cell to a grating pattern moving across the receptive field. [See Fig. 1.15.]. Here, sustained cells responded to higher spatial frequencies while the transient cells responded to movement. They found the optimum target size of the X cell to be $\frac{1}{2}$-1^{o} in diameter, whereas for transient cells it was 1^{o} upwards. This indicates a smaller receptive field central zone for sustained cells. A similar classification can be applied to the primate visual system. Gouras (1969) found that

"transient" retinal ganglion cells in the monkey have faster conduction axons than sustained cells. De Monasterio (1978 a, and b.) working on Macaqu ganglion cells and using the "Null" test of Enroth-Cugell and Robson (1966) classified the ganglion cells as X- or Y- cells on the basis of the linearity or non-linearity of their spatial summation to alternating contrast of drifting gratings. In contrast to the work of Gouras (1969), de Monasterio found colour-opponency in Y- as well as X- cells.

So far, discussion has been restricted to X- and Y-type ganglion cells which are well documented. Another group of cells has been found in the retina and these may also have some role to play in amblyopia. Stone and Hoffmann (1972) found about 15% of retinal ganglion cells which were neither X- nor Y-type and these are known as "W" cells. They have axons which conduct more slowly than X- or Y-axons. Their receptive fields fall into two broad groups; i) each unit has a considerable spontaneous activity which is suppressed by contrast; ii) where this spontaneous activity is excited by contrast, they have a very low rate of spontaneous discharge and are excited by high contrast. Furthermore, these units were responsive only to velocities below $50^{o}Sec^{-1}$. Ikeda and Wright (1974b) also studied "W" cells and found they had small receptive fields and terminated in the superior colliculus. They thought these slow-conducting nerve fibres may be involved in the control of slow tracking eye-movement, and may also be concerned with the maintenance of fixation and thus may function abnormally in strabismus.

Electrophysiological measurements of ganglion cell responses in cat and primate have shown that the level of light adaptation affects primarily the surround region of the receptive field (Barlow et al, 1957). Further, the activity of the surround appears to regulate the centre response, thus maintaining a contrast average discharge over a wide range of luminances (Barlow and Levick, 1965). In contrast, the activity of the centre region is unchanged by the level of light adaptation. Maffei et al, 1971, found that for low light levels, the surround activity was absent and the average discharge level of the centre region increased with increasing background illumination until the surround activity became measurable. The surround response is maximum at high illumination levels, while the centre discharge under these conditions decreases. Over the middle illumination ranges the centre activity remains approximately constant and the gain transfer characteristics show practically no significant dependence on background luminance, (in range 0.5 - 0.05cd/M^2). These results suggest that the coding of stimulus contrast appears largely independent of background luminance at scotopic levels of illumination.

In general, the findings are as follows; transient cells in both cats and primates have larger receptive field sizes, shorter conduction latencies, preferred peripheral distribution, less prominent inhibitory surrounds and non-linear spatial summation. Sustained cells respond with sustained fashion to an intensity gradient in their receptive field, are distributed predominantly in the foveal region, have more pronounced antagonistic surrounds, respond best to slower target speeds

and show linearity of spatial summation. The smaller sustained neurones predominate in or near the area centralis, the larger transient neurones being found mainly in the peripheral retina. (Enroth-Cugell and Robson, 1966; Cleland et al, 1971; Stone and Hoffmann, 1972; Ikeda and Wright, 1974 b; de Monasterio, 1978 a).

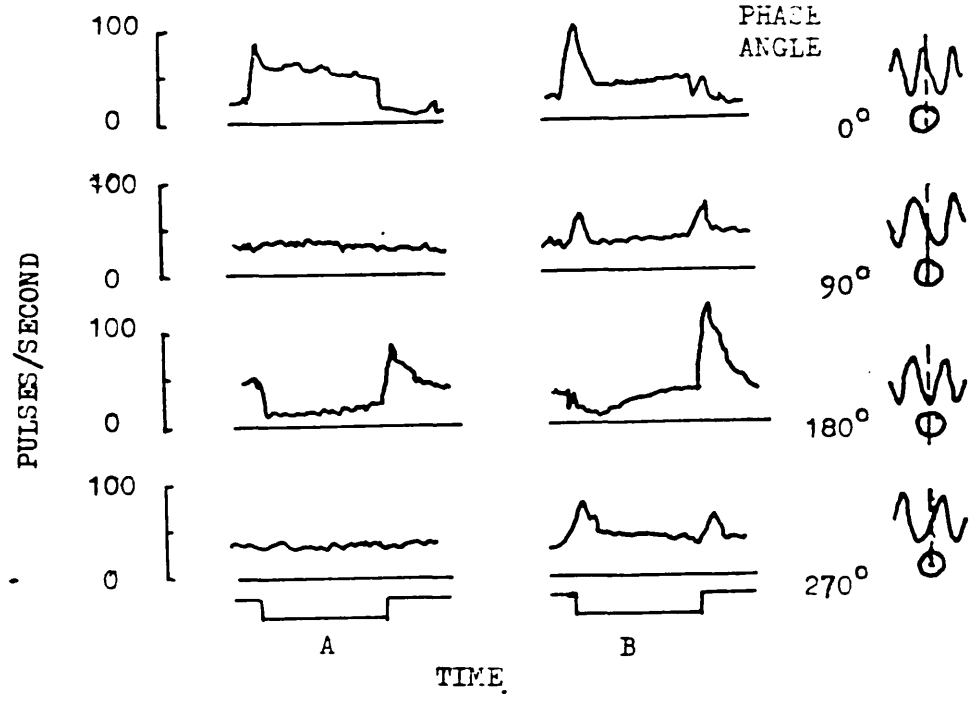

Fig. 1.14 Response of an off-centre X-cell (A) and an off-centre Y-cell (B) to the introduction and withdrawal of a stationary sinusoidal grating pattern. Grating phase angle in relation to receptive field of cell is shown on right. In each example illustrated the total length of the trace corresponds to 2s. (After Enroth-Cugell and Robson, 1966).

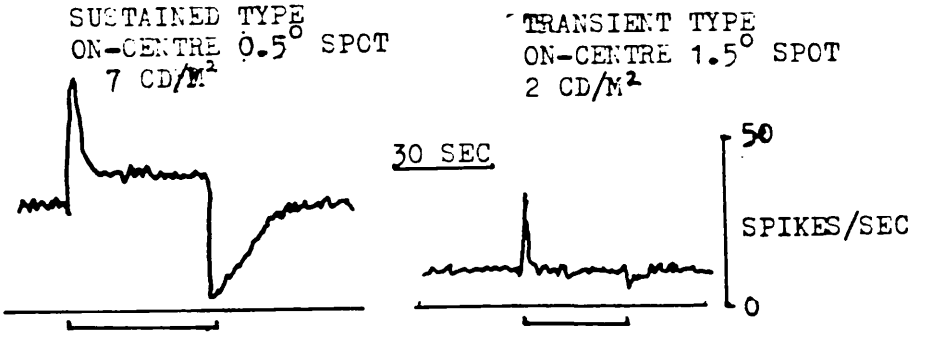

Fig. 1.15 Sustained and transient responses to standing stimulus. Duration of target spot is given by bar beneath each record. (After Cleland et al. (1971).)

1.5.2. Cell Classification in The Lateral Geniculate Nucleus

The centre and surround antagonistic organisation of the majority of retinal ganglion cells is also observed at the L.G.N. and cortical levels. However, the temporal properties of receptive field organisation at the ganglion cell level are different to those of L.G.N. or cortical neurones, (Maffei et al, 1970, Maffei et al, 1971). For ganglion cells, the maximum temporal frequency for which no modulation of a discharge pattern can be detected is in the range 25-45Hz for the centre and some 10-20Hz for the surround. In the L.G.N. however, the responses are up to some 45Hz for the centre and surround. This is attributed to the contribution of many ganglion cells to the surround receptive field of a single L.G.N. neurone. Hubel and Wiesel (1961) found L.G.N. neurones have essentially the basic retinal organisation of receptive fields characterised by ON-centre OFF-surround, or vice-versa. A given geniculate cell is generally, however, influenced by many hundreds of ganglion cell inputs. Cleland et al (1971) examined L.G.B. neurones and discovered

that these were excited by retinal ganglion cells of the same functional types, that is, X-ganglion cells excited X-type L.G.B. cells and Y-type ganglion cells excited Y-type L.G.B. neurones. Measurement of the geniculo-cortical latencies were longer for sustained cells than for transient cells. Ikeda and Wright (1974a) argued that information transmitted by the transient cells will therefore reach the visual cortex first.

Dreher et al (1976) studied lateral geniculate nuclei of primates with micro-electrode recordings. They found both X and Y-type cells within the L.G.N., and showed that the X-type cells were encountered first during an electrode penetration of the L.G.B., with Y-cells located deeper.

Ikeda and Tremain (1978a) studied the development of spatial resolving power in L.G.N. neurones of kittens. They found that the basic concentric organisation of the receptive fields of X-type L.G.N. cells which receive inputs from the area centralis appear to be established by 3 weeks of age. The spatial resolving power of the cells developed gradually to the level of adult L.G.N. cells during the period from 3-12 weeks (the sensitive period), see Fig. 1.16. This development is dependent on the enhancement of distinct inhibitory surround mechanisms taking place during the 6th - 11th week, as is shown by the gradual loss of sensitivity to low spatial frequencies and shift towards high spatial frequencies. Ikeda and Tremain (1978a) compared their

findings with those of Freeman and Marg (1975), and Mitchell et al (1976), see Figs. 1.17, 1.18 and 1.19.

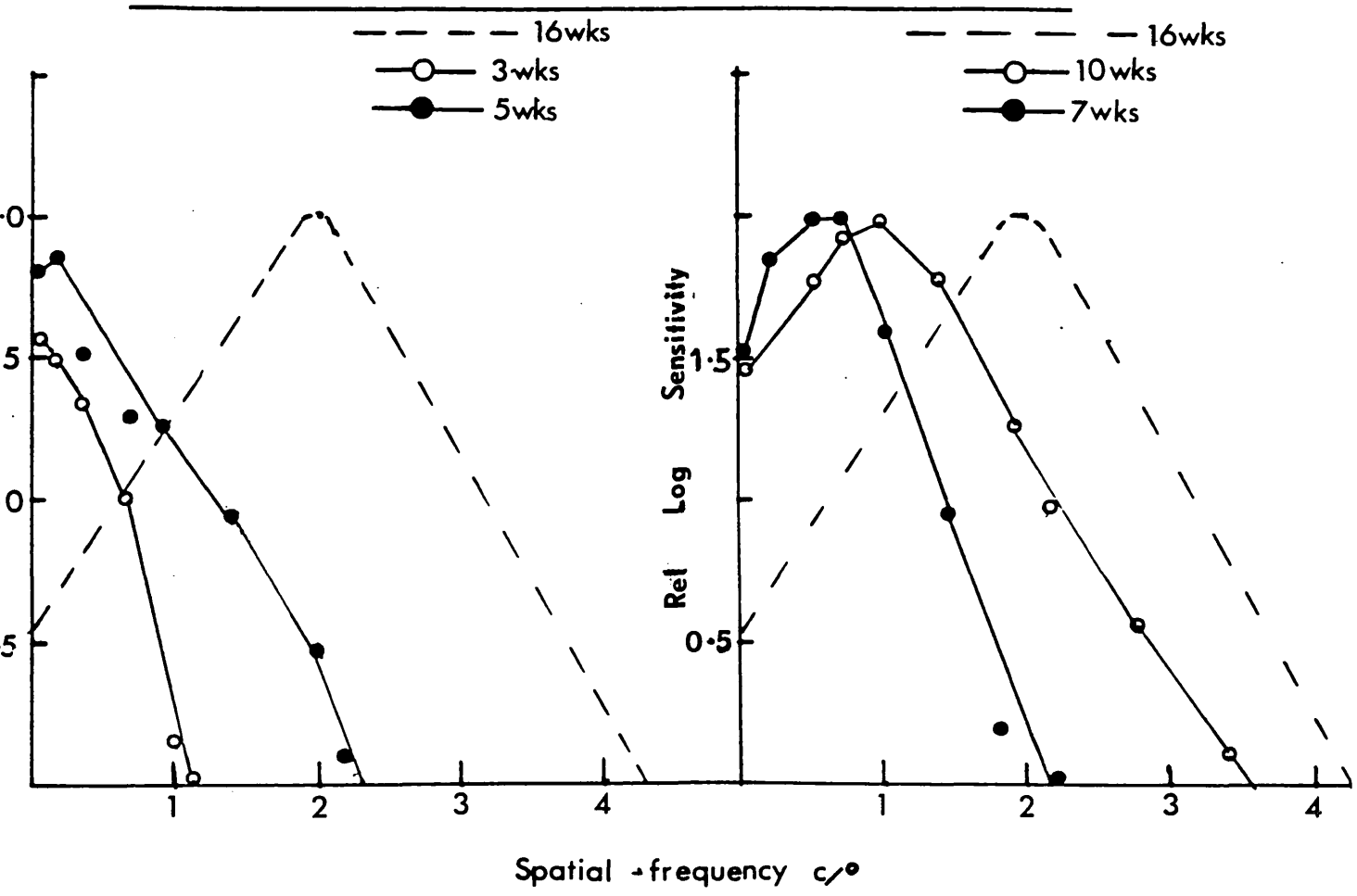

Fig. 1.16 Contrast sensitivity curves obtained from sustained L.G.N. cells driven from the area centralis of the retina recorded from kittens aged 3, 5, 7, 10, and 16 weeks. The curves were obtained by measurements of threshold contrast (the weakest contrast of sinusoidal grating, mean luminance: 10 cd/m^2; drift speed: 1Hz, to which the cell gave just discernable modulation of firing in post stimulus histograms (16 stimulation cycles). The relative log contrast sensitivity is the reciprocal of the threshold contrast. A) the curves obtained from cells recorded from the 3 weeks and 5 weeks old kittens are compared with that obtained from a cell in the 16 week old kitten (dashed curve). B) the curves obtained from cells recorded from the 7 weeks and 10 weeks old kittens are compared with that obtained from a cell in the 16 week old kitten (dashed curve) (after Ikeda and Tremain, 1978a).

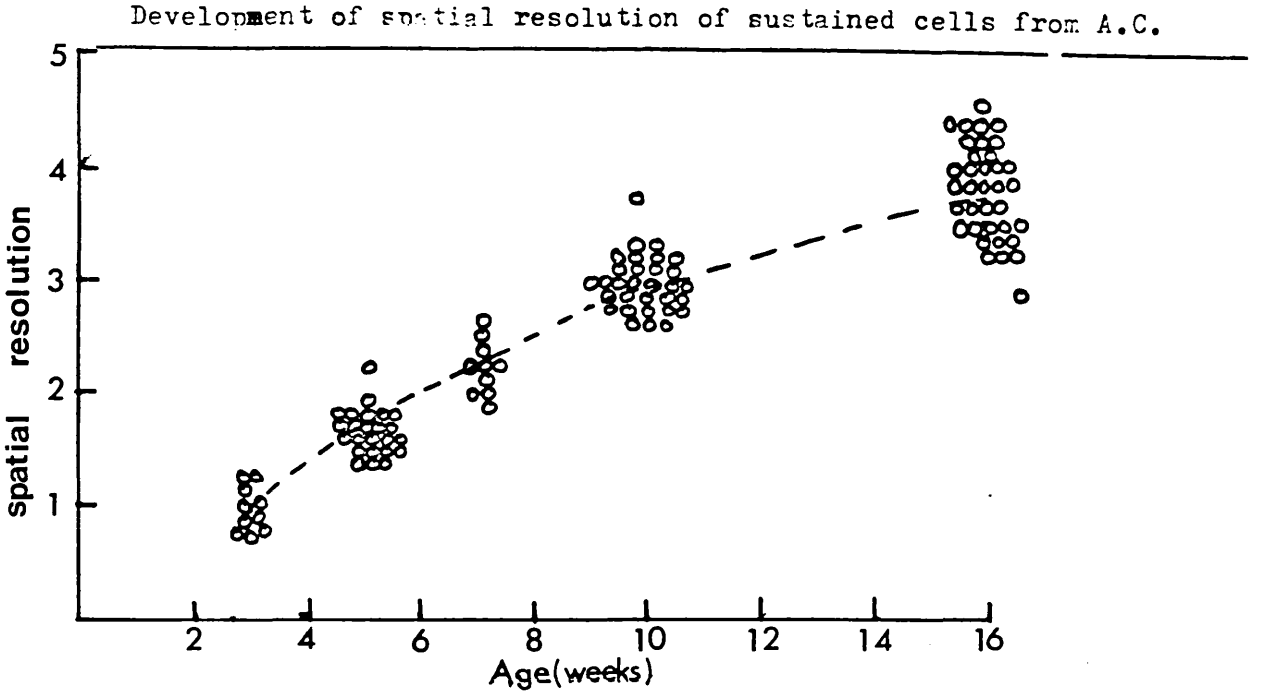

Fig. 1.17 Spatial frequency threshold the highest spatial frequency of a sinusoidal grating (contrast; 0.4, mean luminance: 10cd/m^2, drift speed: 1Hz) to which a cell responded with modulation firing of sustained L.G.N. cells driven from the area centralis of the retina obtained in kittens of different ages. The measurements of spatial frequency threshold were carried out using post stimulus histograms (16 stimulation cycles) in all cells. (from Ikeda and Tremain, 1978a).

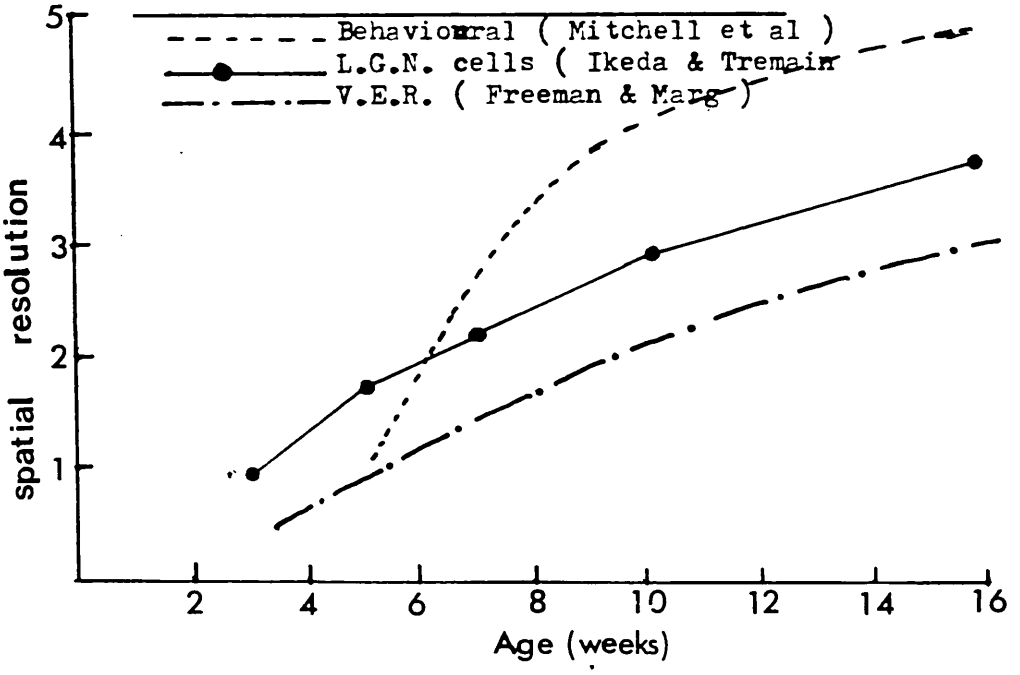

Fig. 1.18 Comparisons of visual acuity developmental curves for kittens obtained by three different methods. The spatial frequency thresholds of sustained L.G.N. cells from kittens of different ages are plotted as filled circles (mean including ±1 S.E. of the points shown in Fig. 1·17) For comparison, the developmental curves for visual acuity obtained by a behavioural technique (Mitchell et al., 1976) and the visual evoked response (V.E.R.) method (Freeman and Marg, 1975) are plotted on the same scale. (from Ikeda and Tremain, 1978a).

Comparison of developmental curves.

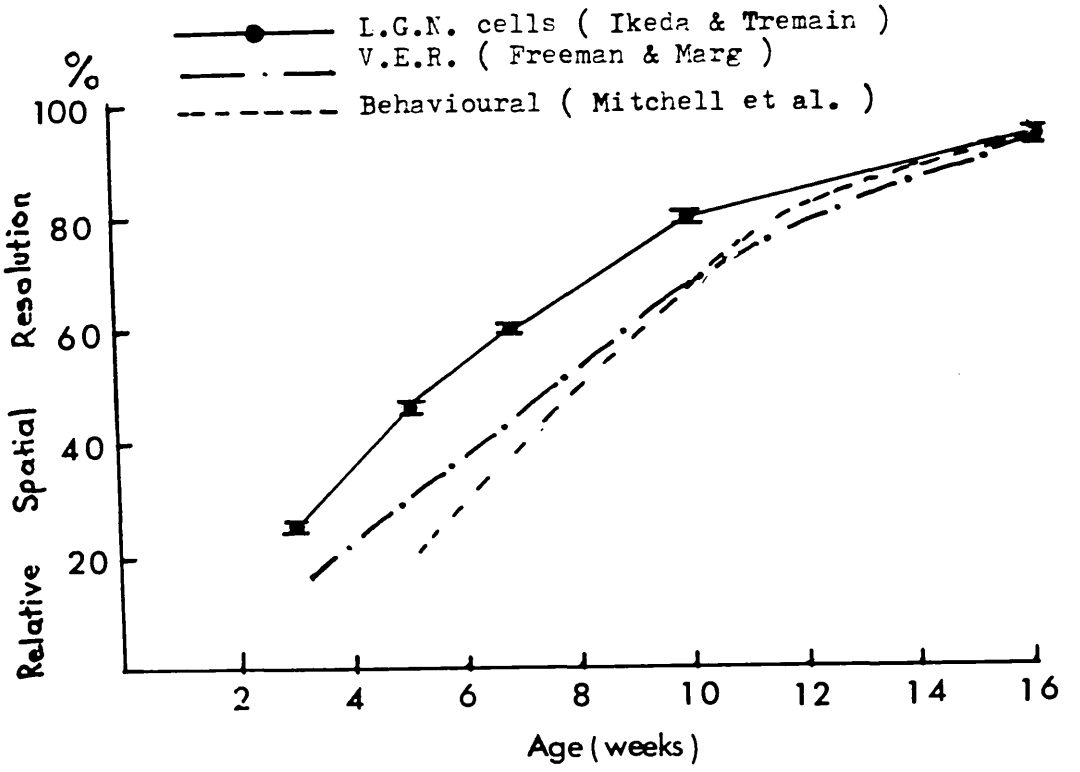

Fig. 1.19 Comparison of visual acuity developmental curves for kittens obtained by three different methods. In order to compare the relative visual acuity, the curves of (Fig. 1·18) have been re-plotted to make the visual acuity at 16 weeks equal to 100 . Note the similarity between the three curves. The data of Mitchell et al. (1976) and those of Freeman and Marg (1975) have been re-calculated for the purpose. (from Ikeda and Tremain, 1978a).

1.5.3. The Striate Cortex

The most striking differences between the receptive field organisation in the striate cortex and the pre-cortical areas, is that of linear rather than circular receptive field and binocular rather than monocular control. Fig. 1.20 (c-g) shows receptive fields of simple cortical neurones. Hubel and Wiesel (1962), found that the slit orientation for maximum response was quite critical and changes of 5 - 10^{o} had a

significant effect. It is assumed that cortical neurones receive their inputs from a number of geniculate cells, each with concentric organisation, the combination of these cells giving a linear array of their receptive fields which behave effectively as a unit with a linear receptive field as shown in Fig. 1.21. By appropriate arrangement of geniculate cells the different types of receptive fields shown in Fig. 1.20 can be constructed. With all these "simple" units a moving stimulus was always very effective, but it is important that the correct orientation of the slit be maintained, the movement being executed at right-angles to the slit direction. In general, the response was the same with forward or backward movement.

In some units such as G in Fig. 1.20, however, the response is very unequal, due to asymmetry in the flanking regions. These units were all described as simple because, like retinal and geniculate fields, they have distinct excitatory and inhibitory regions with summation occurring in each area, also antagonism between each region. The responses for stationary or moving stimuli can be predicted from a map of the excitatory areas (Fig. 1.21).

Another class of units was termed complex because their responses to different stimuli could not be predicted from a map made with circular spot-stimuli. Four different complex units were found by Hubel and Wiesel in the cat (1962). These units were affected by orientation rather than position of

the stimulation. Movement of a slit does not have the phasic effects seen with the simple unit, a continuous discharge throughout the movement is apparent. One of the unit types is an "edge detector", illustrated in Fig. 1.22. When an edge is projected onto the retina, that is half the field is light and the other half being dark, a strong ON response is observed. The response falls as the orientation is changed from the preferred direction and replacement of the stimulus by its mirror image reverse the response, that is, giving inhibition to stimulus ON and excitation to stimulus OFF.

Simple cells can be either "sustained" and "transient" (Ikeda and Wright, 1975), & recordings from cortical cells have shown that simple cells may possess pure X or Y inputs, or mixed X-Y inputs (Lee et al, 1977). Complex cells are probably mixed input cells, however, they may be derived from simple cell outputs (Hubel and Wiesel, 1962).

A third class of cells, the hypercomplex, also exist and these seem to respond to the length of an edge or a bar stimulus.

Fig. 1.23 shows how a group of simple cortical neurones could be connected to a higher order neurone to give a complex field. Similar complex fields could be built up from different groups of simple cortical cells. For these relationships to occur the latencies of complex cells would be longer than for simple cells.

Ikeda and Wright (1974a) classified cells in area 17 of the cat's visual cortex as either "sustained", X-cells, or "transient" Y-cells. They found that the receptive field organisation of "sustained" cells makes them very sensitive to fine details, whereas "transient" cells are sensitive to temporal changes in light distribution and therefore transmit information about the temporal properties of visual stimulation. Ikeda et al (1974a) found that spatial frequency tuning curves for the sustained cells peak at higher spatial frequencies than do those of the transient cells. Further, the spatial frequency bandwidth of sustained cells is narrower than those for transient cells. Orientation selectivity was also observed in cat's cortical cells, the mean spike-frequency changing with the change in direction of the grating. (Campbell, Cleland, Cooper and Enroth-Cugell 1968). Hubel and Wiesel (1962), showed that about 80% of cortical neurones respond to stimulation of either eye, that is, they are binocularly driven. Further, the receptive fields in the two eyes that stimulated a single cortical neurone were similar in both shape and orientation, occupying symmetrical positions in the two retinae. Summation and antagonism occurred between the two receptive fields, thus should the ON area of one eye be simultaneously stimulated with the OFF area of the other eye, the responses are cancelled out. Hubel and Wiesel (1963), found that with visual deprivation from birth, only 1% of cortical cells were driven binocularly. It appears, therefore, that disruption of connections present at birth subsequently occurs, suggesting that the site of the abnormality is in the region of the synapses between the axon

terminals of geniculate cells and cortical cells on which they terminate. Similar results in normal and visually deprived cats were found by Yinon et al (1976).

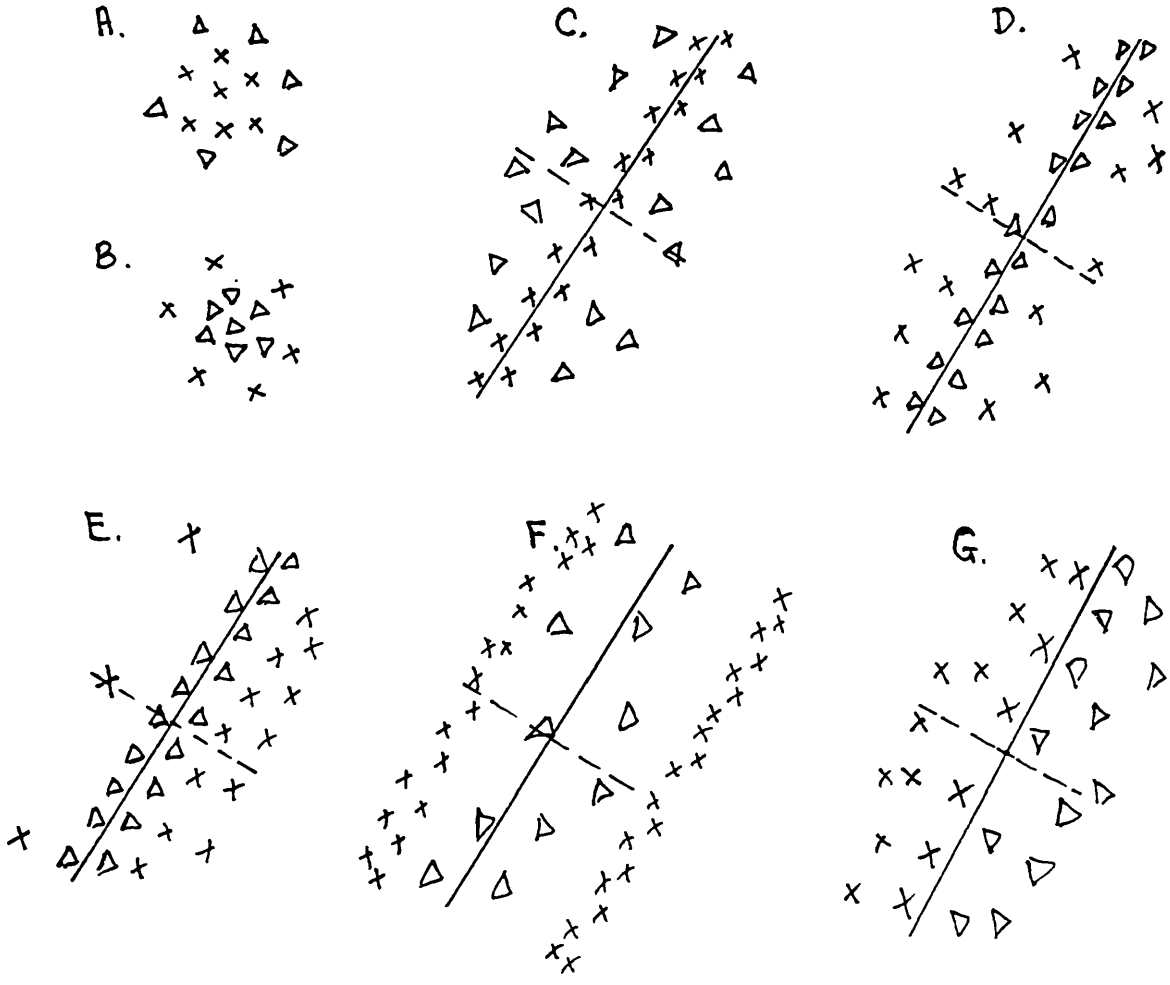

Fig. 1.20 Typical receptive fields, crosses indicate excitatory or ON-responses, triangles indicate inhibitory or OFF-responses. A, ON-centre typical of the ganglion and L.G.B. cells. B, OFF-centre type, otherwise as A. C-G, various arrangements of "simple" cortical fields (Hubel and Wiesel, 1962).

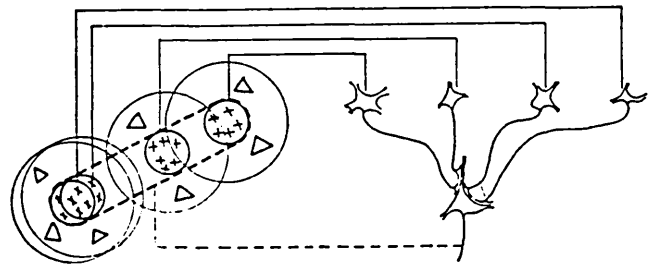

Fig. 1.21 Scheme to explain the organisation of the linear cortical receptive field on the basis of summation of circular fields at the geniculate level (Hubel and Wiesel, 1962).

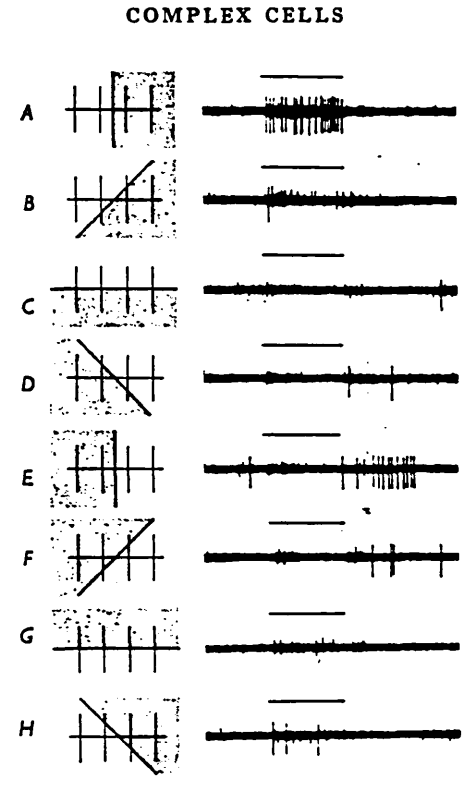

Fig. 1.22 Responses of a cell with a large complex receptive field to an edge projection on the ipsilateral retina so as to cross the receptive field in various directions. (Hubel and Wiesel, 1962).

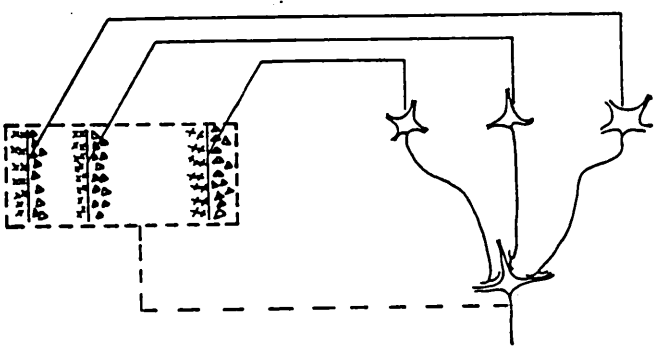

Fig. 1.23 Possible explanation for the organisation of complex receptive fields. A number of cells with simple fields are imagined to project to a single cortical cell of higher order. The receptive field arrangement of the simple cells are shown on the left. The boundaries of the fields are staggered within an area outlined by the interrupted lines. Any vertical-edge stimulus falling across this rectangle, regardless of its position, will cause excitation of the simple cells and thus excitation of the higher-order cells. (Hubel and Wiesel, 1962).

1.5.4. Cortical Architecture

It was shown by Mountcastle (1957) that the Somatosensory cortex of the cat was divided by a system of vertical columns extending from surface to white matter. Hubel and Wiesel (1963) found that in the kitten's visual cortex units which respond to a given slit orientation are also located in columns. Hubel

and Wiesel (1968) showed that in the monkey cortex, an oblique microelectrode gives a step-by-step change in orientation of the receptive fields as the electrode penetrated deeper through adjacent columns, (See Fig. 1.24). Further, horizontal organisation became apparent, showing simple cells to be concentrated in the deep part of layer III and in layer IV, which is where geniculate fibres relay with the cortical cells, and these simple cells were predominantly monocularly driven. The layers above and below contain high proportions of complex and hypercomplex cells. It was also shown in this study that area 17 as well as 18 and 19 contain complex cells. Hubel and Wiesel (1968) found that the dominant eye is more strongly represented than the fellow eye.

Hubel and Wiesel (1965) found projections from area 17 proceeding to areas 18 and 19. The receptive fields of the neurones within these areas were exclusively complex cells, further, a new class of cell known as the hypercomplex cell, was discovered. Within this hypercomplex grouping, both "higher order" and "lower order" cells were found. Area 18 contained predominantly complex cells, as does area 17, plus a few hypercomplex cells, while area 18, contains predominantly hypercomplex cells with a few complex cells. Hypercomplex cells show a size and orientation specificity and no response is achieved if a line of similar orientation is detected by an adjacent antagonistic region. If this occurs, then the hypercomplex cell behaves like two complex cells, one excitatory with its receptive field in the activating retinal

portion, the other inhibitory with its receptive field in the antagonistic portion. It was found that the majority of the neurones in areas 18 and 19, were binocularly driven, with a similar distribution of dominance for all three visual areas.

There is evidence that in the extrastriate cortical areas there are other retinotopic maps, each specialised for a specific stimulus attribute. Zeki (1978), found in area V_4 cells with irregular receptive fields, which appeared to be specialised for the analysis of colour contrast, and in the superior temporal sulcus a map specialised for movement analysis (Zeki, 1974 a and b).

It might be revealed that the two pathways seen in the retina and L.G.N., embodied in the X- and Y-type cell classes, retain their separate identities in these regions to a degree not seen in the primary visual cortex. However, Levick (1980) hypothesised that Y-type cells are confined to pre-cortical levels, and exist to regulate the X-cell activity in the cortex.

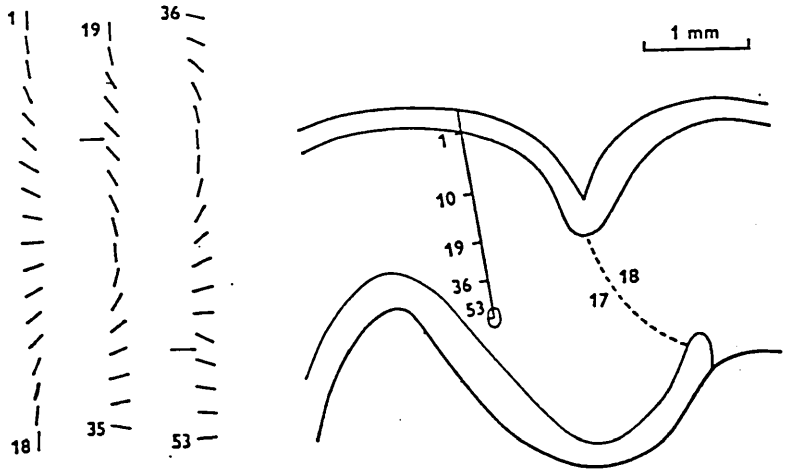

Fig. 1.24 Penetration through the striate cortex about 1mm from the border of areas 17 and 18, near the occipital pole of the spider monkey. On the left are shown the orientation as the column is traversed. (Hubel and Wiesel, 1968).

Chapter Two Psychophysical Techniques used in the Investigation of Normal Human Visual Pathways.

2.1. Psychophysical Investigation in Normal Vision

In the previous chapter the electrophysiological work was discussed. Two distinct channels were demonstrated, the X-type which was characterised by "sustained" firing for the duration of the presence of a stimulus and the Y-type characterised by "transient" firing to both stimulus ON or stimulus OFF. Discussion will now be given to psychophysical experiments which demonstrate the activity of these two channels in human vision.

Kulikowski and Tolhurst (1973) measured sensitivity to temporally-modulated sinusoidal gratings and found that two thresholds could be distinguished. These were the threshold of perceived flicker and that at which spatial structure was detectable. These two thresholds vary independently with temporal or spatial frequency, which indicates two independent systems. The one which detects flicker responds selectively to low and medium spatial frequency, the other, responsible for the discrimination of spatial structure, responds at medium and high spatial frequencies. Thus, flicker detection was mediated by a movement analyser, which gives transient responses, and spatial detection was mediated by a form analyser which yields sustained responses.

Breitmeyer and Julesz (1975) investigated contrast sensitivity to sinusoidal gratings of variable spatial frequency where the onset and offset of their 500ms presentation were either abrupt or gradual. When abrupt onset and offset is used contrast sensitivity at low spatial frequencies increases; no such change occurred with high spatial frequencies

thus , indicating that temporally transient stimulation is preferentially tuned for low spatial frequencies. Legge (1978) also found the same effects using a masking technique.

Harwerth et al (1980) demonstrated by psychophysical experiments on monkeys, functions similar to those found in human observers and the results were compared with electrophysiological evidence for neurones with sustained and transient properties.

Tolhurst (1975) used sub-threshold gratings exposed for a long duration, and then measured the sensitivity to short flashes of the same spatial frequency present during the sub-threshold flash presentation. In the sustained response, the sensitivity to the short flash increased after the onset and then remained until the flash finished. In the transient response however, the sensitivity increased at the onset but then dropped and remained further unaffected. Purely transient responses were obtained at a spatial frequency of 0.2 c/deg, but at 7.6 c/deg or above, the gratings appeared to be detected with sustained responses.

Tolhurst (1973) postulated the existence of two different channels for movement and form detection, the channel dependent on movement of an image having units possessing a low spatial frequency range of <2 cl^{o} and the form channel, independent of movement, with units generally tuned to spatial frequencies greater than 2 cl^{o} carrying no temporal information. Further, he identified these two channel types with the electrophysiological classification of Y and X-type cells of

the retina and L.G.N. (Enroth-Cugell and Robson, 1966), respectively.

In summary, it is generally found that two response channels exist. One having a spatial frequency response confined to the lower end, peaking at about 1 c/° and being specialised for movement and flicker detection; the other responding to higher spatial frequency, with a peak at about 4 c/°, and specific for pattern and form detection (Tolhurst, 1973, Kulikowski and King-Smith, 1973, Holliday and Ruddock, 1983). Most agree that these two systems correspond to the X and Y-type classifications respectively.

Some researchers have demonstrated narrow bandwidth spatial frequency channels which gave rise to the hypothesis that the visual system performs a Fourier analysis of a visual scene. However, recordings from single units can be obtained with non-periodic stimuli at all levels of the visual pathway. Burton, Nagshineh and Ruddock (1977) provided evidence that the positive and negative contrast components of a grating are processed independently, which is contrary to the spatial frequency model. Further, the results of Campbell and Robson (1968) and Sachs, Nachmias and Robson (1971), which compared the contrast thresholds for square, sinusoidal and composite gratings and gave evidence for the Fourier theory, can be explained by observed receptive field properties (Legendy, 1975).

2.2. Two Spatio-temporal Filters in Normal Vision

Recently, two different spatio-temporal filters have been identified in normal observers and the bulk of the

present study is concerned with the measurement of these filter functions in amblyopia and albinism. Details of these experimental methods and results will be given later in the text, but the methods developed by Barbur and Ruddock (1980) and Holliday (1982) (see also Ruddock 1982) are described briefly here.

2.2.1. Spatio-temporal Filter Type 1

Barbur and Ruddock (1980) described a spatial response known initially as the I.M.G. function, which stands for Interaction between Motion perception and background Grating. This function has more recently been called ST spatial response and is associated with a visual spatio-temporal filter, type 1. In this thesis the underlying mechanism will be called the ST filter. In their experiments a circular target moved at constant velocity across a spatially modulated background grating of square waveform with bar width d, giving a fundamental spatial frequency fs = $[2d]^{-1}$ The subject adjusted the illumination of the circular target, I_t, in order to obtain threshold illumination for its detection. I_t was measured as a function of the background grating periodicity fs, and measurements were made for a number of different mean illumination levels of the background gratings. It was found that for constant mean background illumination the threshold detection illumination, I_t, varies with the background periodicity, fs (Fig. 2.1.). Two characteristic response curves were observed; for mean background illumination below 2.0log trolands, the response curve peaks at fs equal to 4 to 5 cycles deg^{-1}, whereas at higher background illuminations it peaks at 8 to 10 cycles deg^{-1}. Thus there appear to be two

spatial response functions, one of which mediates detection at low (<2.0log trolands) illuminations levels , the other at high (>2.0log trolands) illumination levels. This response is essentially independent of stimulus parameters such as target size and velocity and importantly, the orientation of the background grating. For viewing at a non-foveal location, 30deg. off-axis, there is a shift to lower spatial frequencies in the response, with peak values of 1 to 2 cycles/deg for low illumination levels and up to 4 cycle/deg at higher illumination levels. The spatial distribution associated with these responses is circularly symmetric, with centre and surround regions of opposite response polarity, thus it is similar in form to the receptive fields of retinal ganglion cells (Fig. 2.2a and b). (Barbur, computer receptive field for foveal and 30° off axis).

Barbur, Holliday and Ruddock (1981) measured the temporal frequency response of the STI filter and found that it is low-pass in nature, with bandwidth which increases as the mean illumination increases (Fig. 2.3).

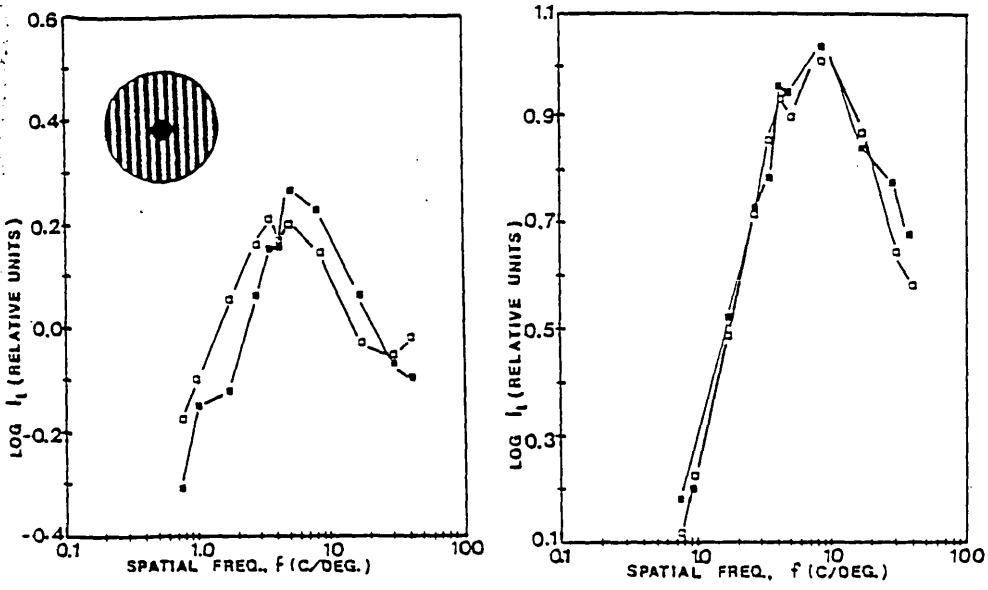

Fig. 2·1 The spatial responses obtained with a target moving over an unmodulated grating. (The IMG response) Two response types are found: a)one peaking at ≈5c/o for background field illuminations, I_b,below some 2.0 log Trolands; b)one peaking at ≈8 c/o for I_b above 2.5 log Trolands. The figure shows both response types. In each case target threshold illumination, log I_t, is plotted against the fundamental spatial frequency of the background. The target was a 3.5° diameter white circle moving at 15°/S horizontally over the central 8° of a 17° diameter circular vertically oriented 90% contrast background grating. The background field illuminations used were a) 1.4 log Trolands (circles) b)3.4 log Trolands (triangles). Results for subjects JB (full symbols) and V W (open symbols). Mean standard deviation=0.03 log units (from Barbur 1980)

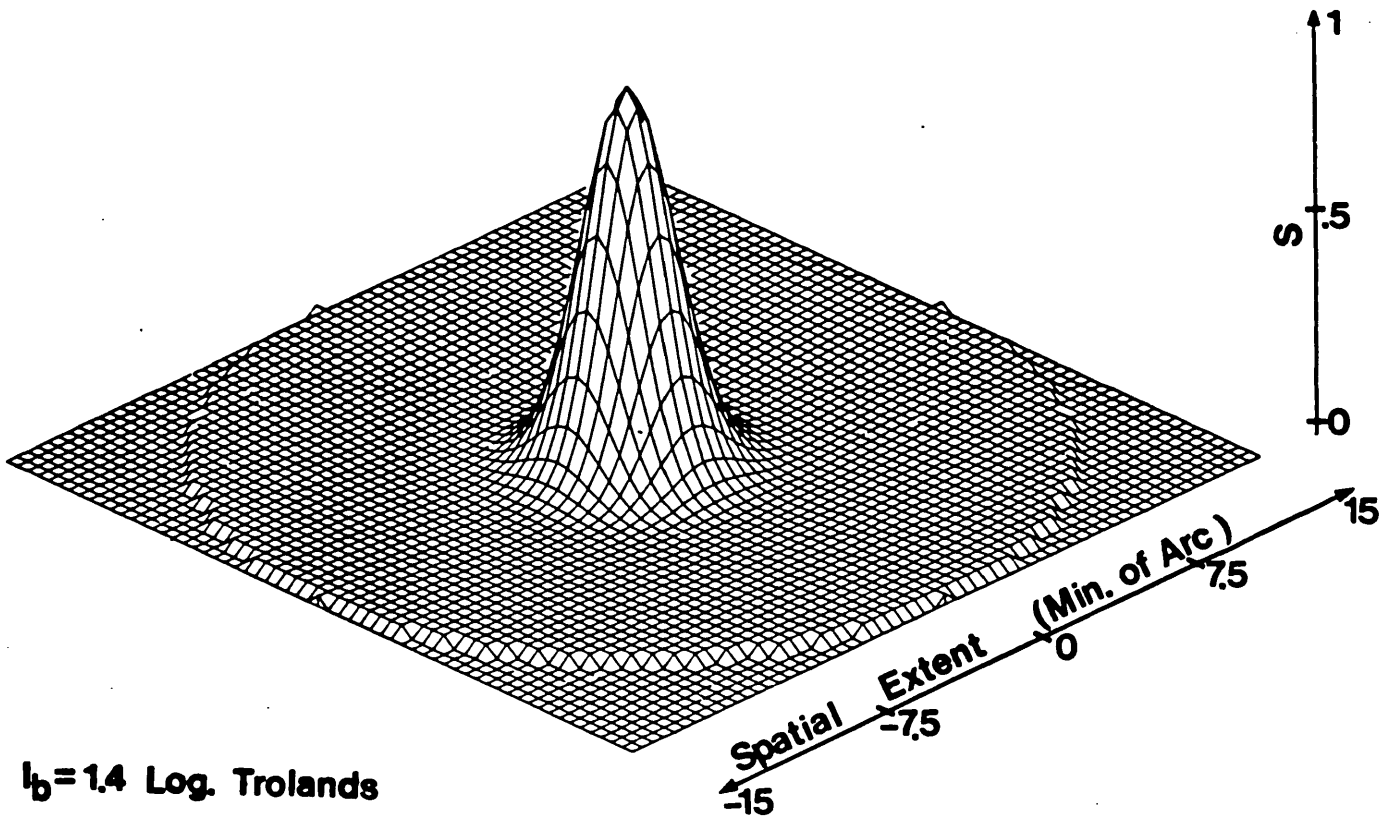

Fig. 2.2a Computed point spread functions for the mean background light level. ST1 spatial response mechanism at 1.4 log trolands. The X-Y plane is the spatial extent of the filter and the Z-co-ordinate is the sensitivity of the filter. The overall shape is of a sharply peaked central lobe surrounded by a shallow negative trough.

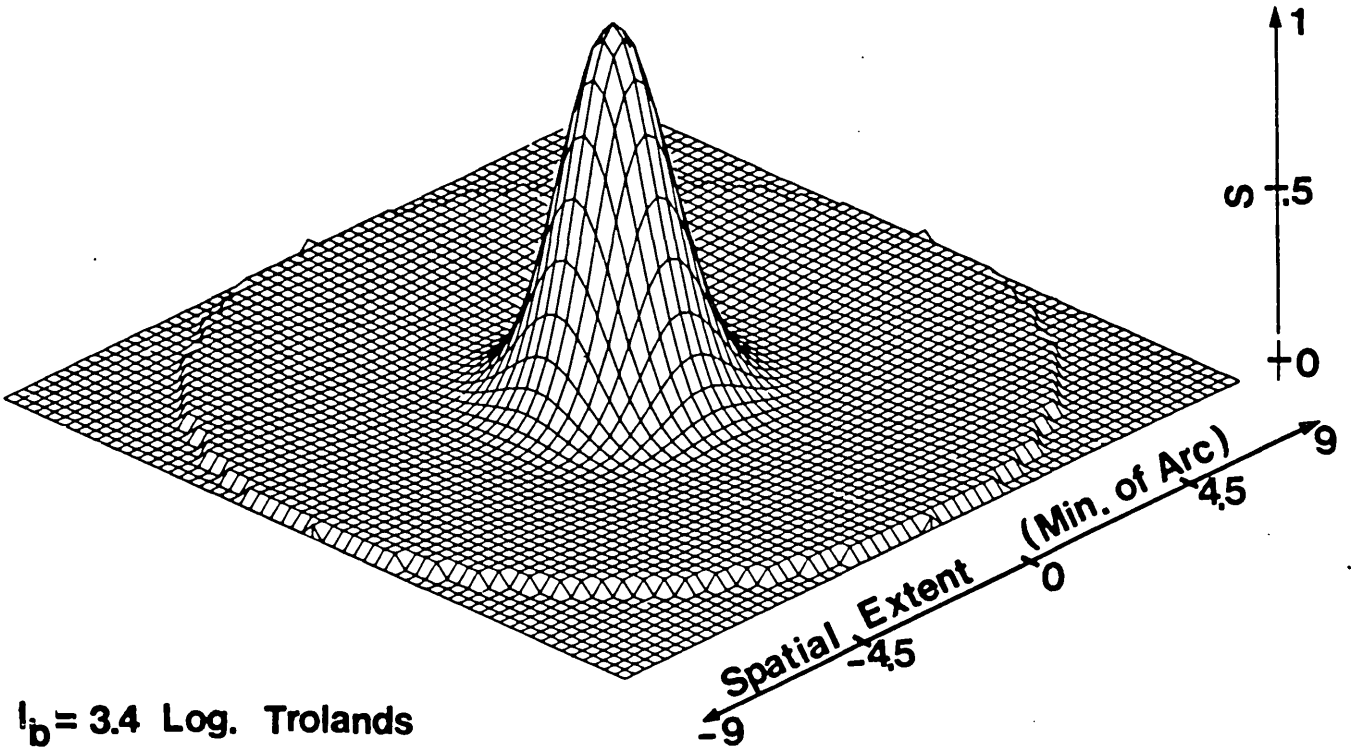

Fig. 2.2b Computed point spread function for the ST1 spatial response mechanisms at 3.4 log trolands mean background illumination level. The X-Y plane is the spatial extent of the filter and the Z-co-ordinate is the sensitivity of the filter. The overall shape is of a sharply peaked central lobe surrounded by a shallow negative trough.

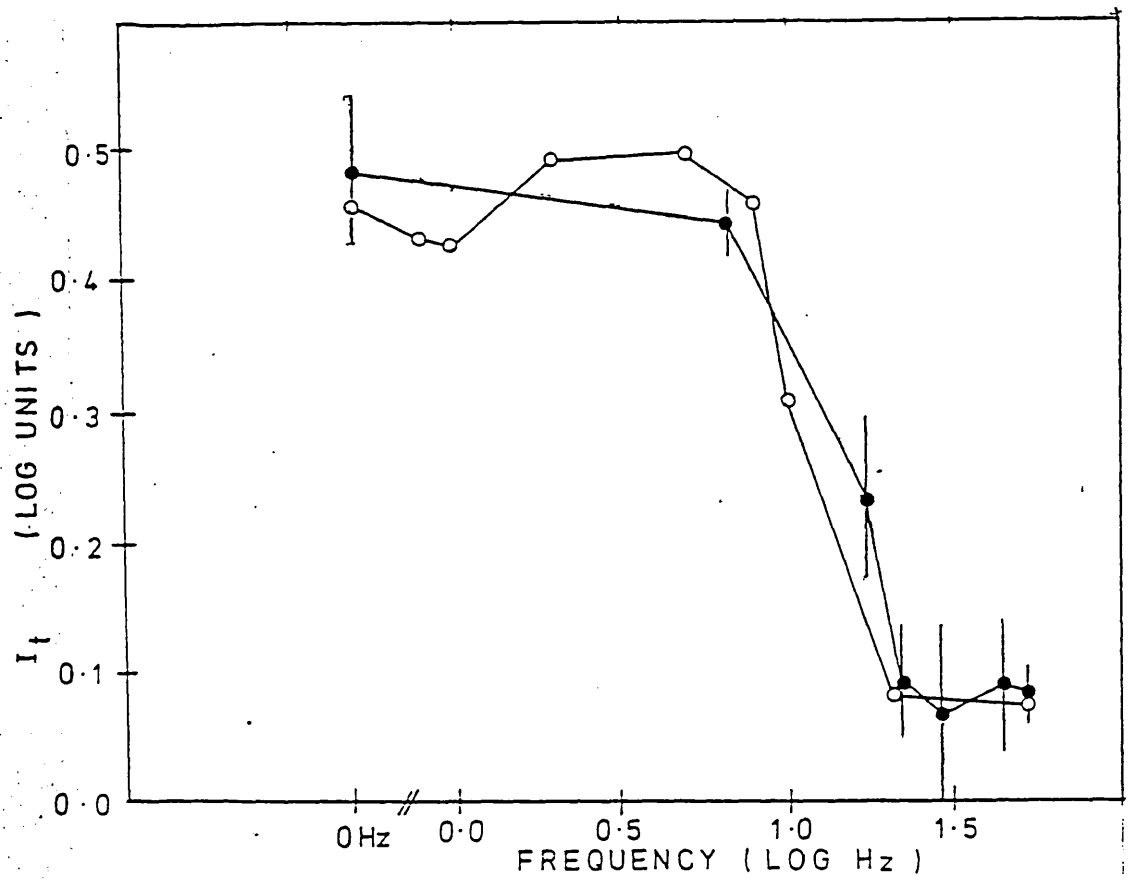

Fig.2.3 Temporal response of the IMG response. Target threshold is plotted against the background modulation frequency for a circular test presented flashed stationary in the centre of two 17° diameter circular 4.3 c/° square waveform gratings in spatial and temporal anti-phase (fig 2.16.For subject IEH ○ the test was 1.4° in diameter and was red (600nm). The background was broad band red light from two l.e.d's driven by the counterphase modulator (sec.2.3.7). For subject PS● the test was 1.4°in diameter and was white. The background was also white, th e modulation being provided by a sectored disc driven by a servo-motor chopping beams 2 and 3 (fig 2.1b) in antiphase. For both subjects the mean background field illumination was 1.7 log Trolands, and the test presentation was in a 1s/3s cycle. Mean standard deviation =0.05 log units.

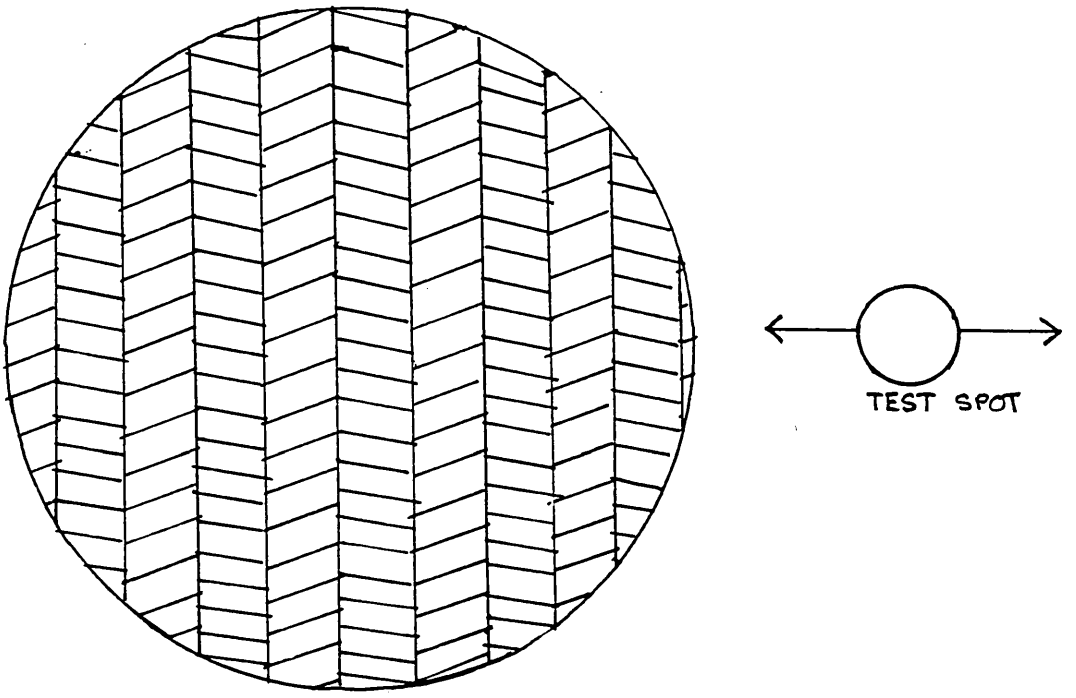

Fig. 2.4. The background field consists of alternate steady and flickering bars of equal bar width. The mean illumination level of the modulated bar is equal to the luminance of the unmodulated bar, that is 2.7 log trolands.

2.2.2. A Second Spatio-Temporal Filter, ST2

In addition to the ST1 filter characteristics described in the previous section a second set of filter characteristics attributed to the so-called ST2 filter, were revealed (Holliday and Ruddock, 1983 and Ruddock 1983). The experimental method used was similar to that applied in the case of the ST1 filter, namely threshold illumination I_t, for detection of a circular target moving across a modulated background field. The different filter characteristics were revealed by choosing different background field structures (see Chapter 4, section 2.3. for details). The ST2 spatial response was found by measuring I_t as a function of the

periodicity, f_s, of a background grating, constructed of alternate steady and flickering bars (Fig. 2.4.). The mean illumination of the steady and flickering bars was the same, so this background field provides spatial modulation which depends on the (transient) flicker of alternate grating bars. The spatial response obtained is shown in Fig. 2.5. and as is clear, it differs from the ST1 spatial response in that it peaks at 1 cycle/deg. and it does not change as the background illumination increases to 2.7 log Trolands. The parametric properties of this response can be summarised as follows:- it is invariant under change in orientation of the background grating and for eccentric fixation of the target less than 30^{o} off axis along the horizontal meridian. It is also independent of target size for circular targets of diameter greater than 1 degree diameter and for target velocities greater than 5 deg./sec.$^{-1}$. For targets of lower velocities and smaller diameter, however, the response peak shifts to 4 cycles/ deg.$^{-1}$ and the curve becomes similar to the ST1 spatial response.

The temporal response corresponding to the low-frequency ST2 spatial response can be determined by using a fixed spatial frequency for the background grating and finding threshold detection illumination, I_t, as a function of the temporal frequency, f_t, of the flickering bars. In practice, however, similar results can be obtained, more readily, by using a spatially uniform, flickering background field. Results obtained in this way are shown in Fig. 2.6., and it can be seen that the temporal response is bandpass in nature quite different from the lowpass response found for the ST1 filter (Barbur, Holliday and Ruddock, 1981). Further, as the background illumination

increases, both the frequency, f_t, for peak response and the cut-off frequency increase, in a manner similar to that observed in measurements of critical fusion frequency (de Lange, 1958). The other important parametric properties of this temporal response are that its amplitude increases rapidly as the modulation depth of the flickering bars increases to 25% but then saturates, and as the target velocity falls to 1 cycle/deg. or less, the response disappears. As in the case of the ST2 spatial response, the temporal response is essentially invarient for measurements up to 30 deg. eccentricity in the horizontal meridian and for circular targets of diameter greater than about 1 deg.

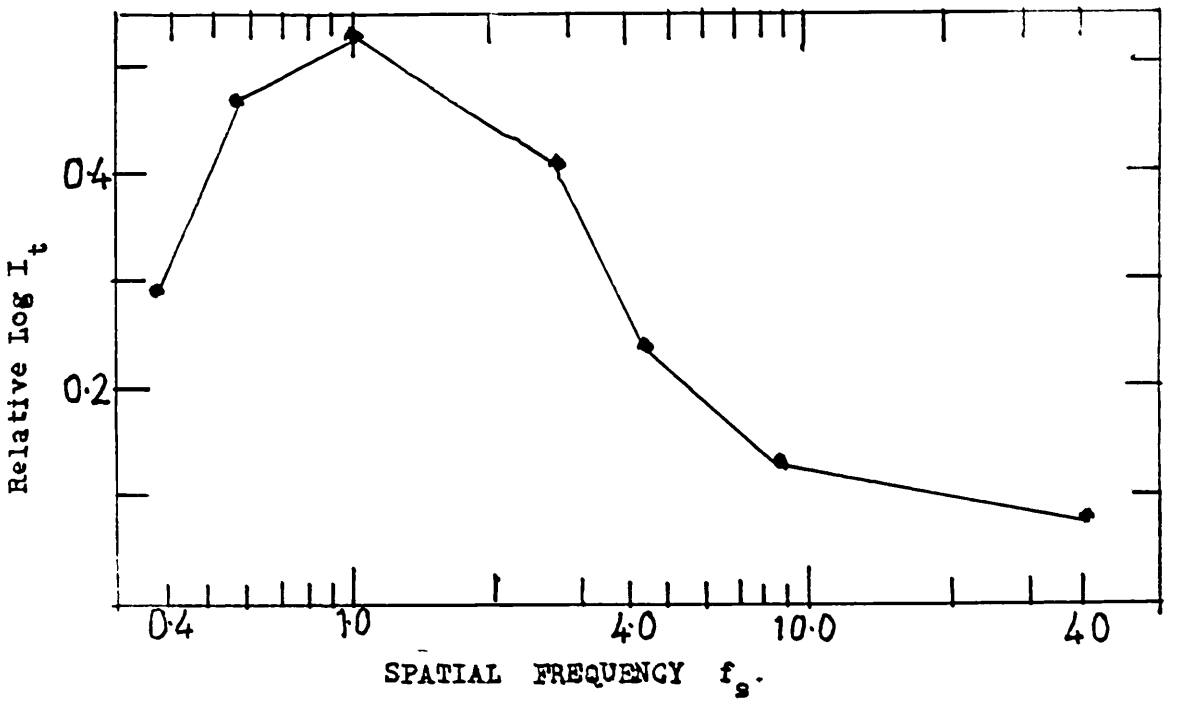

Fig. 2.5. The ST2 spatial response curve is shown. Illumination I_t, for detection of the moving target is plotted against the spatial frequency, f_s, of the background grating. The target was a 1.5 $deg._1$ diameter white light spot, moving at 15 deg./sec.$^{-1}$ along the horizontal meridian. The background consisted of alternate steady and flickering bars of equal width, forming a vertically orientated background grating of fundamental spatial frequency, f_s, See Fig. 2.4. The background field was of mean illumination level 2.7 log trolands, and the alternate flickering bars were 100% modulated at 20Hz around this average value.

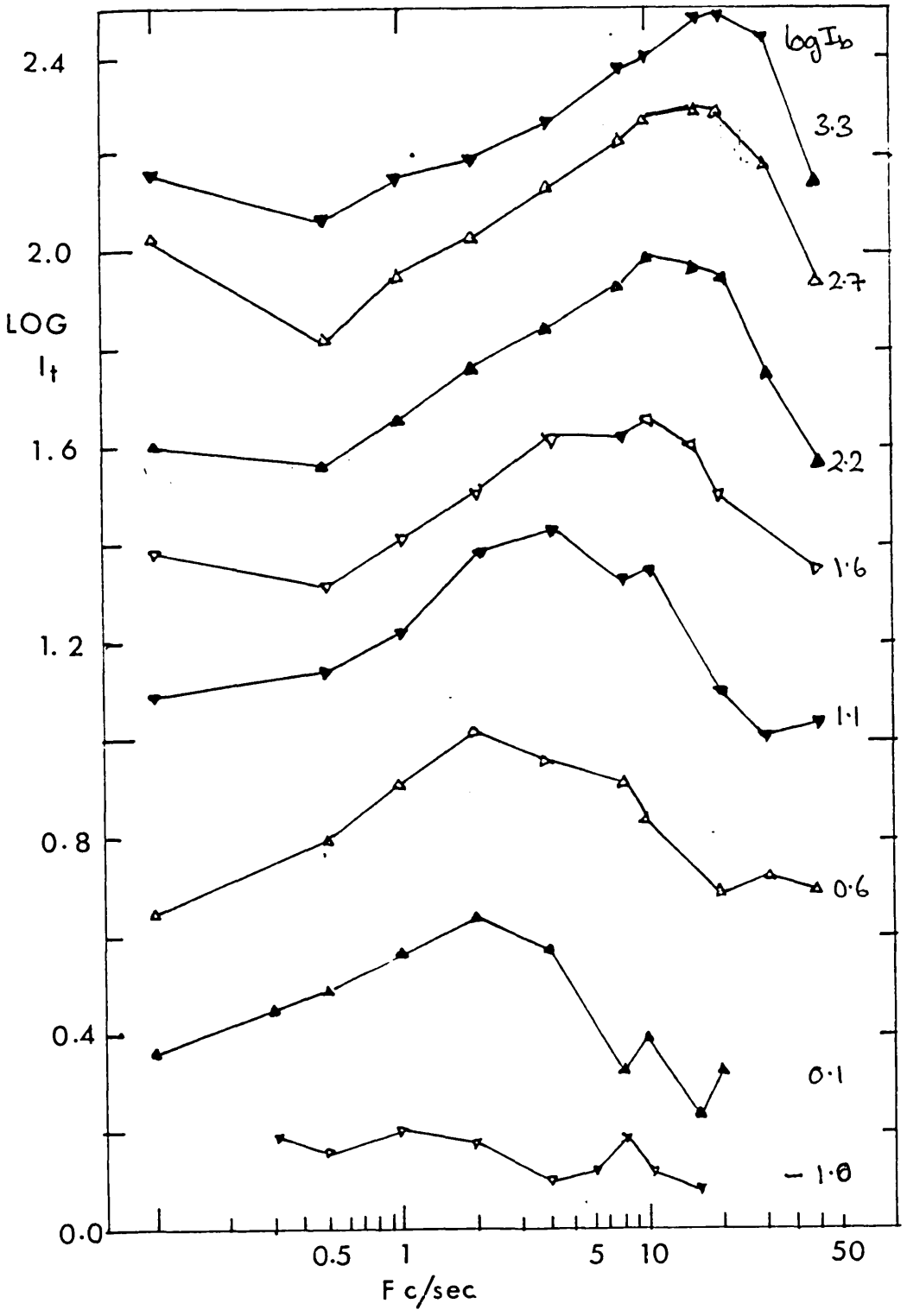

Fig. 2.6 Effect of mean background field illumination (I_B). Log target threshold illumination (log I_t) is plotted against background field modulation frequency for a 1.4° target moving horizontally at 15°/s across the central 8° of a 17° diameter, spatially uniform 25% modulated flickering background field, for 8 values of I_B, which are shown in units of log Trolands to the right of each curve. For clarity, the different sets of data have been shifted arbitarily along the log I_t axis. Transfoveal presentation. OBSERVER IEH. Mean standard deviation = 0.05 log units.

2.2.3. The Organisation of Two Spatio-Temporal Filters

The experiments reviewed in the previous Sections 2.2.1 and 2.2.2, provide spatial and temporal response data for two filters which contribute to the detection of moving targets. The first, ST1, has bandpass spatial response with relatively high frequency peaks at 4 cycles/deg. or 8 cycles/deg. depending on whether average background illumination is below or above 2.0 log trolands respectively, and has lowpass temporal response, the bandwidth of which increases with increase in background illumination. The second filter, ST2, has passband spatial response with relatively low frequency peak at 1 cycle/deg. and passband temporal response, the peak frequency being displaced to higher frequencies as background illumination increases. These two filters have been modelled by a two-stage network (Holliday, 1982, Ruddock, 1983; Holliday and Ruddock, 1983) in which the ST1 filter preceeds and provides the input to the ST2 filter (Fig. 2.7a and b). Two spatially distinct ST1 filters connect with each ST2 filter, where their inputs are subtracted algebraically to provide the ST2 output. In order to predict the temporal response of the ST2 filter a delay, τ, is introduced between the two ST1 inputs to ST2, and by choosing τ in the range 100mSec. for very low illumination levels, rising to 20mSec. for high levels, the experimental data is accurately predicted. The spatial responses of the two filters are considered to be independent of each other, with the finely tuned ST1 responses summed at the input stage of the ST2 filter to give its coarser spatial response

The two filters revealed by the background modulation method provide finely tuned spatial responses, combined with a sustained temporal response (filter ST1) and a coarser spatial response combined with a transient temporal response (filter ST2). The existence of two parallel pathways possessing this general type of response characteristic has been suggested by other psychophysical data (see Table 2.1.), but previously, no precise data for the response characteristics of the two filters has been given. Reference has already been made to the properties of the X- and Y-type ganglion cells, with sustained and transient temporal responses respectively (Chapter 2 Section 2·1). In the case of the macaque retina the X-type receptive fields are small, with centres of diameter 0.04 to 0.09 degrees for cells with red or green cone driven receptive field centres, and of diameter 0.16 deg. for those with less frequent blue cone driven centres. These values are constant for retinal eccentricities up to 20 degrees. The Y-type cells have larger receptive fields, those with colour opponent responses increase from about 0.9 degrees diameter at the fovea to o.24 degrees diameter at an eccentricity of 10 degrees. Y-type responses decay more rapidly than X-type and exhibit conspicuous "on" and "off" transients, while X-type have very few transients, (De Monasterio, 1978a&b). Correspondingly, the ST1 filter possesses sustained (low-pass) temporal responses and have small receptive field centres of 0.04 to 0.08 degrees diameter (Barbur and Ruddock, 1980a). The ST2 filter appears to correlate with the Y-type mechanisms as they respond to transient stimuli and have larger receptive fields as indicated by the lower spatial frequency responses of the ST2 filter.

TABLE 2.1

REFERENCES	FORM CHANNEL	MOTION CHANNEL
Holliday and Ruddock, 1982 Barbur et al, 1981.	Low pass temporal response (of ST1 filter (I.M.G.))	Bandpass temporal response. Peak shift with background illumination. Spatial response peak at 1 c/°.
Barbur and Ruddock, 1980.	Spatial (S.T.1) Mechanism peaking at 4 or 8 c/°.	----------
Roufs and Blommaert, 1981	0.8' spot give low pass temporal mechanism.	1° spots give bandpass, time course depends on an illumination.
Blommaert and Roufs, 1981	Point spread function similar to ST1 filter.	----------
Breitmeyer et al, 1981.	Uniform field flicker, no effect for spatial frequencies above 4 c/°.	Increased thresholds for spatial frequencies below 4 c/° with 5Hz flicker.
Green, 1981	Uniform flicker, no effect for spatial frequencies above 4 c/°. Low pass temporal response.	Bandpass temporal response for low spatial frequencies peak at 6Hz.
Burr, 1981	Low pass temporal response. Cut-off at 16Hz.	Bandpass mechanism for large spots.
Keck et al, 1976	----------	Non-linear dependence on contrast (motion after effect.
King-Smith and Kulikowski, 1975.	Spatial response peak at 5 c/° low pass temporal response.	Spatial 1.5 c/° peak. Temporal bandpass response.
Kulikowski and King-Smith, 1973.	Point spread function similar to I.M.G. (ST1 filter) response.	----------

The recent work of Barbur and Ruddock, (1980), Barbur, Holliday and Ruddock, (1981), and Holliday and Ruddock, (1983) has provided new psychological techniques which can be applied in the study of visual defects. In general, visual defects which change visual spatial resolution change the ST1 filter. Recent electrophysiological findings in cats with surgically induced squints show that there is a deficit in the X-cells spatial response while the Y-cells show little change, thus it was decided to use the techniques reviewed in this section to assess the changes in psychophysical filters corresponding to the electrophysiological X- and Y-systems in human amblyopic subjects.

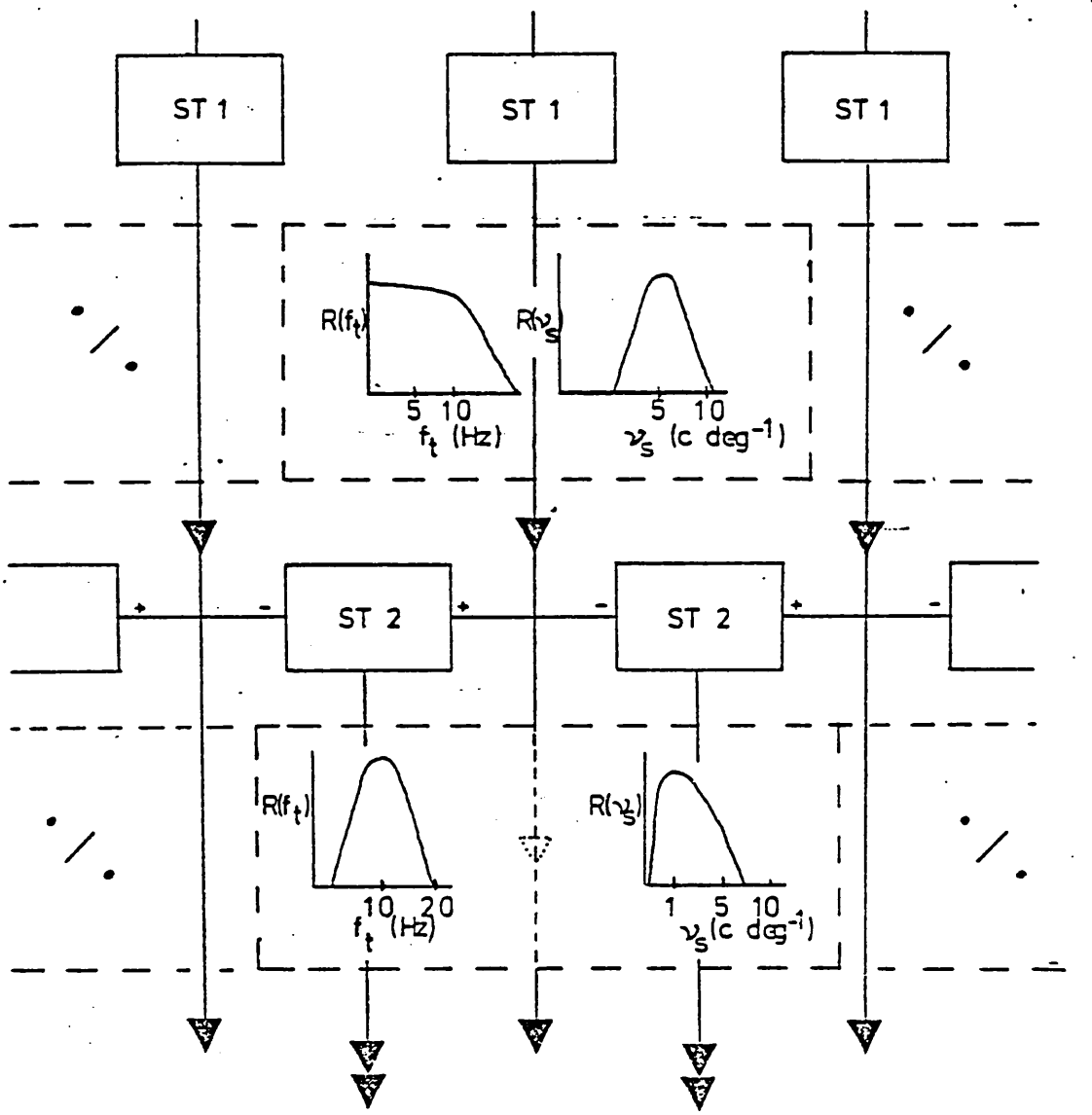

Fig. 2.7. a) The model network proposed for linking the ST1 and ST2 psychophysically determined filter mechanisms. The small rectangles enclosing the symbols ST1 and ST2 represent individual filter mechanisms. These filters are in two rows, and the full vertical single arrowed lines show the signal direction is from the ST1 filters downwards. The ST2 filters have horizontal linkages to the ST1 filter outputs and these perform a subtraction operation, their outputs being labelled with double arrows. Below the rows of ST1 and ST2 filters the general form of their temporal ($R(f_t)$) and spatial ($R(v_s)$) responses are shown, the position of the dotted boxes and the sign indicating such responses obtain for each individual mechanism. After Holliday and Ruddock, 1983.

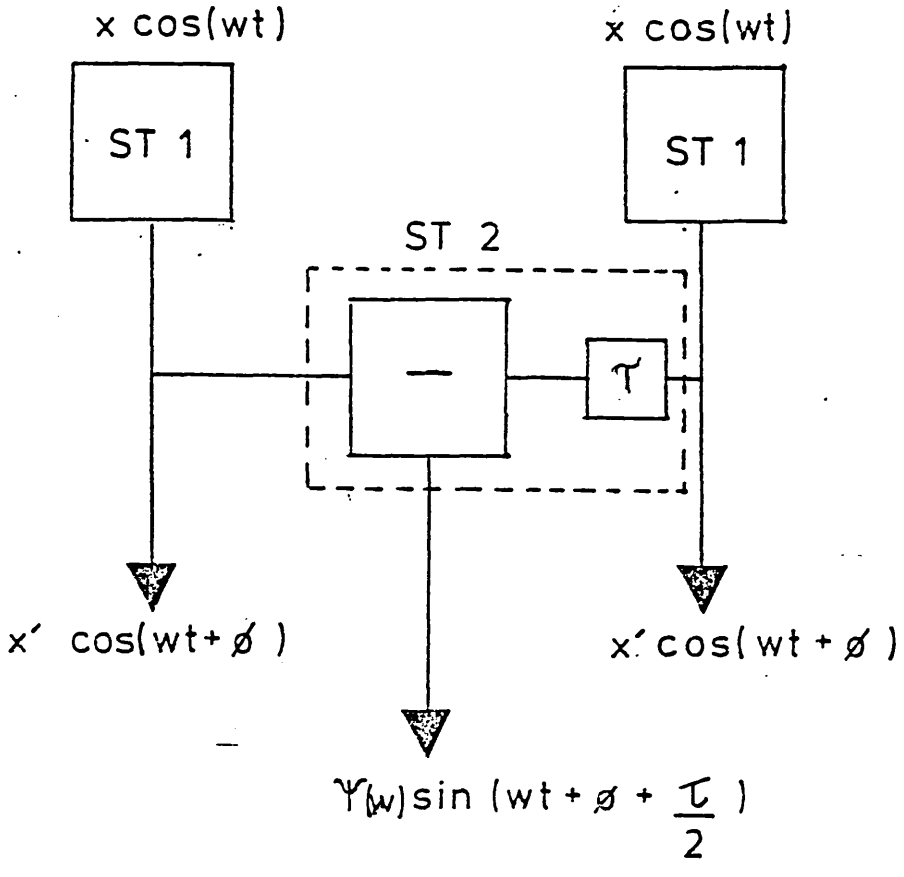

Fig. 2.7 b) The detailed operation of the ST2 filter mechanism. The ST2 filters perform a subtraction operation on two ST1 outputs, one of which is subject to a time delay τ. The input/output relationship is shown explicitly on the figure, (After Holliday and Ruddock, 1983).

Chapter Three Clinical, Electrophysiological and Psychophysical Details on Amblyopia

3.1. Amblyopia

Amblyopia is the term applied to certain conditions leading to poorer than normal resolving power. There are many causes of such a loss of resolution but in this study we confine ourselves to the functional amblyopia. A definition given by Lyle and Wybar (1962) is, "A condition of diminished visual form which is not associated with any structural abnormality or disease of the media, fundi or visual pathways, and which is not overcome by correction of any refractive error." Adaptations to the presence of a squint are variable between subjects. A manifest squint which is present from birth results in a failure of development of the normal binocular reflexes so that the adaptations which occur are different from those which take place when a squint arises in a young child whose binocular system is partly or fully established; in such a child active suppression must result to prevent diplopia. This process of suppression, is the result of a cerebral inhibition designed to give complete dominance to the non-deviant eye. There are two main types of inhibition, faculative and obligatory, the latter type often being followed by an eccentric fixation (use of a non-foveal point for both monocular and binocular fixation). Faculative inhibition occurs in the squinting eye only during the time when it is squinting and disappears when the eye takes up fixation, and thus it does not result in a permanent loss of vision. Obligatory inhibition, occurs in the squinting eye whether it is fixating or not and occurs commonly in uniocular convergent squints. Faculative inhibition is generally a sequel of the inhibitory type.

Eccentric fixation is the term applied to an alteration which may occur in the fixation of the squinting eye following the development of an obligatory inhibition, and is normally preceded by a condition known as abnormal retinal correspondence (A.R.C.). It is a sensory adaptation which eliminates diplopia and confusion by reorientation of the image of the squinting eye relative to the non-squinting eye, a phenomenon dependent on an altered sensoral relationship between the two eyes. Thus the point on the retina which receives the same input in the squinting eye as the fovea of the normal eye, correspond with each other under binocular conditions. This gives, in some cases, a rudimentary binocular vision and eliminates diplopia and confusion. However, the anomalous "fovea" of the squinting eye is only used under binocular conditions, the normal fovea being used under monocular conditions. If the abnormal retinal correspondence (A.R.C.), is not eliminated it will eventually progress to eccentric fixation and under this condition, the "false fovea" is also used under monocular viewing conditions, hence both abnormal retinal correspondence and eccentric fixation are forms of sensory retinal reorganisation.

3.1.1. Theories concerning Amblyopia, Eccentric Fixation and Motor Anomalies

Over the years many theories have been put forward in an attempt to explain the subnormal level of visual acuity found in amblyopic eyes, whether of strabismic or anisometropic (unequal refractive errors in each eye) origin. The classical sensory theory developed by Worth (1903) and Chavasse (1939) states that amblyopia is a loss of central visual acuity which

is the result of suppression of a deviating eye in strabismus, or due to a blurred image in anisometropia, see Fig. 3.1.. Eccentric fixation is often found in amblyopic eyes and was believed by Worth (1903) to occur where the central loss is so great that foveal acuity is less than that of the surrounding area. The amblyopic eye then fixates at a more sensitive site to enhance visual resolution. The classical theory is supported by the work of Shapero (1971) who argues that the reduction of central acuity can be attributed to relatively long-standing suppression, inhibition, disuse or non-use of the central impulses from one eye. Impulses arriving at the visual cortex from the foveal area of the amblyopic eye provide information which is either in conflict with, or inferior to, the information from the normal eye. The cortical response to such bilateral input is to respond only to the impulses from the normal eye, suppressing those from the other.

An alternative theory is the motor theory, in which acuity is related directly to the eccentric part used. Weymouth (1958) found that in nine eccentrically fixating strabismics the acuity was analogous to the peripheral acuity at the same distance from the fovea in untrained normal observers. Flom and Weymouth (1961) thought that at least some amblyopias could be the result of eccentric fixation - a motor anomaly - without resorting to an inhibition of acuity. Mallet (1969) argues that the vast majority of strabismic amblyopes have some degree of eccentric fixation, and that the amount of eccentricity is predictable from their acuity with some accuracy. Hess (1977) compared ten strabismic amblyopes' acuity at their eccentric fixation position with that

of normal subjects viewing eccentrically. Both the Llandolt C and gratings were used to assess acuity. Hess found two types of amblyopia; in some he found that the acuity was predictable by the region used for fixation, whereas the remainder showed a further reduction in acuity beyond that expected at the retinal locus used for fixation. Kirshen and Flom (1978), measured the acuity in eccentrically fixating subjects across the retina. Acuities were determined at various eccentricities in the visual field. In all cases they showed that maximum acuity was at the fovea and not at the eccentric point. They also noted a uniform drop in acuity both nasally and temporally on leaving the fovea. They concluded that the acuity loss exhibited by the amblyopic eyes have a sensory (inhibition) component and a motor (retinal-locus) component, the sensory component being greater for small degrees of eccentric fixation, while a motor component was greater for large amounts of eccentric fixation.

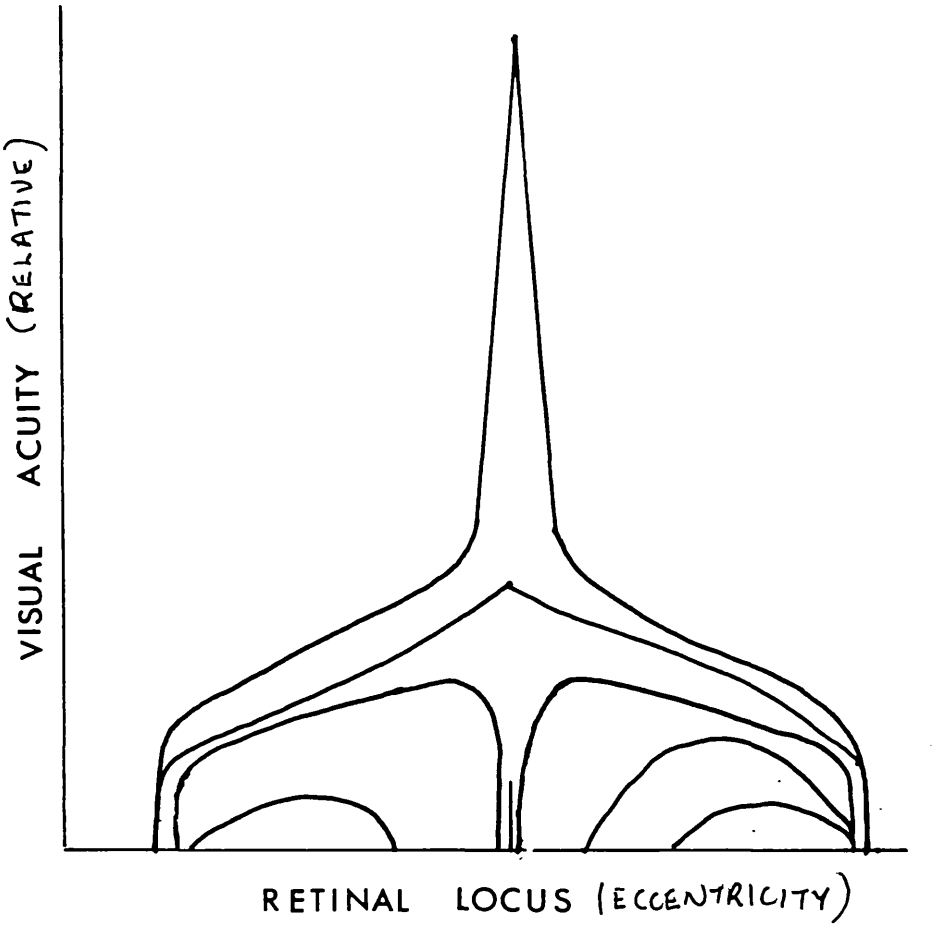

Fig. 3.1. Chavasse's notation of acuity in an amblyopic eye. Upper curve shows acuity in the normal eye. The lower curves show the results of different degrees of central retinal inhibition in amblyopic eyes. (After Chavasse, 1939).

3.2. Electrophysiological Studies on Amblyopia

In recent years many researchers have investigated various stages along the visual pathways by microelectrode recordings, and a brief resumé of some of their work follows.

3.2.1. Electrophysiology of the Amblyopic Retina

Acuity in amblyopia is largely related to the foveal region. In cats, Ikeda and Wright (1974b) found that small sustained neurones predominate in or near the area centralis , the larger transient neurones being found mainly in the peripheral retina.

The sustained cell has a well defined inhibitory surround where the cell becomes more sensitive to stimulus "off" than to "on". Beyond this inhibitory surround is a region known as "disinhibitory" where the cell becomes again sensitive to stimulus "on". These properties give a capacity for fine spatial discrimination, thus allowing high visual acuity. Transient cells have a lower sensitivity at the receptive field centre than sustained cells, the sensitivity gradient is shallow and never drops to zero or exhibits a distinctive surround region. Peripheral transient cells, therefore, have large receptive field centres and weak surrounds so they have poor spatial discrimination. In contrast, they are very sensitive to large,high-contrast flickering targets.

Ikeda and Wright (1974b, 1975) investigated the effects of defocus on both X and Y ganglion cells,(see Fig. 3.2.). As can be seen, the Y-cells under defocussed conditions act as light-catching devices, the activity of the field edges becoming greater than in the focussed condition. The receptive field of the X-cells on the other hand, does not expand, but retains its symmetrical response profile to the point where response fails; this is when light was defocussed dioptrically to a value greater than 8 dioptres, High visual acuity is therefore dependent on sustained retinal ganglion cells in the foveal area, which require a sharply-focussed, small, temporally-stable object for optimum stimulation.

Ikeda and Wright (1972a)examined the relationship between refractive error and the spread of the image on the cat's retina. Having measured the retinal image under different blurred

conditions they confirmed that the changes noted in different ganglion cell behaviour cannot be due to optical differences between the central and peripheral retina, but arise from differences in the receptive field organisation of central and peripheral ganglion cells.

Abnormal visual experience during the sensitive period of development produces physiological abnormalities in the visual system. (Wiesel and Hubel, 1963; Blakemore and Cooper, 1970). Wiesel and Hubel (1963) proposed that a neural connection must receive adequate stimulation during the sensitive period in order to remain effective & Ikeda and Wright (1974b) have suggested amblyopia may be the result of lack of adequate foveal stimulation during the sensitive period of development and that functional degeneration in the sustained pathways could therefore occur at the retinal ganglion cell level. Ikeda and Wright, 1976, Ikeda et al, 1978, & Ikeda and Tremain 1979, showed that regardless of the type of squint, the number of binocularly driven cortical cells is reduced, while loss of visual acuity only occurs in mono-fixational strabismus. Hubel and Wiesel (1965) used cats reared with surgically produced divergence but found no amblyopia, only loss of binocularly driven cortical cells. Blakemore and Eggers (1977) found the same results with convergent squinters, but in both of these studies alternating strabismus was produced. Ikeda and Tremain (1979) argue that the surgical technique used in the other studies tended to produce alternation, so in their study on eleven cats, they used their own method to produce convergent strabismus, which involves removing the lateral rectus and the superior oblique muscles and all the connective tissue from the lateral side of the eyeball. A further two cats had convergent squint produced

by removal of the lateral rectus muscle only and the connective tissue, and one cat was raised with a divergent squint produced by removing the medial rectus. The results of the different surgical procedures were as follows: cats with oblique and rectus muscle plus connective tissue removed produced large angle squints with a degree of hypertropia; those with rectus muscle removal only, generally had a smaller angle squint but no vertical tropia; all these cats had amblyopia and a reduction of binocularly driven cortical cells. The one cat with lateral rectus disinsertion and also the divergent squinter proved to be alternators and were not amblyopic, but did show a reduction of binocularly driven cells.

The spatial resolution of a cell was determined by the sinusoidal grating with the highest frequency to which the cell gave a modulated response to grating movement (Ikeda and Tremain, 1979) Recordings were taken from four of the cats, including one control cat, the two alternators, and one of the monofixational convergent squinters. The results are shown in Fig. 3.3. and as can be seen, only the monofixational squinter shows amblyopia. The resolving power of the amblyopic eye was poorer, with a mean 1.4c/^{o}, the normal eye averaging at about 4.5c/^{o}. The other three cats showed mean peaks for both eyes at around 4.5c/^{o}. Transient cells 2^{o} from the area centralis were examined (Y-cells); these cells have very little spontaneous activity and their responses decreased for gratings of higher spatial frequencies. The resolving power from the normal eye was about 2c/^{o} whereas in the amblyopic eye it was about 1.5c/^{o}. Fig. 3.4. shows the spatial resolution of 71 X-cells from normal eyes and 83 from

amblyopic eyes. The lower graph shows the spatial resolution of 47 Y-cells from normal eyes and 44 from amblyopic eyes, these data being plotted against retinal eccentricity. The acuity of the sustained retinal ganglion cells of normal eyes resembles that of sustained L.G.N. cells of normal eyes (Ikeda and Wright, 1976; Ikeda and Tremain, 1978b). It was found that, strabismus has no effect on the acuity of peripheral cells beyond 10^{o} of the area centralis. A minor degree of amblyopia is found in transient cells of the L.G.N.. (Ikeda and Wright, 1976).

Figs. 3.5. and 3.6. show the contrast sensitivity curves for "sustained" and "transient" cells of a normal control cat and of a monofixational squinter respectively. The sustained responses of the amblyopic eye is generally reduced in amplitude and shows a particularly noticeable high spatial frequency cut off. The transient cell for the amblyopic eye shows a slight general reduction for all frequencies. The receptive field sensitivity gradient of both sustained and transient retinal ganglion cells in the area centralis of a normal eye and of an amblyopic eye are shown in Fig. 3.7. The centre-surround responses in amblyopia are less pronounced, particularly in sustained cells, the effect being less marked for transient cells.

The work of Ikeda and co-workers has therefore provided evidence for changes in retinal ganglion cells in amblyopic eyes. The X-cells, as has been seen are predominantly affected. Additional evidence for Ikeda's work on retinal ganglion cells has been provided by Chino, Shansky and Hamasaki, 1980.

In a recent study (Cleland et al, 1982) the findings of Ikeda et al and Chino et al, 1980, were not confirmed. Although the cats were behaviourally amblyopic, recordings from retinal ganglion cells were said to be normal, but, in a poster presented by these authors at the Fifth European Conference on Visual Perception they state that the acuities of brisk-sustained, X-type, ganglion cells were slightly lower than normal for cats with convergent strabismus caused by removal of the muscle bodies of the lateral rectus and superior oblique muscles, a technique similar to that used by Ikeda and co-workers. Yinon et al, (1976), found that even when three extra-ocular muscles are sectioned a few cats ended up with almost straight eyes and tended, therefore, to alternate. It was thought that sectioned muscles might have grown back, as was found by Wickelgren-Gordon, (1972), in cats operated on to induce strabismus. Further evidence for sectioning causing low angle strabismus with a tendency for alternating fixation was given by Ikeda and Tremain, 1979, when they reproduced the sectioning techniques of Hubel and Wiesel, 1965, and Blakemore and Eggers, 1977, and produced alternating strabismus. Cleland et al, 1982, also found a distinction between the two different surgical techniques when examining the response of the L.G.N.. Thus, when the whole muscle is removed - myectomy - a reduced soma size in the laminae of the nucleus receiving input from the strabismic eye is noticed, whereas the sectioning technique, -tenotomy- gave little measureable changes in the soma size. Hence, their results differ from those of Ikeda and co-workers, but they used a different surgical technique, one which has already been shown to be ineffectual in producing monofixational strabismic cats. (Yinon et al, 1976,

and Wickelgren-Gordon 1972). The absence of changes in X-cell recordings would be easily explained if their cats were alternators, but such animals would not show behavioural amblyopia as the VA of the two eyes would only differ very slightly if at all.

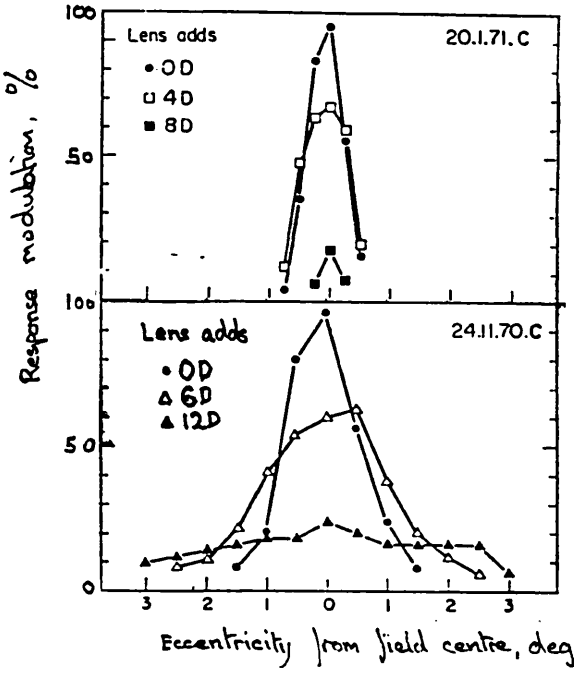

Fig. 3.2 Effect of defocusing on transient cell response and sustained cell responses. (Ikeda and Wright (1974b).)

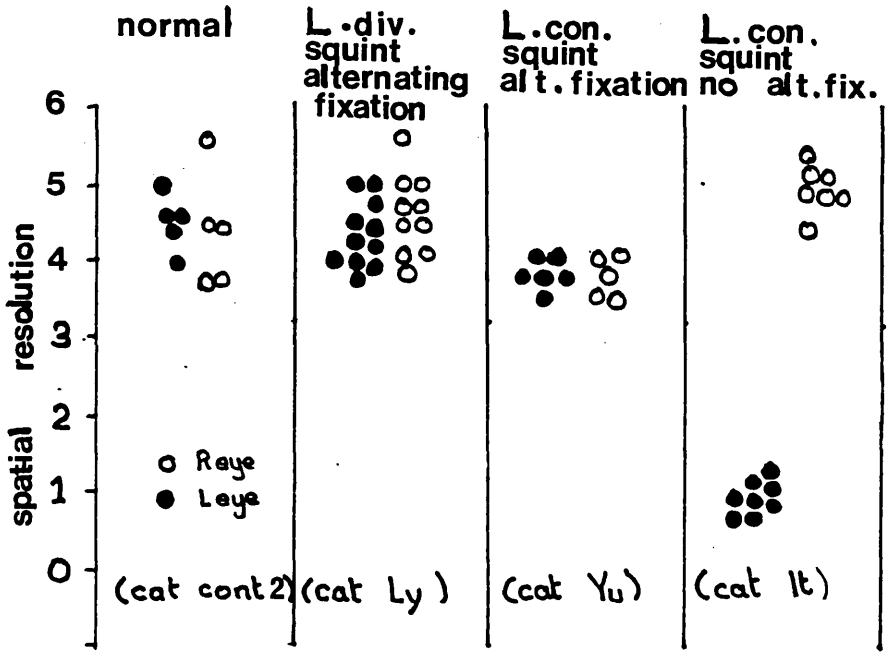

Fig. 3.3 Spatial resolution of sustained retinal ganglion cells in the area centralis of each eye of four cats. Spatial resolution is the highest spatial frequency of a sinusoidal grating (contrast 0.4 mean luminance, 10cd/m^2, drift speed 1Hz). (Ikeda and Tremain, 1979).

Visual acuity of Retinal Ganglion Cells at Different Distances from Area Centralis (AC).

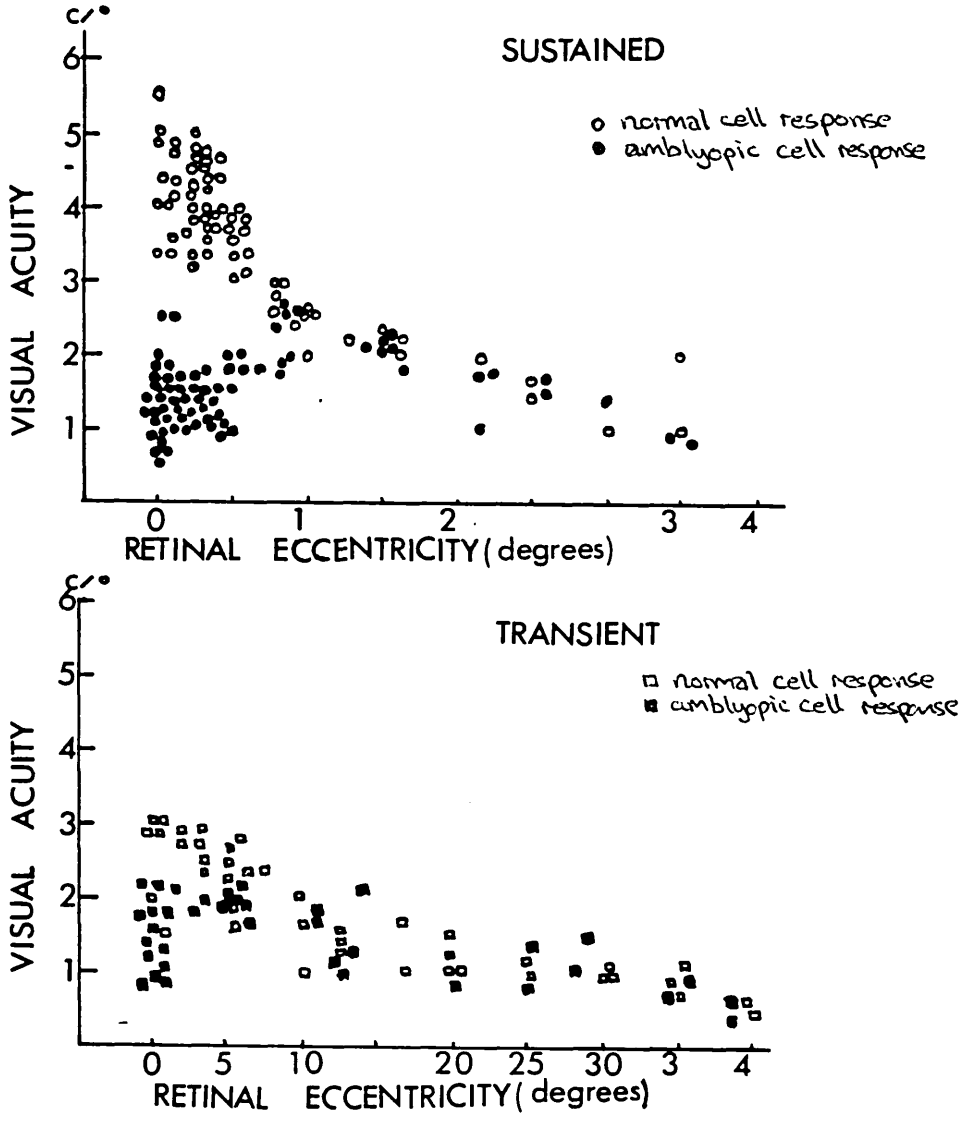

Fig. 3.4 Plots of spatial resolution of sustained and transient retinal ganglion cells against retinal eccentricity, for cells in the normal and squinting eye of the cats left convergent squint without alternating fixation. (Ikeda and Tremain, 1979).

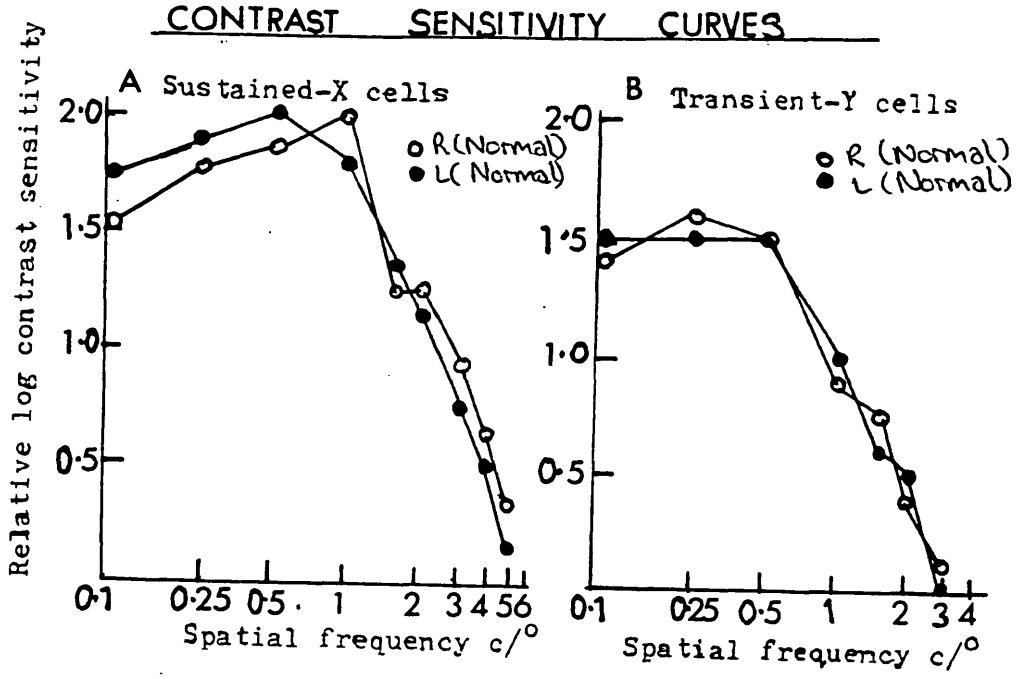

Fig. 3.5 Comparison of contrast sensitivity curves obtained from two sustained cells in the area centralis of the left and right eyes of a control cat (A), and from two transient cells near the area centralis of the left and right eyes of the same cat. The curves were constructed by measurements of threshold contrast (the weakest contrast of a sinusoidal grating with mean luminance of 10cd/m^2) to which the cell gave just discernable modulation of firing in post stimulus histograms (16 stimulation cycles). The relative log contrast sensitivity is the reciprocal of the threshold contrast. Note the similarity of the two curves in A and B. (After Ikeda and Tremain, 1979).

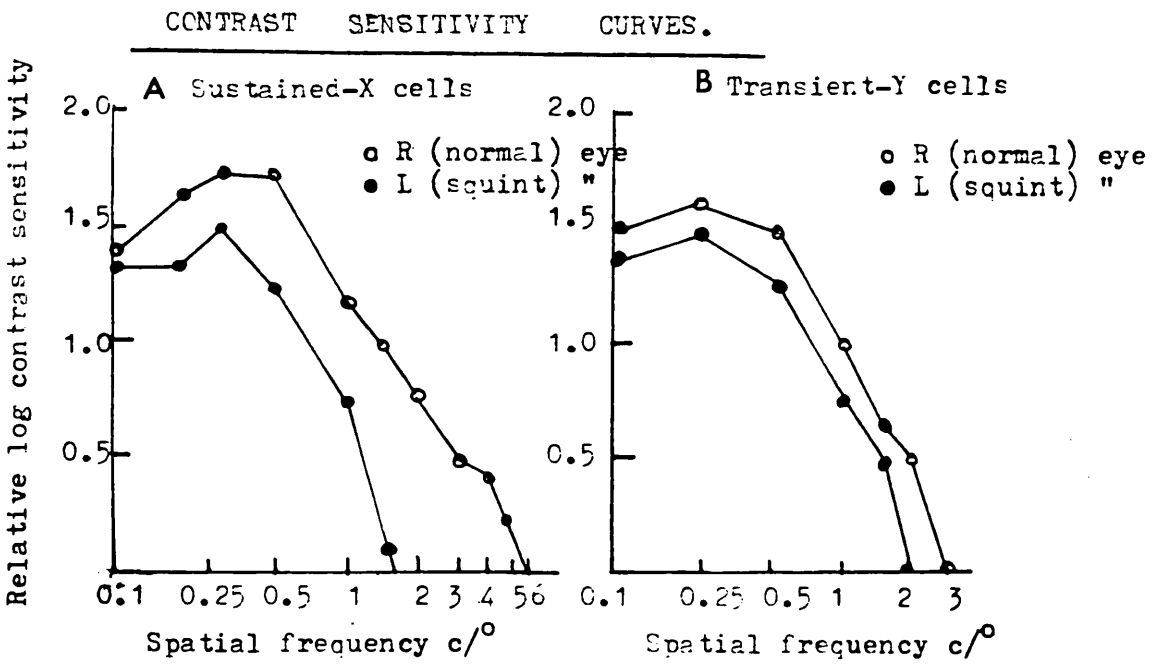

Fig. 3.6 Comparison of contrast sensitivity curves obtained from two sustained cells in the area centralis of the normal and the squinting eye of a cat (Cat Is) with a left convergent squint without alternating fixation (A) and that of the curves obtained from two transient cells near the area centralis of each eye of the same cat (B). The stimulus conditions were exactly the same as those used for the cells from the control cat illustrated in the previous Figure. Note that the curve for the sustained cell from the squinting eye in A and that for the transient cell from the squinting eye in B are displaced to the left and downwards compared with the curves for the cells from the normal eye. (After Ikeda and Tremain, 1979).

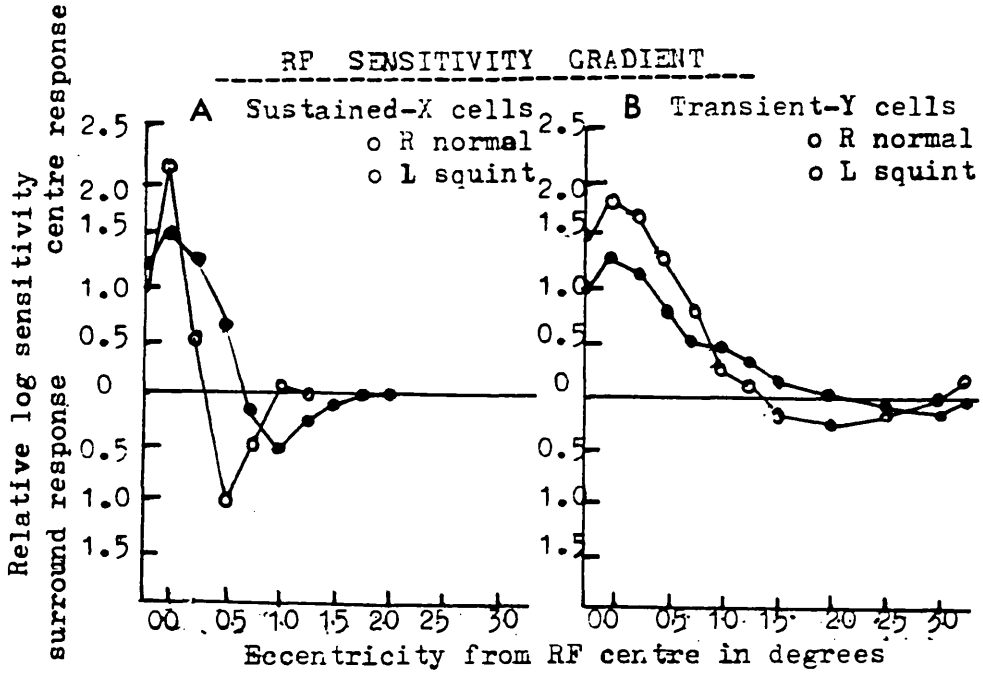

Fig. 3.7 Receptive field sensitivity gradient of sustained retinal ganglion cell in the area centralis of the squinting eye compared with that of a sustained cell of the area centralis of the normal eye obtained from a cat (Is) with convergent squint without alternating fixation. The sensitivity values are the reciprocals of threshold contrast of a single bar generated at different positions along the radius of the receptive field. The bar stimulus was 0.2° in size and was changed from light to dark above and below the mean luminance ($10 cd/m^2$) of background, at the rate of 1Hz. Centre response indicates response of the cells to the "on" of the light phase of the bar and surround response, to the "on" of the dark phase of the bar. Note that the sensitivity profile of the receptive field of the normal eye cell shows a steep sensitivity gradient and widely spread centre and surround. B Comparison of the sensitivity gradients of the receptive fields of two transient cells near the area centralis of the normal and the squinting eye of the same cat (Is). (After Ikeda and Tremain, 1979).

3.2.2. Electrophysiology of the L.G.N.

Ikeda et al (1978) studied the spatial resolution of L.G.N. neurones in cats raised with strabismus surgically induced at different ages from 3 weeks to 16 weeks. The earliest point of the sensitive period of development in kittens has been shown to be at 3 weeks of age, (Hubel and Wiesel, 1970; Blakemore, 1974), hence the choice of 3 weeks for the earliest operation to be performed. Yinon (1976) in his work on cortical cells, also showed that age of onset of strabismus was important.

Recordings from the cat's L.G.N. for normal and squinting eyes at a series of ages are shown here in Fig. 3.8, with the mean of the data plotted against age in Fig. 3.9 and the best fitted line of regression is drawn.

Fig. 3.10 is a plot of the relative spatial resolution of "sustained" cells driven by the area centralis against age at which squint was induced and the broken lines represent data taken from Ikeda and Tremain (1978 a). Fig. 3.11 compares the contrast sensitivity curves of "sustained" L.G.N. cells driven by the area centralis of the normal and amblyopic eyes of these cats, with the similar curves obtained from untreated normal cats.

Ikeda et al (1978) found close agreement between the sensitivity curve of cells driven by the squinting eye of the young adult, with that of normal cats whose true age corresponds with the age at which a squint was induced. Comparison of the data from the squinting eye of young adult cats, whose squint was

induced at 3 weeks of age, with those of a normal 3-week old kitten, revealed some sign of low cut in the sensitivity curve of the squinting eye. It is suggested that this low spatial frequency loss in contrast sensitivity indicates the presence of an inhibiting surround in the receptive field. So, despite the squint, some inhibitory surround development occurs after 3 weeks of age, although high spatial frequency sensitivity does not develop in these early onset squints. In general, the contrast sensitivity curve of a "sustained" cell from a squinting eye has a lower spatial frequency peak, and exhibits a gross loss of sensitivity to higher spatial frequencies. Ikeda also found that both retinal ganglion cells and L.G.N. cells showed severe loss in and around the area centralis.

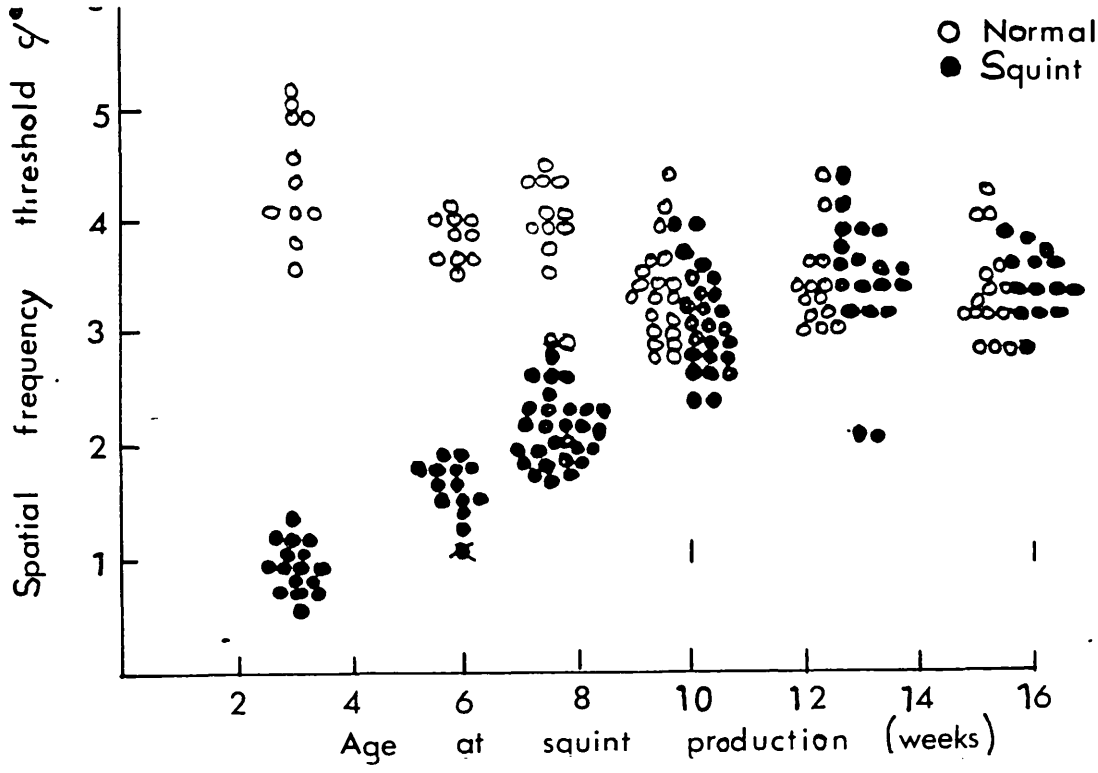

Fig. 3.8. Spatial resolution of "sustained" L.G.N. cells receiving inputs from the area centralis of normal eyes and amblyopic eye. (Ikeda et al, 1978).

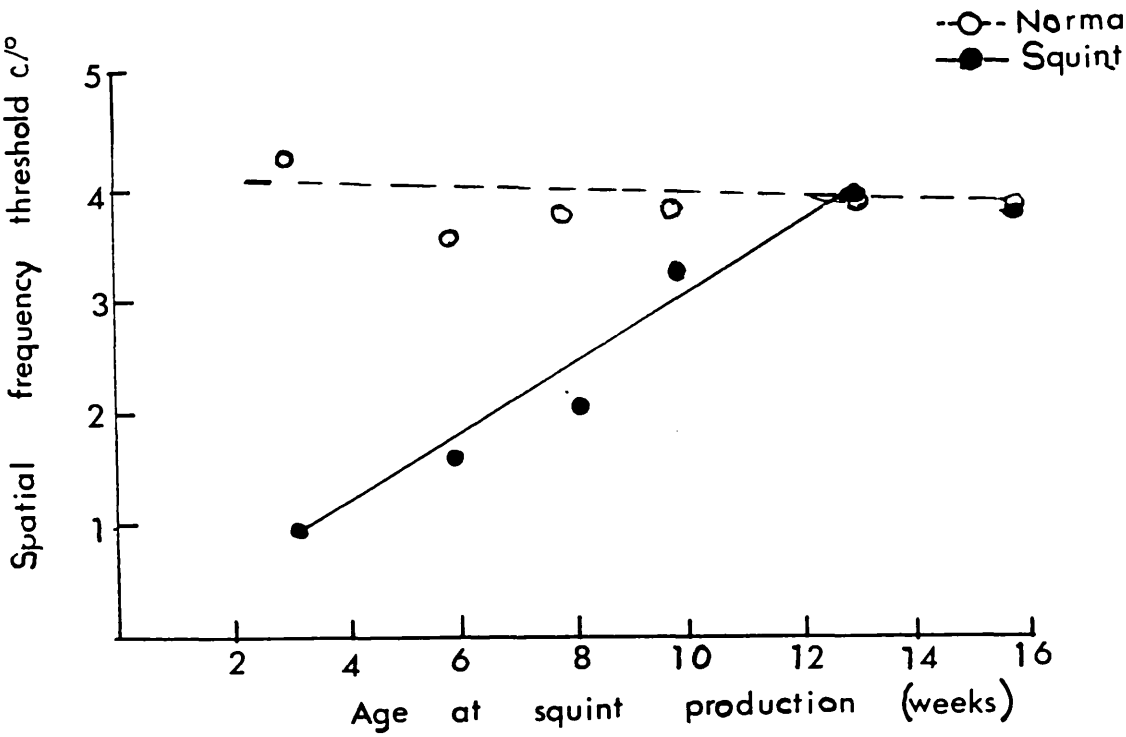

Fig. 3.9. Mean highest spatial frequency of "sustained" cells as in Fig. 3.8. (Ikeda et al 1978).

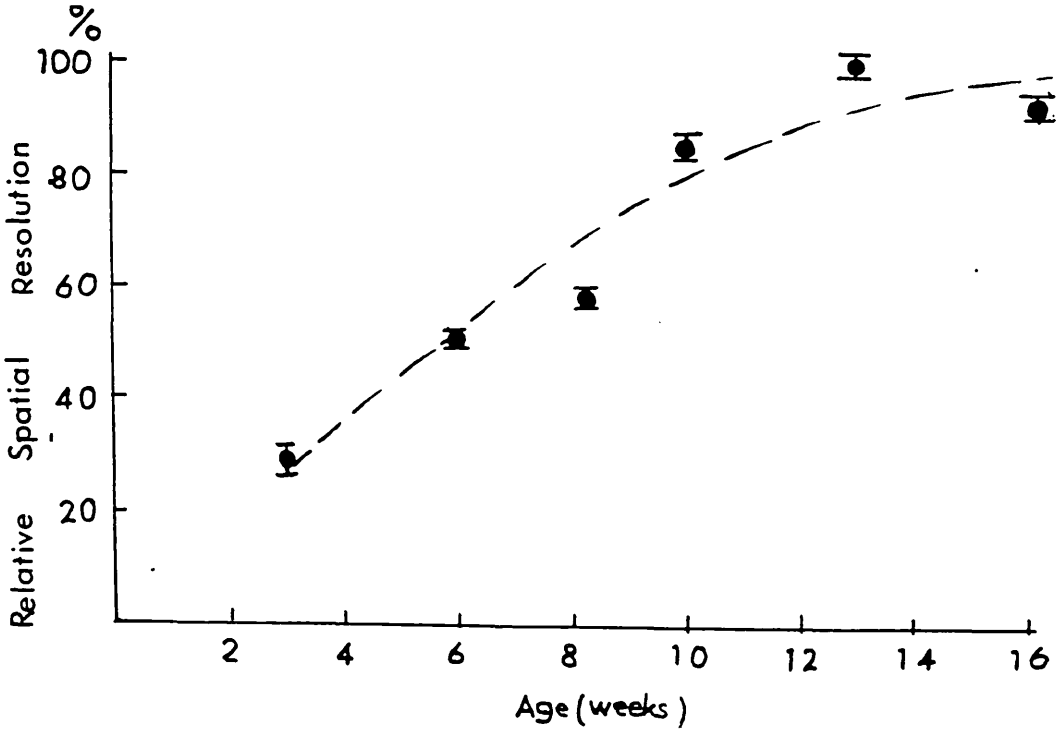

Fig. 3.10. The relative spatial resolution of "sustained" cells driven by the area centralis of the squinting eye as a function of age of squint production. The dashed line is the normal development curve of spatial resolution of "sustained" L.G.N. cells (from Ikeda and Tremain 1978a and Ikeda et al 1978).

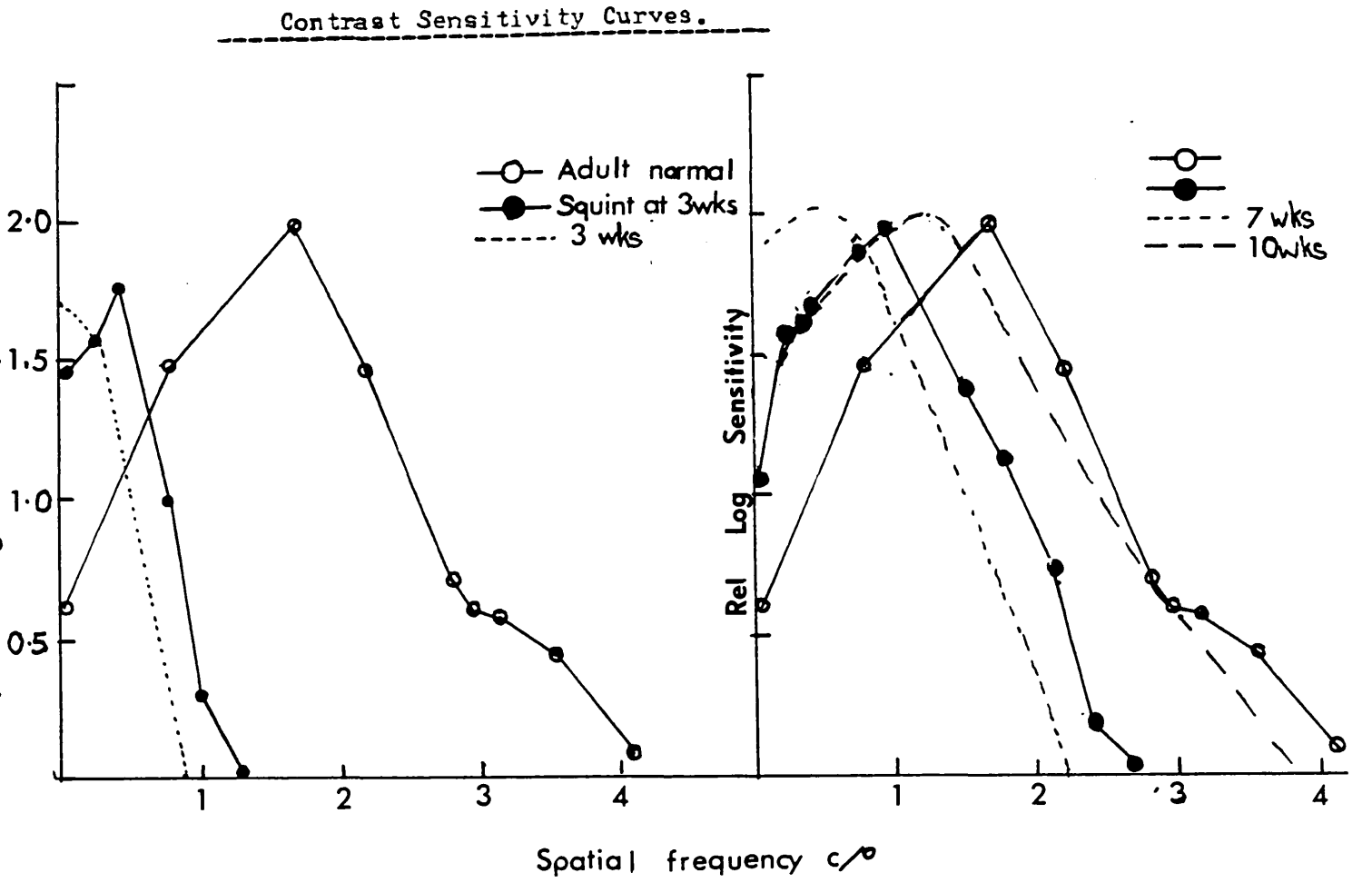

Fig. 3.11. Comparisons of contrast sensitivity curves of "sustained" L.G.N. cells driven from the area centralis of the normal eye and the squinting eye of young adult cats and those of "sustained" L.G.N. cells driven by the area centralis of normal kittens. A, compares curves for cells driven by the normal eye and the squinting eye of a young adult cat whose squint was produced at 3 weeks of age and a cell from a three week old normal kitten. B, compares curves for a cell driven by the squinting eye of a young adult cat whose squint was produced at 8 weeks of age, with cells from the normal eye of kittens of different ages (7, 10 and 28 weeks). The relative log contrast sensitivity is the reciprocal of the threshold contrast of a sinusoidal grating (mean luminance, 10cd/m, drift speed, 1Hz) determined in post stimulus histograms (16 stimulation cycles) showing just discernable modulation of firing. (Ikeda et al 1978).

3.2.2.1 Histological Studies on the L.G.N. in Amblyopic Cats

Ikeda et al (1977), found on histological examination of the L.G.N. that there was a reduced soma size of the layers receiving inputs from the amblyopic eye. These findings were also found by Cleland et al, (poster for ECVP) in cats which were myectomised, although they did not find any changes in somal dimensions in tenotomised cats.

3.2.3. Electrophysiological Investigation of the Visual Cortex

Yinon et al (1976) recorded from neurones in the visual cortex of cats raised with divergent and convergent squint. Their results showed that in five normal cats 70.7% of the neurones responded to binocular stimulation. They studied twelve cats with convergent squints and four divergent squints; 27.2% of neurones responded binocularly in the convergent cats and 63.6% in divergent cats. Furthermore, 65.2% of the monocular neurones were found to react through the normal eye the remainder through the strabismic eye. Their results show very little difference in the recordings of monocularly driven neurones in normal eyes and those studied with divergent strabismus.

Wiesel and Hubel (1963), working on kittens with one eye deprived of visual stimulus from birth for two or more months, found that only 1% of cortical cells were driven binocularly, whereas in normal eyes, 80% of cells in the striate cortex are driven binocularly. The cortical cells of the very young, visually inexperienced kittens had previously been found to be normal and it appears, therefore, that disruption of connections present at birth subsequently occurs. They suggested that the

abnormality was in the region of the synapse between the axon terminals of geniculate cells and the cortical cells on which these terminals end. Eggers and Blakemore (1978), recording from the visual cortex of kittens which received their only visual experience whilst wearing goggles containing a high-power lens before one eye, thereby creating a defocus effect, found that most neurones are dominated by input from the normal eye, with X-cell type units receiving inputs from the amblyopic eye having poorer resolving power and contrast sensitivity.

A study on kittens following lid suture was carried out by Tsumodo and Suda (1978), who found that almost all neurones in the visual cortex became unresponsive to visual stimuli presented to the deprived eye. Investigations had shown that if the normal eye were removed after the critical period of development, the deprived eye was capable of some recovery particularly after the application of bicuculline, an antagonist of GABA-mediated inhibition in the visual cortex. This suggests that some excitatory connections from the geniculo-cortical afferents of the deprived side remain after monocular deprivation. They therefore studied the V.C. neurones of such connections more directly by recording intra-and extracellularly following electrical stimulation of both optic nerves, as well as after visual stimulation. The existence of excitatory connections to a significant number of cortical neurones from the deprived eye, and of inhibitory circuits operated mainly by the non-deprived eye, was suggested.

Hubel and Wiesel (1965) working on cats, and Baker, Grigg and Van Noorden (1974); & Crawford and Van Noorden (1979), working on primates, studied the effects of surgically induced strabismus on the development of the visual cortex, finding substantial deficits in binocular neurones and in those normally driven by the amblyopic eye.

Fox et al (1978) studied the effects of monocular lid closure on the development of receptive-field properties in the superior colliculus in the rabbit. One eyelid was sutured, the other being left to develop normally. Recordings were taken from both the normal and abnormal colliculi. The units which respond to orientation selectivity are significantly affected by lack of visual input, resulting in only about a quarter of the normal number being present at about 4 weeks of age. A corresponding increase in the number of indefinite cells is also found compared to the normal eye. In contrast, units which are not orientation specific remain unaffected.

3.2.4. Changes in the E.R.G. in Amblyopia

The E.R.G. was measured by Hamasaki and Pollack (1972) in cats deprived of light stimulation, who found that light deprivation caused a temporary depression of components of the E.R.G., including the late receptor potential. These results were confirmed neither by Wiesel and Hubel (1963) nor by Van Noorden, Dowling and Ferguson (1970), who both reported that visual deprivation does not affect the E.R.G. Hamasaki and Pollack (1972) argue that lack of support for E.R.G.

depression was due to incomplete visual deprivation in the studies of other groups. They consider that the light deprivation alters the metabolism of the retina, thereby affecting the standing potential across the eye. Other workers who have reported evidence for light deprivation altering retinal metabolism are Brattgard (1952), Liberman (1962), Glow and Rose (1964), Maraini and Carta and Frangueli (1969). Weiskrantz (1958), examined retinas from kittens raised in the dark and found the inner plexiform layer was much thinner than in normal eyes.

Both Hubel and Wiesel (1963) and Hamasaki and Pollack (1972) found it difficult to isolate units from the L.G.N. of deprived cats, & Garey et al (1966a) argue the weak response of L.G.N. units may be related to the decrease in the b-wave of the E.R.G. of visually deprived eyes of cats. Thus, light deprivation can affect the initial part in the visual process. The input to the cortex from the visually deprived layers of the L.G.N. is different from that of normal layers. If several L.G.N. cells are required to fire in a specific pattern to stimulate a simple cortical cell in area 17 (Hubel and Wiesel, 1962) then the alteration at the cortical level may be partly due to changes at the L.G.N.

3.2.5. Psychophysical and Behavioural Studies in Amblyopia

In recent years psychophysical studies in human amblyopic subjects and behavioural studies on cats and primates have been reported. In the following sections, brief consideration will be given to some of this work.

3.2.5.1.Behavioural Studies in Animals with Induced Amblyopia

In behavioural studies on cats, the jump technique of Mitchell et al, 1976 and also 1977 , was used. This involves each animal being trained to discriminate between a square-wave grating and an adjacent uniform field of the same space-average luminance situated beneath the animal on the jumping stand. The animals were trained to jump towards the grating by rewarding them with petting and food or drink. If the animals jumped towards the uniform field the reward was denied. The grating spatial frequency was increased until on a number of trials, a certain percentage of correct responses was not achieved; this frequency was then deemed not resolved.

Cleland et al (1982), using a method similar to that described above, were able to record the VA of both the normal and amblyopic eyes of their strabismic cats, finding on average a drop in VA of 1½ octaves between the amblyopic and normal eyes. They did not, however, find a correlation between this VA drop and electrophysiological retinal ganglion X-cell recordings, as was found by Ikeda (1980) and Jacobson and Ikeda (1979), who using a similar assessment method, found that there is a close correlation between receptive field sizes of X-type retinal ganglion cells and behavioural VA recordings. Fig. 3.12 shows the results of the behaviourally determined visual acuity of normal cats (dashed line, triangles), and amblyopic adult eyes (full line, circles) plotted as a function of the age at which the squint was produced.

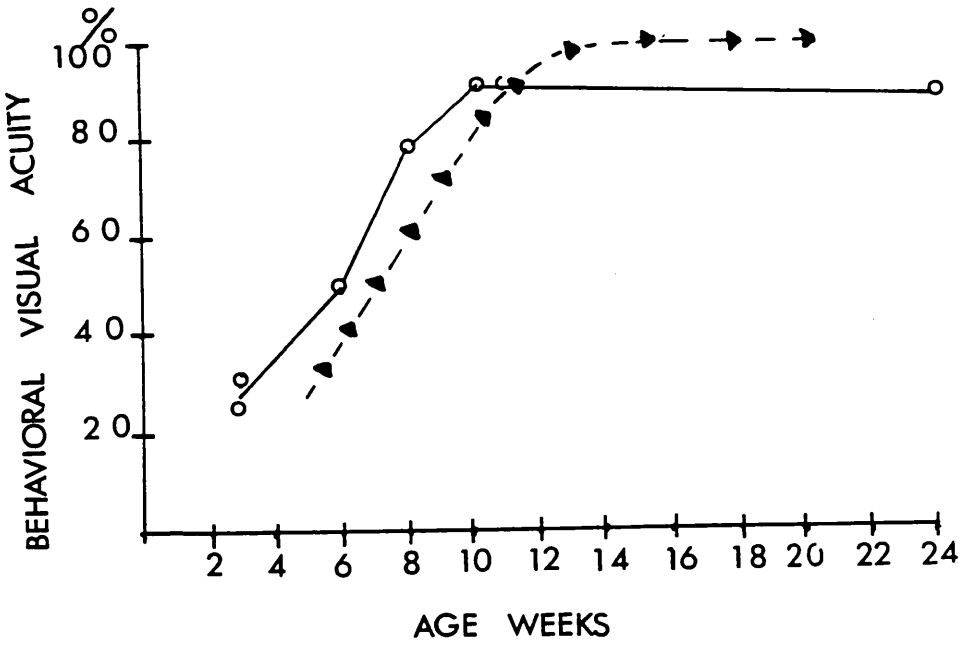

Fig. 3.12 The behaviourally determined visual acuity of normal kittens (dashed line, triangles), and adult cats with induced squints (full line, circles) as a function of the age at which the squint was induced, (from Ikeda, 1980).

3.2.5.2. Psychophysical Studies in Amblyopia

Harwerth and Levi (1978) measured the photopic-luminosity functions for two amblyopic subjects, using a CFF detection task. The results obtained were similar to those for normal observers, therefore indicating a normal transient response channel. Lavergne (1967) also found a normal CFF in amblyopic subjects, while Roth (1968) found that colour vision was normal in the amblyopic fovea. These results indicate that the amblyopic fovea as a whole, cannot be suppressed as some visual functions are intact. Harwerth and Levi (1978) also performed experiments on increment threshold spectral sensitivity and showed that very much higher background intensities were required

to show colour apponency of the amblyopic eye. This indicates a functional anomaly of the sustained channels of the visual system, Harwerth & Levi, 1978 also reported that contrast sensitivity at all spatial frequencies is abnormally low in amblyopia, and peaks at a lower spatial frequency than normal. They found that the extent to which sensitivity is depressed for low spatial frequencies is related to visual acuity. Tests of reaction time for detection of suprathreshold stimuli indicate that there may be deficits in both transient and sustained systems, but that the sustained cells are more severely affected than the transient cells.

Hess and Howell (1977), using a contrast sensitivity technique, postulated two types of amblyopia; one type showing a general depression at all spatial frequencies, the other having predominantly high spatial frequency cut off (see Fig. 3.13 and 3.14). On close inspection of their subject data (table 3.1), however, it seems that those showing a general depression at all spatial frequencies have the following characteristics; they are early onset squinters, have responded less well to treatment, showing higher levels of eccentric fixation and poor VA. The selective high spatial frequency loss is present in those subjects with predominantly later onset strabismus, better VA and lower eccentric fixation (table 3.1). It appears, therefore, that the overall sensitivity loss type is a simple extension in severity of the high spatial frequency loss type. An exception to the afore mentioned seems apparent in subject JP, who was 7 years of age when unilateral blur was first noticed. However, if we consider the refractive error of

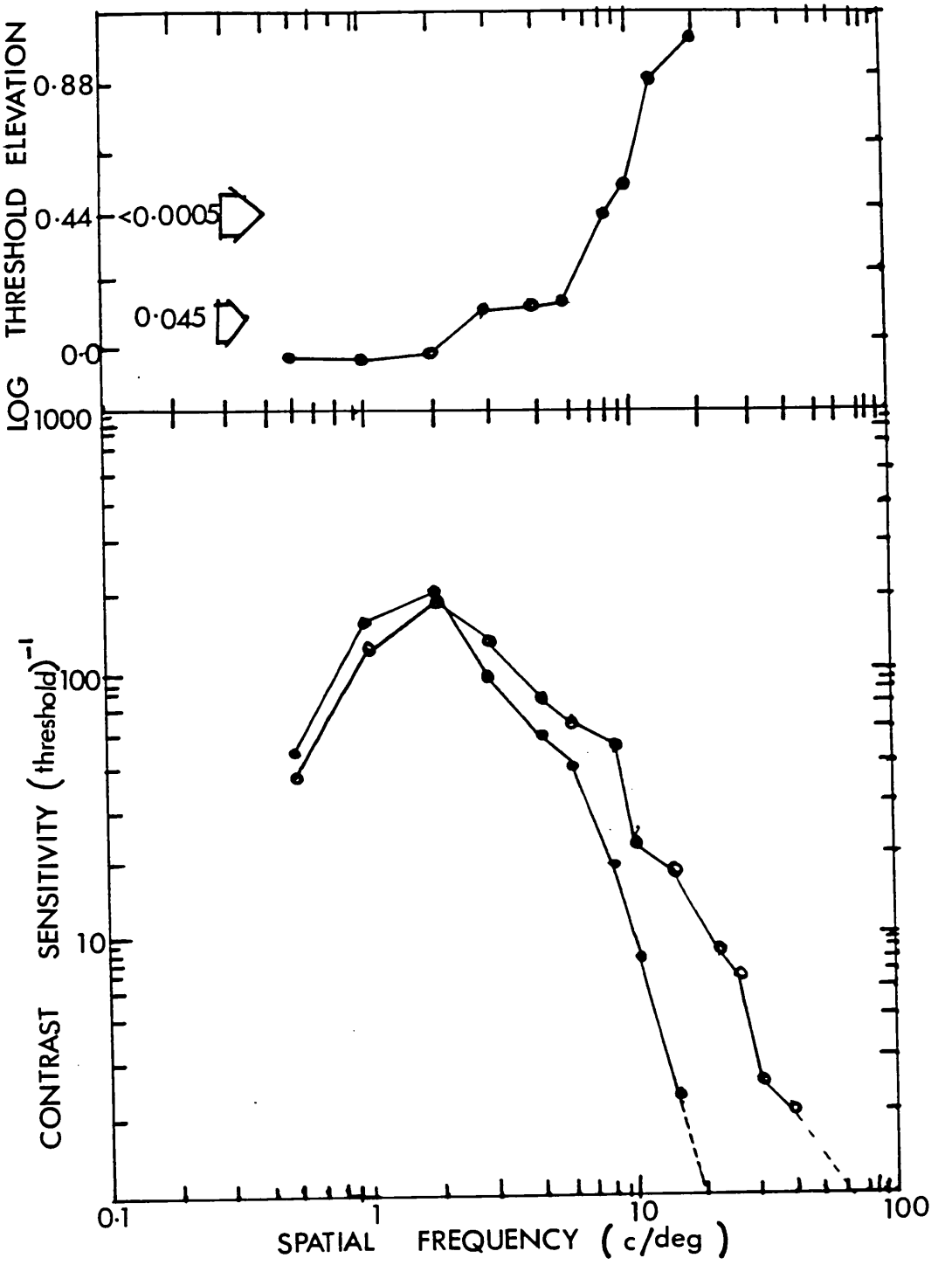

Fig. 3.13 The contrast sensitivity results for subject K.S. are plotted as contrast sensitivity, which is the reciprocal of the contrast threshold (log scale) against spatial frequency in cycles per degree (log scale). Contrast is defined as (Lmax - Lmin)/(Lmax + Lmin) where Lmax and Lmin are the maximum and minimum luminances of the light and dark bars respectively. In the lower, the "normal" eyes response (open circles) is compared with the fellow amblyopic eye's response (closed circles) at each spatial frequency. The departure of the normal from the amblyopic response is plotted in the upper figure as log threshold elevation with probability levels indicated. This subject had abnormal contrast sensitivity for only high spatial frequencies. (After Hess & Howell, 1977).

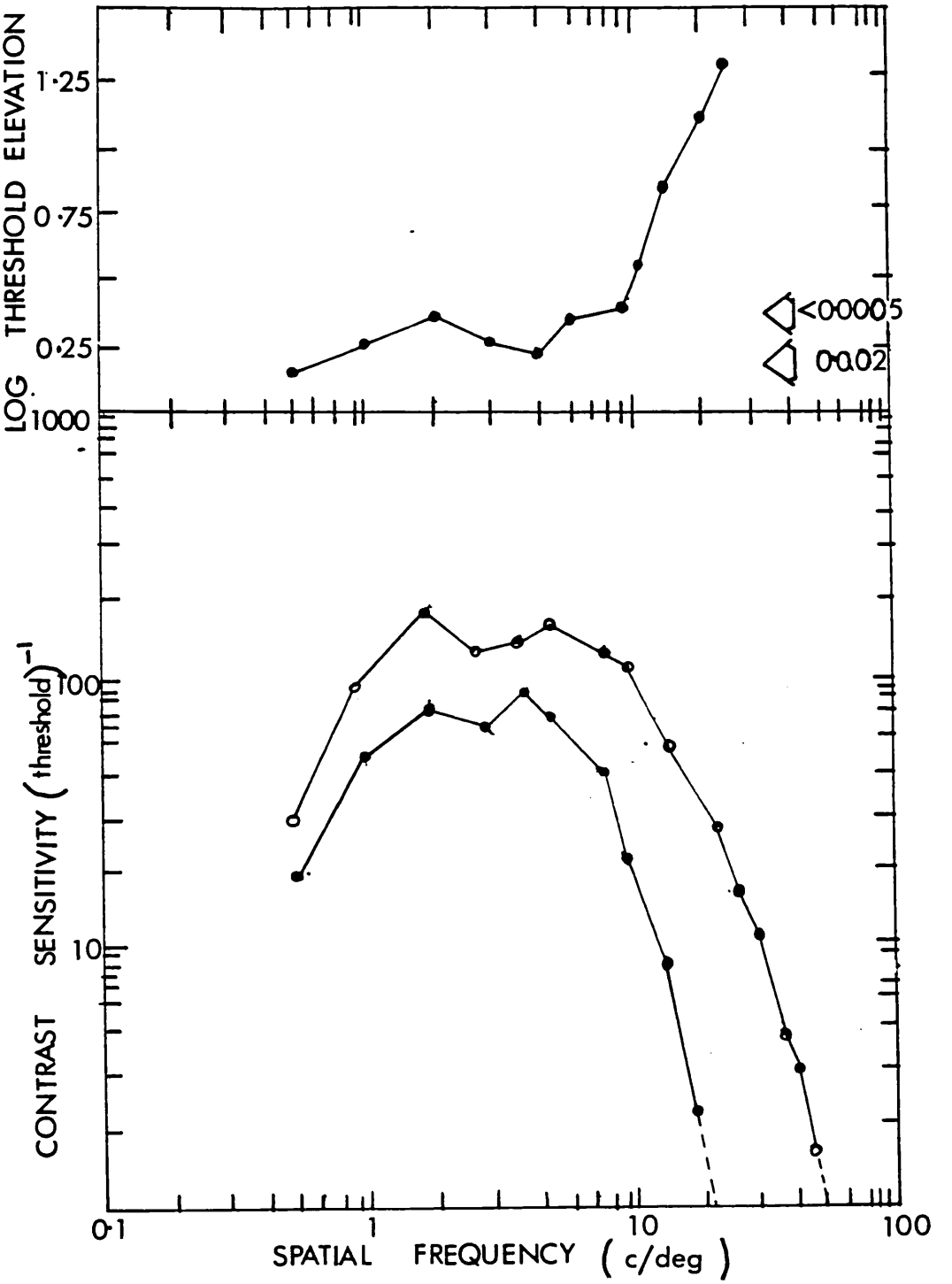

Fig. 3.14 The contrast sensitivity result for subject (J.L) are plotted as described for Fig. 3·13 When the "normal" eye's response (open circles) is compared with the amblyopic eye's response (closed circles), at each spatial frequency (lower circles), the contrast sensitivity abnormality is seen to affect all spatial frequencies tested. The upper curve (log threshold elevation curve) which represents the departure of the normal from the amblyopic eye's response shows the form of the abnormality with probability levels indicated. (After Hess & Howell, 1977).

Patient	Sex/ Age	Cycloplegic Refraction (5mm at Pupil)	Snellen Acuity ($30cd/m^2$)	Psychometric L and C Acuity ($30cd/m^2$)	Monocular Fixation (deg)	Angle and Type of Duration (6m photography) (deg)	Age First Noticed	Details of Amblyopia/ Strabismic (therapy)
High frequency only less class								
P.M.	F 22	$RO\frac{+.75D}{-.75}x20$	$R^{6}/_{9}$	$R^{6}/_{8.3}$	R Central	2R.exotropia	9 yrs.	Decreased vision in R.F. detected at age 9 years. R_x worn until age 12. Squint detected at age 16. No therapy undertaken.
		$LO\frac{+.50D}{-0.50}x20$	$L^{6}/_{5}$	$L^{6}/_{6}$	L Central			
K.S.	F 18	$R1\frac{-.25D}{-.00}$	$R^{6}/_{21}$	$R^{6}/_{8.9}$	R 1.8^{o}	4R.esotropia	5 yrs.	Total direct occlusion at $5\frac{1}{2}$ yrs. for 2 6-week periods. Therapy discontinued at age 6 yrs.
		$L\frac{-1.00}{-0.50}x70$	$L^{6}/_{5}$	$L^{6}/_{5.4}$	L Central			
S.W.	F 17	$R1\frac{+.00D}{}$	$R^{6}/_{7.5}$	$R^{6}/_{6.4}$	R Central	3L.esotropia	3 yrs.	Total direct occlusion at 3 yrs. for 1 yr. followed by R_x worn with one lens for 2 yrs. Minimal improvement.
		$L3\frac{+.50D}{}$	$L^{6}/_{1.5}$	$L^{6}/_{10.4}$	L 1.3^{o}			
P.C.	F 35	$RO\frac{+.75D}{-.50}x25$	$R^{6}/_{9}$	$R^{6}/_{6.1}$	R Central	6R.exotropia	6 yrs.	R_x worn from age 6-13 yrs. No other treatment.
		$L+0.75D\frac{}{-0.50}x140$	$L^{6}/_{4.3}$	$L^{6}/$	L Central			
A.S.	M 25	$RO\frac{+.25D}{-.25}x105$	$R^{6}/_{21}$	$R^{6}/_{10.1}$	R 0.86^{o}	4R.esotropia	7 yrs.	exercises and total direct occlusion for 2 yrs. Therapy discontinued at age 12 yrs.
		$LO\frac{+.50D}{-.75}x30$	$L^{6}/_{6}$	$L^{6}/_{6.4}$	L Central			
Low and High less class								
J.L.	F 24	$RO\frac{+.75D}{}$	$R^{6}/_{4.5}$	$R^{6}/_{4.5}$	R Central	3R.exotropia	18 Months	Large exotropia - total occlusion at age 2 yrs. for 6 months. Squint op. at age 5 yrs. followed by occlusion, etc.
		$L+0.75D\frac{}{-0.25}x140$	$L^{6}/_{30}$	$L^{6}/_{15.5}$	L 2.5^{o}	3L.hypertropia		
J.P.	F 23	$R6\frac{-.00D}{-.50}x135$	$R^{6}/_{5}$	$R^{6}/_{6.6}$	R Central	11L.exotropia	7 yrs.	Unilateral blur. Age 11 yrs. Squint op. No other therapy.
		$L19\frac{-.00D}{}$	$L^{6}/_{90}$	$L^{6}/_{76.2}$	L 2.6^{o}			
C.N.	F 23	$RO\frac{+.25D}{-.50}x20$	$R^{6}/_{15}$	$R^{6}/_{7.5}$	R Central	4R.exotropia	3 yrs.	Total direct occlusion at age 3 yrs. for 6 to 8 months. At age 10 yrs. 5^{o} esotropia with $^{6}/_{15}$ till age 12 yrs.
		$L\frac{plano}{-0.59}x100$	$L^{6}/_{4.5}$	$L^{6}/_{4.3}$	L Central			
S.C.	F 23	$R4\frac{+.75D}{-0.75}x115$	$R^{6}/_{5}$	$R^{6}/_{4.4}$	R Central	21L.esotropia	9 Months	Squint op. at age 1 yr. R_x worn for 4 yrs. Occlusion for 3 weeks at age 8 yrs. etc.
		$L+6.50D\frac{}{-1.50}x170$	$L^{6}/_{84}$	$L^{6}/_{39.9}$	L 3^{o}			
H.A.	F 24	$R2\frac{+.50D}{-0\ \ 0}x40$	$R^{6}/_{5}$	$R^{6}/_{4.1}$	R Central	5L.exotropia	3 yrs.	Amblyopia detected at age 3 yrs. No thera) or etc.

Table 3.1

this subject we find an anisometropia of around 12 diopters. Although it is not impossible for one eye to develop this difference in refraction, it is unlikely and it is more probable that this level of anisometropia was always present, but was not appreciated by the subject until the age of 7 years. If this is indeed the case, then the squint is probably not the primary effect but secondary to a refractive amblyopia, a view which is supported by the fact that the squint is divergent.

In a series of experiments involving contrast sensitivity, Hess and Howell and Hess et al, 1978 found the following. When contrast sensitivity is measured for sine-wave profile gratings as a function of the length and number of bars, they found that an effect on the thresholds only occurred when the resultant height or width was less than a size which was equivalent to ten periods of the grating at all spatial frequencies. This suggests the presence of a functional summation of responses for detecting elements at threshold over an area, the size of which is reciprocally related to the spatial frequency.

In their third paper, they checked the luminance dependent nature of strabismic amblyopia. A clinical test known as the 2 neutral density check has been used in the past to quickly distinguish strabismic amblyopia from other forms. When a 2 ND filter is placed in front of an amblyopic eye, Snellen acuity will stay the same or improve in strabismic amblyopia, while in refractive amblyopia and in normal eyes,

the acuity will generally drop by about 2 lines. When contrast sensitivity is checked under progressively lower background luminances, it is found that in strabismic subjects there is a point at which responses become normal under mesopic or scotopic conditions (normalisation) and this point is frequency dependent, see Fig. 3.15. They postulate three possible explanations for the luminance - dependent nature of amblyopia. Firstly, the amblyopic abnormality may be pre-ganglionic and involve only cone-disfunction. Secondly, the results may be explained in terms of a visual loss centred in the fovea, having greater effect on the central cone-only projection as compared with the extrafoveal rod-cone projections; thirdly, amblyopic detectors may themselves exhibit a luminance-dependent saturation effect at photopic levels. In Fig.3.15,the results of two subjects are shown, one who has an overall sensitivity loss for all spatial frequencies, the other having only a sensitivity loss at high spatial frequencies. It is note-worthy that the "normalisation" occurs at higher illumination levels in the subject K.S. who has a high frequency loss only, than in subject S.C. who has an overall sensitivity loss at all frequencies. The VA of K.S.'s amblyopic eye is $\frac{6}{21}$ and eccentric fixation was reported as being 1.8°, while S.C.'s VA is $\frac{6}{84}$ with an eccentric fixation of 3°, the other main difference between the two subjects is age of onset of squint being 5 years in the case of K.S. and 9 months for S.C. As "normalisation" only occurs in strabismic amblyopes and eccentric fixation occurs in strabismic amblyopia, then perhaps the level of eccentric fixations is responsible for the luminance dependence of the "normalisation" point.

Hess, Campbell and Zimmerman (1980) found that the "normalisation" observed in strabismic amblyopia does not occur in anisometropic amblyopia. They hypothesised that in normal vision, reduction of luminance biases detection progressively towards more peripheral receptors, thus normal and amblyopic responses should converge. They measured contrast sensitivity functions in a normal eye with an artificial central scotoma and found that a similar "normalisation" occurs under reduced background luminance. Consequently, it was proposed that the visual abnormalities in strabismic amblyopia are largely restricted to the central visual field. Thus, anisometropia amblyopia seems consistent with the notion of deprivation due to restricted input, while strabismic amblyopia with its visual field specificity must involve a different process.

Hess and Bradley (1980) showed that the threshold deficits measured in amblyopia are not related to what happens above threshold. They found no contrast coding abnormality in strabismic amblyopia at the high-contrast range which is typical of everyday vision. Hess (1980) studied the contrast threshold elevation effect (Gilinsky 1968; Pantle and Sekuler, 1968, and Blakemore and Campbell, (1969)) in amblyopia. Subjects were adapted to a grating of fixed spatial frequency and the induced threshold elevation effect for a number of gratings of different spatial frequencies was measured. After adaptation to an equal number of log units above the individual (each eye) contrast threshold, he found similar size selective channels

in both the amblyopic and normal eyes.

Hess, Burr and Campbell (1980) examined frequency discrimination tests, and found that normal eyes can discriminate differences in spatial frequency to within 2-5%. Such fine discrimination requires co-operation between a number of size channels. Amblyopes are able to discriminate normally for low spatial frequencies but abnormally for higher spatial frequencies. Hess and Campbell (1980) found that spatial summation of sinusoidal gratings was normal in amblyopes and they infer from this that the number of detectors contributing at any one spatial frequency is normal. As a result of the afore-mentioned studies, Hess et al (1980) concluded that size-selective channels exhibit normal spatial bandwidths, and normal spatial summation at threshold. There are, however, abnormalities in the ability to make size judgements in the abnormal frequency regions. They suggest that this could result from a reduction in the co-operative activity of the channels within this range, rather than from a decrease in sensitivity of individual detectors.

Hess, Howell and Kitchin (1978) checked the temporal properties of pattern and movement thresholds in amblyopia. They find that "movement" is not abnormal in amblyopia, see Fig. 3.16, while "form" vision is. They argue that in order for an amblyope to have a form abnormality without a movement abnormality for the same low spatial frequency grating requires normal pre-ganglionic retinal function, and they conclude that

this result provides evidence for a ganglionic or post-ganglionic site of strabismic amblyopia.

Levi et al (1979) have shown that humans deprived of normal binocular vision have binocular interactions tuned to both size and orientation. These subjects deprived of binocular vision did, however, show a failure of binocular summation at threshold or sub-threshold contrast levels. In contrast, strabismic and refractive amblyopia disrupted the normal excitatory interactions between the two eyes but cortical inhibitory binocular connections seem not to have been disrupted.

Fig. 3.15 The effect of luminance on contrast sensitivity for normal (o) and the fellow eye (●) of amblyope K.S. The retinal illumination is indicated to the left of each function. The average standard error for both eyes was equal to less than a symbol size. This amblyope has only high frequency photopic contrast sensitivity abnormality.

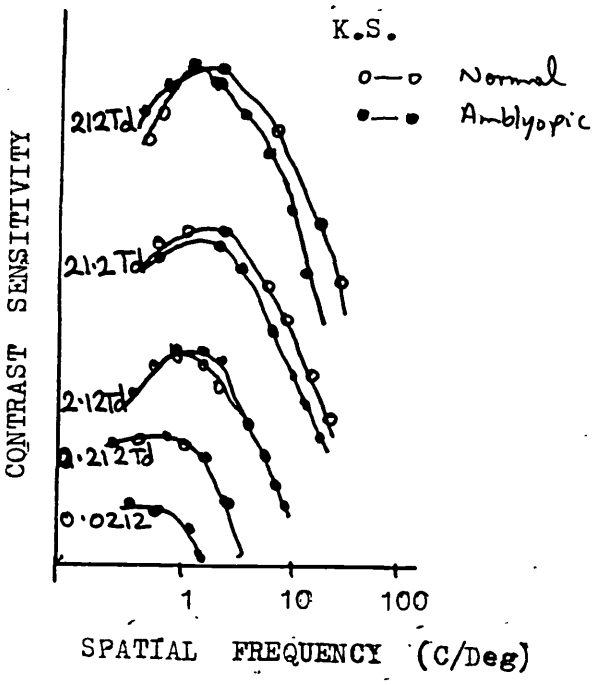

The lower graph shows the results of amblyope S.C. with (o) normal eye and (●) the amblyopic eye. Retinal luminance is again indicated to the left of each function while standard error was equal to less than the symbol size for both eyes. This amblyope has a low as well as high frequency photopic abnormality. (After Hess and Howell, 1978).

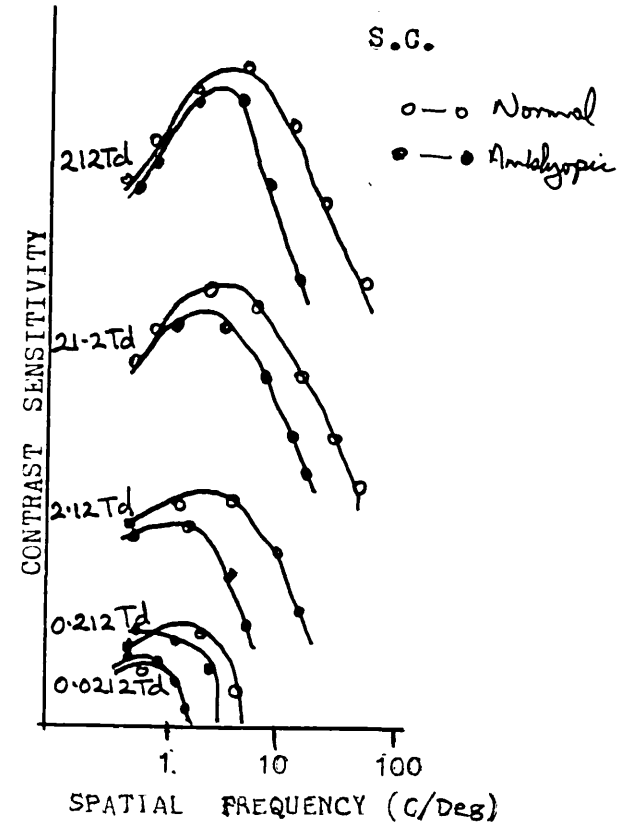

3.3 Summary

The research of Ikeda and co-workers has shown that in amblyopic cats a deficit in the X-cell system in the L.G.N. and retinal ganglion cells is observed, while the transient Y-cell system is only very minimally affected. Ikeda and Tremain (1977) suggest that the cause of amblyopia is retinal while binocular loss is central, as agreed by others (Hubel and Wiesel, 1965; Baker et al, 1974; Blakemore and Van Sluyters, 1974; Gordon and Gummows, 1975; Yinon et al, 1976; Van Noorden, 1974). They therefore suggest that unwanted inputs from the squinting eye are suppressed to prevent diplopia, Plasticity is therefore necessary in the synaptic organisation of the brain.

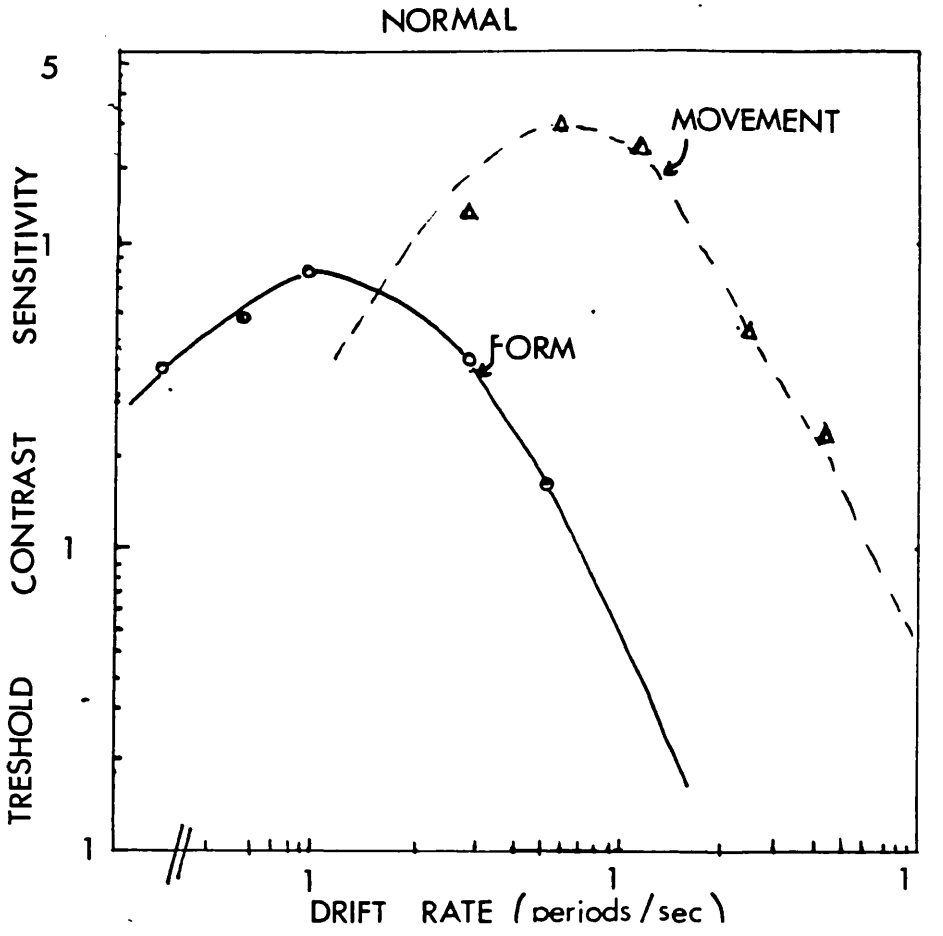

Fig. 3.16a) Temporal properties for form (O) and movement (△) thresholds for normal observer EHH. At the movement thresholds only movement was perceived. The spatial frequency was 0.2c/deg, (After Hess et al, 1978)

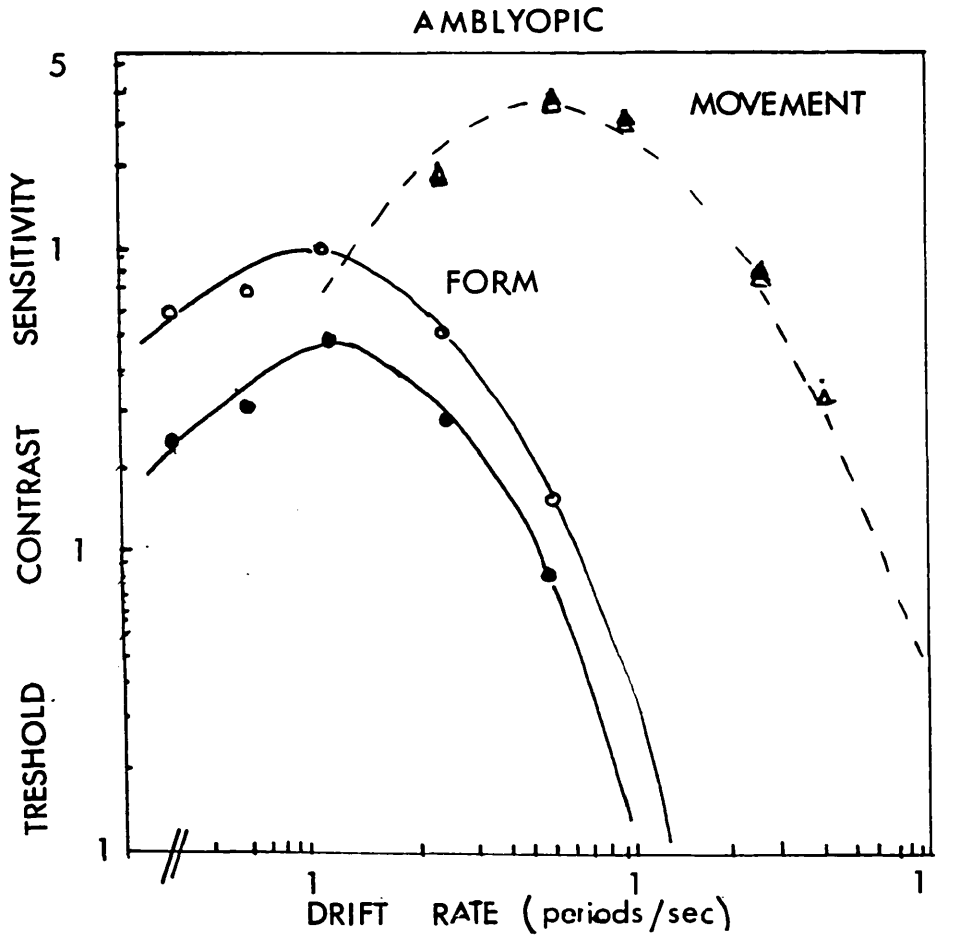

Fig. 3.16b) Temporal properties for form (0,0) and movement (Δ,Δ) thresholds for the normal (0,Δ) and amblyopic (0,Δ) eye of amblyope J.L. has a low as well as high frequency form abnormality. (After Hess, Howell and Kitchin, 1978).

Chapter Four Details of the Equipment, General Techniques for Data Collection and the Clinical Data of the Subjects of this Study.

The equipment used for the experiments reported later, was originally designed and built by Dr. J.L. Barbur (1980) and modifications to the basic instrumentation were subsequently made by Dr. I.E. Holliday (1982).

4.1 Description of the equipment (Fig. 4.1)

The instrument to be described has a four-channel Maxwellian view optical system designed for psychophysical studies of movement perception. The light source was a Quartz Halogen 100W/12V lamp (Atlas, 12V A1/45) driven by a Roband (Model 67-1019/12V) stabilised power supply. The lamp was positioned by moving the mount vertically and/or transversely on the optic axis of the instrument. Emmitted light was collimated by achromatic doublet lenses (L_1) forming two beams. Beam 1 passed first through a neutral density filter holder (ND1) proceeding through a logarithmic neutral density wedge (W1) and then through a mechanical slide (OP1). The test transparency was mounted in this slide carrier and driven laterally across the back focal plane of the lens (L_2) by a d.c. servo motor, giving constant speed in the range 0.1deg/sec. to 100deg./sec. The beam then passed through a series of beam-splitters and multi-element lenses (TAKUMAR) culminating with a 50mm f1.2 Pentax Camera lens (L_3). An image of area 1.5mm x 0.75mm of the source was produced in the exit pupil, which was adjusted to fall in the observer's pupil plane, an arrangement known as the Maxwellian viewing condition. The second beam was directed by a front silvered mirror and passed through a glass plate (GP); half of the light continued as beam 2, the other half forming beam 3, which provided a uniform field of up to 48° diameter

Beam 2 passed through a glass plate (GP) half of the light passing straight through and continuing as Beam 2, the deflected half having formed Beam 3. Beam 2 passed, after deflection by a mirror (M), through a neutral density wedge (W_2), positioned by a second d.c. servo motor (dc_2), then through a second neutral density filter (ND_2) and continued to provide a 17.5° background field. Beam 3 passed through a neutral density filter holder (ND_3) providing yet another 17.5° background field. This beam was used in some experiments to provide a fixation spot, in this case a red filter and a small hole were placed in (ND_3). Beams 2 and 3 were deflected by 90° by mirrors M_3 and M_4 respectively. Beam 2 then passed through object plane (OP_2) and on to the beam splitter (BS_1), while Beam 3 passed through object plane (OP_3) and then proceded to beam splitter (BS_2). Both beams 2 and 3 then recombined with Beam 1, the target beam, which proceded through a system of lenses to the exit pupil. The eye piece consisted of a 3.5mm artificial pupil in a hollow cylinder which had an eyecap fitted both to aid observer comfort and to minimise stray light.

The observer used a dental bite made from stents thermoplastic mounted on an aluminium blank. This was fixed to a rigid clamp which is adjusted for height, lateral movement and distance from the eye piece.

Three neutral density Wratten filters (NDF) provide coarse adjustment of the illumination level of beams 1 and 2.

Fine adjustment was achieved with the logarithmic attenuators (W_1 and W_2). These wedges were mounted in a vertical slider/frame arrangement similar to that of the target carrier OP_1, to be discussed later. W_2 was driven by a servo motor (Electrocraft S-586-5A) fitted with a 30:1 gearbox (McLennan Engineering AM5020). A precision 10 turn potentiometer supplied the command voltage which caused rotation of the shaft. This was connected by a string and pulley system to the slider, thus providing vertical movement. A second 10 turn potentiometer, driven by a rack and pinion system which was fixed to the frame, gave a slave signal to the servo-control unit. This signal was compared to the command signal and appropriate shaft rotation returns the slider to the null position. Limit switches placed at the extremes of travel of the slider prevented overrun. The driving motor of the test wedge (W_1) was controlled by the subject, by rotation of a wheel and in this way threshold settings, were achieved.

In the object plane of the target beam (OP_1) transparencies produced by high contrast graphic arts film (Kodalith Ortho Film, Type 3) were placed in the carrier and the transparency was mounted in twin glass slides which are fixed on the slider. The visual angle through which the target movement can be observed was controlled by a mask placed in front of the carrier. The carrier allows a lateral movement of 20cm and was driven via a rack and pinion system powered by an electric d.c. servo motor (Electrocraft 586-5A) fitted with a 30:1 gearbox (McLennan Engineering, AM5020). The motor-carrier combination produces smooth, quiet movement with speeds

stabilised to 1% in the range 0.1 to 100 deg/sec. by a tacho feedback mechanism. The speed was controlled by a voltage, provided by a converter, whose input was derived from the setting of three BCD (binary coded decimal) switches. The output was inverted and either polarity applied to the command line of the servo-motor, by a 2-pole toggle analoque switch grating DG201. Limiting switches were placed at the extremes of the slider travel to prevent overrun. The design of the controller/motor combination was such as to allow start/stop times of about 40mSec. at full speed. The rotation of the motor and, therefore, the direction of the test object, was controlled by the polarity of the command voltage. The toggle switch was controlled by the observer and thus target movement and direction were controlled. In order to allow temporal modulation of one beam, an analysing polaroid disc was placed perpendicular to the beam in front of a rotating polaroid disc. The rotating disc received motion via a third d.c. servo-motor (Electrocraft S-586-5A). Command voltages were supplied from a precision 10-turn potentiometer. Tacho-feedback provided stabilised rotation for a frequency range of 0.05 to 100Hz.

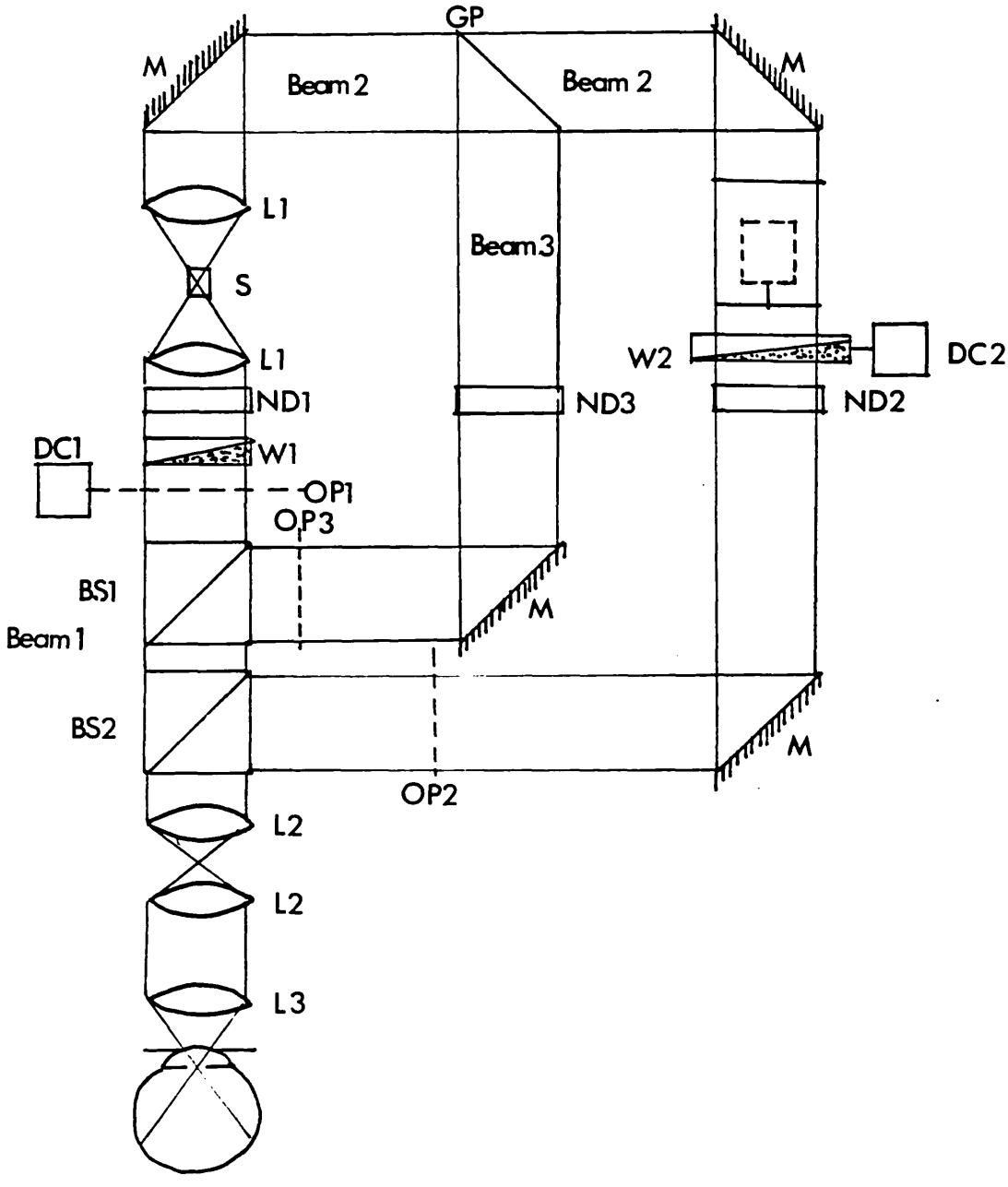

Fig. 4.1 Plan of the Maxwellian view optical system used for all the experiments discussed later. A detailed description of this equipment appears in the text.

4.1.1. Calibration and Measurement Techniques

Experimental data were initially gathered by a purpose-built 8-channel data logging system (Barbur and Nunn, 1978). All parameters were simultaneously recorded on paper tape, and were later analysed by a computer. A minicomputer has recently replaced the previous system for data aqcuisition and analysis. This has extensive facilities for input and output of analogue and digital signals which were under program control (Analog Devices, MACSYM II). Multi-turn potentiometers were coupled to the different sliders, carrying targets, and logarithmic attenuators (W_1, W_2). Calibration of the attenuators in terms of their potentiometer voltages was used in the program to compute the illumination levels of the different beams. The target speed was set by BCD switches whose output was recorded directly. When the observer depressed a button to signal the completion of a set of results, the data was recorded on the tape.

4.1.2. Calibration of Neutral Density Attenuators (Figs. 4.2 and 4.3)

The wedges were calibrated in white light and for spectral bands isolated by insertion of Balzer B40 interference filters into the appropriate beams in front of the wedges. A Macam 3010 radiometer/photometer was used to measure the light flux at the exit pupil. The position of the wedges was translated as voltages by precision potentiometers. The radiometer was checked over a range of 5 log units and found to be linear to within 3% in comparison with a photomultiplier (EMI, Model 9558) which sampled the same beam via a beam splitter.

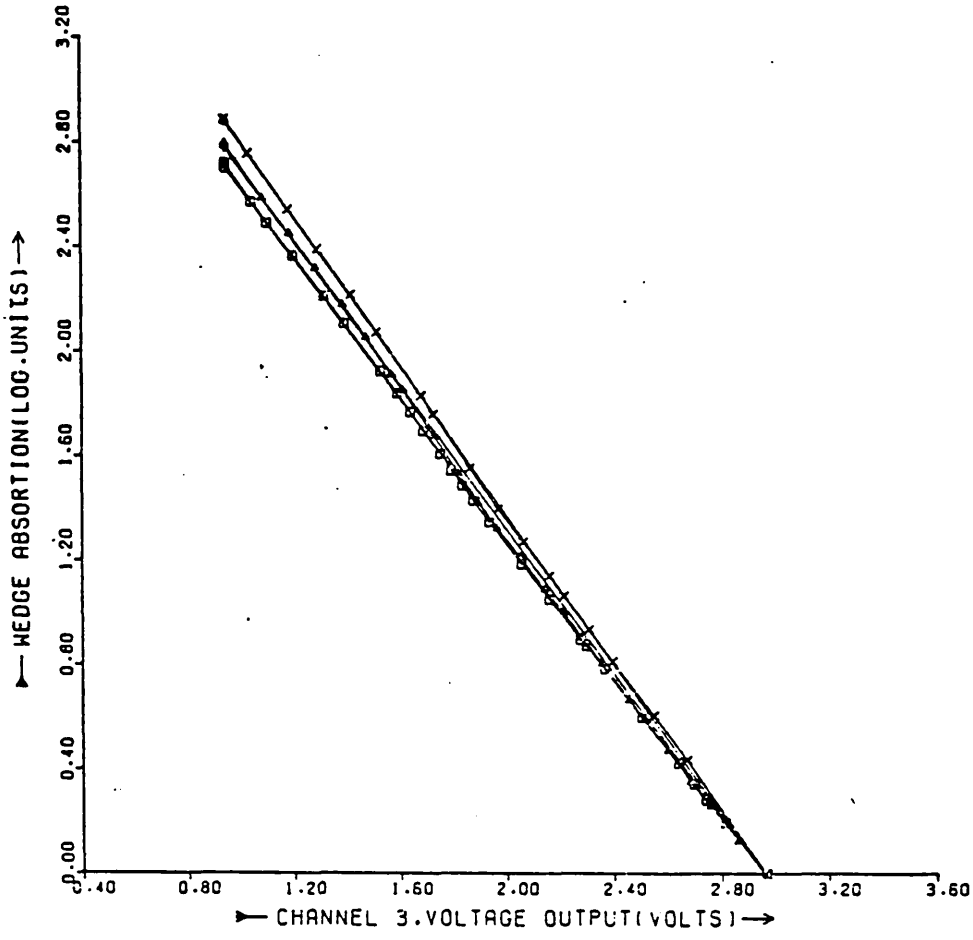

Fig. 4.2 Calibration curves for the logarithmic attenuator in beam 1. (W_1. fig. 4.1). Absorption is plotted as a function of transducer output voltage for three stimulus wavelengths: 512nm (triangles), 446nm (crosses) and 611nm (squares). A least squares line is fitted to each set of data.

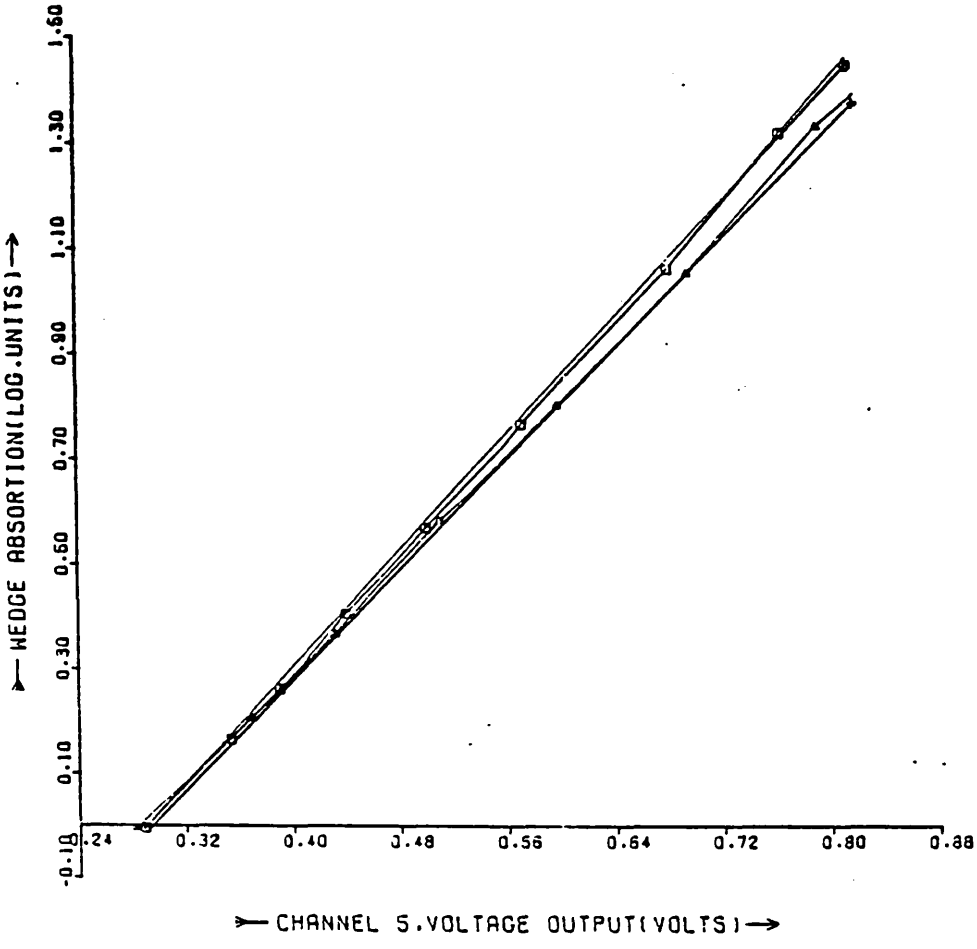

Fig. 4.3 Absorption of wedge W_2 is plotted against transducer output voltage for stimulus wavelengths of 446nm (squares), 512nm (crosses), and 611nm (triangles). The data are fitted by least squares lines.

4.1.3. Calibration of the Temporal Modulation Frequency

Polaroid rotation produced temporal modulation of Beam 3. When the rotation frequency was below 2Hz a cardboard sector disc with 180° gap was fixed on the motor axis. Rotation of this disc interrupted light falling on a light activated switch, then registered on a timer. By starting and stopping the motor in the dark phase of the cycle, the duration of the cycle was measured accurately. When the speed was between 2Hz and 5Hz the sector rotated continually, with the timing triggering a pulse. These pulses were counted and by measuring the accumulated time the angular speed was calculated. For speeds in excess of 5Hz, an oscilloscope was used to display the voltage waveform produced. The oscilloscope timebase was compared with the digitimer generated waveform in order to calibrate it. See Fig 4.4.

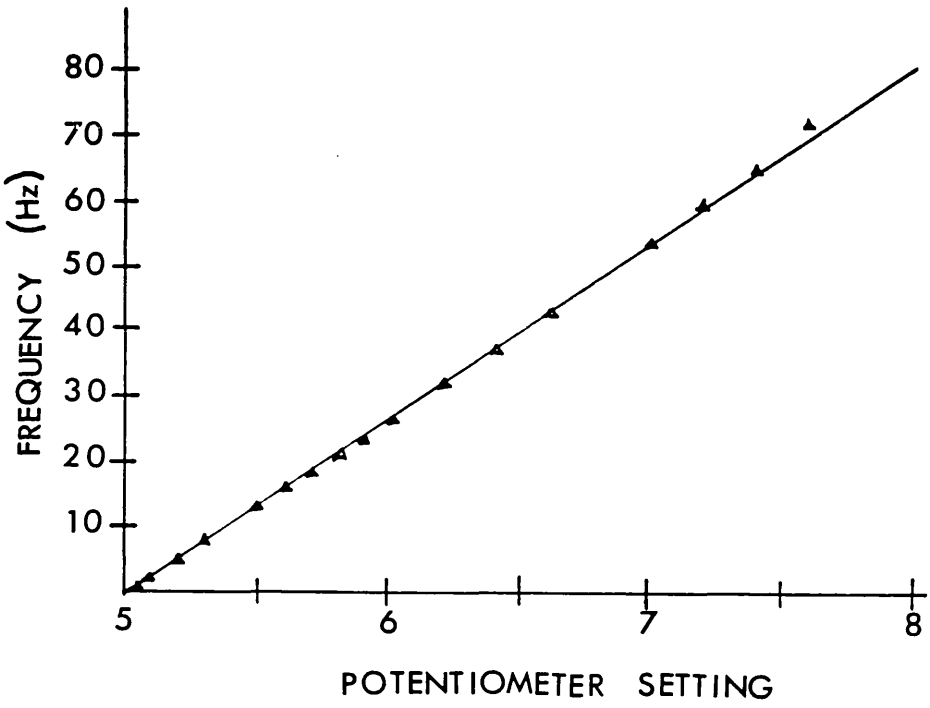

Fig. 4.4 Calibration of polaroid rotation. The modulation frequency of light transmitted by the polariser/rotating analyser combined in Beam 3 is plotted against the potentiometer setting the motor drive voltage. Triangles represent data points, which are fitted by a least squares line.

4.1.4. Calibration of Transmission Through the Polaroid

The polaroid was calibrated for transmission against angle of rotation by measuring the transmitted light level with the Macam 3010 photometer, the angle of the polaroid setting being denoted by a pointer moving over a radial scale. The transmission deviated by less than 1.5% from the expected $\cos^2$ distribution

4.1.5. Calibration of the Target Slider Speed

The calibration method was similar to that used for angular speed calibration; light emitted by L.E.D. was directed towards a light activated switch and was interrupted by a dark bar on a transparency fixed in the target slider. The length of this bar was accurately measured by a travelling microscope. By measuring the time for which the L.E.D. beam was interrupted, the traverse time was calculated to an accuracy of 1msec. Different speeds were selected from the available range by setting three B.C.D. switches. The calibration data are fitted in two parts to give increased accuracy in the lower speed range (see Figs. 4.5. and 4.6.). The lower calibration was used for target speeds of less than 3.5°/sec. Calibration of the slider was performed on several occasions and the accuracy of the fit of the least squares approximation line to that data was better than 3 per cent.

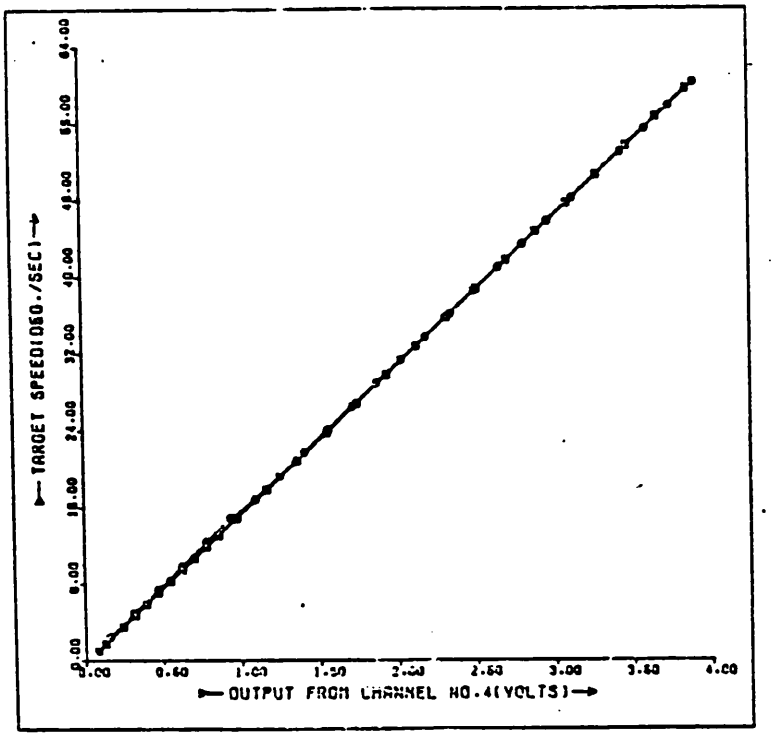

Fig. 4.5. Target speed in deg/sec. is plotted against the motor drive voltage with a least squares line drawn through the data.

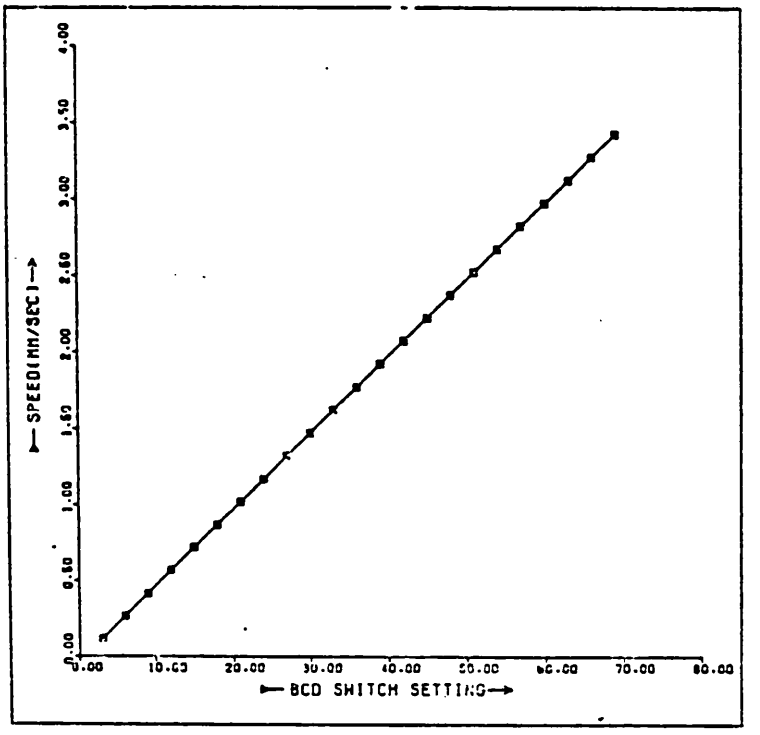

Fig. 4.6. For target speeds below 3.5deg/sec. the speed calibration was separately fitted. Here target speed is plotted against the B.C.D. switch setting.

4.1.6. Square-Wave Grating Targets

These were produced by standard photographic techniques on Kodak "Kodalith Orthofilm". This film gives high density where exposed and almost zero density elsewhere. The transmission ratio between dark/light bars was approximately 4 log units. Square-wave gratings of various spatial frequencies were produced by this method.

4.2. Details of Stimulus Configuration used in the Different Experiments

In all experiments threshold settings were made for a white circular target moving at 15°/Sec. Each of the three classes of response to be discussed in this thesis were obtained for target movement against a particular class of background field and these will now be discussed in detail. Before doing this I describe the principle of the threshold perturbation technique.

4.2.1. The Threshold Perturbation Technique

This is based on the hypothesis that the response of a psychophysical mechanism to a particular stimulus parameter can be studied by superimposing a constant test stimulus upon a background stimulus, and obtaining the threshold for detecting the test as a function of the background field parameter of interest. Its success is dependent upon choosing the correct background and target stimuli so the mechanism of interest can be isolated, otherwise intrusion of other mechanisms will occur. In order to make the correct choice, a parametric study was undertaken for a series of target sizes and speeds and

background illumination and contrast, (Holliday, 1982). The choice of stimulus parameters for the work presented in this thesis was based on the results of that study.

4.2.2. General Experimental Design and Execution

The subject was seated comfortably in an adjustable chair & a dental bite for each subject was mounted on an aluminium blank which was secured to a three-dimensional carriage at the exist pupil of the instrument. By suitable adjustment of the carriage for height and lateral positioning the subject's eye pupil could be lined up with the optical axis of the equipment. The mouthpiece could then be moved backwards and forwards so that the pupil was filled with the illumination from the equipment light source. The visual fields in each of the experiments consisted of two components; the background field and the target or test field. Gratings of different spatial frequencies were placed in OP_2 in Beam 2, to provide the spatially structured component of the background field and focus for each subject was achieved by a backwards or forwards movement of OP_2, (see Fig. 4.1). Beam 3 provided a uniform circular background field of diameter 17.5deg. and was uniform spatially for two out of the three experiments & Beam 2 and Beam 3 were combined to give the full background stimulus. The mean background illumination of Beam 2 and Beam 3 were adjusted prior to a recording session to the required level (usually 1.4 log trolands) by means of neutral density filters. The target consisted of a single circular spot, and in most of the experiments to be described, it was of diameter 3.5 deg. and moved at 15 deg. sec^{-1} along the horizontal meridian. A mask was placed within the

carrier OP_1 which restricted the visibility of the target to the central 8° of the 17.5 deg. background field (see Fig. 4.7 for a general view of the visual function). The subject had manual control of the neutral density wedge W_1 and by rotating a wheel controlling a pulley mechanism, threshold settings for each grating could be taken. The subject also controlled the movement of the carrier with the target and by operating a rocker switch, the direction of the movement could be reversed, hence the target was moved laterally from side-to-side and the subject gradually reduced its illumination by setting the wedge until the target was just no longer detected. The subject then pressed a button and the computer recorded the neutral density and wedge position. The wedge was then reset to give a suprathreshold illumination level and the measurement was repeated five times for each background and the computer worked out the average and standard error of each data point, which were printed out. These averaged threshold illumination levels I_t were plotted as a function of the background field parameter which formed the measurement parameter (see Section 4.2.3. below).

For non-foveal presentation the subject was asked to fixate a red spot which was provided by Beam 3 as described in Section 4.1 of this chapter & this spot was placed in a suitable position to give the desired eccentricity for measurement.

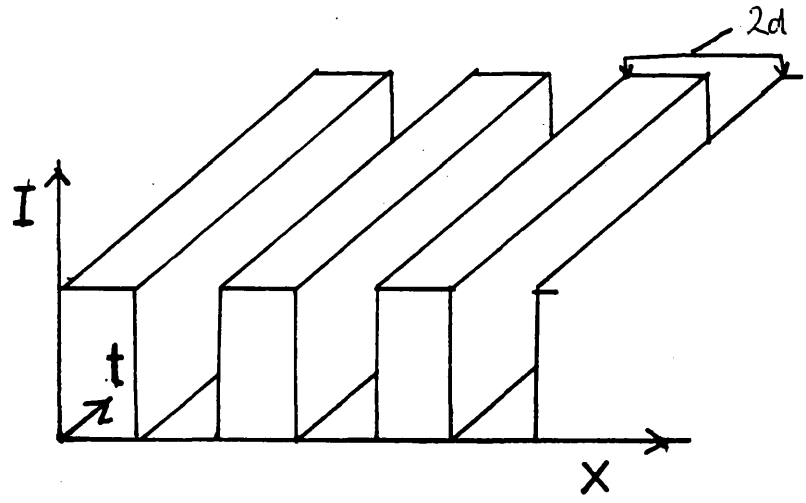

Fig. 4.7. Here is shown the spatio-temporal stimulus used to elicit the Type 1 response. It consists of a square-waveform grating superimposed on a uniform background field with the same mean luminance.

4.2.3. The Background Fields Used in Each Experiment

Several different background field configurations were used in the experiments and these will now be discussed.

4.2.3.1. Simple Spatial Modulation for Measurement of the ST1 Spatial Response

This was the background field used by Barbur and Ruddock (1980) when investigating the spatial response of the ST1 filter. Square-wave gratings with bar width d (Fig. 4.7) giving a fundamental spatial frequency $f_s = (2d^{-1})$, were used. The gratings were produced by placing a high contrast negative into the object plane of Beam 2 & its contrast was controlled by superimposing the uniform field (Beam 3) on the grating field, (see Fig. 4.7.). Log threshold illumination, log I_t, for the detection of the target was measured as a function f_s.

4.2.3.2. Simple-Temporal Modulation (Fig. 4.8) for Measurement of the ST2 Temporal Response

A circular, spatially uniform background field of 17° diameter was temporally modulated by placing an analysing and a rotating polaroid in Beam 2. This beam was combined with a uniform field of 17° diameter (beam 3) in order to control the flicker modulation depth. If the modulated Beam 2 gives an output illumination

$$I = I_3(\cos^2\omega t)$$

and Beam 3 has uniform illumination I_2, then the modulation of the background is given by

$$M = \frac{I_{max}-I_{min}}{I_{max}+I_{min}} = \frac{I_3}{2I_2+I_3} \qquad (1)$$

and the average illumination of the background

$$I_b = I_2+\tfrac{1}{2}I_3 \qquad (2)$$

therefore, from (1), $M = \frac{I_3}{2I_b}$

$$= 1-\frac{I_2}{I_b}$$

The illumination levels of Beams 2 and 3 were controlled by suitable adjustment of the neutral density filters, and that of Beam 2 could also be varied continuously with the motorised wedge W_2. Therefore, the modulation M and the average illumination level could be set. Log threshold illumination, $\log I_t$, for detection of the circular target was measured as a function of f_s.

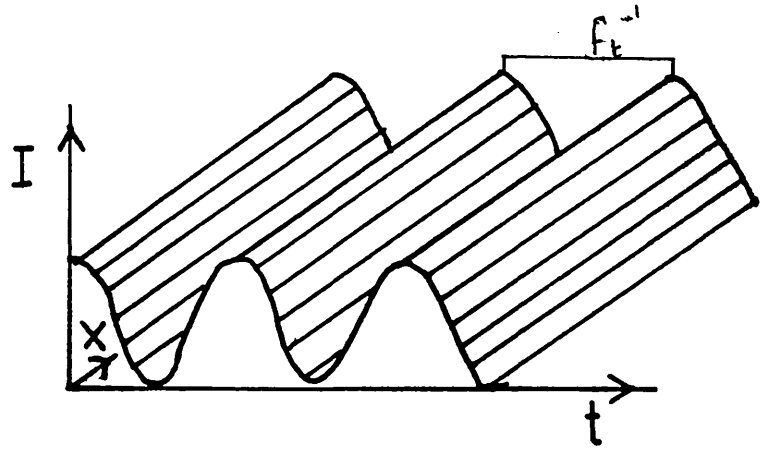

Fig. 4.8. The spatio-temporal stimulus used to elicit the ST2 type temporal response. The uniform field is modulated at different frequencies (Hz) by placing an analysing and a rotating polaroid in Beam 2.

4.2.3.3. Spatio-Temporally Modulated Background for Measurement of the ST2 Spatial Response

In this case, two identical square-waveform gratings, one located in Beam 2 and the other in Beam 3, were set to the same mean illumination and arranged in antiphase. One grating is sinusoidally modulated whilst the other remains unmodulated, giving the spatial and temporal distribution of illumination shown in Fig. 4.9. In order to achieve this, an analysing polaroid disc is placed in Beam 2, and this is then combined with the unmodulated grating in Beam 3. Both gratings were placed in the object planes OP_2 and OP_3 and the components of the background fields were adjusted to the same mean illumination by neutral density filters and the motorised wedge W_2 in Beam 2. The output of the instrument was monitored at the exit pupil with a Macam 3010 photometer.

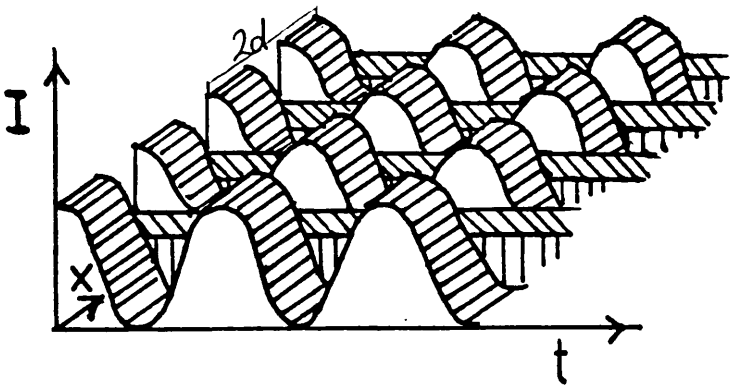

Fig. 4.9. The spatio-temporal stimulus used to elicit the ST2 type spatial response. Here two spatially identical gratings are used and positioned such that the dark bars of one grating appear in the light spaces of the other gratings. One grating is modulated, the other is unmodulated.

4.3. Factors which Influence the Type of Squint

Central mechanisms favouring the development of binocular vision are concerned with the act of fusion, which is a sensory phenomenon, and also with the cortical control of ocular movement which is a motor phenomenon. The visual image of an object is built up of two separate halves with the object divided vertically. a composite picture of the whole object is built up by the activity of the striate areas of both hemispheres of the visual cortex. The final analysis is implemented by the higher visual centres in the adjacent parastriate and peristriate areas. When fusion is unable to take place a breakdown in binocular vision occurs. The factor of age has an appreciable influence on the type of squint which may follow an upset in the AC/A (accommodative convergence versus accommodation) relationship. The significance of uncorrected hypermetropia becomes progressively less

after the early years of life because of the natural reduction in the amount of hypermetropia, resulting in a diminished need for accommodative effort. Conversely, the significance of uncorrected acquired myopia is seldom evident in the earlier part of life because, except in the relatively rare type of congenital or infantile myopia, it generally develops after fusion has occurred. The fusion reflexes acting as a barrier to the development of a divergent squint. Uncorrected astigmatism, particularly of myopic type, tends to result in a divergent squint either manifest or latent, due to lack of the normal exercise of the AC/A ratio.

Finally, anisometropia (that is a different refractive error of one eye relative to its fellow) can affect the accommodative-convergence/accommodative reflex. If the dominant eye has only a slight level of hypermetropia, the other eye tends to remain straight irrespective of its refractive error. If the dominant eye has a high degree of hypermetropia, the other eye will tend to converge irrespective of its own refractive error. When the dominant eye is myopic, the fellow eye will remain straight or may tend to diverge. If neither eye is dominant and one eye is favoured for distance and the other for near, divergence may occur because there is no use for the AC/A relationship. Anisometropia of a marked degree even when corrected, tends to favour the development of a squint in certain cases due to different retinal image sizes (aniseikonia) which prevents fusion despite two clear images. This inability to fuse the images often leads to a positive attempt to prevent fusion by deviation. Finally, a

squint is frequently congenital. There is a strong familial tendency for squints and this is probably due to an inheritance factor which acts as an obstacle to the development of binocular function. This may take the form of an abnormality of one or more extrinsic ocular muscles, but more commonly if an abnormally high refractive error, generally hypermetropia is present.

4.4. Clinical Data for the Amblyopic Subjects

Firstly, I review the techniques used to obtain the relevant clinical data. The visual acuity was assessed by a Snellen chart at six metres, and each eye was checked individually. Stereopsis was checked with the random dot stereograms of Julesz (1971). The amount of eccentric fixation was assessed with an ophthalmoscope with a macula fixation star. The observer was asked to look in the centre of the star and the foveal reflex displacement was assessed. (See Fig. 4.10). The Linksz star graticule is used with a green (red free) filter, the concentric circles subtending angles of 3° and 5° respectively. With this target, the presence of eccentric fixation and the degree of eccentricity may be determined quickly and accurately. The appropriate angle of squint was assessed visually by the cover test, but it should be noted that this value is that at the time of experiments and does not reflect the initial value, which may have been changed surgically. Unfortunately, hospitals are reluctant to reveal clinical details of patients so I do not have any information on V.A. immediately after treatment which might have been very

useful in the analysis of the results. The data on past history has therefore been gleaned from the subject's own knowledge and their parents' memory of what occurred and when, and has therefore to be considered as less than complete.

I shall start by considering the strabismic subjects followed by the refractive's and finally details will be given of an albino subject.

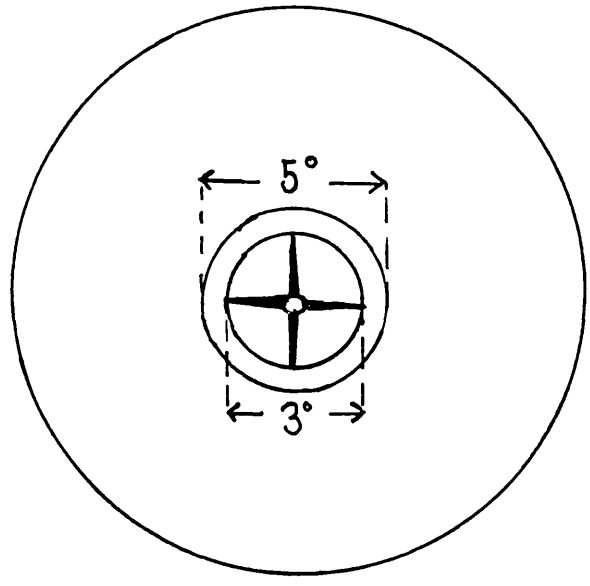

Fig. 4.10. The Linksz Star Graticule 1330E

This graticule is used with a projectoscope or suitable ophthalmoscope in conjunction with a green (red free) filter. The concentric circles subtend 3° and 5° from the centre of the star. By projecting the star on to the retina, and instructing the patient to look directly at the centre of the star, the position of the foveal reflex in relation to target can be assessed.

4.4.1. Strabismic Amblyopes

Observer S.B., a male aged 20, has a small divergent strabismus of approximately 5° which was not detected until his late teens. Consequently no treatment was attempted and as spectacles are not required for the normal eye, none were issued.

Snellen acuity at the time of the experiment was recorded as $\frac{6}{5}$ in his normal eye and $\frac{6}{9}$ in the amblyopic eye. Ophthalmoscopy showed no abnormality and no eccentric fixation was found with the Linksz star; stereopsis was not present with the Julesz (1971) stereograms.

Observer P.M., a male aged 24, has a small divergent strabismus of approximately 7°, detected at age 16 years. No treatment was attempted nor were spectacles prescribed. His VA is $\frac{6}{5}$ in the normal eye and $\frac{6}{24}$ in the amblyopic eye. No abnormality was found by ophthalmoscopy and eccentric fixation of approximately $\frac{1}{2}^{\circ}$ was shown with the Macula star. No stereopsis was present with the Julesz stereograms.

Observer N.C., a male aged 20, has a moderate convergent strabismus approximately 12°, which was first noticed at age 18 months. He was treated for many years orthoptically and received several long periods of patching. Ophthalmoscopy showed no fundal abnormality and eccentric fixation of some 2° was found. The VA of the normal eye was recorded as $\frac{6}{5}$ while that of the amblyopic eye was $\frac{6}{24}$; no stereopsis was found.

Observer G, a male in mid-fifties, has a large divergent strabismus of about 35° with a 5° hypertropia. The squint developed following a fall at age 9 months and no treatment was attempted. Ophthalmoscopy showed no abnormality and an eccentric fixation of about 3° was present. The VA of the normal eye was $\frac{6}{5}$ and $\frac{1}{60}$ in the amblyopic eye, and no stereopsis

was present. Spectacles are worn for hypermetropia.

Observer J.R., a male aged 42, has an alternating micro-exotropia of about 3°. It was not detected until his late teens when spectacles were prescribed for hypermetropia. Otherwise no treatment was given. The VA's of the two eyes are $\frac{6}{6}$ and $\frac{6}{9}$ which indicates a slight fixation preference. Stereopsis was found up to the stereogram containing 50% binocular correlation (F) level with the Julesz stereograms. Ophthalmoscopy was normal and no eccentric fixation was found.

Observer R.W., a male aged 29, has a small alternating exotropia of approximately 6°. He displays equal VA's of $\frac{6}{12}$ in both eyes and no treatment has ever been given. The squint was first detected at age 3 years, and spectacles have never been worn. Ophthalmoscopy was normal and fixation central; nil stereopsis was present.

Observer K.M., a male aged 20, has a moderate divergent squint of about 15° with a 3° hypertropia. The age of onset was about 1 year. He was treated for long periods, i.e. several months at a time, by patching of the normal eye and also received other orthoptic training on a synoptophore. His VA's are $\frac{6}{6}$ in the normal eye and $\frac{6}{36}$ in the amblyopic eye. Ophthalmoscopy was normal and eccentric fixation of 3° was present, no stereopsis was found.

Observer S.W., a female aged 20, has a convergent strabismus of 10°. The squint was first noticed at age 18

months and patching over several periods, each lasting for several months was undertaken. She had corrective surgery at ages $2\frac{1}{2}$, 3 and 4 years to reduce the angle to the present cosmetically acceptable level. Orthoptic treatment, plus patching of the normal eye continued to the age of 7 years. The VA of the normal eye is $\frac{6}{6}$ and the amblyopic eye is $\frac{6}{24}$. Ophthalmoscopy showed no apparent defect and an eccentric fixation of $1\frac{1}{2}^{\circ}$ was found; nil stereopsis was present. In this case, there was a family history of strabismus as one Aunt, two Cousins and a younger Sister all have convergent strabismus with hypermetropia. Our subject wore spectacles constantly in childhood but now only wears them for prolonged close work.

Observer C.L., a male aged approximately 40, has a large convergent strabismus of about 25°, which was first noticed at age 1 year. Patching was attempted but was not successful in improving VA and it was therefore thought that his amblyopia might have been of congenital origin. His VA in the normal eye is $\frac{6}{6}$ and $\frac{1}{60}$ in the amblyopic eye. Ophthalmoscopy showed a macula disturbance in the amblyopic eye which is probably of congenital origin. Fixation was variable so a measurement was not possible, no stereopsis was present.

Observer S.Be., a female aged 20, who has a convergent squint of angle 8° with spectacles and 12° without spectacles. She is moderately hypermetropic and has an accommodative strabismus or Donders squint. The squint was first noticed at age 18 months and received patching for several months at a time. She had two operations but the age at which these were

performed is not known. Ophthalmoscopy was normal and eccentric fixation of 2° was observed. No stereopsis was present and her Snellen acuity was $\frac{6}{5}$ in the normal eye and $\frac{6}{24}$ in the amblyopic.

Observer D.F., a male aged 22, has a convergent squint of 12° increasing to 15° without spectacles. He is moderately hypermetropic, about 5 diopters, and as in the above case has an accommodative element to the esotropia. The squint occurred at about 2 years of age and he was treated with some patching. He also had two operations to reduce the angle of the esotropia plus other orthoptic treatment. Ophthalmoscopy showed no defect and eccentric fixation is about $\frac{1}{2}^{\circ}$. The VA of the normal eye was $\frac{6}{6}$ and the amblyopic eye was $\frac{6}{24}$ & no stereopsis was found.

Observer J.F., a male aged 19, has a micro-esotropia of about 5° which was not detected until age 8 years. He was given part-time occlusion for only 1 hour a day for a few months. Ophthalmoscopy showed no defects and eccentric fixation was about 1°. The VA of the normal eye was $\frac{6}{6}$ and the amblyopic eye was $\frac{6}{12}$, & stereopsis was not found.

Observer M.T., a male aged 21, has a convergent squint of angle 10°. The esotropia was first noticed at age 18 months. Three operations were performed between the ages of 2 and 5 years. He received full-time occlusion for periods of several months over a two-year span. Ophthalmoscopy showed a normal fundus, with eccentric fixation between 1.5 - 2°. The VA of the normal eye was $\frac{6}{6}$ and $\frac{6}{36}$ in the amblyopic eye. No stereopsis was present to the Julesz stereograms.

Observer D.D., a male aged 45, has a convergent strabismus of 12°. This was detected at about 18 months and surgical correction was performed, but it is not known at what age or how many times. Occlusion was carried out for prolonged periods in early chindhood but no spectacles were worn. Ophthalmoscopy was normal and eccentric fixation of about $1\frac{1}{2}^{\circ}$ was present. VA was $\frac{6}{6}$ in the normal eye and $\frac{6}{24}$ in the amblyopic eye. Stereopsis was not present with the Julesz stereograms.

Observer C.C., a female aged 21, has a convergent squint of about 9°. This was first noticed at about 18 months. Patching and orthoptic treatment was carried out up to age 7 years. Two operations to reduce the angle of squint were performed between the ages of 3 and 5 years. Ophthalmoscopy showed no fundal defect and eccentric fixation was found to be about 2°. The normal eye has a VA of $\frac{6}{5}$ and the amblyopic eye $\frac{6}{24}$; no stereopsis was found.

Observer T.S., a male aged 19, has a micro-esotropia of about 5°. This was first detected at about 12 months of age and orthoptic treatment and patching was carried out until 6 years of age. He had one operation at age 3. Ophthalmoscopy showed no apparent defect and eccentric fixation was about 1°. The normal eye had a VA of $\frac{6}{5}$ with the amblyopic eye recording $\frac{6}{12}$; stereopsis was absent.

Observer J.B., a male aged 18, has a convergent squint of angle 8°. The age of onset is unknown but it was early. He received patching, orthoptic treatment and operations, but does

not know at what age they were undertaken. Ophthalmoscopy showed no defect and eccentric fixation was shown to be about 1°. The VA was $\frac{6}{5}$ in the normal eye and $\frac{6}{24}$ in the amblyopic; Stereopsis was absent.

Observer J.D., a male aged 19, has a convergent squint of angle 10°. The age of onset was about 2 years. He had patching and orthoptic treatment until age 6 years. Two operations were performed between ages $2\frac{1}{2}$ and 4 years. Ophthalmoscopy was normal and eccentric fixation was measured to be about $1\frac{1}{2}^{\circ}$. The VA was $\frac{6}{6}$ in the normal eye and $\frac{6}{24}$ in the amblyopic; Stereopsis was absent.

4.4.2. Refractive Amblyopes

Observer M.J., a male aged 22, has refractive amblyopia which was first detected at the age of 10 years, but no treatment or refractive correction was attempted. Ophthalmoscopy was normal and fixation central, but no stereopsis was present. The VA of the normal eye was $\frac{6}{5}$ and $\frac{6}{12}$ in the amblyopic.

Observer C.H., a male aged 19, is an unusual refractive amblyope. His amblyopic eye is of smaller dimensions than the normal eye, a condition known as microphthalmus. The amblyopia was first noticed at age $2\frac{1}{2}$ and was originally thought to have been due to a microtropia. He received patching for several months at a time for approximately 1 year with no sign of improvement. After further specialist examination the true condition was found and it was discovered that the

dimensions of the external eye were such that the lens had insufficient room to change shape (accommodate) and thus alter focus. This was considered to be the cause of the amblyopia and no further treatment was attempted. Ophthalmoscopy shows a normal fundal appearance. Neither eccentric fixation nor stereopsis were found. The normal eye's VA is $\frac{6}{5}$, while the amblyopic eye acuity is only $\frac{3}{60}$.

Observer A.G., a female aged 28, has no deviation, amblyopia being of refractive origin. This was first detected at age 7 years but no treatment attempted except for spectacles worn from about 5 years of age. Ophthalmoscopy showed no apparent defect and no eccentric fixation was found. The VA of the better eye is $\frac{6}{6}$ and $\frac{6}{9}$ in the weaker eye. At the age of 20 part-time occlusion and orthoptic exercises were attempted which restored a reasonable level of stereopsis. On examination of stereopsis using the Julesz stereograms depth was detected up to a 60% binocular correlation (E).

Observer J.Bo, a male aged 29, whose amblyopia was first noticed at age 7 years. He wore spectacles from this age but no other treatment was attempted. Ophthalmoscopy was normal and no eccentric fixation was present. The VA of the normal eye is $\frac{6}{6}$ and the amblyopic eye is $\frac{6}{12}$. Stereopsis was checked by the Julesz stereograms and depth was noticed up to the 40% binocular correlation level (G).

Observer V de A, a male aged 21, has no deviation. His refractive amblyopia was first noticed at the age of 11 years, and spectacles have been worn since that time. Ophthalmoscopy

showedno defects and no eccentric fixation was present. The acuity was $\frac{6}{6}$ in the normal eye and $\frac{6}{12}$ in the amblyopic; no stereopsis was found.

Observer RR, a female aged 23, whose refractive amblyopia was first noticed at the age of 8 years. No treatment other than spectacles was given and these were worn for a two-year period and then discontinued. Ophthalmoscopy showed a normal fundus and no eccentric fixation was present. Stereopsis was checked with the Julesz stereograms and depth was appreciated up to the 40% binocular correlation level (G). Acuity was measured as $\frac{6}{5}$ in the normal eye and $\frac{6}{12}$ in the amblyopic.

4.2.3. Albino Observer

Observer D.C., a male aged 37, who is a severe tyrosan type albino. He also has an alternating strabismus with equal VA's of $\frac{3}{60}$ R and L and no stereopsis; no binocular vision is present, presumably due to abnormal projections from each eye to the visual cortex. Ophthalmoscopy shows a typical albinoid fundus with prominent view of choroidal vessels, and coarse nystagmus is also present.

A total of 25 subjects with abnormal vision took part in this study and comparison measurements were also made for 7 normal subjects. The abnormal subjects included one albino, six refractive amblyopes and eighteen strabismic amblyopes of which six are divergent squinters, two of these having alternating exotopias.

Chapter Five Characteristics of the Spatio-Temporal Filter Type 1 (ST1) in Abnormal Visual Systems.

5.1. Introduction

It has been argued by Ikeda and her co-workers that for normal visual development to occur, a clearly focussed retinal image is required throughout the critical period of development and that image blur or eccentricity caused cessation of the normal development of the X-cell acuity, whereas the Y-type cell responses remain essentially unaltered. Behavioural studies have confirmed the electrophysiological results both in demonstrating the relationship between age of onset and visual acuity (Fig. 3.12). Studies on the effect of image defocus have shown a drastic reduction in the firing of X-cells (Ikeda 1980). The equivalence between the psychophysical ST1 and ST2 response mechanisms and the X and Y-type electrophysiological mechanisms, respectively, have been noted in Chapter 3, Section 3.25, thus the two psychophysical mechanisms have been studied in human subjects exhibiting amblyopic vision. 25 subjects were investigated; six have amblyopia of refractive origin, one was an albino and the remaining 18 were strabismic amblyopes. Of the strabismic amblyopes, two had alternating divergent strabismus, five had mono-fixational divergent strabismus and the remainder were convergent strabismics. A detailed description of each subject's condition, including operations and attempted treatment appears in Chapter 4, Sections 4.4.1. and 4.4.2.. For ease of reference a table is presented containing the relevant details (Fig. 5.1.). The ST1 spatial response function of Barbur and Ruddock (1980), see also Section 2.2.1., has been measured for both eyes of 24 amblyopes and also for the amblyopic eye of one other subject. Comparison data are presented for a group of 7 normal subjects.

Subjects	S.T.1 Spatial Peak Position cycles deg^{-1}		Visual Acuity		Age of Onset or Age First Found	Eccentric Fixation In Degrees	Treatment
Strabismics	N	A	N	A			
S.B.	4.3	2.87	6/5	6/12	Teens	Nil	Nil
P.M.	4.3	1.73	6/5	6/24	16	0.5	Nil
S.W.	2.87	1.73	6/6	6/24	18 Months	1.5	Patching
C.L.	1.00	1.00	6/6	1/60	Birth	Variable	Patching
J.R.	3.61	3.61	6/6	6/9	Unknown	Nil	Nil
R.W.	1.73	1.73	6/12	6/12	3 Years	Nil	Nil
S.Be	2.87	1.73	6/5	6/24	18 Months	2.0	Patching
D.F.	3.61	2.87	6/6	6/24	2 Years	0.5	Brief
J.F.	3.61	1.73	6/6	6/12	7 Years	1.0	Nil
M.T.	2.87	1.73	6/6	6/36	18 Months	1.5 - 2.0	Patching
G.	4.3	0.75	6/5	1/60	9 Months	3 - Variable	Nil
D.D.	2.87	1.73	6/6	6/24	18 Months	1.5	Patching
N.C.	2.87	1.73	6/5	6/24	18 Months	2.0	Patching
C.C.	3.61	1.73	6/5	6/24	18 Months	2.0	Patching
T.S.	1.73	1.00	6/6	6/12	12 Months	1.0	Patching
K.M.	-	1.00	6/6	6/36	12 Months	3.0	Patching
J.B.	2.87	1.00	6/5	6/24	Unknown	1.0	Patching
J.D.	2.87	1.73	6/6	6/24	2 Years	1.5	Patching

CONTINUED.....

Fig 5.1

Subjects	Peak Position in cycles deg^{-1}		Visual Acuity		Age First Found	Eccentric Fixation In Degrees	Treatment
Refractives	N	A	N	A			
A.G.	4.31	2.87	6/6	6/9	7 Years	Nil	Nil
J.Bo.	4.31	2.87	6/6	6/12	7 Years	Nil	Nil
V de A.	3.61	2.87	6/6	6/12	11 Years	Nil	Nil
R.R.	4.31	1.73	6/5	6/12	8 Years	Nil	Nil
M.J.	4.31	2.87	6/5	6/12	10 Years	Nil	Nil
C.H.	2.87	1.73	6/5	3/60	18 Months	Nil	Patching
Albino							
D.C.	0.40	0.40	3/60	3/60	Birth	Nystagmus	Nil

Normal	Peak Position in cycles deg^{-1} R	L	Visual Acuity R	L	Age When Tested	Sex	N/A
J.B	4·31	4·31	6/5	6/5	25	M	—
V.W.	4·31	4·31	6/5	6/5	22	F	—
I.E.H.	4·31	4·31	6/6	6/6	24	M	—
I.H	4·31	4·31	6/5	6/5	22	F	—
P.S.	4·31	4·31	6/6	6/6	21	M	—
E.I.	4·31	4·31	6/5	6/5	22	M	—
R.G.	4·31	4·31	6/5	6/5	31	M	—

Fig. 5.1. Table of the relevant details of all subjects included in this study

5.2. The Foveal ST1 Spatial Filter: Results for Mean Background Illumination equal to 1.4 log Trolands

The results of seven normal subjects and twenty-five amblyopic subjects, (one subject had only his amblyopic eye examined) were examined for a background light level of 1.4 log Trolands, see table 5.1. The method used to obtain the results has already been discussed in Chapter 4, Sections 4.2.2. and 4.2.3.1., and each value of log threshold illumination for detection of the moving target, log I_t, is the mean of five readings. Standard errors for these readings were typically 0.05 log units. In each figure, values of log I_t, normalised to the same peak value, are plotted against fs, the spatial periodicity of the background grating expressed in cycles deg^{-1}. Fig. 5.2. shows a multiple plot for all the normal subjects and shows a well-defined tuning curve, with log I_t peaking at background fundamental spatial frequency, fs, of about 4 cpd for all subjects. Further, the shape of the tuning curve shows very little inter-subject variation, hence only very slight scatter is present between subjects. Fig's. 5.3. and 5.4. refer to amblyopic subjects and show the collected plots for the normal eyes (A-N) and amblyopic eyes (A-A) of 12 strabismic amblyopes, [the 13th subject only had his amblyopic eye evaluated]. These data differ from the normal data in peaking at a lower spatial frequency value than the 4 cycle deg^{-1} value for normal vision, and there is considerably greater inter-observer spread in the response curve. It must be noted that these comments hold for both the normal and amblyopic eyes of the strabismic amblyopes.

Average values taken from each of the sets of data (Fig's. 5.2., 5.3. and 5.4.) are plotted in Fig. 5.5. with error bars showing the standard error associated with each point. The shift in the position of the peak response is clearly seen in this figure, which shows that the curves for the amblyopic eyes (A-A) peak at a lower spatial frequency than those of the normal eyes (A-N). The difference between data for the "normal" and amblyopic eyes of the strabismic subjects is shown in Fig. 5.6. with the error bars again denoting the standard errors in the points. This difference plot shows that the data for the amblyopic eyes are shifted to lower spatial frequencies than those of the "normal" eyes. Data similar to those presented in Fig. 5.3. and 5.4. were obtained for a group of 6 refractive amblyopes and are presented in a similar way. Thus, normalised values of log I_t are plotted against fs for the normal eyes (Fig. 5.7.) and amblyopic eyes (Fig. 5.8.) of each refractive amblyope. The response curves for all but two of the normal eyes peak at the same value of fs as those for the normal subjects (Fig. 5.2.), but the data still exhibit greater inter-subject scatter than do the normal data. In the case of the amblyopic eyes (Fig. 5.8.), the curves all peak at a lower frequency than do the curves for normal subjects. The average values taken from Fig.'s 5.2. (normal subjects) and 5.7. and 5.8. are plotted in Fig. 5.9.; these show both that the curves for the refractive amblyopic eyes are displaced to lower spatial frequencies relative to the normal data, and that there is little high frequency loss in the normal eyes of these subjects. The difference, Δ, between the averaged log I_t values of the "normal" and amblyopic eyes of these refractive amblyopes are plotted

against fs in Fig. 5.10. The relationship between fs and Δ, differs from that found for the strabismic amblyopes (Fig. 5.6.), in that at low spatial frequencies, Δ approaches zero for the refractive subjects but increases to a large value for the strabismic subjects. This may reflect fundamental differences between the mechanisms of the two types of amblyopia as suggested in some previous studies (Hess and Bradley, 1980).

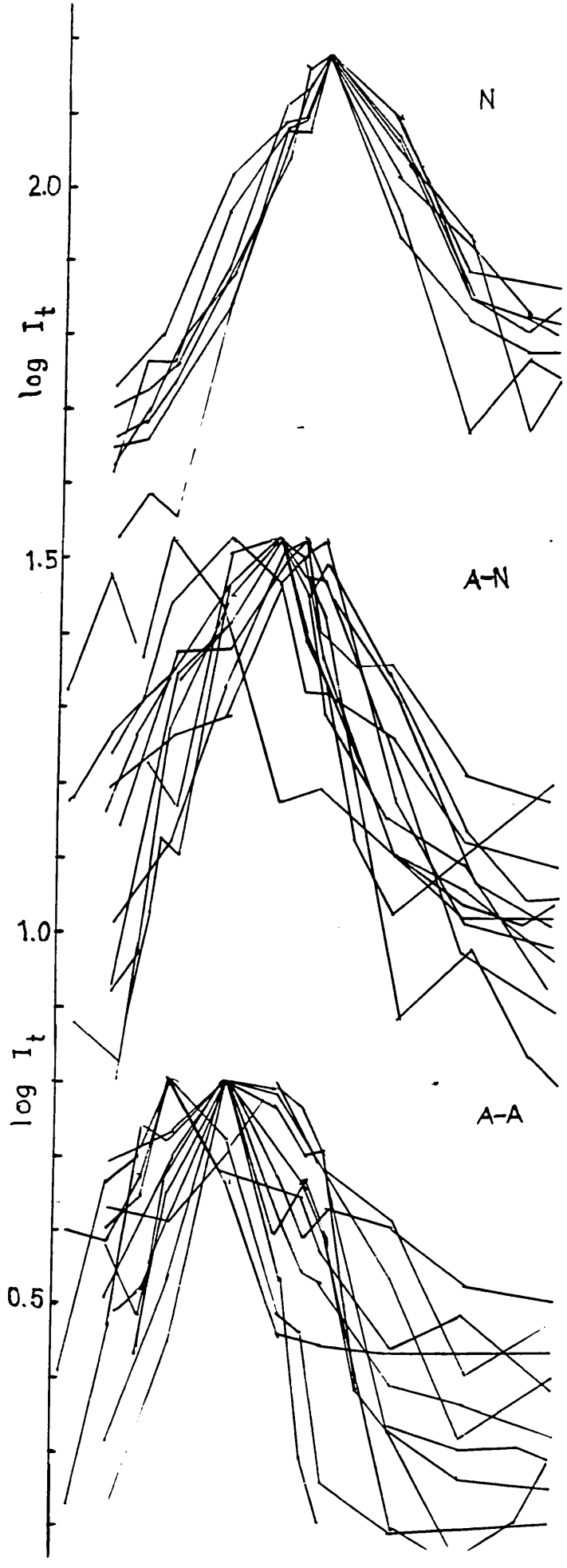

Fig. 5.2.

ST1 spatial response for 7 normal subjects. Threshold illumination I_t, for detection of a circular white light target (diameter 3.5deg.) moving across the grating fundamental spatial frequency, fs. The curves all peak at 4.3 cycles deg^{-1} and there is little subject variability. The mean illumination level of the background field was 1.4 $\log_1$ trolands and the target speed 15 deg. $sec.^{-1}$.

Fig. 5.3.

As for Fig. 5.2., but data for12 strabismics who have amblyopic vision. The data were measured for the "normal" eyes of each subject. The significant inter-subject variability should be noted.

Fig. 5.4.

As for Fig. 5.2., but data for the amblyopic eyes of the same 12 strabismic subjects plus a further result from a 13th subject.

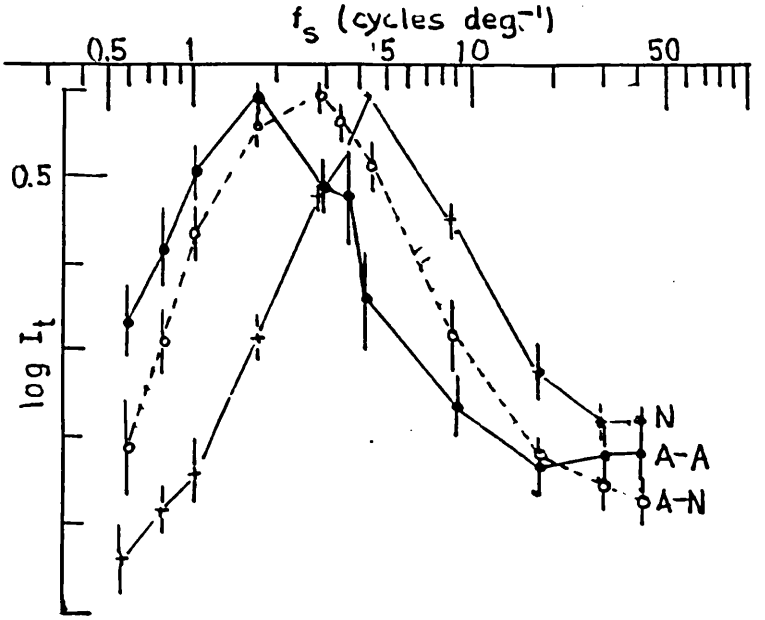

Fig. 5.5 This graph shows the average response measured from all the response curves of Fig's. 5.2, 5.3 and 5.4 (●——● Amblyopic subjects amblyopic eyes, (A-A); O---O amblyopic subjects normal eyes (A-N); +——+ normal subjects (N)). The error bars show ± standard error associated with the average values.

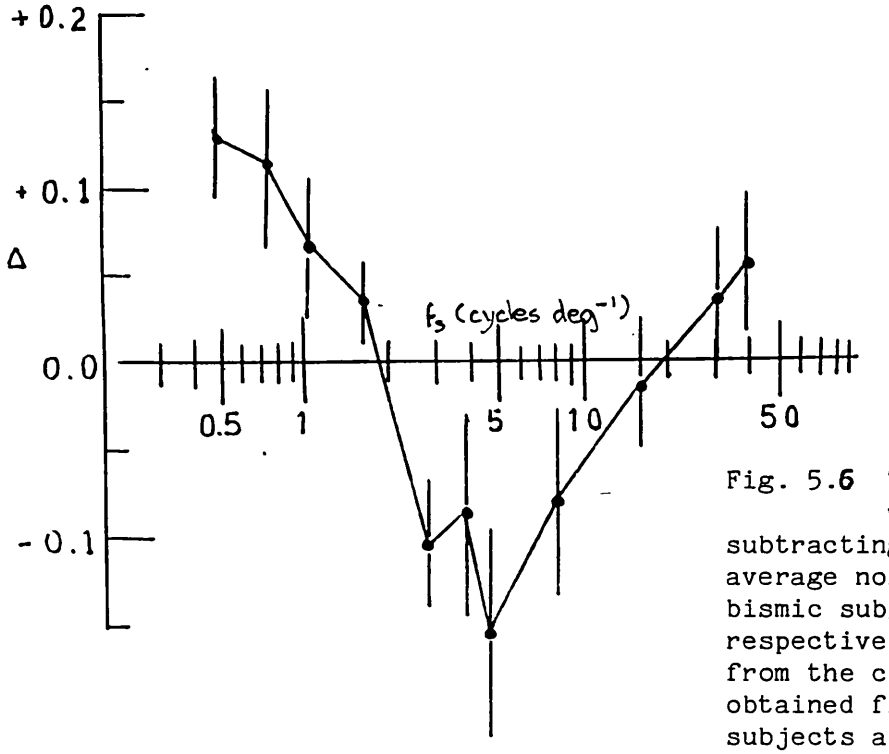

Fig. 5.6 The difference graph was obtained by subtracting the value of the average normal eye of the strabismic subjects (A-N) at each respective spatial frequency from the corresponding value obtained from the amblyopic subjects abnormal eyes (A-A). Thus ($(\log I_t)_{AA} - (\log I_t)_{AN}$) gives the response curve shown on this graph, with error bars denoting the standard errors ±, for each spatial frequency.

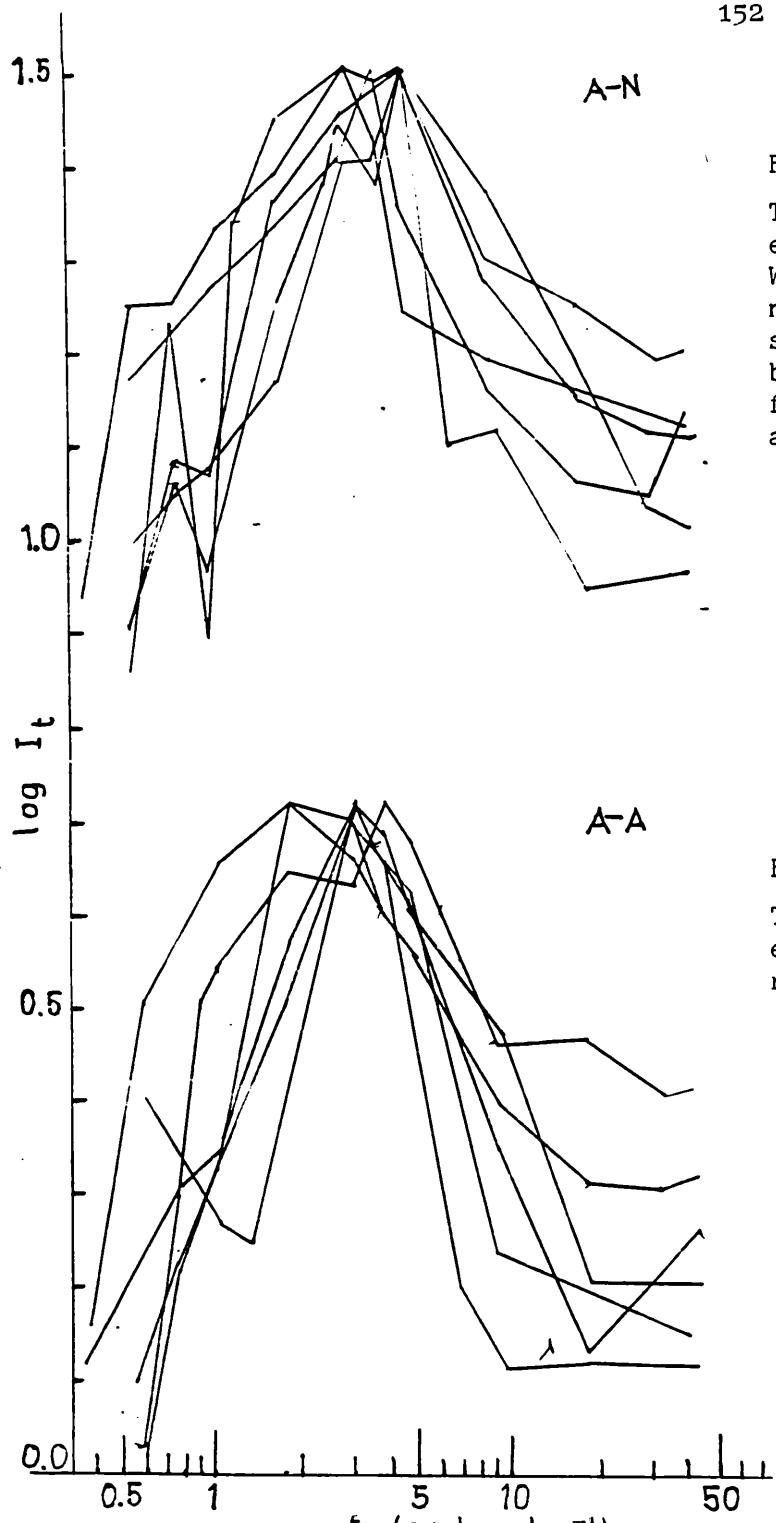

Fig. 5.7.

The ST1 spatial responses for the normal eyes (A-N) of 6 refractive amblyopes. When compared to the responses of the normal observers (see Fig. 5.2), it is seen that there is greater variability between observers, though not as great as for the "normal eyes" of the strabismic amblyopes. (See Fig. 5.3.)

Fig. 5.8.

The ST1 spatial responses for the "amblyopic" eyes of the amblyopes. Note that all the response curves peak below 4 cycles deg^{-1}.

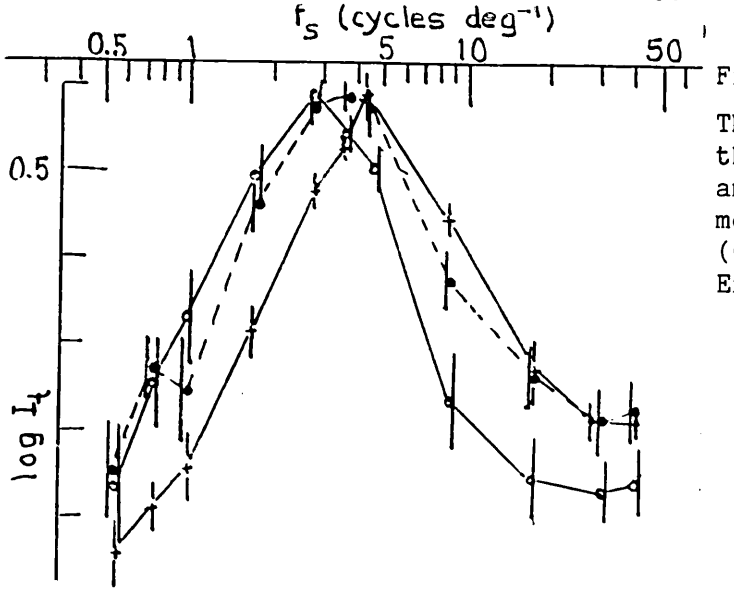

Fig. 5.9.

The average (mean curves) from the data of the refractive amblyopes shown in Fig. 5.7. and 5.8. are drawn here together with the mean curve obtained from Fig. 5.2., (O——O), (A - A); (●---●), (A - N), and (+——+), (N). Error bars denote ±1 standard error.

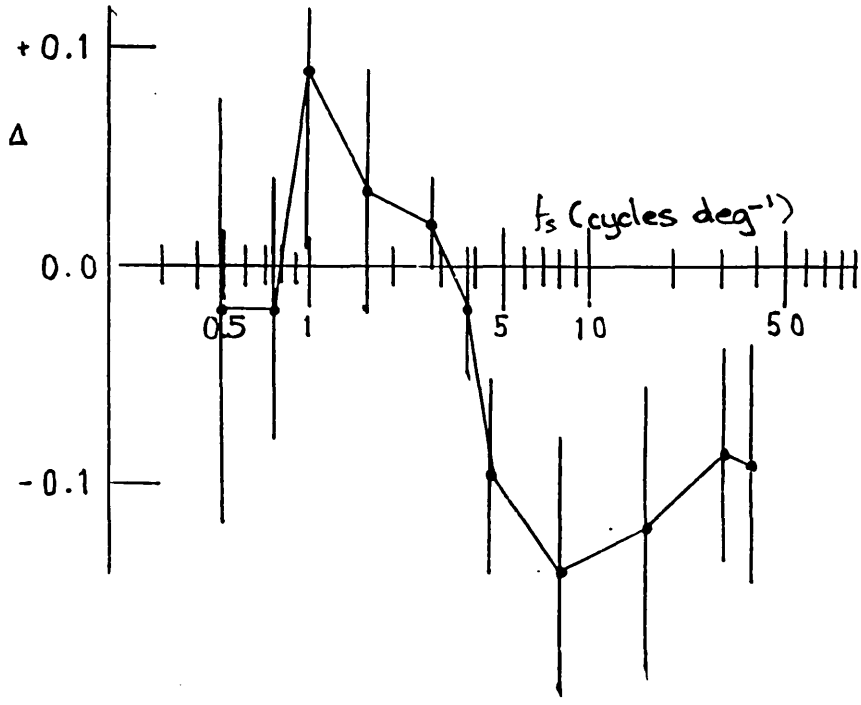

Fig. 5.10 The difference graph was obtained by the same method as Fig. 5.6., that is, ((log I_t) AA - (log I_t)AN) using the averaged results for the "normal" and amblyopic eyes of the refractive subjects shown in Fig. 5.9. Error bars denote ± 1 standard error.

5.3. The Foveal ST1 Spatial Filter. Results for Mean Background Illumination equal to 3.2 log Trolands

In the original study on the ST1 spatial mechanism, it was found that two different responses are obtained, dependent on the average illumination I_b of the background grating. For values of I_b below 2.2 log trolands the response curve peaks for a background grating of spatial frequency f_s, equal to 4 cycles deg^{-1}, whereas for higher values of I_b, the peak occurs for f_s of 8-10 cycle deg^{-1} (Barbur and Ruddock, 1980, see also Chapter 2, Section 2.2.1.). In the previous section, data corresponding to the lower illumination level response were presented and in this section, restricted data for the higher illumination level are described. Data are presented for three amblyopic subjects and, for comparison purposes, for five subjects with normal vision. The first amblyopic subject, a refractive amblyope R.R, has a relatively normal response at lower illumination level for her normal eye (Fig. 5.11), and as the illumination level is increased to 3.2. log trolands, the curve remains essentially constant. For her amblyopic eye, the curve at low illumination level is shifted to the low frequency side of the normal eye (Fig. 5.11) with its peak at 1.7 cycles deg^{-1} and as illumination level increases to 3.2 log trolands it is displaced to higher spatial frequencies with response peaks at 4.3 cycles deg^{-1}. For subject S.W, a strabismic amblyope, both the normal and amblyopic eyes give low frequency responses at low illumination level with the peak occurring at 1.7 cycles/deg for the amblyopic eye and at 3.6 cycle/deg for the normal eye. As illumination level increases to 3.2 log trolands, however, there is a marked upward shift in the frequency response for both eyes,

with the peak shifted to about 8 cycles deg^{-1}, similar to the value found by Barbur and Ruddock (1980) for normal vision (Fig.5.12). The third amblyope,C.C. also strabismic, exhibits low illumination responses similar to S.W with the curve for the "normal" eye peaking at 3.6 cycles deg^{-1}. and that for the amblyopic eye at 1.7 cycles deg^{-1}. At 3.2 log trolands, both curves are shifted to higher frequencies, with that for the normal eye peaking at 6 cycles deg^{-1} (Fig. 5.13) Thus, as background illumination level increases, then ST1 spatial responses are displaced to higher frequencies in all cases, except that of R.R's "normal" eye. In the course of these experiments, data were obtained for normal subjects both to confirm the original observations of Barbur and Ruddock and to provide comparison data for the results of the study on amblyopia. Three of these normal subjects give ST1 responses which are clearly displaced to higher spatial frequencies as background illumination increases from 1.4 to 3.2 log trolands (Fig. 5.14), in much the same way as was described by Barbur and Ruddock. For the other normal subjects, however, there is no significant change in the responses as illumination level increases from 1.4 to 3.2 log trolands (Fig.5.15), thus there appears to be some variability for normal subjects in the extent to which the high level response function can be observed. In view of this variability amongst normal subjects, it was decided that no definitive information about the differences between amblyopic and normal vision could be derived from the studies on the high level illumination level function. All the remaining data and discussion are, therefore, concerned only with the low illumination level response.

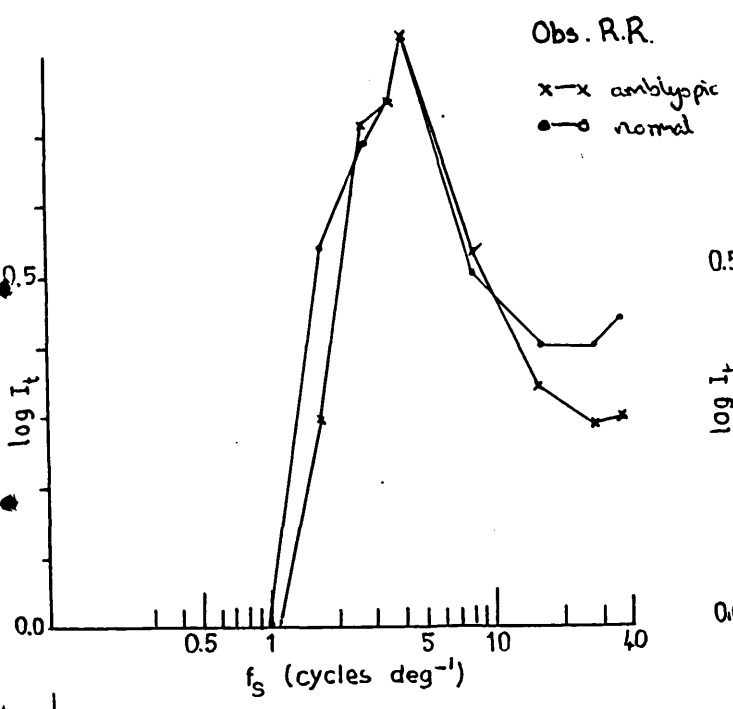

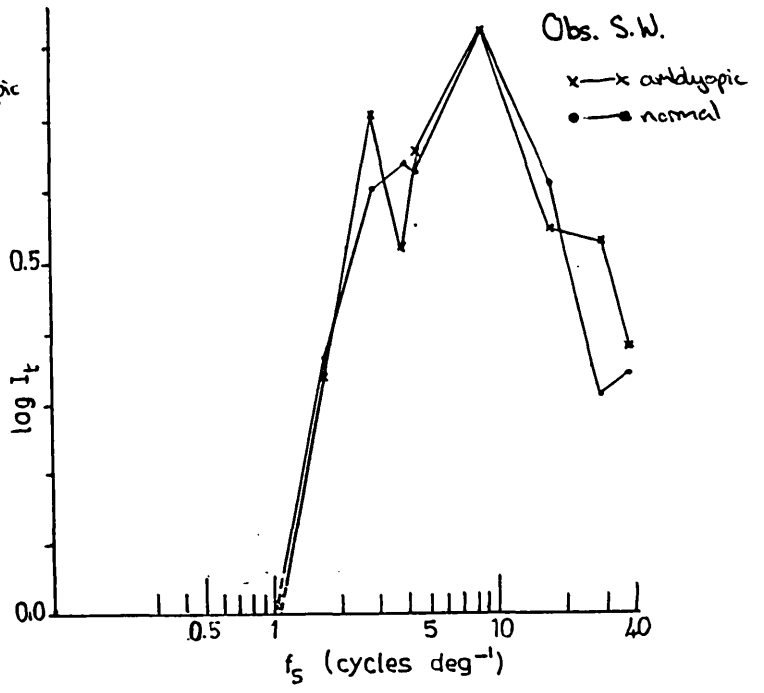

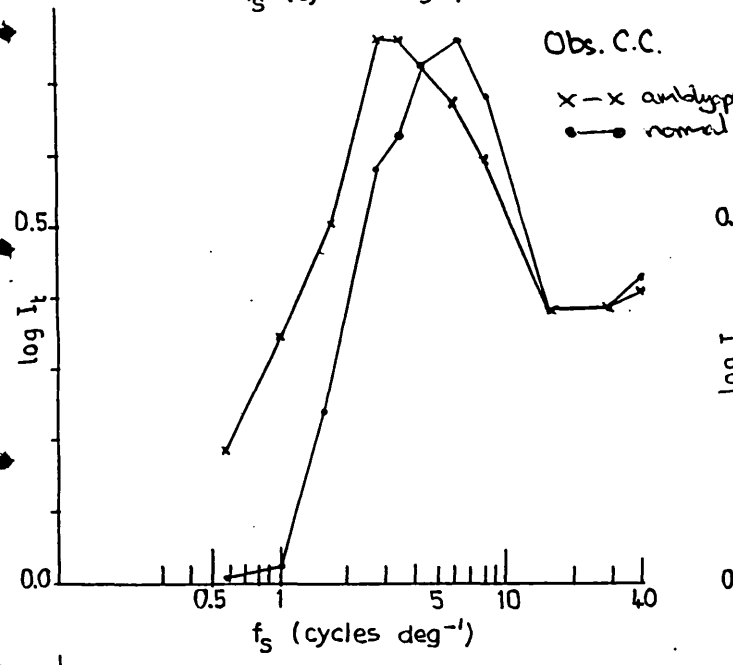

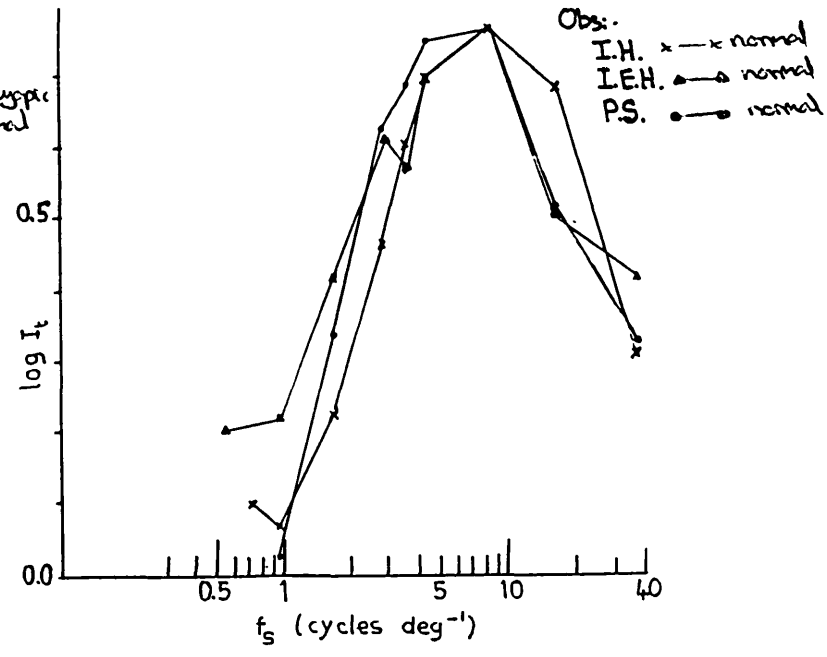

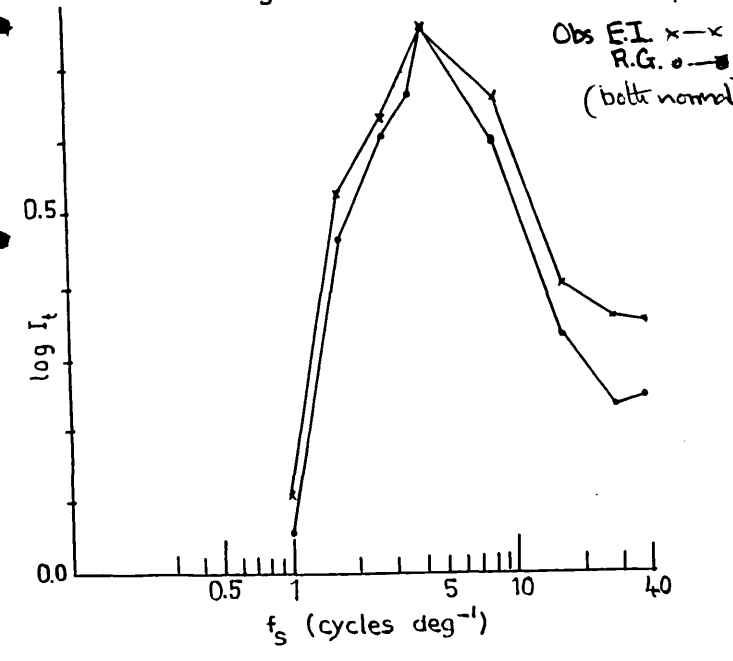

Fig. 5.11 to 5.15

ST1 spatial response curves are shown for 3 amblyopic subjects, 1 refractive and 2 strabismic. Figs. 5.11, 5.12 and 5.13 and 5 normal subjects, Figs. 5.14 and 5.15. Threshold illumination I_t, for detection of a white light spot stimulus of diameter 3.5° moving across a background grating is plotted against the grating funddamental frequency, f_s. The mean illumination level of the background field was 3.2 log trolands and the target speed was 15 deg. sec^{-1}.

5.4. ST1 Spatial Responses for Two Subjects with Alternating Divergent Strabismus

Strabismic subjects who alternate fixation between the two eyes should not penalise either eye in relation to the other, thus there should be no difference in the visual performance of the two eyes. Measurements of the ST1 spatial response confirms this conclusion for two subjects who exhibited alternating fixation (Figs. 5.16 and 5.17). Thus for observer J.R, who has relatively normal VA in each eye, $\frac{6}{6}$pt R & L the ST1 spatial response for each eye peaks at 3.6 cycle/deg. For observer R.W, who has lower VA's in both eyes, being $\frac{6}{12}$+R and L, the tuning curves for each peaks at 1.73 cycles deg^{-1}. In the latter case, there appears to be some factor, perhaps congenital, which causes loss of visual acuity. It should be noted that surgically induced strabismus which leads to an alternating squint fails to produce loss of visual acuity (Hubel and Wiesel, 1965; Blakemore and Eggers, 1976; Yinon et al, 1976 and Ikeda et al,1977). See Chapter 3.

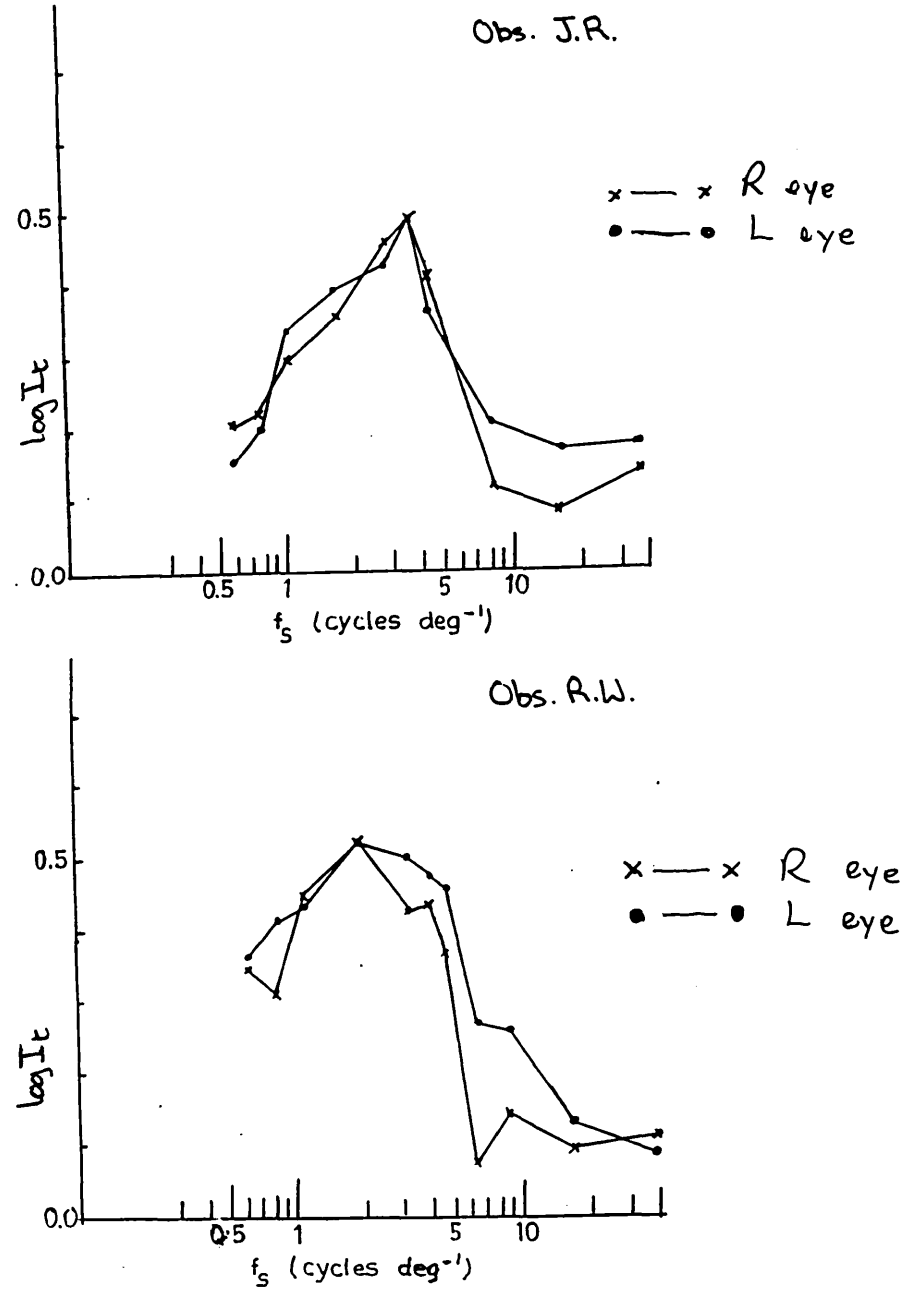

Fig's 5.16 & 5.17 The ST1 spatial responses for both eyes of two alternating strabismic subjects J.R and R.W. Threshold illumination I_t, for detection of a white light spot stimulus of diameter 3.5^o moving across a background grating is plotted against the grating fundamental frequency, fs. The mean background illumination level was 1.4 log trolands and the target speed was 15 deg. sec^{-1}. Note that both eyes of each respective observer peak at the same spatial frequency.

5.5. ST1 Spatial Response: Data for an Albino Subject D.C. (Fig. 5.18).

Observer D.C. is classified by the hair test as Tyrosinase Negative (a severe form of Albinism). He exhibits a marked nystagmus and low spatial resolution, with Snellen acuity of $\frac{3}{60}$ in each eye. (see also Section 4.2.3. of Chapter 4). His spatial response to the ST1 filter is shown in Fig. 5.18, and the peak is clearly shifted from that of the normal observer, with a peak position of 0.4c/°.

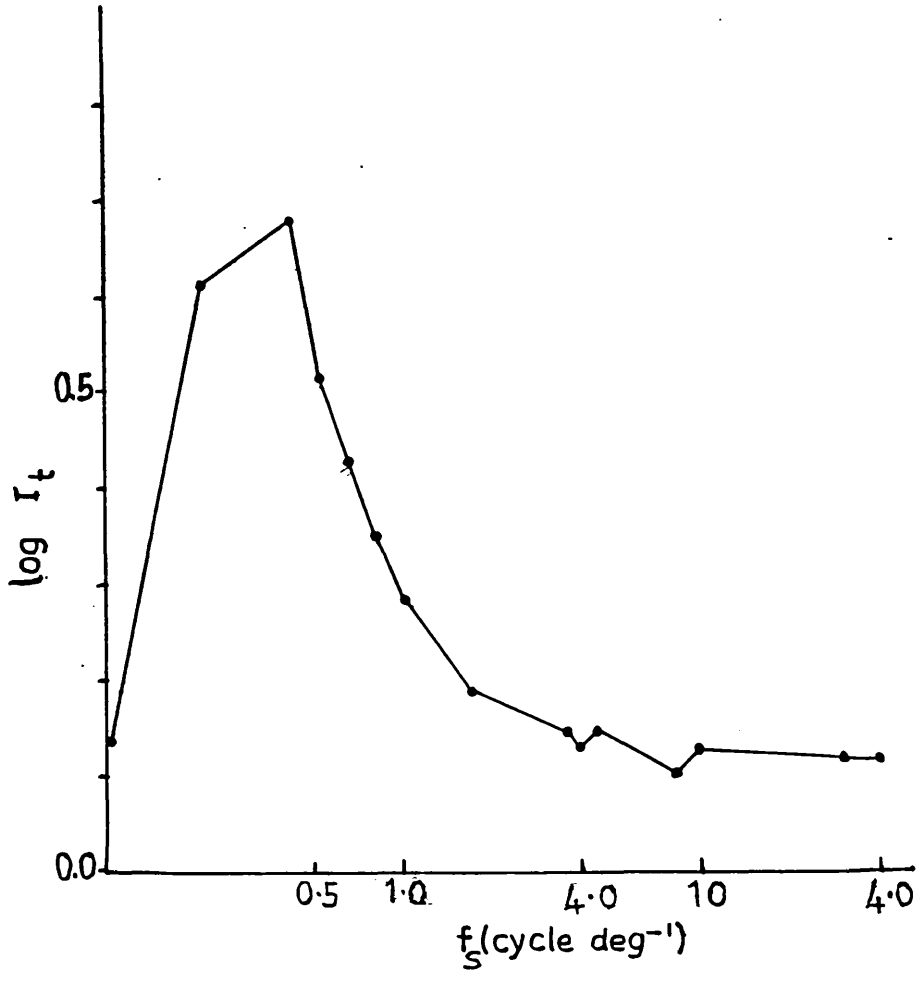

Fig. 5.18 The ST1 spatial response curve of an albino observer D.C., measured for mean background illumination of 1.4 log trolands. Note the peak is shifted to a very low spatial frequency, 0.4c/°.

5.6. ST1 Spatial Response: Data for Eccentric Vision

It has been proposed that amblyopia represents visual function through non-foveal receptors, (see Chapter 3, Section 3.1.1.), and in order to examine this proposition the spatial ST1 response was measured for eccentric fixation of the moving target. This was achieved by placing in the visual field a red fixation spot, located either 10 deg. or 20 deg. from the centre of the background grating, that is, at the centre of the displacement path for the moving target (Fig. 5.19). The experimental procedure is otherwise the same as for the foveal measurements. In each case the fixation point was located along the horizontal meridian, such that the target was moved on the horizontal meridian in the temporal retina.

ST1 spatial responses for the normal subjects, R.G. and I.H. measured at different retinal locations are plotted in Fig. 5.20, and in the case of subject R.G., data are given for both eyes. It is apparent that as retinal eccentricity increases the peak of the ST1 spatial response curves shift to lower spatial frequencies, and the data for each eye of the subject R.G. are closely similar in this, as in all other respects. Electrophysiological findings (Ikeda et al, 1978, but cf. de Monasterio, 1978a) have shown that receptive field sizes of X-cells increase with increasing eccentricity from the fovea, thus these results are consistent with the view that the ST1 mechanisms correlate with X-type electrophysiological mechanisms. Similar data were also obtained for two refractive subjects and four strabismic amblyopes, and are plotted in Figs. 5.21, 5.22

and 5.23, with log threshold illumination I_t plotted against the spatial frequency, f_s, of the background grating. Data are given for both the normal and amblyopic eyes of the refractive amblyopes A.G. and C.H., and the strabismic amblyopes, P.S., J.F. and N.C., but only for the amblyopic eye of P.S. The plots show that in each case, the peak of the ST1 spatial response shifts to lower spatial frequencies as target eccentricity increases, but for the amblyopes, the functions for the "abnormal" eyes are displaced to lower spatial frequencies than those for the "normal" eye at all retinal locations (Figs. 5.24, 5.25 and 5.26).

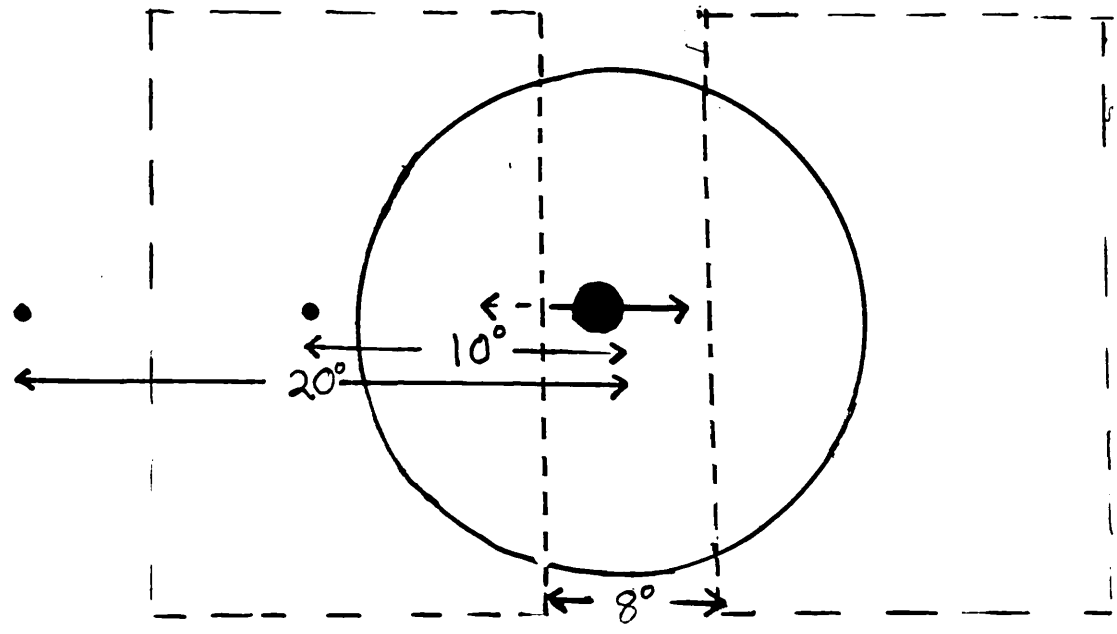

Fig. 5.19 The visual field arrangement for non-foveal measurements. The fixation point was located at the required angular distance from the centre of the 8 deg. path over which the target travelled. Other stimulus parameters as for Fig. 5.2.

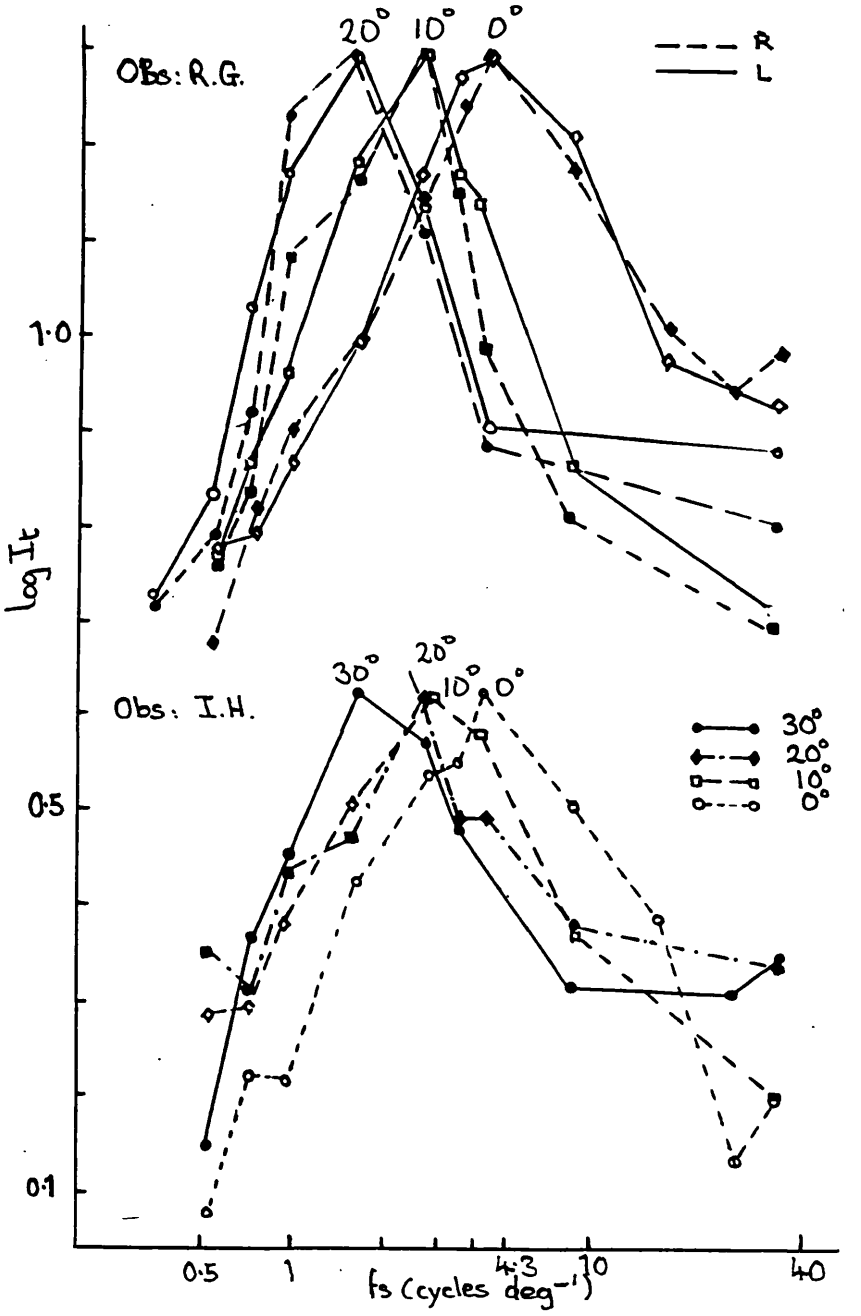

Fig. 5.20 ST1 spatial responses for two observers with normal vision measured foveally and at 10^{o} and 20^{o} eccentricity in observer R.G. and foveally, at 10^{o}, 20^{o} and 30^{o} eccentricity in observer I.H. In the case of R.G., data are given for both eyes and there is little difference between the two eyes.

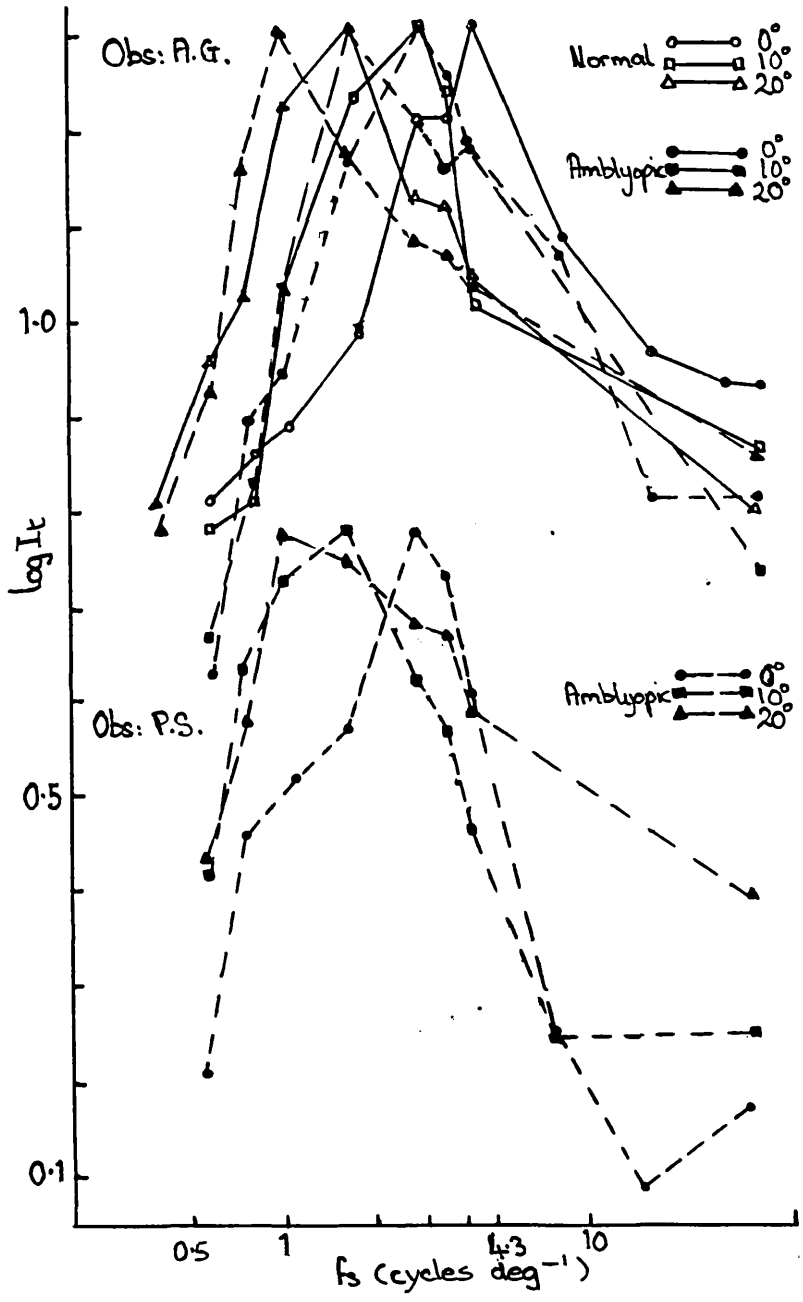

Fig. 5.21 As in Fig. 5.20 the plots for foveal, 10° and 20° eccentricity are shown for a group of amblyopic observers and data are given for both the "normal" and amblyopic eyes.

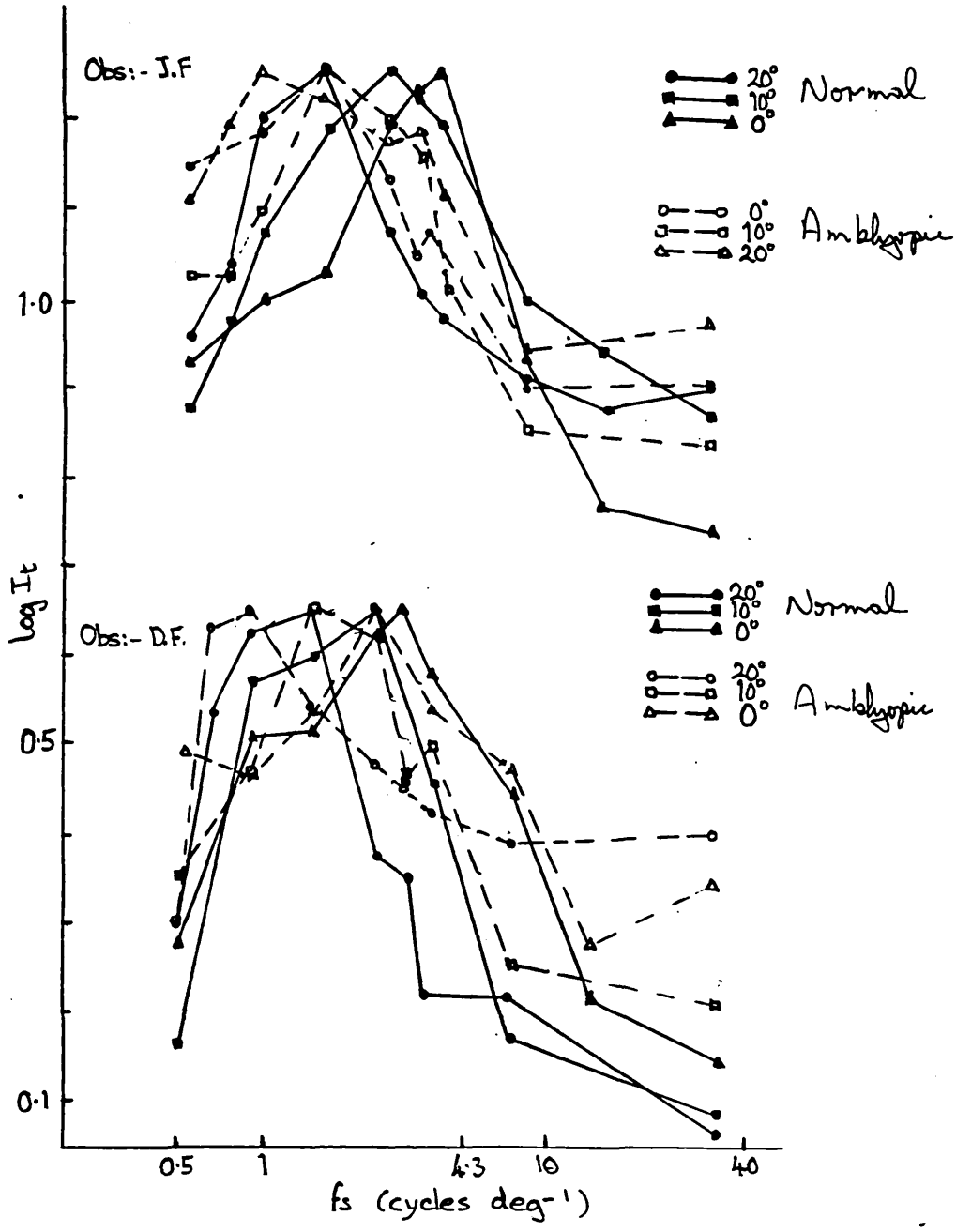

Fig. 5.22 As in Fig. 5.20 the plots for foveal, 10° and 20° eccentricity are shown for a group of amblyopic observers and data are given for both the "normal" and amblyopic eyes.

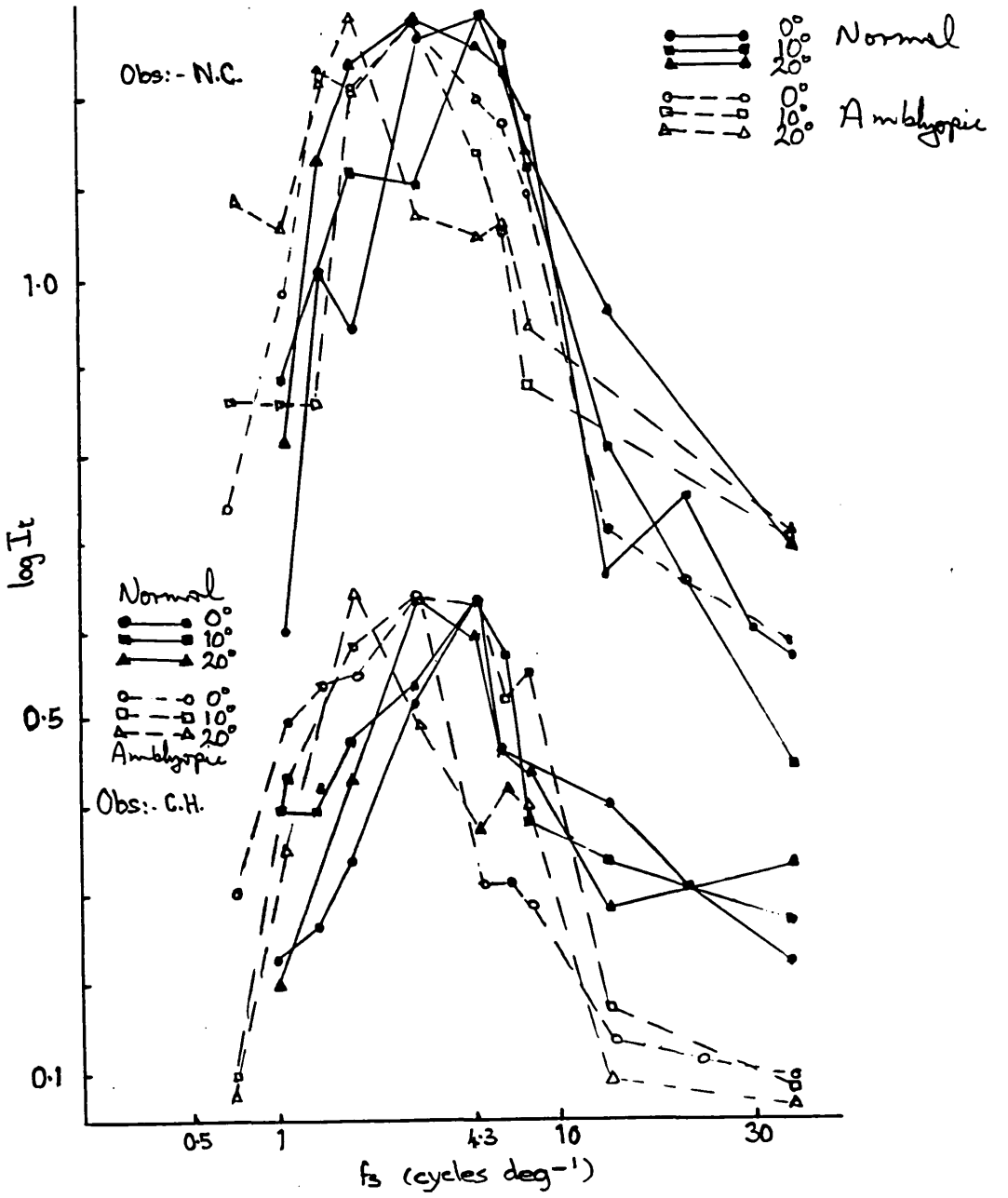

Fig. 5.23 As in Fig. 5.20 the plots for foveal, 10° and 20° eccentricity are shown for a group of amblyopic observers and data are given for both the "normal" and amblyopic eyes.

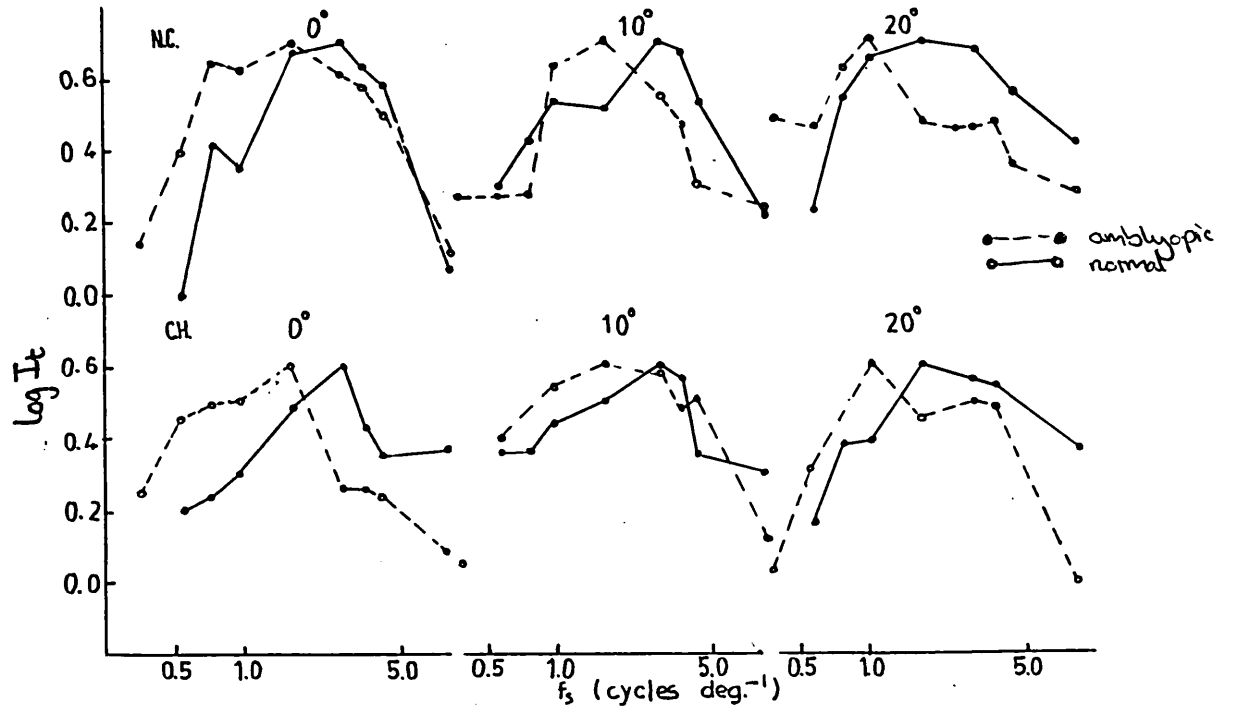

Fig. 5.24 The data of Fig. 5.20 to 5.23 replotted so that data for the different amblyopic subjects referring to a given retinal location are plotted on a single figure.

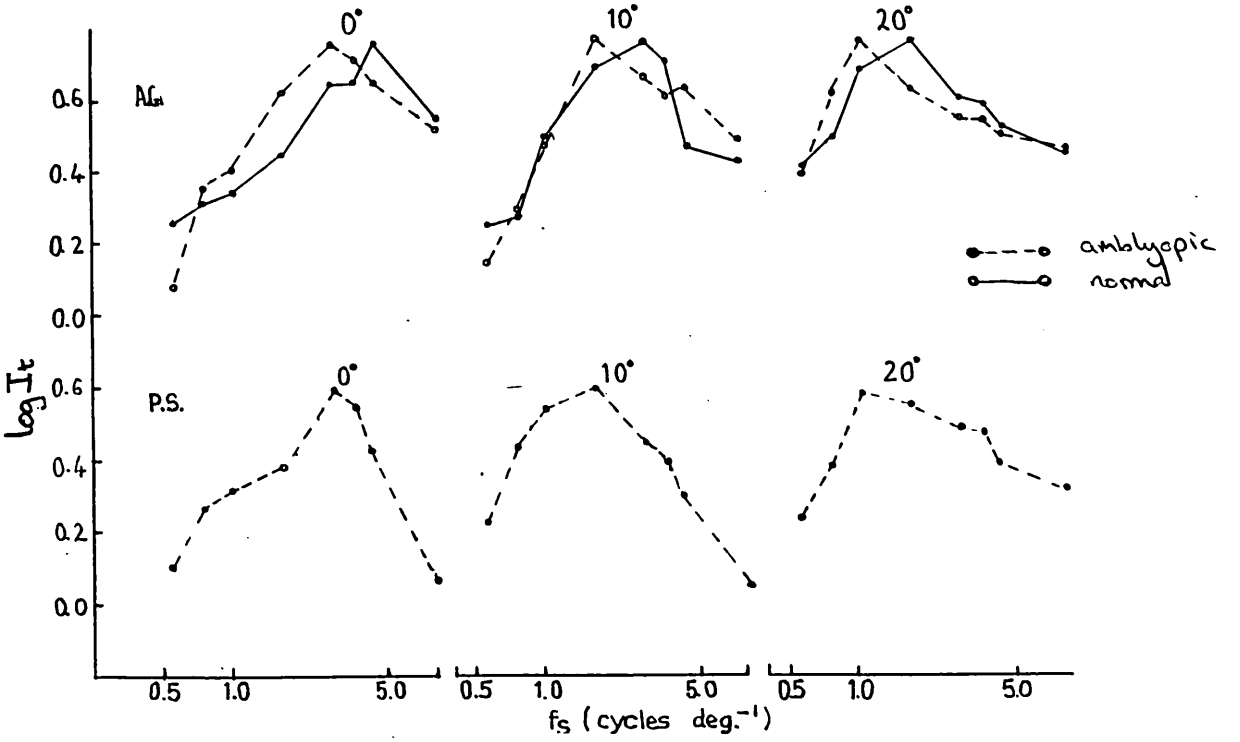

Fig. 5.25 The data of Fig. 5.20 to 5.23 replotted so that data for the different amblyopic subjects referring to a given retinal location are plotted on a single figure.

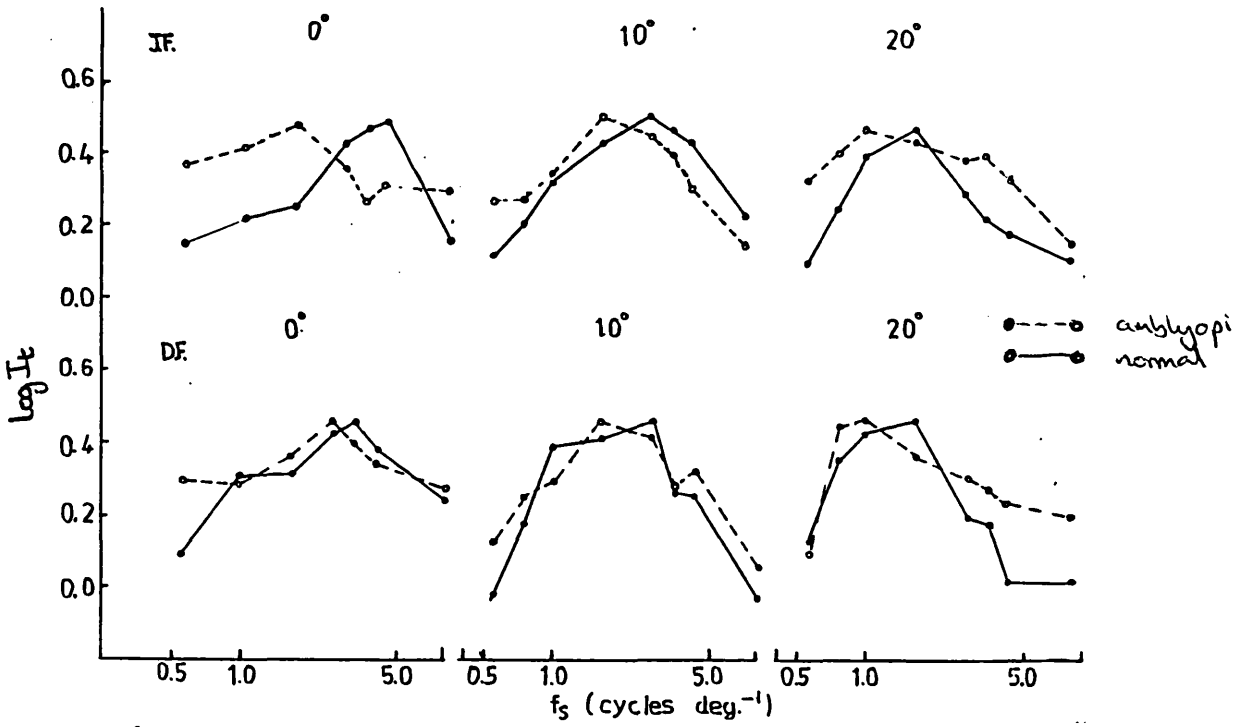

Fig. 5.26 The data of Fig. 5.20 to 5.23 replotted so that data for the different amblyopic subjects referring to a given retinal location are plotted on a single figure.

5.7. General Discussion: Features of Amblyopic ST1 Responses

The experimental results show that in amblyopic eyes the ST1 spatial response is shifted to low spatial frequencies relative to the corresponding data for normal vision. Unexpectedly, this is also observed in the case of normal eyes in most of the strabismic amblyopes. Abnormally low spatial frequency response implies that the receptive field associated with the response mechanism is larger than the response mechanism for normal vision. A method for computation of the ST1 receptive field from the frequency response data is given by Barbur and Ruddock (1980, Appendix) and can be applied to the amblyopic data. The cross-section through the receptive field corresponding to the average data for the amblyopic eyes of the strabismic subjects (Fig. 5.4.) is plotted in Fig. 5.27, together with the data for normal vision taken from Barbur and Ruddock. The significant broadening of the receptive field in amblyopia is clearly

illustrated by this figure. This result correlates with the electrophysiological finding, that in cats with surgically induced amblyopia, the X-type response mechanisms suffer loss of spatial resolving power (Ikeda, 1980). In the remainder of the discussion, several different aspects of this general result, a loss of acuity associated with amblyopia, will be discussed.

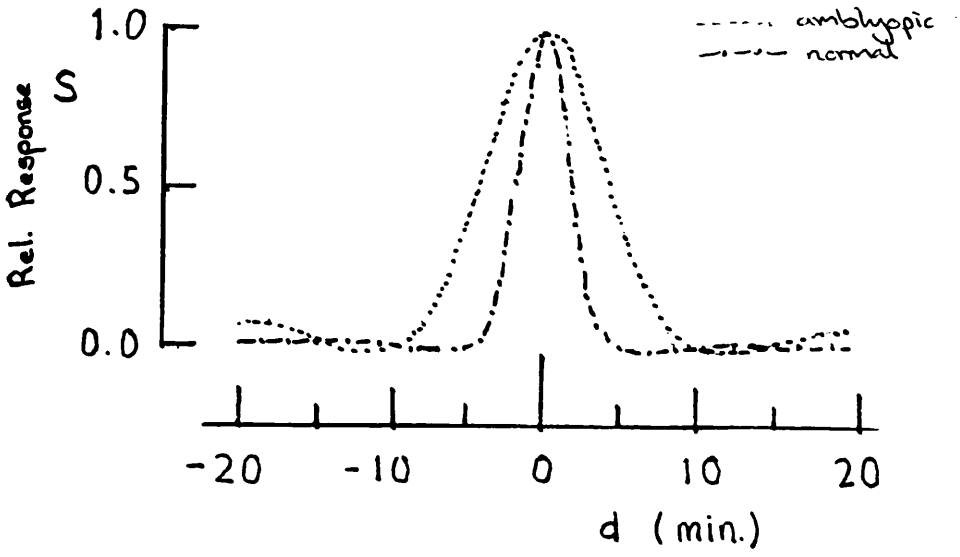

Fig. 5.27 Cross-sections through the spatial responses corresponding to the ST1 data for normal vision, and for the average ST1 data for the amblyopic eyes of the strabismic subjects (Fig. 5.5.). The receptive fields were obtained by the method described by Barbur and Ruddock (1980).

5.8. The Abnormal Responses Found in the "Normal" Eyes of Strabismic Amblyopes.

The most unexpected aspect of the experimental data is that the ST1 spatial responses for the normal eyes of strabismic, but not refractive, amblyopes are displaced to low spatial frequencies relative to the normal data is similar to, but less marked, than that for the amblyopic eyes.

In attempting to interpret this finding it was noted that all strabismic amblyopes included in the study had received long-term patching of the normal eye during the critical development period. In contrast, none of the refractive amblyopes had received any treatment whatsoever, thus an obvious possibility is that the differences between the normal eyes' performance of the two types of amblyopia reflects the difference in treatment. Most of the subjects in this study and all those who had contributed to the data presented so far were students between 18 and 20 years of age at a time when long-term patching for the treatment of amblyopia was in vogue. More recently, however, such treatment has been considered unnecessary and by some opthalmologists, as possibly harmful. The idea behind such treatment is that occlusion of the good eye for many months at a time, encourages use of the weakest eye. Such treatment not uncommonly results in reversal amblyopia or transfer amblyopia, which refers to the situation when, following such occlusion, the amblyopic eye has improved to a near normal VA while the eye which previously had good VA becomes amblyopic.

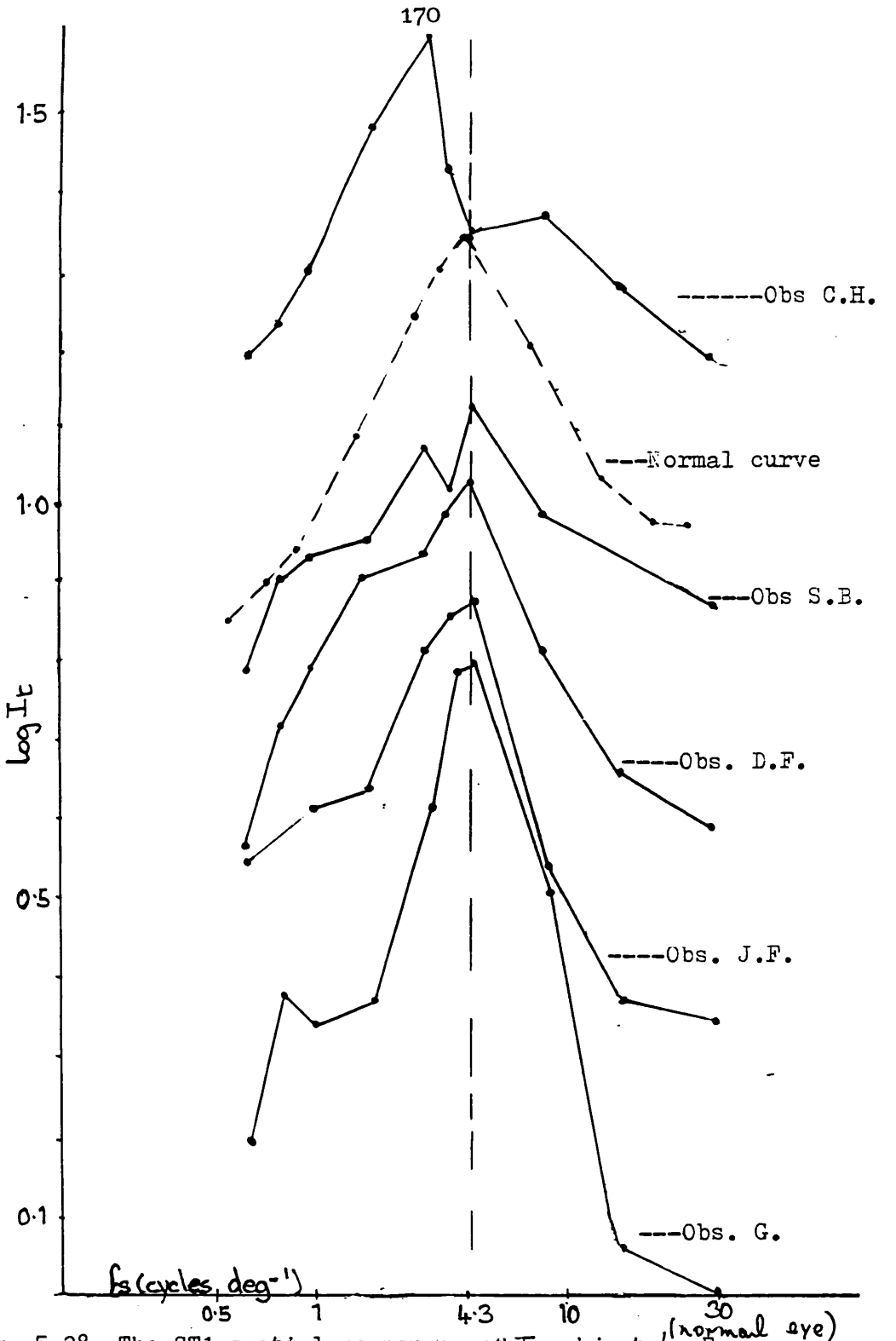

Fig. 5.28 The ST1 spatial responses of 5 subjects. Four are untreated strabismic amblyopes, the other, C.H, is a patch treated refractive subject. It is apparent that the response curves of 4 untreated strabismic amblyopes is similar to the averaged normal response curve from Fig. 5.5, which is drawn on this graph as a dashed line. The response curve of C.H (treated refractive amblyope) by contrast has a peak displaced to a lower spatial frequency. All stimulus parameters as for Fig. 5.2.

As occlusion therapy is carried out during the critical development period it seem inevitable that long-term occlusion will cause some detrimental effects on the occluded, normal, eye. It is possible, therefore, that the better eyes of the treated subjects of this study may have suffered some deficit in development, resulting in the displacement of the ST1 spatial response to lower frequencies relative to the function for normal eyes. In order to test this hypothesis strabismic amblyopes who had not received any treatment and refractive amblyopes who had received patching treatment, were sought. Such subjects proved difficult to find, but eventually a few strabismic subjects, none of whom had received long-term patching, and one refractive who had been treated by such occlusion, were found. The ST1 spatial response was measured for those subjects and the data for the "normal" eyes are plotted in Fig. 5.28. It is apparent that the responses for the un-treated strabismic subjects are closely similar to the normal average curve, whereas for the treated refractive amblyope the peak shifted to a lower spatial frequency, with a peak at $2.89c/^{o}$.

In order to examine further this hypothesis, the data for all the amblyopes have been replotted, but divided into two groups, those treated and those un-treated. Fig. 5.29 shows the results for the amblyopic eyes (A-A) of the treated subjects and it is apparent that all the log I_t vs, fs curves peak at spatial frequencies below the normal peak of $4.3c/^{o}$. Fig. 5.30

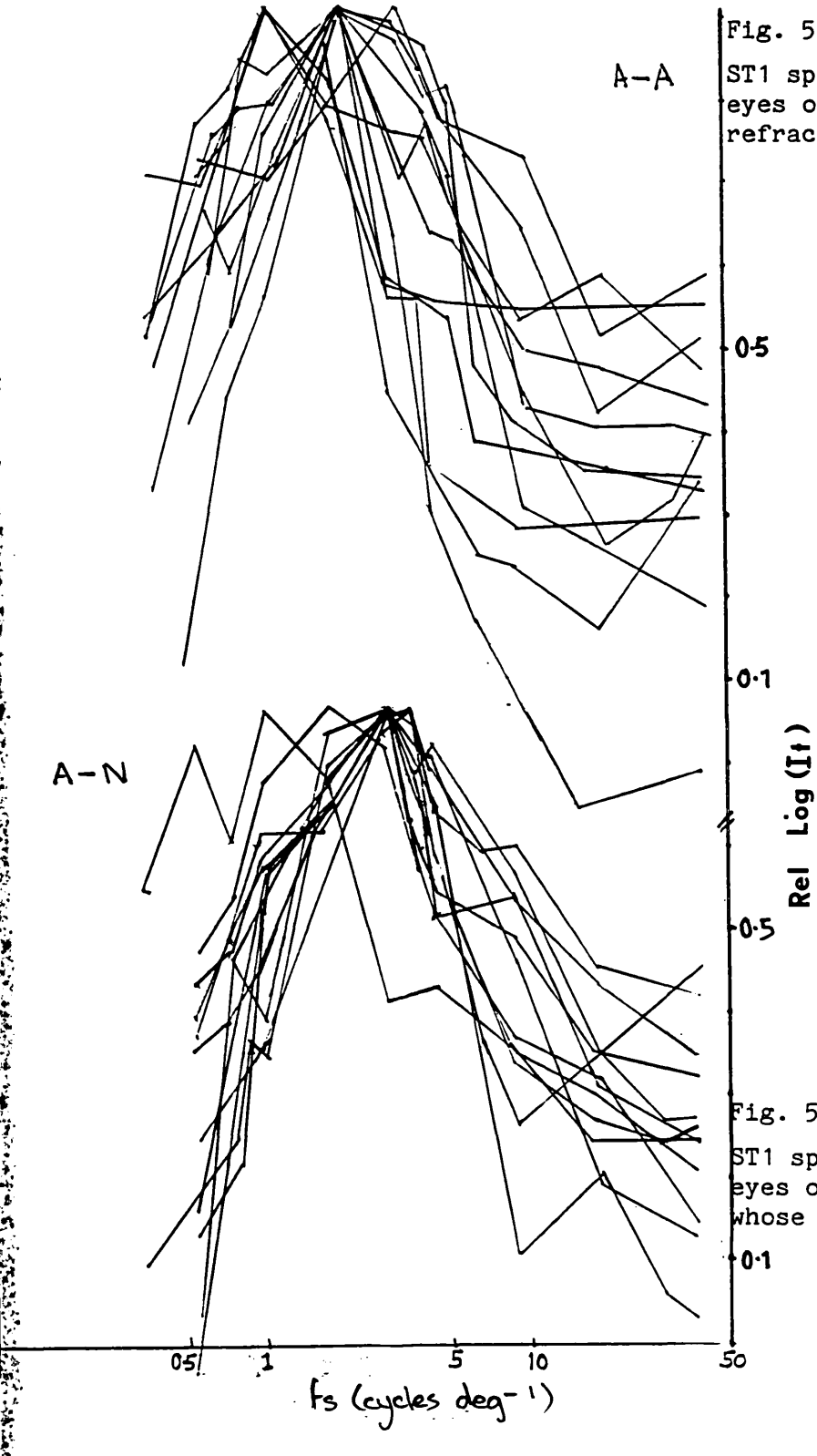

Fig. 5.29

ST1 spatial responses for the amblyopic eyes of 13 amblyopes (strabismic and refractive) treated by patching.

Fig. 5.30

ST1 spatial responses for the "normal" eyes of 12 of the 13 strabismic amblyopes whose "abnormal" eye data are in Fig.5.29

shows the multiple graph of the "normal" eyes of these subjects and again all the peaks are below 4.3c/^{o} although the average peak position for the "normal" eyes (A-N) is closer to the position for normal subjects than that for the amblyopic (A-A) eyes. Fig. 5.31 shows a frequency histogram of all the peak positions of both the amblyopic (A-A) and "normal" (A-N) eyes of the treated subjects. An averaged normalised plot of all the "amblyopic" and "normal" eyes is plotted in Fig. 5.32 together with the normal curve from Fig 5.5. A difference graph, in which the difference of each subject's points are taken individually and then averaged are plotted in Fig. 5.33, in which the subjects "normal" eye results are represented by the line AB. It can be seen that the deviation of the amblyopic eye from that of the "normal" eyes' response represented by AB, shows a significant difference.

Plots for nine untreated subjects are shown in Figs. 5.34 (for the amblyopic eyes) and 5.35 (for the normal eyes). Fig.5.36a and b shows the frequency histograms of the peak positions. The A-A (amblyopic eyes) show a deviation of the peak position towards lower spatial frequencies whereas the A-N (normal eyes) are similar to the normal tuning curve.Fig. 5.37 shows the averaged normalised ST1 response curves for the amblyopic (A-A) and "normal" (A-N) eyes of the untreated amblyopes and the average curve for the normal subjects. It is apparent on inspection that the responses for the normal eyes of the amblyopes are similar to those of the normal subject, whereas the amblyopic eyes, A-A, give significantly different results with the curves shifted to low spatial frequencies. In Fig.5.38, the

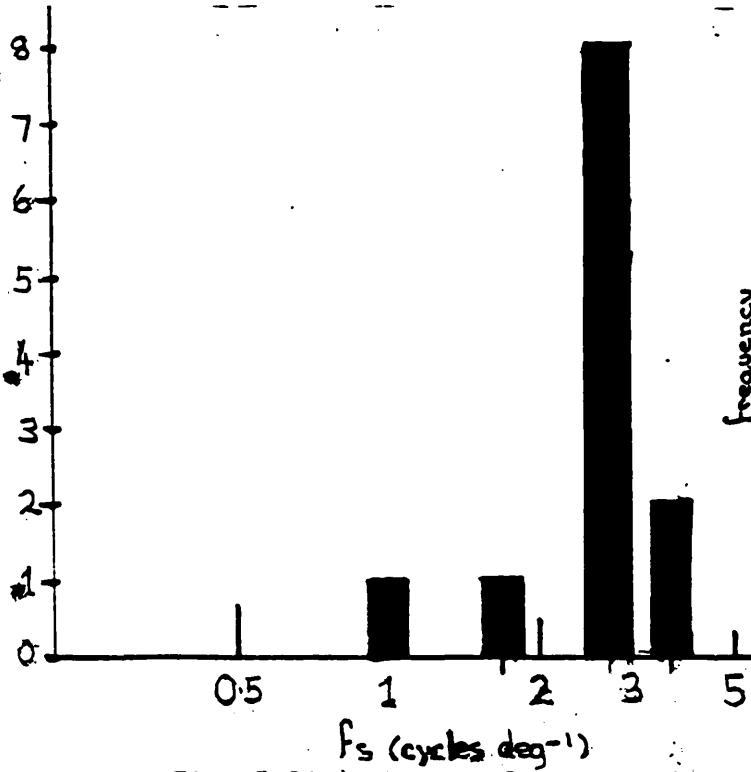

Fig. 5.31a) shows a frequency histogram of the peak positions of the response curves shown in Fig. 5.29.

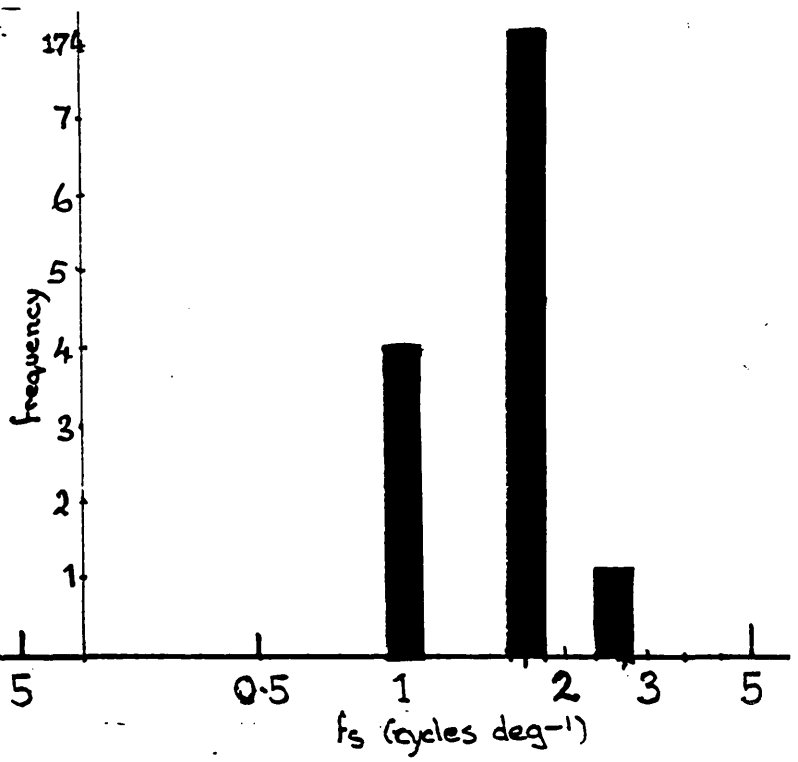

Fig. 5.31b) shows a frequency histogram of the peak positions of the response curves shown in Fig. 5.28.

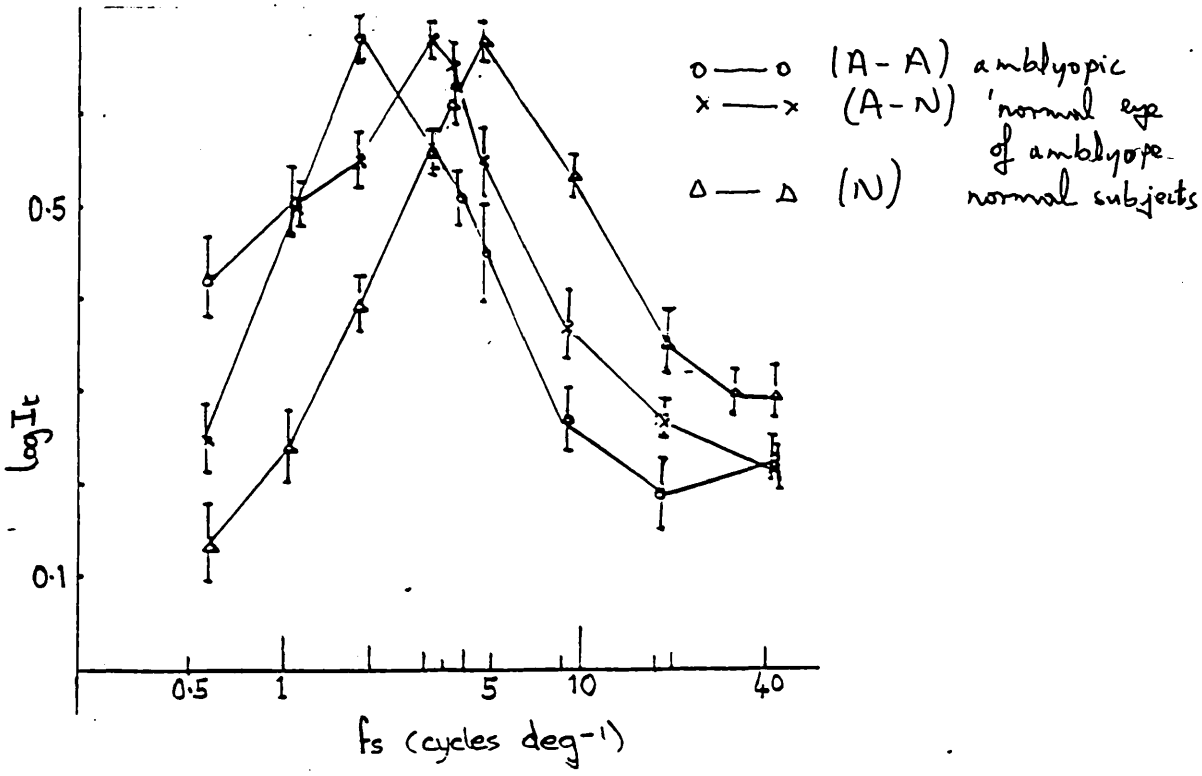

Fig. 5.32 The mean ST1 spatial response curves of the plots of the A-A eyes (O-O) from Fig. 5.29 and the A-N eyes (X-X) from Fig. 5.30, are plotted with the mean curve from the plots of normal observers shown in Fig. 5.2.

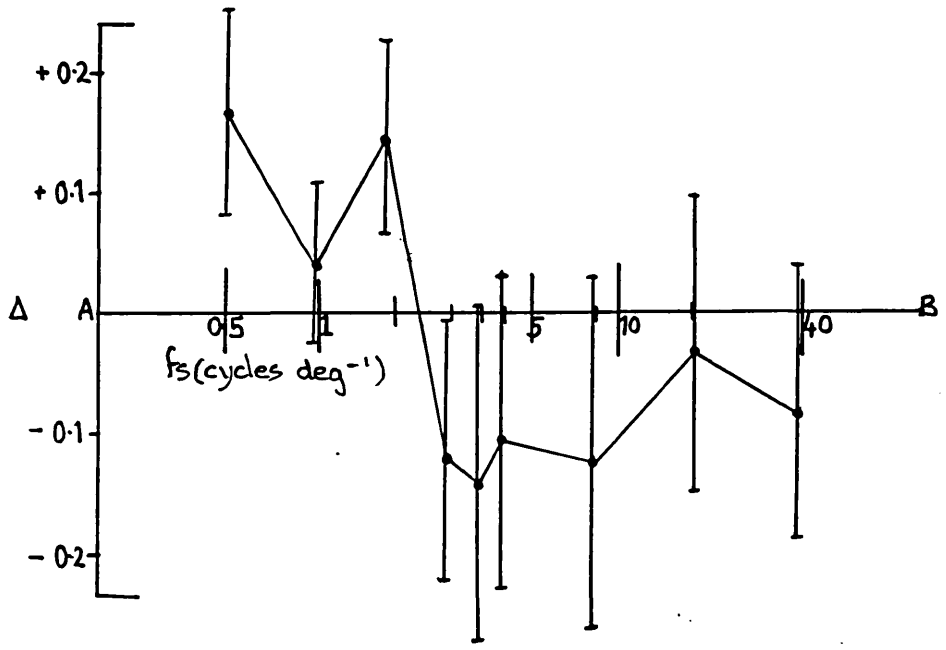

Fig. 5.33 This shows the difference graphs of the amblyopic and "normal" eyes of the treated amblyopic subjects. The response curve is derived from the equation $(\log I_t)_{AA} - (\log I_t)_{AN}$.

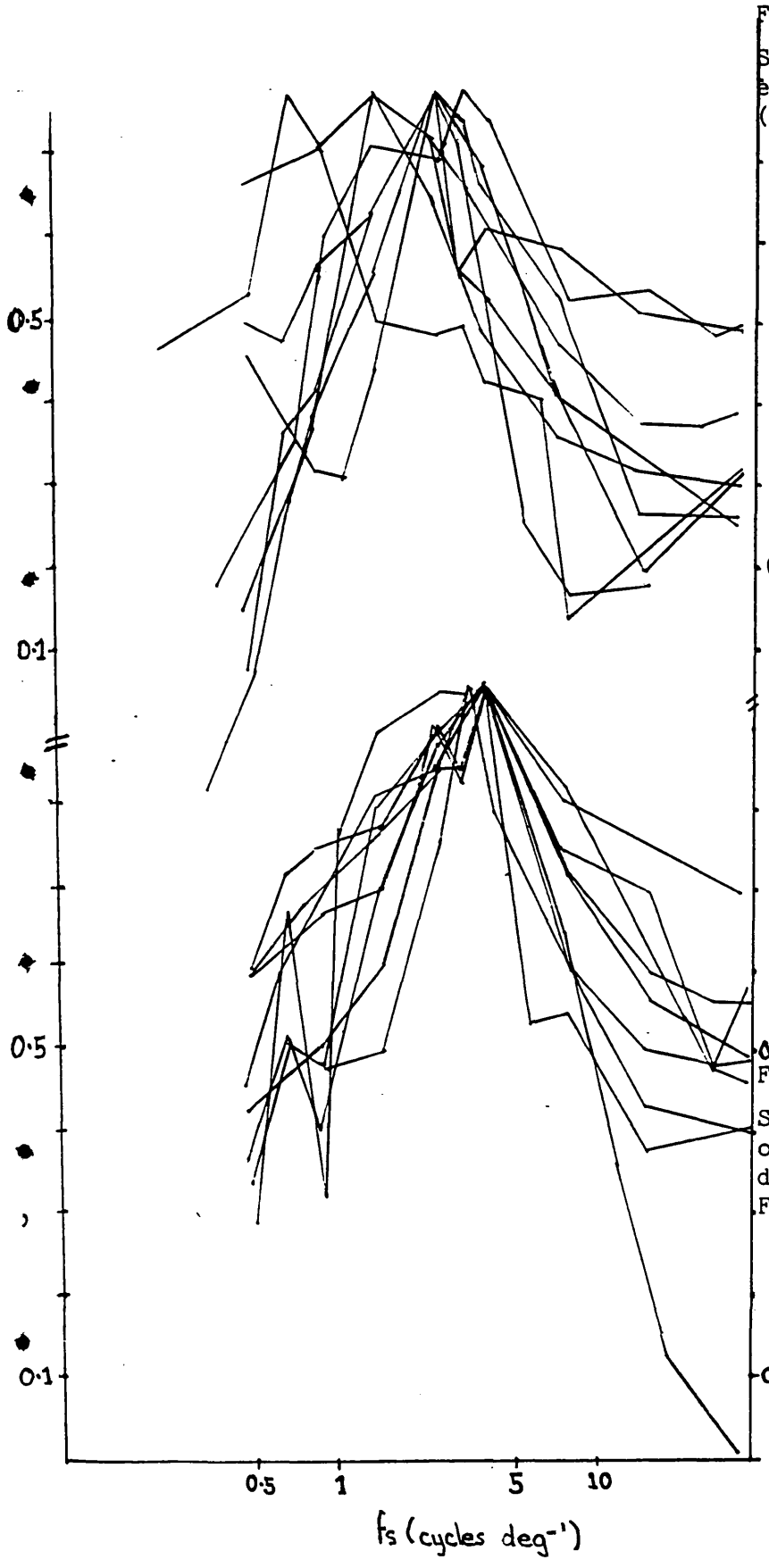

Fig. 5.34

ST1 spatial responses for the amblyopic eyes of nine untreated amblyopes (Strabismic and refractive).

Fig. 5.35

ST1 spatial responses for the normal eyes of the nine untreated amblyopes, with data for the "abnormal" eyes given in Fig. 5.34.

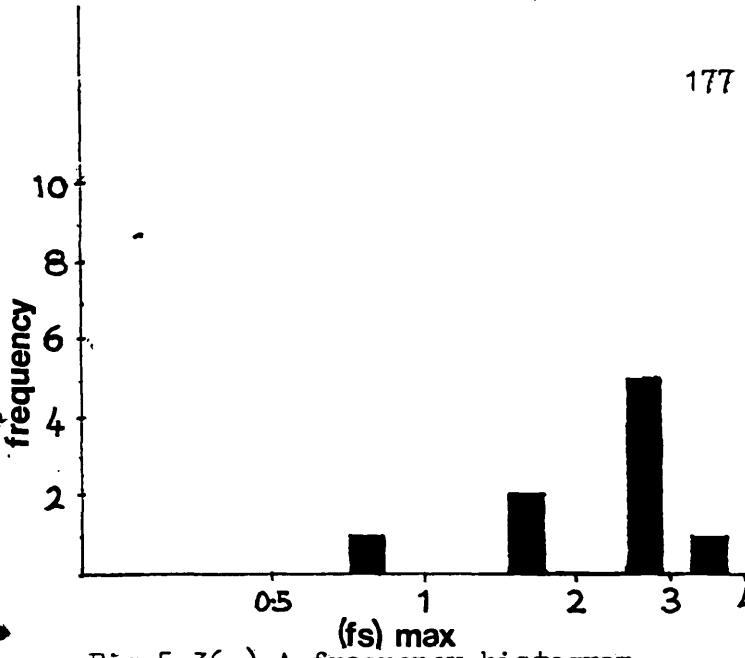

Fig.5.36a) A frequency histogram of the peak position of the response curves shown in Fig.5.34.

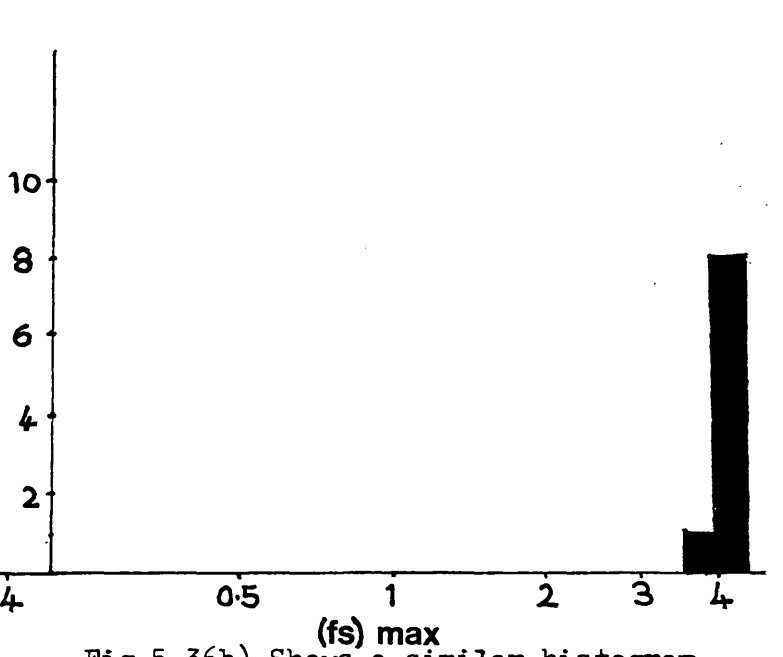

Fig.5.36b) Shows a similar histogram of the peaks of the response curves from Fig.5.35 (normal eyes).

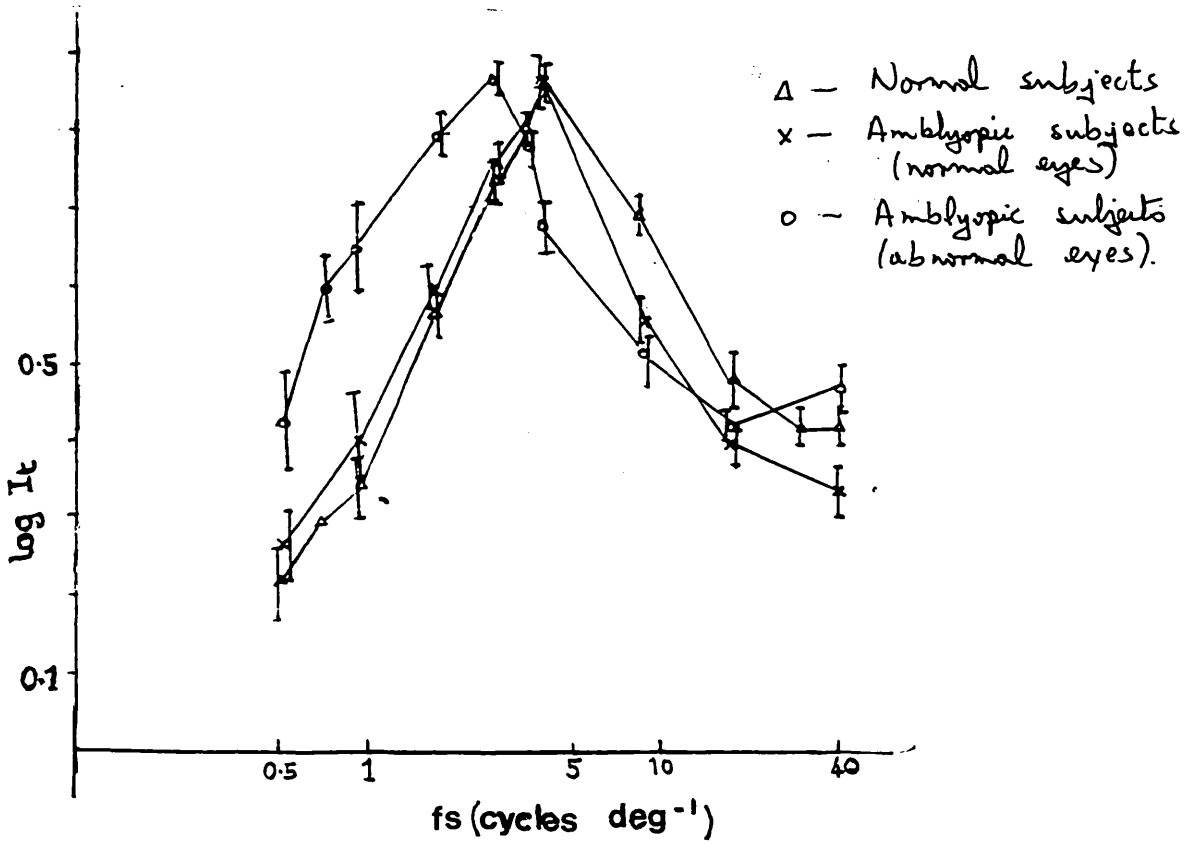

Fig. 5.37 Mean ST1 spatial response curves taken from the data for the untreated amblyopes (amblyopic eyes, Fig.5.34) and normal eyes (Fig.5.35). Also shown are the mean values for seven normal subjects (Fig.5.2).

difference between data for the "normal" and "abnormal" eyes are plotted and it can be seen that the A-A response deviates from the "normal" eyes response represented by line AB. By inspection of Figures 5.28 and 5.37 the experimental results seem consistent with the suggestion that the "normal" eyes are influenced by patching treatment.

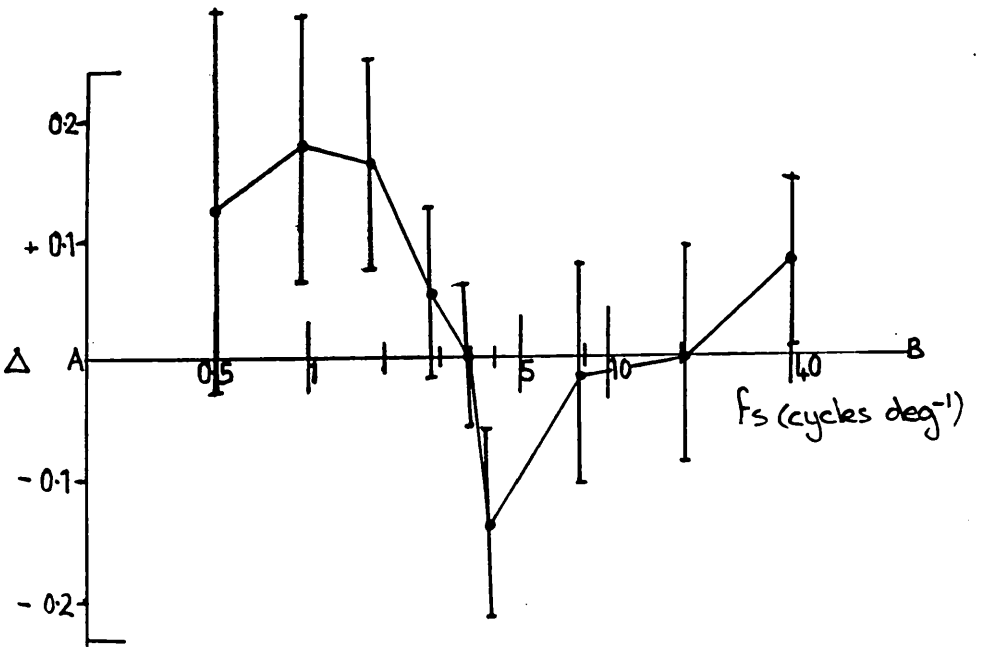

Fig. 5.38 The difference graphs are determined by the equation $((\log I_t)_{AA} - (\log I_t)_{AN})$ as for Fig. 5.33.

The Influence of Age of Onset of Amblyopia on the ST1 Spatial Response

In studies of X-cell recordings and in behavioural tests on cats with surgically induced amblyopia (Ikeda, 1980), it has been shown that receptive field size of ganglion cells is related to age of onset. The frequency for peak ST1 spatial response for each subject is therefore plotted against age of onset as shown in Fig. 5.39. A line of regression was drawn for each respective set of data and is shown on the figure. The following features of this plot should be noted a), In untreated amblyopes, the amblyopic eyes have in the main lower peak frequencies than do the normal eyes, with a tendency that the earlier the age of onset the lower the peak frequency (symbol,●). In the case of the amblyopic eyes, the responses include data for two subjects with congenital visual defects, a rod monochromat and an albino, both of which may be regarded as forms of amblyopia. Inclusion of their data provides a better distribution of points over the age range, as in most of the untreated subjects, amblyopia was not detected until after 7 years of age.

The correlation coefficient for the untreated amblyopic eyes is 0.80, significant at 0.01 level.b) For the untreated amblyope's "normal" eyes (symbol,+), (f_s) max. is almost exclusively equal to 4.3 cycles deg^{-1}, the peak position for normal vision, thus there is no correlation with age as the values are essentially constant; c) In treated subjects the value (f_s) max. for the amblyopic eyes (sumbol, ●), shows a progressively higher spatial frequency as the age of onset increases, and a strong linear correlation is found (coefficient r = 0.78 significant at 0.01 level.d) The"normal"

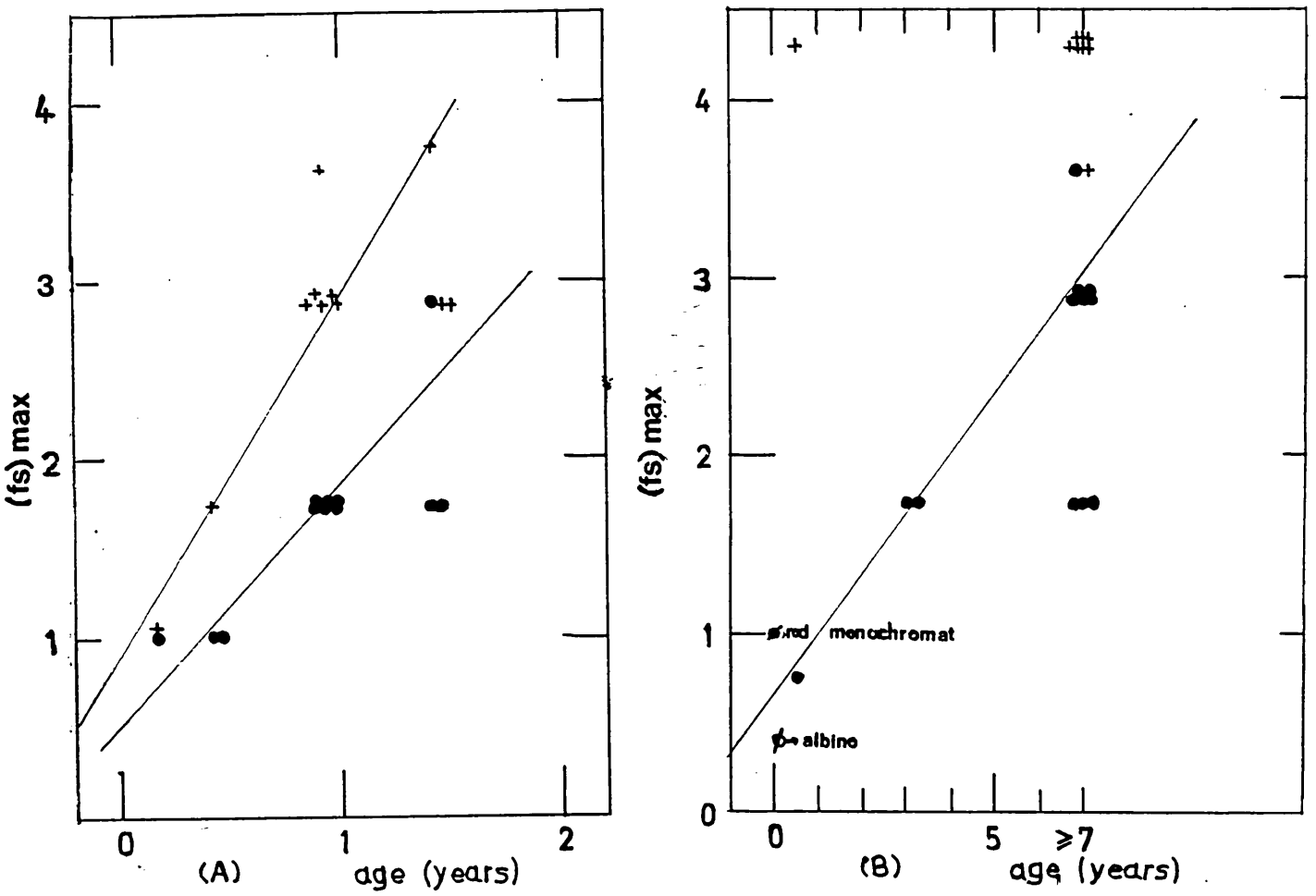

Fig.5.39 The peak positions of the ST1 spatial response curves of the amblyopic observers are plotted against age of onset/age first noticed.
A. gives the responses of the treated subjects (+),=the ' normal ' eyes results ;(●),= the amblyopic eyes responses.
B. gives the responses of the untreated subjects symbols as for A. On this diagram also appears the results of a rod monochromat (ø), and an albino (ø).

eyes of patch treated subjects (symbol, +) show a change of (f_S) max. with age of onset, similar to that of the amblyopic fellow. As for the amblyopic eye of the treated subject a strong linear correlation is found (coefficient r = 0.81, significant at 0.01 level). In the treated subjects the data is restricted to the age range up to two years. Patching treatment commenced at the time when amblyopia was first noted, thus the age axis corresponds to the "age at which treatment commenced". It has been shown that in three out of four classes of eye there is a significant positive correlation between the age at which amblyopia was noted and the value of (f_S) max. and such correlation implies that the younger the age at which amblyopia occurs, the greater is the low frequency displacement of (f_S) max. relative to the normal value. Ikeda and Tremain (1978) showed that in cats with surgically produced squints, amblyopia was more severe as the age of its induction decreases, corresponding to arrested visual development in the kittens. No data is presented for the ST1 responses in children between the ages of 1 to 7 years, therefore we do not know whether the age changes in (f_S) max. values correspond to arrested development in their amblyopic eyes. It should be noted when considering the data present here that the ST1 spatial responses were determined only at discrete values of the spatial frequency variable, f_S, and that the age at which amblyopia was first noted does not necessarily correspond to the age of its onset.

5.10 The Relationship Between the ST1 Spatial Response and Visual Acuity

The ST1 spatial response is relatively finely tuned, and is therefore likely to be involved in the task of spatial resolution, as are the X-type electrophysiological mechanisms to which they correspond. The observation that in amblyopic subjects, the ST1 mechanism has abnormally coarse spatial response, is thus consistent with the reduced visual acuity associated with amblyopia. The peak frequencies (f_S) max for the ST1 spatial responses of all the amblyopicsubjects, including two congenital defectives, have therefore been plotted against Snellen visual acuity (Fig. 5.40). The open circles denote the data for the amblyopic eyes and the full circles those of the "normal" eyes. It is seen that (f_S) max. increases significantly with visual acuity. The line of best fit for the data is plotted on the graph and the coefficient of correlation $r = 0.65$, is significant to the 0.01 level. In the normal eyes (full circles) the scatter in peak frequency values is not reflected in the visual acuity values. The lack of one to one correlation between visual acuity and (f_S) max, may result from the choice of the Snellen chart for acuity measurement. The Snellen chart consists of high contrast figures which are familiar to the subject, thus "resolution" may involve mechanisms other than purely visual ones. In retrospect, it would have been advantageous to measure acuity with neutral targets such as gratings and perhaps to measure vernier acuity. Unfortunately it was impossible to undertake a further set of time-consuming experiments with the same subjects. Another factor which could affect acuity is the patching treatment discussed in the previous section. Thus, it was decided to re-plot the data of Fig. 5.40 excluding subjects

who had received patching. The data is presented in Fig. 5.41, and show a better linear correlation than between (f_s) max. and V.A. in the data of Fig. 5.40. A stronger linear correlation is found with the data of Fig. 5.41, with a coefficient of correlation $r = 0.72$, significant to the 0·01 level. It should be noted that in Fig. 5.41, all values of V.A. of $\frac{6}{60}$ or below are recorded at the value for $\frac{6}{60}$, plotted on the graph as 0.1 , while recorded Snellen acuities of $\frac{6}{6}$ or better are recorded as $\frac{6}{6}$, plotted as unity on the graph, and this assists in producing the better correlation. The improved correlation between (f_s) max. and V.A. which is observed in untreated amblyopes probably reflects the disturbance of visual acuity development which accompanies extensive patching treatment. The ST1 mechanism acts as a general, early stage visual filter subserving high spatial resolution (Holliday and Ruddock, 1983), thus its low frequency response characteristics in amblyopia should result in reduced spatial resolution. Similarly, low-frequency spatial response in X-type ganglion cells of amblyopic cats leads to low visual resolution (Ikeda, 1980). Some support to the above is given by the data but considerable scatter is present, particularly in the "normal" eyes. Acuity cannot be uniquely defined by (f_s) max. thus factors other than the ST1 spatial response must also influence visual resolution. This implies that acuity may be being altered by subsequent operations on the filter outputs, such as the extraction of "zero-crossings" as proposed by Marr and Hildreth (1980). The experimental data obtained requires that such operations are subject to variation in amblyopia, and so cause the observed variations in visual acuity for a given value of (f_s) max.

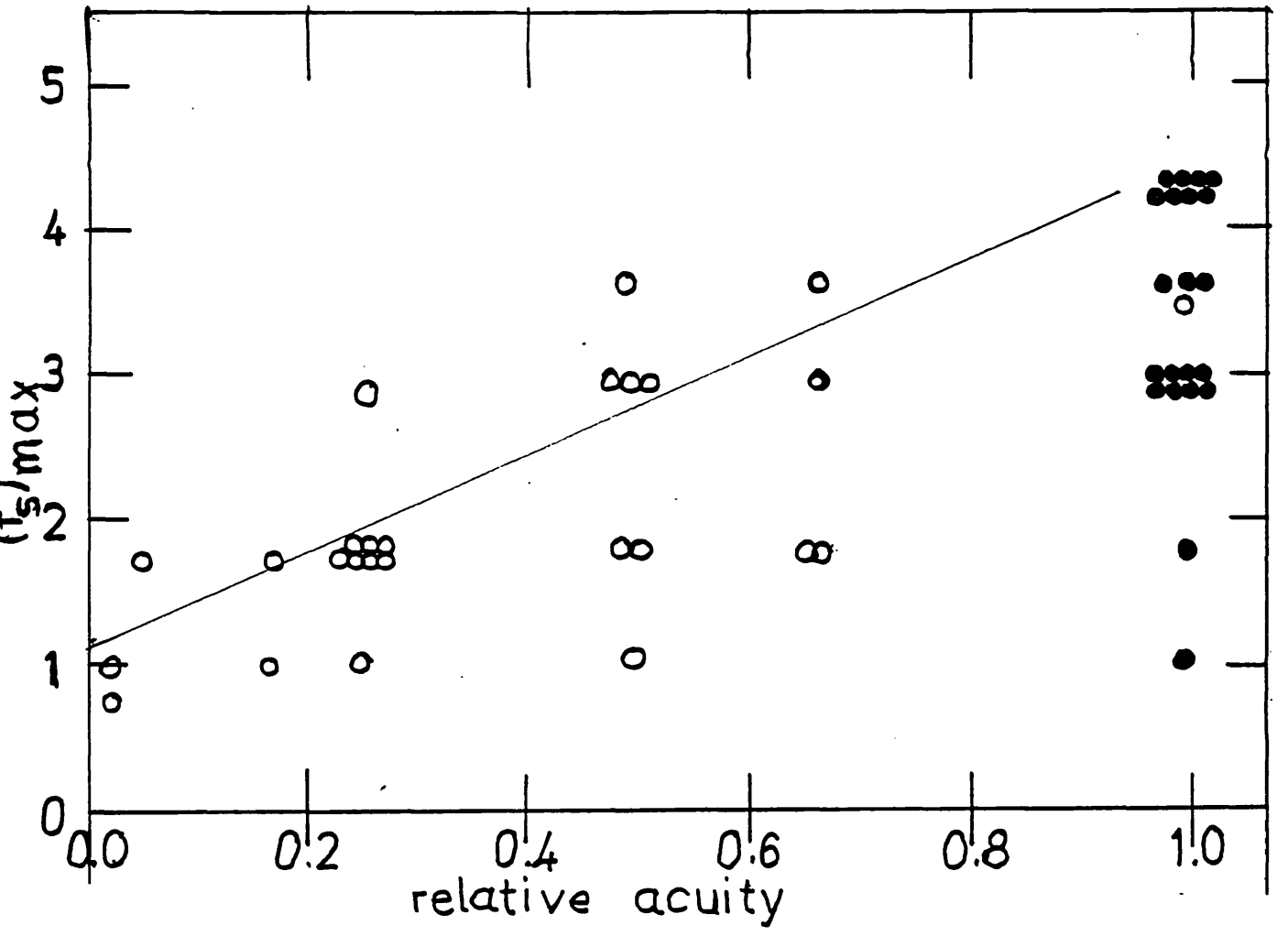

Fig. 5.40 Spatial frequency for the peak of the ST1 spatial response curves plotted against relative visual acuity. Filled circles denote data for normal eyes and open circles data for amblyopic eyes.

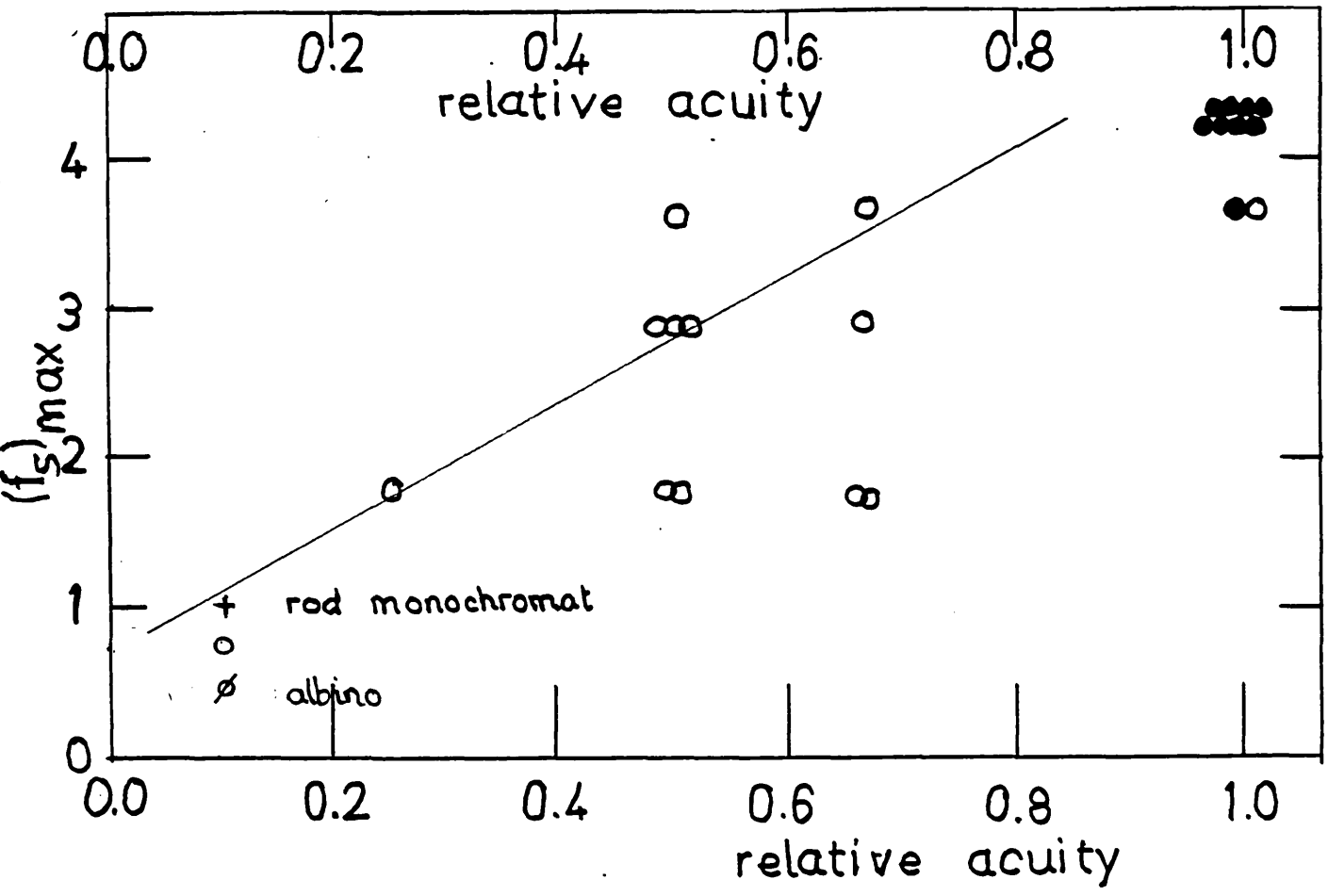

Fig.5.41 Spatial frequency data for the peak of the ST1 spatial response curves plotted against relative acuity. Full circles denote data for normal eyes and open circles data for amblyopic eyes of untreated amblyopes. The responses of a rod monochromat (+), and for an albino (ø).

5.11 The Influence of Eccentric Fixation on the ST1 Spatial Response

Nearly all the strabismic subjects had some degree of eccentric fixation, and it has been argued that accentric fixation is always present in strabismics (Mallet, 1969). As is seen from the table of Fig. 5.1, all subjects with constant eccentric fixation, fixate at 3° or less from the fovea and two of the subjects have wandering fixation, averaging at 5°, due to very poor V.A. In the ST1 measurements the target moves over the central 8° of the visual field, (see Chapter 4, Section 4.2.2) which is a considerably larger angle than that associated with eccentric fixation as observed in our subjects, thus it is unlikely that the changes in the ST1 spatial responses caused by strabismic amblyopia can be the consequence of eccentric fixation. Further, the data recorded at different retinal eccentricities shows that for normal subjects, the ST1 spatial response for 20° eccentricity (Fig. 5.20) is displaced to higher spatial frequencies than the "foveal" responses of some amblyopes (Fig. 5.4.) and this, again, is consistent with the view that amblyopia cannot be explained simply in terms of eccentric fixation. A plot of the frequency, (f_s) max., for the peak ST1 spatial response (data for amblyopic eyes) against the degree of eccentric fixation in degrees, does, nonetheless, produce a significant correlation (Fig. 5.42). The coefficients of correlation, r, is equal to -0.60 , significant at 0.01 level. It has been suggested that the reduction of visual acuity in amblyopia simply reflects the normal reduction in acuity associated with non-foveal stimulus presentation (Flom and Weymouth, 1961 and Mallet, 1969), however, this theory is not supported by quantitative analysis (Hess, 1977 and Kirshen and Flom 1978). It has clearly been shown that there is a

correlation between the frequency at which the ST1 spatial response peaks and the age of onset of the squint (Fig. 5.39). Generally, subjects with higher levels of eccentric fixation have poorer visual acuity, and if eccentric fixation is plotted against V.A. a reasonable correlation is again achieved, with r at -0.53 , significant to 0·02 level. (Fig. 5.43).

In general then, V.A. correlates with the ST1 spatial frequency peak position, which in turn is representative of the receptive field size, showing a similar relationship to that found in electrophysiological studies (Ikeda, 1980).

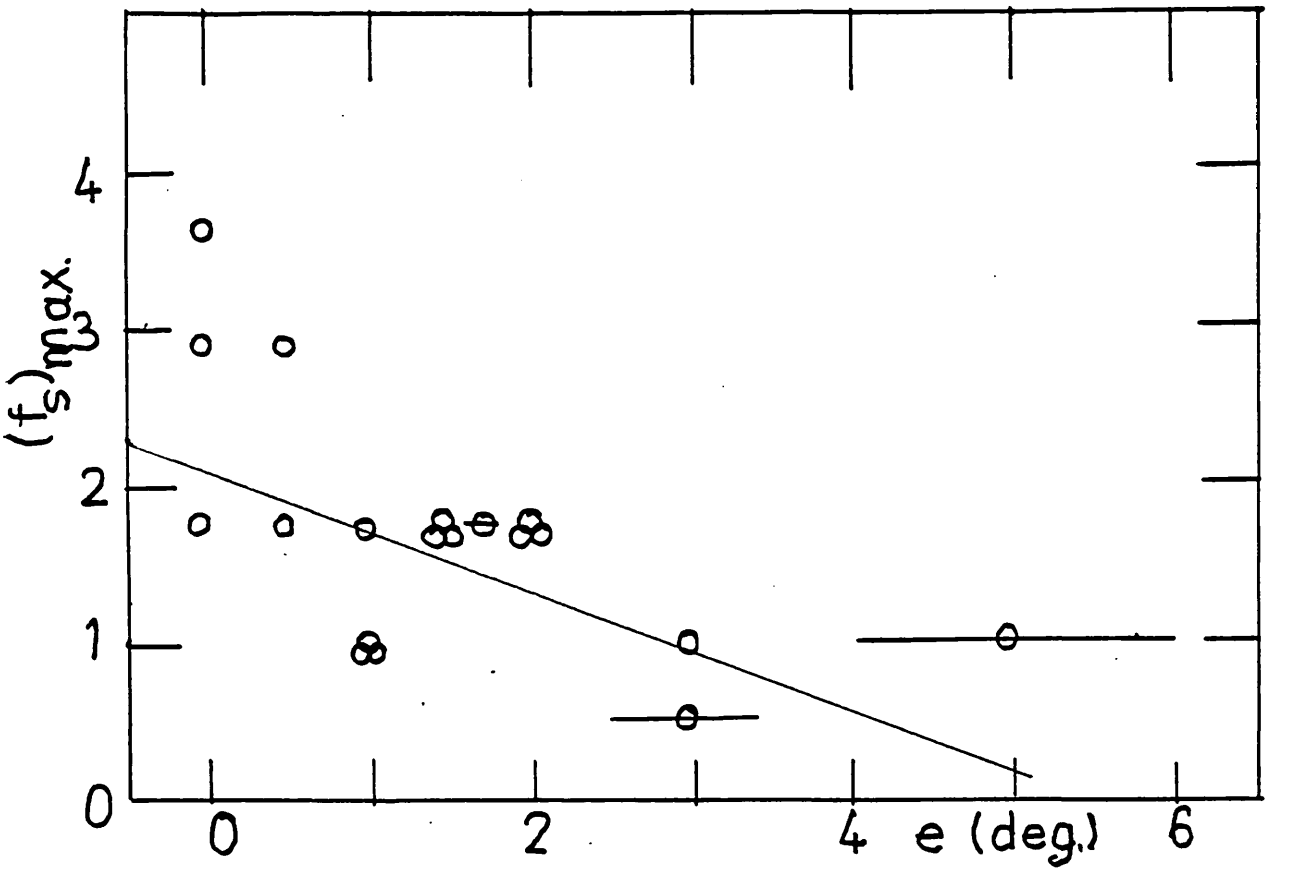

Fig. 5.42 Spatial frequency for the peak ST1 spatial response plotted against eccentric fixation angle. Data refer to the amblyopic eyes of strabismic subjects. Three results are shown with a horizontal line passing through the symbol. This line length denotes the variable fixation range of these subjects.

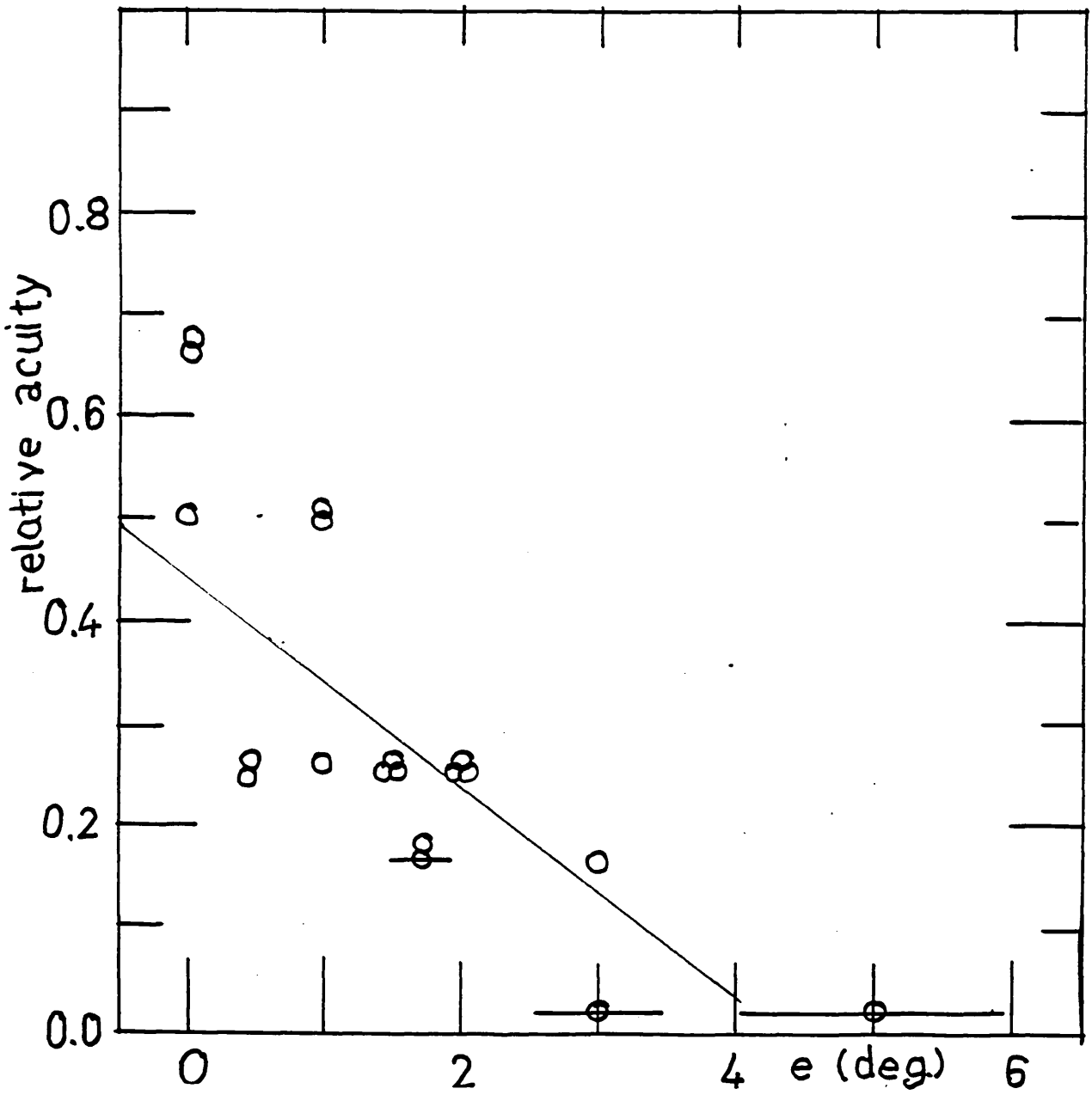

Fig.5.43 The angle of eccentric fixation (in degrees) is plotted against relative visual acuity. Data is for the amblyopic eyes of the strabismic subjects. As in Fig.5.42 three responses have horizontal lines denoting the range of variability of eccentric fixation of these subjects.

Chapter Six Characteristics of the Spatio-temporal Filter Type 2 (ST2) in Abnormal Visual Systems.

6.1. Introduction

The background modulation method for the isolation of spatio-temporal visual response mechanisms reveals, in addition to the ST1 filter examined in Chapter 5, a second filter designated ST2. The response characteristics of this filter suggest that it correlates with the Y-type psychophysical mechanisms. The temporal and spatial responses of the ST2 filter have been measured for 9 amblyopes, 7 strabismic and 2 refractive, taken from the larger group for which the ST1 spatial response was measured. Data were also obtained for a group of 6 subjects with normal vision.

6.2. The ST2 Temporal Response in Amblyopia

The ST2 temporal response was obtained as explained in Chapter 4, Section 4.2.3.2. and is displayed as log illumination, log I_t, for detection of the circular moving target, plotted against the temporal flicker frequency of the background field. ST2 temporal response curves for individual subjects, normalised to give the same peak value, are plotted in Fig. 6.1 and 6.2, the former referring to the "normal" and the latter to the amblyopic eyes of the 9 amblyopes. Each data point is the mean of five readings with standard error of the order ± 0.3 log units in log I_t. The average values of the data points in Fig. 6.1 and 6.2, normalised to give the same peak, are plotted in Fig. 6.3a, with error bars denoting the standard errors of the data points. Also shown in Fig. 6.3a is the mean normal response curve for 6 normal subjects. The difference Δ, between the mean curves for the normal and

amblyopic eyes are plotted against fs, in Fig. 6.3b. The data shown in these three figures establish that the ST2 temporal response curves for each eye of the amblyopes and for the normal subjects are all similar to each other. There appears, however, to be a greater spread between individual data curves for the "amblyopic" eyes than is observed for the "normal" eyes of the amblyopes (Fig. 6.1 and 6.2).

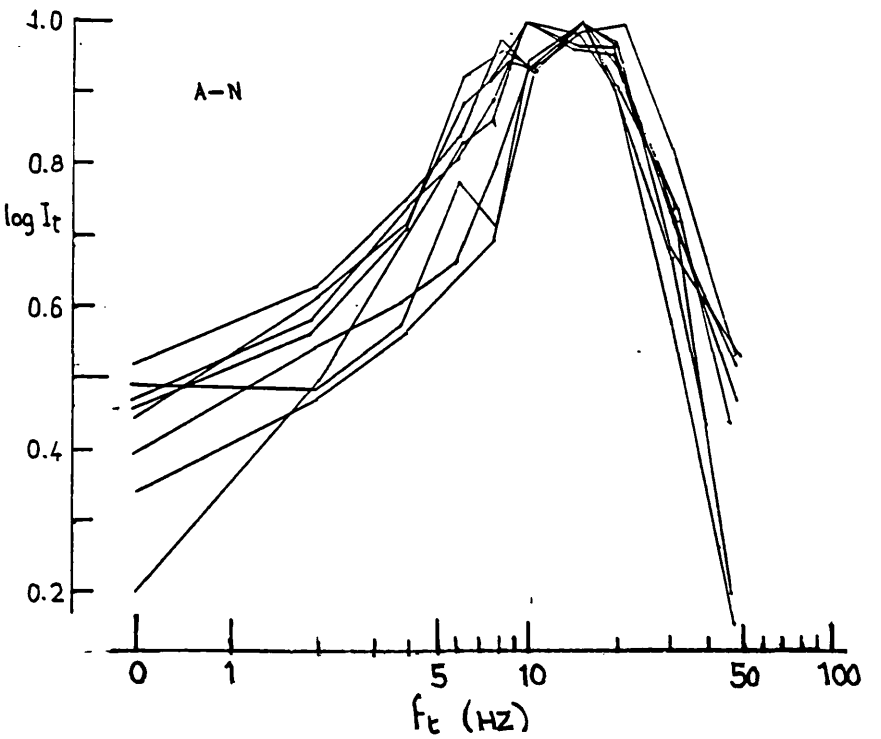

Fig. 6.1 ST2 temporal responses for the normal eyes of 9 amblyopes. Log threshold illumination for detection of the moving circular target is plotted against the modulation frequency of the background field moving horizontally at 15 deg/Sec^{-1}. The target was of diameter 1.4 deg and the background field was of average illumination 2.7 log trolands.

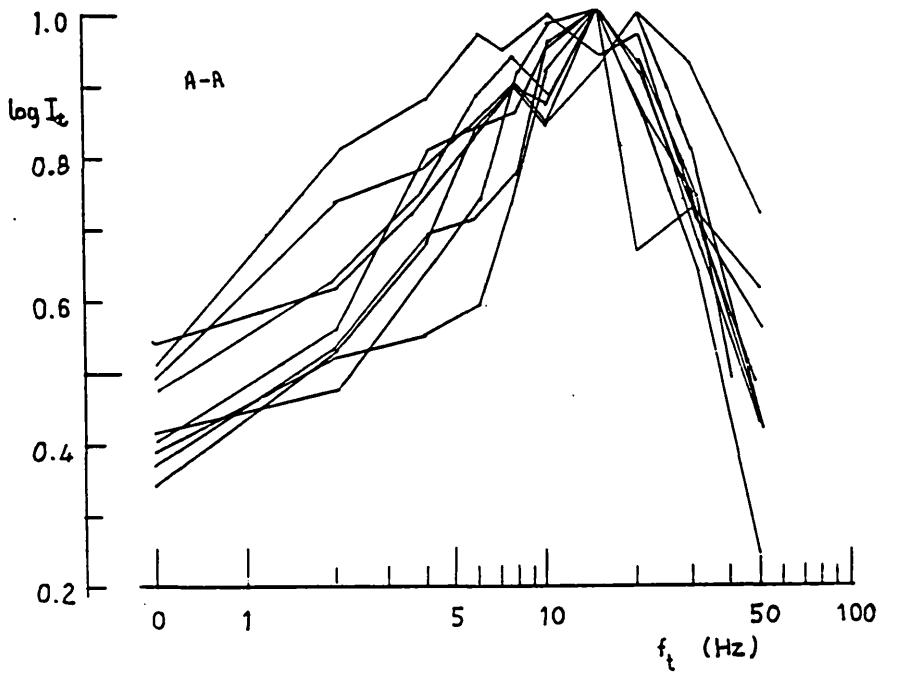

Fig. 6.2 As for Fig. 6.1 but for the amblyopic eyes of the 9 amblyopes. Other parameters as for Fig. 6.1.

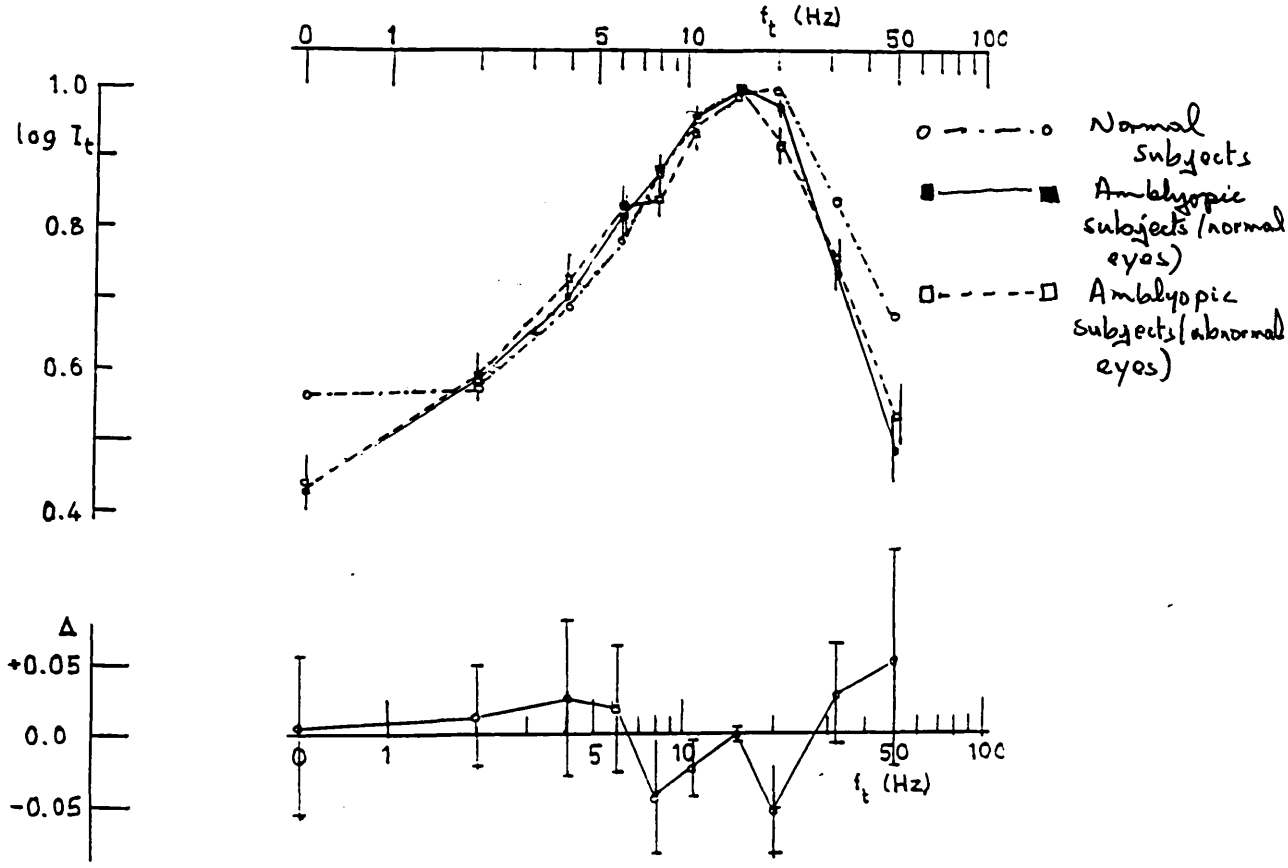

Fig. 6.3a) Shows the mean ST2 temporal responses of 9 amblyopic observers taken from Fig. 6.1 (normal eyes) and Fig. 6.2 (abnormal eyes) together with the average values for five normal subjects. Error bar denote ± 1 standard error.

Fig. 6.3b) This gives the difference graph determined by the equation $(\log I_t)_{AA} - (\log I_t)_{AN}$. Error bars denote ± 1 standard error.

6.3. The ST2 Spatial Responses in Amblyopia

The spatial responses of the ST2 filter were measured in the same 9 amblyopes for whom the corresponding temporal responses are given in Fig. 6.1 and 6.2, & 6 normal eyes were also checked by way of comparison. Measurements were made by the techniques described earlier in the methods chapter (Chapter 4, Section 4.2.3.3.). Thus, a circular target of 1.4^{o} diameter is moved laterally at 15^{o}/sec. across a background grating, which consisted of inter-digitated alternate steady and flickering (at 20Hz) bars (see Fig. 4.9). The average luminance of the flickering bars was maintained at the same level as that of the steady bars, namely 2.7 log trolands. The threshold, I_t, for detection of the moving target was measured as a function of the grating periodicity, fs. The spatial response data of the 6 normal subjects are plotted in Fig. 6.4, those for the normal eyes of the amblyopic eyes are plotted in Fig. 6.5 and those of their amblyopic eyes are plotted in Fig. 6.6, with all curves normalised to give the same peak value. Each point is the mean of five readings with typical standard deviation $\pm$0.03 log units. The mean values taken from each of Figs. 6.4 to 6.6 are plotted in Fig. 6.7a), and all three sets of data have been normalised to give the same peak value (the error bars are $\pm$1 standard error). In Fig. 6.6b), the difference Δ, between the mean $(\log I_t)_{AA}-(\log I_t)_{AN}$ log threshold values for the "normal" and the amblyopic eyes are plotted against fs. The results plotted in Figs. 6.4 to 6.7 show that like the temporal responses, the ST2 spatial responses are similar for all three groups of eyes, i.e. those of normal

subjects and the "normal" and amblyopic eyes of the amblyopes. Only in one case does the response curve for the amblyopic eye peak at a spatial frequency below 1 cycle deg^{-1}, and the peak for the normal eyes and the data for this subject will be discussed together with those for an albino subject, D.C, which are presented in the next section.

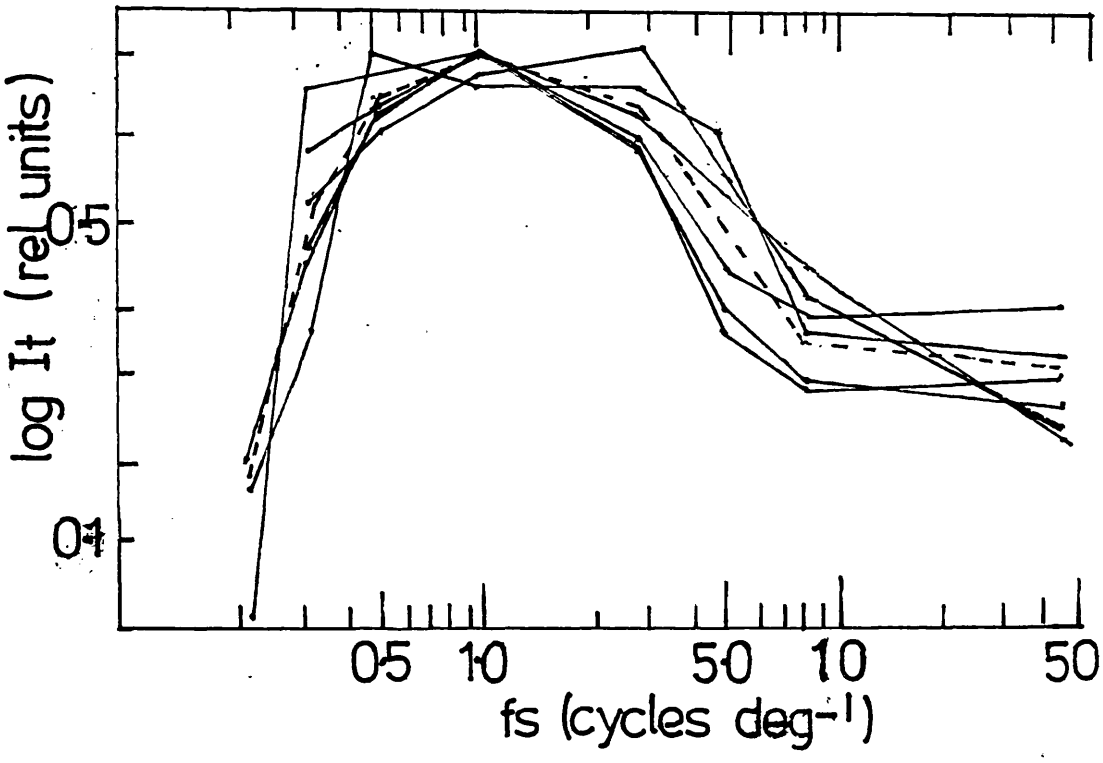

Fig. 6.4 Normalised ST2' spatial response curves measured for 6 subjects with normal vision. Illumination, I_t, for detection of the moving target is plotted against the spatial frequency fs, of the background grating. The target was a 1.5deg. diameter white light spot, moving at 15 deg. sec.$^{-1}$ along the horizontal meridian. The background consisted of alternate steady and flickering bars of equal width, forming a vertically orientated background grating of fundamental spatial frequency, fs. The background field was of mean illumination level 2.7 log trolands, and the alternate flickering bars were 100% modulated at 20Hz around this average value. Dashed line shows the mean response curve of the 6 subjects.

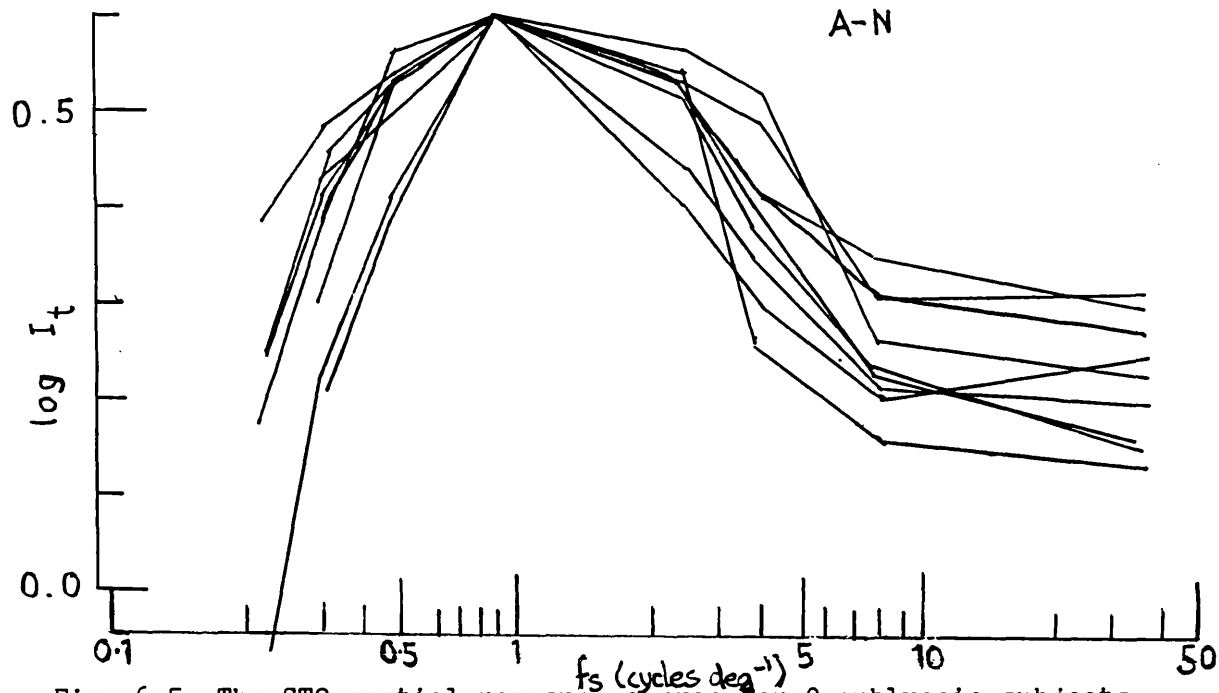

Fig. 6.5 The ST2 spatial response curves for 9 amblyopic subjects, measured for the normal eyes. Other parameters as for Fig. 6.4.

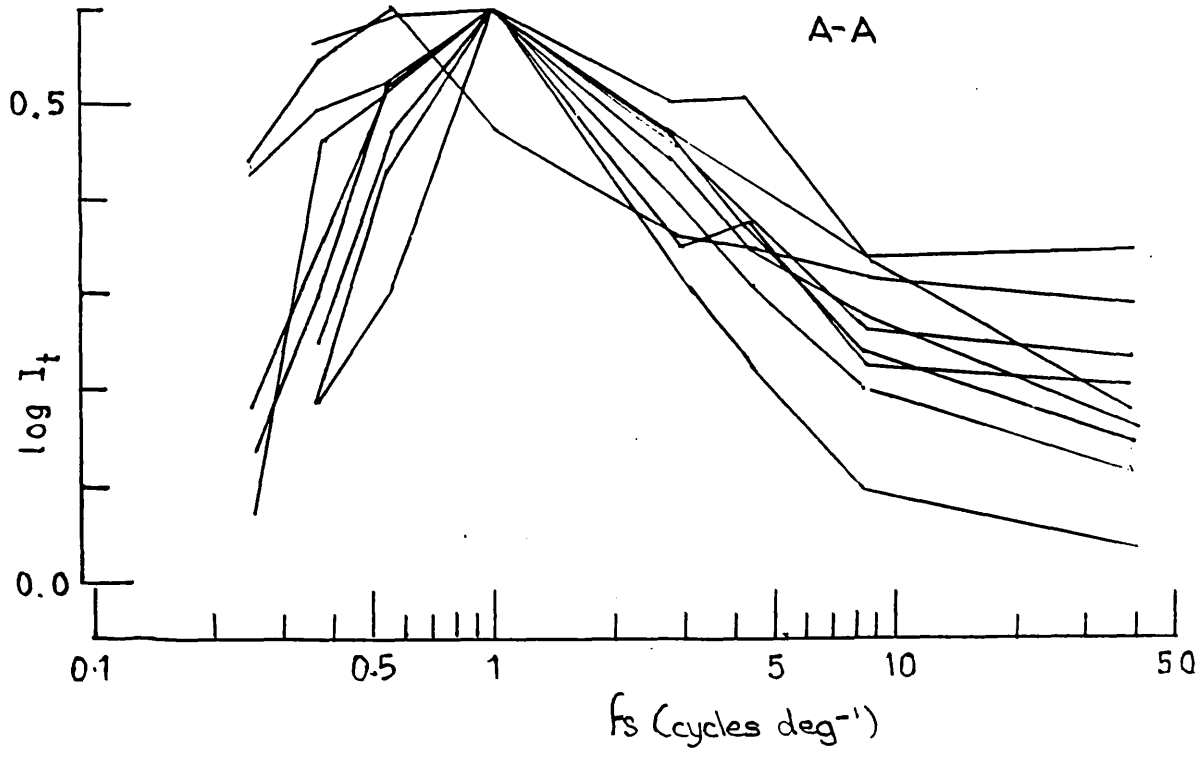

Fig. 6.6 The ST2 spatial response curves for 9 amblyopic subjects, measured for the amblyopic eyes. Other parameters as for Fig. 6.4.

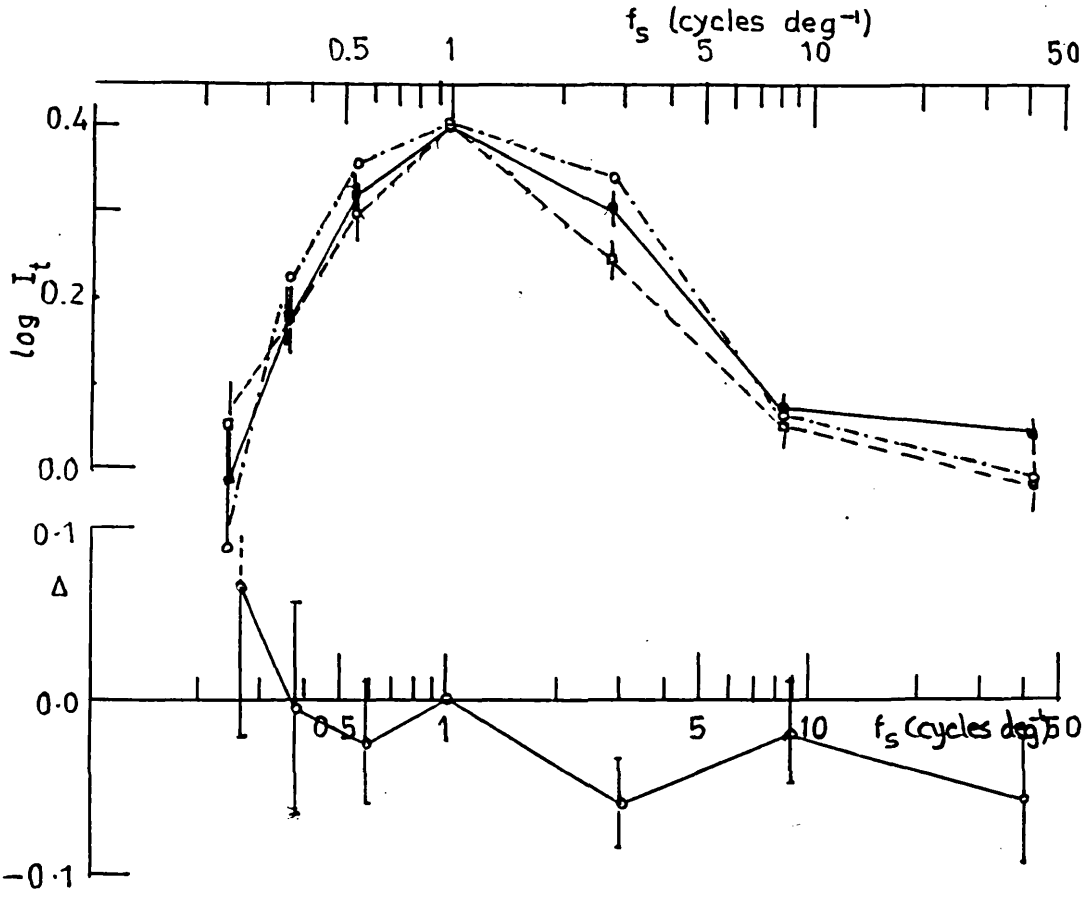

Fig. 6.7a) Average ST2 spatial responses for the 6 normal subjects (O---O), for the amblyopic eyes (●-●) and the "normal" eyes (□-□) of the 9 amblyopes, taken respectively for Figs. 6.4, 6.5 and 6.6. Error bars denote ±1 standard error.

Fig. 6.7b) The difference between log I_t for the abnormal and normal eyes of the 9 amblyopes, given by

$$(\log I_t)_{AA} - (\log I_t)_{AN})$$

plotted against fs.

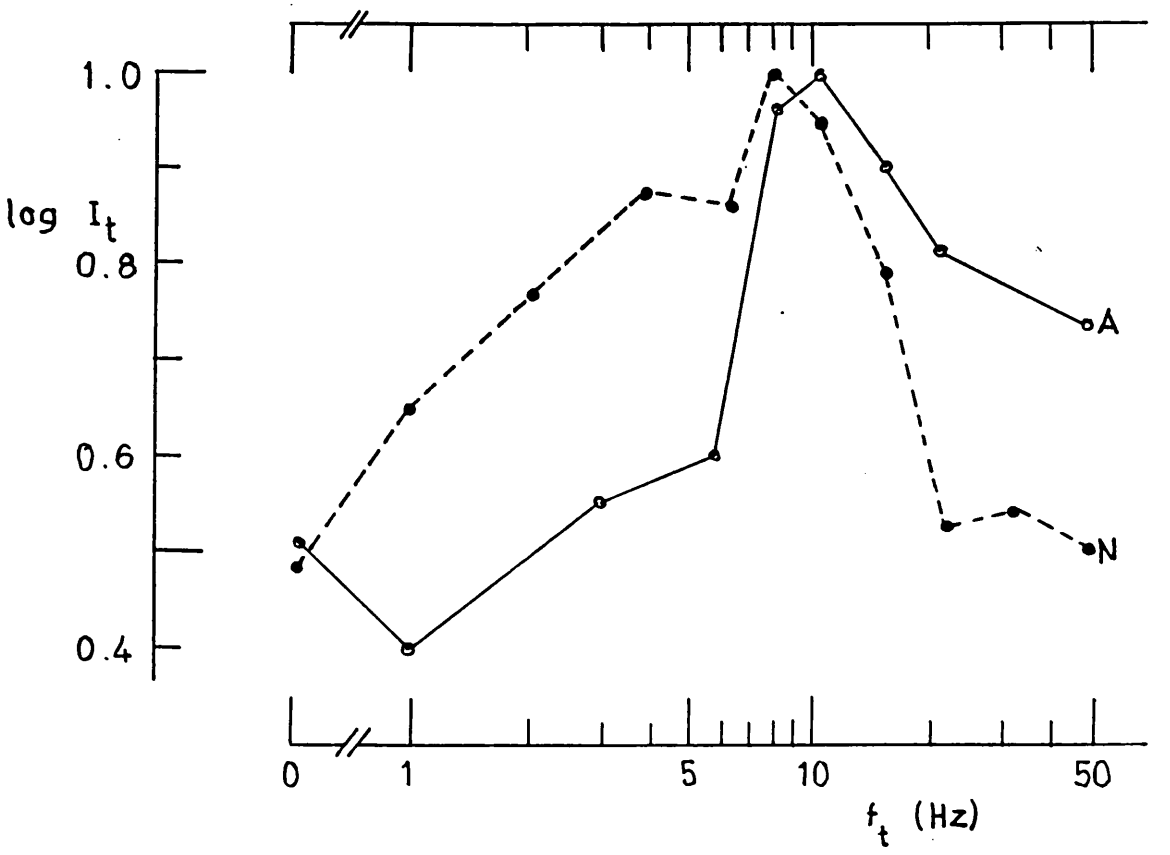

Fig. 6.8 ST2 temporal response for a normal observer I.H (full circles) and an albino D.C (open circles). Threshold illumination log I_t, for detection of 3.5 deg circular target is plotted against the background temporal modulation frequency f_t, the target moved horizontally at 15 deg sec^{-1} and the mean background illumination was 2.7 log trolands.

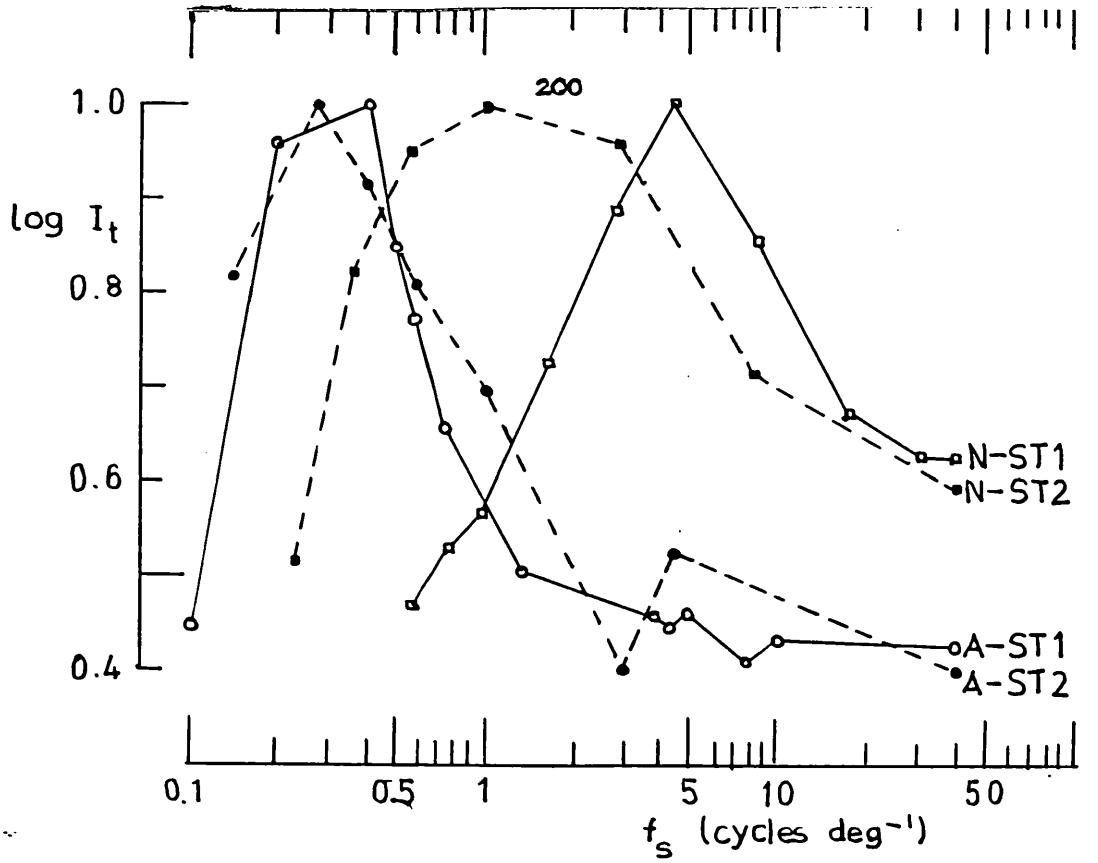

Fig. 6.9 The ST1 and ST2 spatial responses for the albino subject D.C (open and closed circles respectively) and the corresponding average curves for normal subjects taken from Fig. 5.2 (open squares) and Fig. 6.8 (closed squares). The stimulus parameters for D.C were the same as those used in the corresponding measurements for the normal subjects.

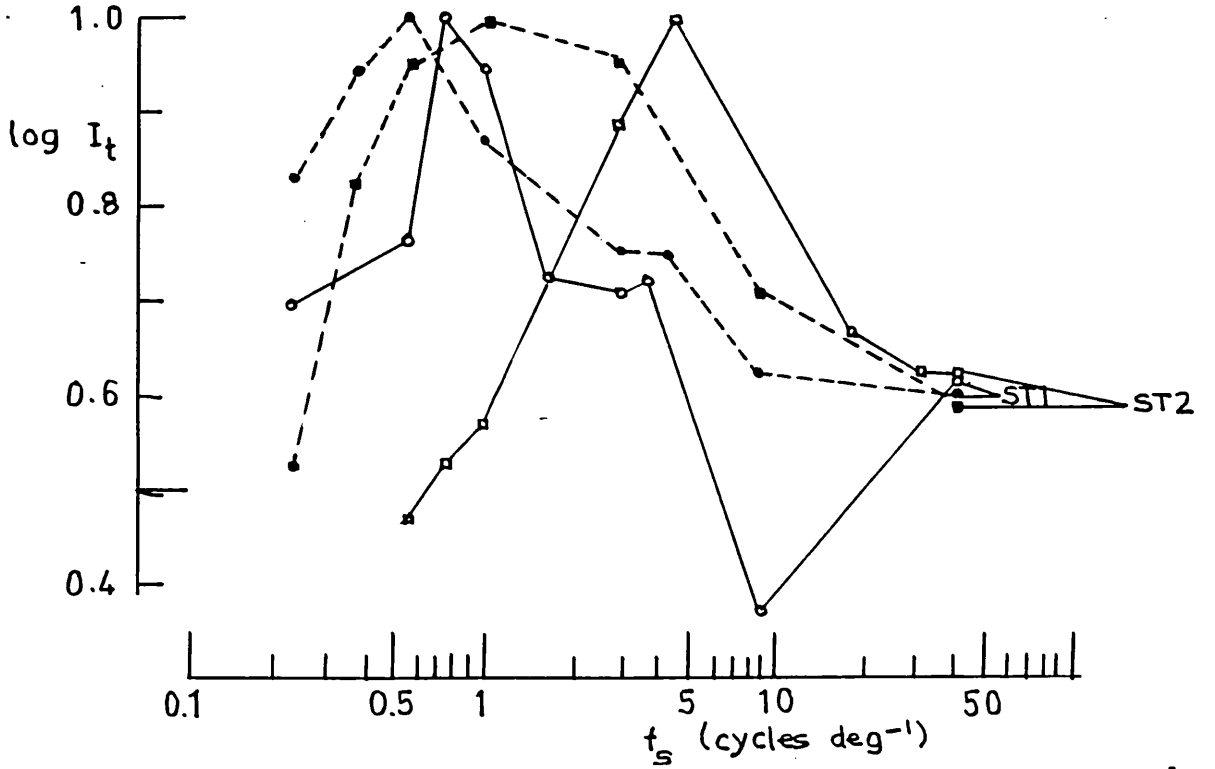

Fig. 6.10 As for Fig. 6.9, but data for a strabismic amblyope G.

6.4. ST2 Responses for an Albino Subject D.C

This subject is classified as tyrosinase negative on the basis of the hair test, and exhibits marked nystagmus coupled with very low spatial resolving power, corresponding to $\frac{3}{60}$ Snellen in each eye. His ST1 spatial response has already been measured by Barbur et al, 1980 (and discussed in Chapter 5, Section 5.5), who also showed that his poor resolution is post-receptoral in origin. His ST2 temporal response, measured for a 1.4 log Troland background, is plotted in Fig. 6.8 (open units) and is similar to the data recorded for a normal subject (closed circles). D.C's ST2 spatial response is plotted in Fig. 6.9 (full circles) together with his ST1 spatial response (open circles) and the normal ST1 and ST2 spatial responses (squares). It is clear that D.C's ST2 and ST1 spatial responses are similar to each other and that both are displaced to low spatial frequencies relative to the normal ST2 spatial response curve.

6.5. Discussion of the Amblyopic ST2 Response Data

The experimental results show that the ST2 temporal results for amblyopic vision are essentially normal (Fig. 6.1 to 6.3) which is consistent with the results of previous studies showing that critical fusion frequency is unaltered in amblyopia (Lavergne, 1967). The more significant result is that the ST2 spatial response is, with the exception of the strabismic amblyope G, essentially normal in amblyopia, in marked contrast to the ST1 spatial response. Thus, it appears that the spatial response of the ST1 filter can be changed without affecting the ST2 spatial response. This is consistent with the network

model of the two filters proposed by Holliday and Ruddock (1982), (Chapter 2, Section 2.2.3.). The spatial response of the ST2 filter is determined by the spatial array of its inputs from the ST1 filters, and should not depend on the spatial response of the ST1 filters themselves, except in the situation where the ST1 spatial distribution exceeds that of the normal ST2 response. This latter is the case for two of the subjects, the albino subject D.C (see Fig. 6.9) and the strabismic amblyope G, whose data are plotted separately in Fig. 6.10. For both these subjects, the ST1 response is shifted to a lower spatial frequency than the normal ST2 response, that is, it is spatially coarser. In both cases, the ST2 spatial response is also shifted to lower spatial frequencies than the normal counterparts, and is similar to the ST1 spatial responses. As explained previously, this is consistent with the sequential organisation of the ST1 and ST2 filters shown in Fig. 2.7a, and b.

The conclusions regarding the ST1 and ST2 spatial responses are entirely consistent with the results obtained by Ikeda and her co-workers in their electrophysiological studies on cats with surgically induced squints (see Chapter 3, Section 3·2·1). They concluded that squint induced during the critical period of development leads to broadening of the receptive fields of X-type neurones, which exhibit marked loss of visual acuity. In contrast, the Y-type neurones remain essentially unchanged in their spatial properties. As was discussed in Chapter 3, Section 3·2·1 the ST1 and ST2 psychophysical mechanisms correspond to the X and Y-type electrophysiological mechanisms, thus the present observations that the former become spatially coarser in amblyopia while the latter are in most cases unchanged,

is consistent with the electrophysiological observations.

CHAPTER 7

Principal Results and Conclusions

The principal results and conclusions of this study are summarised below.

1) The ST1 spatial responses of the amblyopic subjects and one albino were measured for a mean background luminance of 1.4 log trolands. The response curves of both the amblyopic and, in many cases, the "normal" eyes are displaced to lower spatial frequencies than those obtained for "normal" subjects, (see Figs. 5.5 and 5.9). The majority of strabismic amblyopes exhibit a low frequency shift in the "normal" eye, whereas the majority of refractive amblyopes do not.

After careful inspection of the data of each subject it was found that those subjects who had received long-term direct patching, whether refractive or strabismic, show a low frequency shift in the ST1 spatial response of the normal eye, although the shift is less than for the amblyopic eye. In contrast, the ST1 spatial response, measured for the normal eyes of untreated subjects, is similar to the normal response in normal subjects, although their amblyopic eyes show a characteristic shift towards lower spatial frequencies. (Figs. 5.27, 5.28, 5.30, 5.32, 5.33 and 5.35).

It is postulated that the abnormal ST1 spatial responses of normal eyes in patch-treated subjects is the consequence of developmental impedance during the critical period, caused by

long-term occlusion of the normal eye.

2) The displacement of the ST1 response curve to lower spatial frequencies implies that there is a loss of fine spatial tuning in amblyopia and this is shown by the computed "receptive field" profile for the amblyopic eyes of the strabismic subjects (Fig. 5.25).

3) Eccentric fixation is present in most of our strabismic subjects but it is not thought to be a significant factor in the changes found in the I.M.G. (ST1 spatial response) for the following reasons:-

a) None of the refractive amblyopes have eccentric fixation, yet they too exhibit a low spatial frequency response for the ST1 mechanism.

b) The target used for these experiments was 3.5° in diameter and it remained visible whilst traversing 8° of visual angle. As the strabismic subjects with eccentric fixation suffered at worst 5° angular displacement of fixation which obviously lies well within the area of retina being examined, it cannot be of any direct influence. As already discussed in the text, however, it may have some indirect relationship to the severity of the amblyopia and to the peak shift. (Chapter 5, Section 5.11, Fig. 5.42).

c) When the ST1 spatial function is measured at varying degrees of eccentricity in normal subjects, it is found that an eccentricity of at least 20° is required to produce a response function with its

peak in the same position as that found in the ST1 spatial responses of 12 strabismic subjects, and 20° is far greater than the degree of eccentric fixation present in the subjects (Fig's 5.20 →5.23 inclusive).

4) When the ST1 spatial response is measured in the peripheral retina at progressively greater degrees of eccentricity, a gradual change in peak position towards progressively lower spatial frequencies is apparent (Fig's. 5.18, 5.19, 5.20 and 5.21). Furthermore, the amblyopic eyes show the same effect, only in there case the peak position appears at a lower spatial frequency than that of the normal control eyes, at all retinal locations (Fig's. 5.22, 5.23 and 5.24).

5) The ST2 spatial response was measured for both eyes of 9 amblyopic subjects (7 strabismic and 2 refractives). In all but one subject, the response curve was similar to that of 6 normal subjects (Fig's. 6.4, 6.5, 6.6a and b).

6) The average ST2 temporal response for the same 9 amblyopes and that for an albino subject did not differ from the normal ST2 temporal response. (Fig's 6.1, 6.2 and 6.3a and b).

7) For the albino and for one severe divergent strabismic subject, G, both the ST1 and ST2 spatial responses are shifted to low spatial frequency relative to the normal ST2 spatial response curve. For each subject the ST1 and ST2 curves are similar to each other, peaking at 0.3 to 0.4 cycles per degree for the albino, and at 0.56 to 0.75 cycles per degree in the strabismic amblyope G. It is argued that the loss of fine spatial tuning which occurs in the ST1, but not generally in the ST2 spatial responses in the amblyopes, is consistent with the sequential organisation of two classes of psychophysical filter proposed by Holliday and Ruddock (1982). This model (see Fig's. 2.7a and b) predicts that the peak of the ST2 spatial response will fall below its normal value when the ST1 spatial response is shifted to lower spatial frequency than the normal ST2 spatial response. The ST1 spatial response of both the albino (D.C.) and the strabismic amblyope (G) are shifted to lower spatial frequencies than the normal ST2 curve (Chapter 6, section 6.5, fig. 6.8 and 6.9).

8) In conclusion the findings show that in amblyopic subjects the ST1 function is significantly shifted to lower spatial frequency whilst ST2 functions are largely unaffected.

It has been shown, (Chapter3, section 3.2.1 and Chapter 6, section 6.2 and 6.3), that the psychophysically- determined ST1 function corresponds to the neurophysiologically- determined spatial frequency tuning of X-cells and the ST2 function, to that of Y-cells Thus our results are consistent with the findings of Ikeda and her co-workers, (Ikeda et al,1978, Ikeda and Tremain,1979, Ikeda, 1980), in the experimentally induced amblyopia in strabismic cats in which the spatial resolution of X- cells are significantly affected but that of Y- cells only to a minor degree.

DATA APPENDIX

In this section all the individual response curves for each observer, for ST1 spatial and ST2 spatial and temporal filter classes are presented, and the respective caption now follow.

Fig. D.A.1 shows the ST1 spatial responses of twelve treated strabismic amblyopes. Note that the peaks of the response curves are all shifted to lower spatial frequencies relative to the normal position which is indicated by the vertical dashed line. As can be seen, the amblyopic eyes (A) peak at lower f_s than do the fellow normal eyes (N).

The mean background light level was 1.4 log trolands and threshold settings were measured for a 3.5° white spot moving across a grating background at 15°/sec. (See Chapter 5, Section 5.2)

Fig. D.A.2a) shows the ST1 spatial responses of six refractive amblyopes. It is noted that again, in most cases the response curve peaks are shifted to lower f_s is than normal (dashed line). However, the displacement of the peak f_s is generally less marked and also the "normal" eye is only slightly displaced from the normal peak position. All other conditions are as above.

b) shows the ST1 spatial responses of four untreated strabismic amblyopes. Here it is noteworthy that only the amblyopic eyes (A) show response curve peaks lower than the normal peak value of $f_s = 4.3$ c/$^{\circ}$ (shown as dashed line). The normal eyes here show no peak displacement from the normal position (dashed line).

All other conditions as in D.A.1. (see Chapter 5, Section 5.8).

Fig. D.A.3 shows the ST2 temporal response for nine amblyopic observers. Here the response curves of the two eyes, amblyopic (A) and the normal (N), show very little difference. Log threshold illumination for the detection of a moving circular target is plotted against the modulation frequency of the background field moving horizontally at 15 deg sec.$^{-1}$. The target was diameter 1.4 deg. and the background field was of average illumination level 2.7 log trolands. (See Chapter 6, Section 6.2).

Fig. D.A.4. shows the response curve for the ST2 spatial filter of nine amblyopes (same observers as in Fig. D.A.3.). In all but one case (see Chapter 6, Section 6.3) the curves of both the amblyopic (A) and the normal (N) eyes show little variation in peak f_s position.

Threshold illumination I_t, for detection of a white circular target of diameter 1.5 deg. moving at 15 deg. sec.$^{-1}$, are plotted against the spatial frequency f_s, of the background grating. The background consisted of alternate steady and flickering bars of equal width with a fundamental spatial frequency, f_s. The mean background illumination level was 2.7 log trolands and the flickering bars were 100% modulated at 20Hz. (See Chapter 6, Section 6.3).

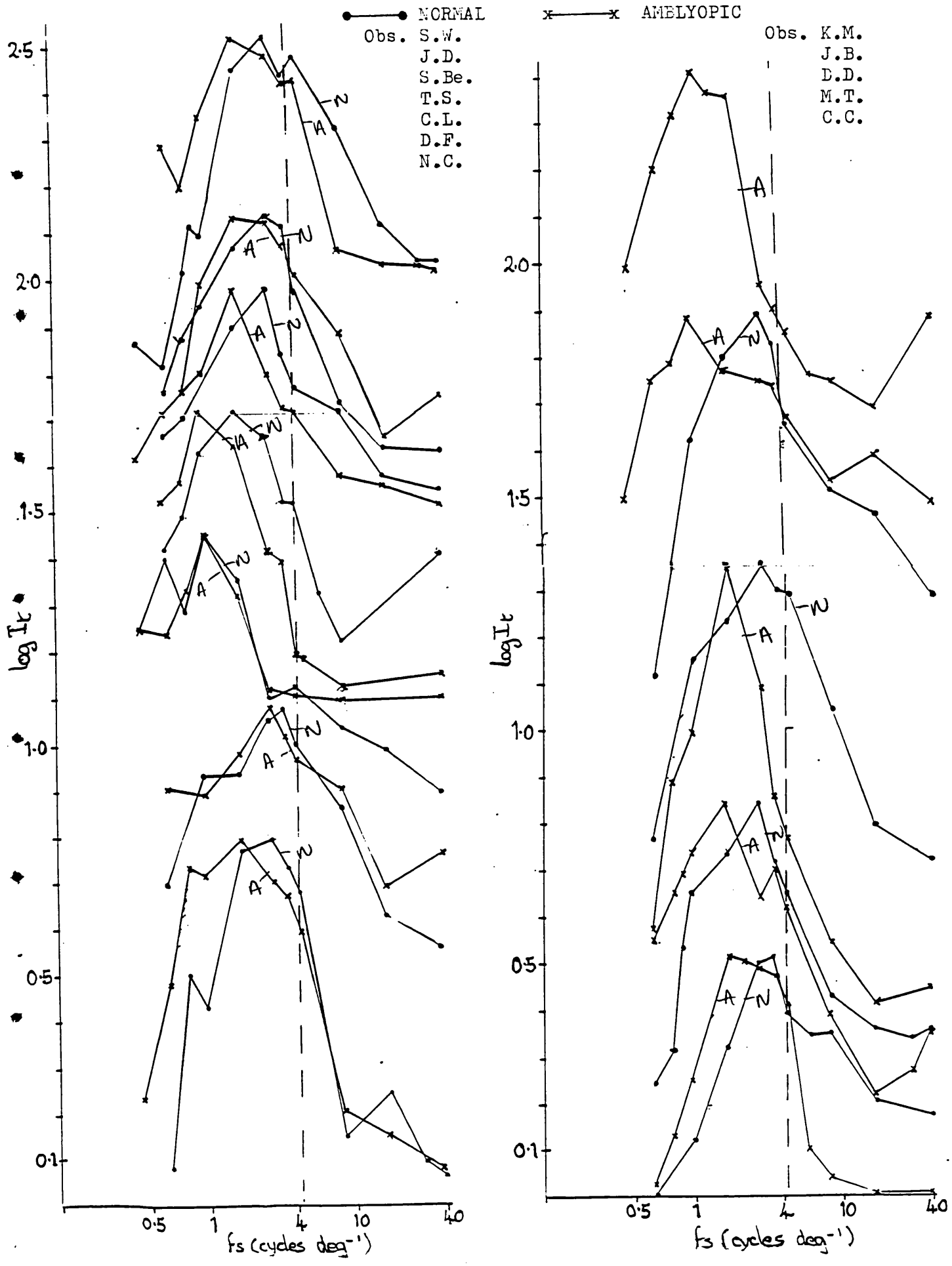
NORMAL
AMBLYOPIC
Obs. S.W.
J.D.
S.Be.
T.S.
C.L.
D.F.
N.C.
Obs. K.M.
J.B.
D.D.
M.T.
C.C.
log Ir
fs (cycles deg⁻¹)
0·5
1
4
10
40
2·5
2·0
1·5
1·0
0·5
0·1
A
N

Fig.DA.1a, b,

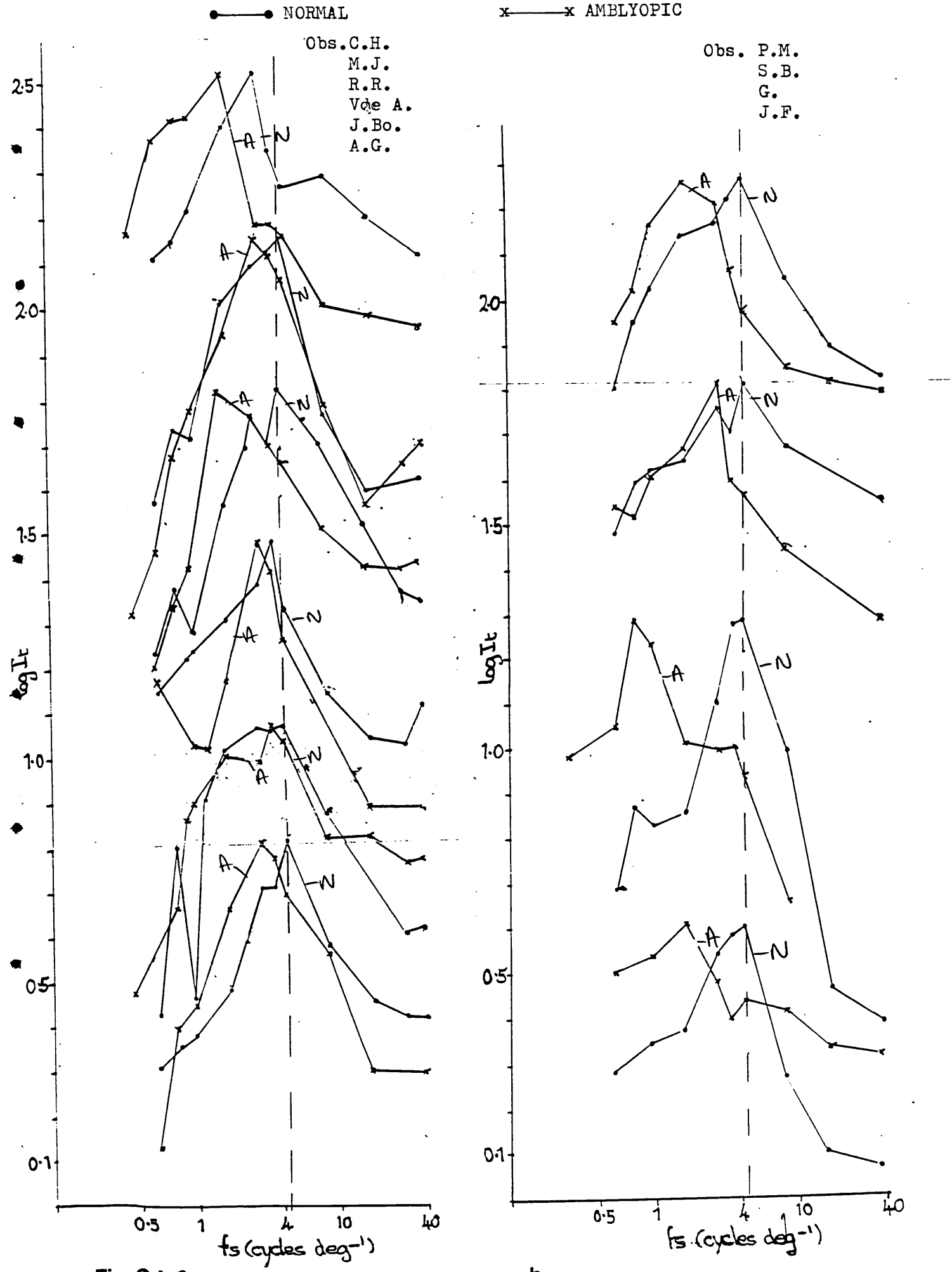
NORMAL
AMBLYOPIC
Obs.C.H.
M.J.
R.R.
Vde A.
J.Bo.
A.G.
Obs. P.M.
S.B.
G.
J.F.
A
N
2·5
2·0
1·5
1·0
0·5
0·1
log It
0·5
1
4
10
40
fs (cycles deg⁻¹)

Fig. DA. 2a, b,

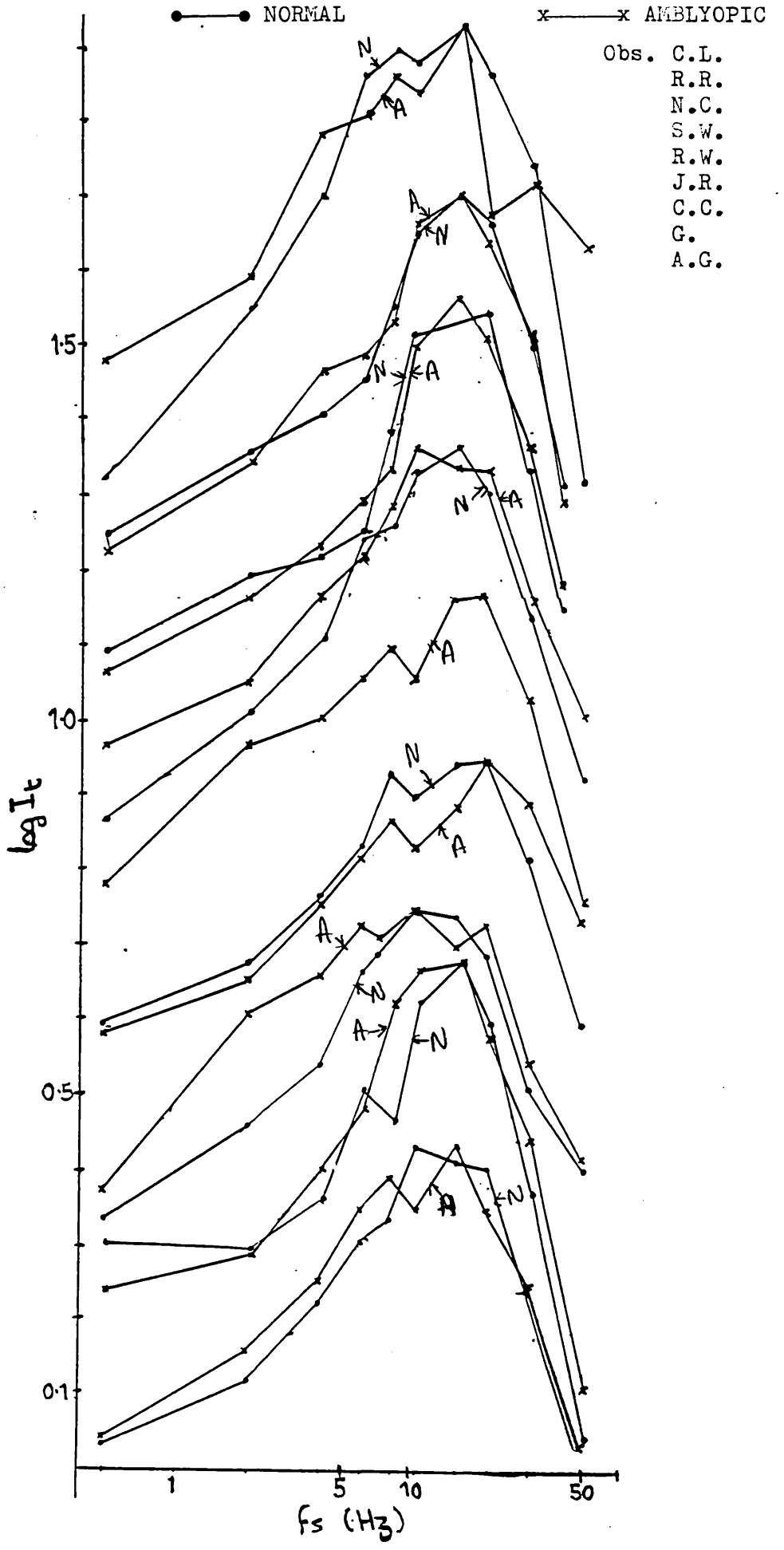
NORMAL
AMBLYOPIC
Obs. C.L.
R.R.
N.C.
S.W.
R.W.
J.R.
C.C.
G.
A.G.
log I_t
1·5
1·0
0·5
0·1
1
5
10
50
fs (Hz)
N
A

Fig.DA.3

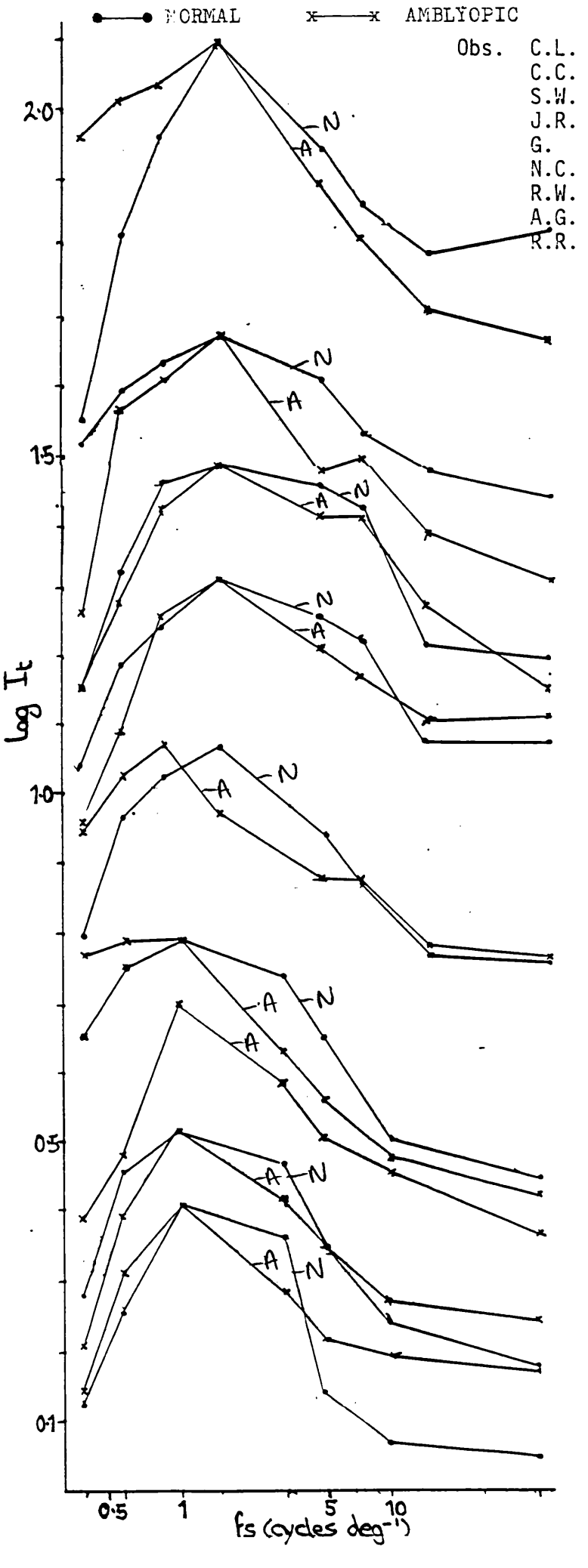
NORMAL
AMBLYOPIC
Obs.
C.L.
C.C.
S.W.
J.R.
G.
N.C.
R.W.
A.G.
R.R.
N
A
2·0
1·5
1·0
0·5
0·1
Log It
0·5
1
5
10
fs (cycles deg⁻¹)

Fig. DA. 4

REFERENCES

APTER, J.T.; Projectionsof the retina on superior colliculus of cats. J. Neurophysiol. 8, 123-134 (1945).

BAKER, F.H., GRIGG, P. and VAN NOORDEN, G.K.: Effects of visual deprivation and strabismus on the response neurones in the visual cortex of the Monkey, including studies on the striate and prestriate cortex in the normal animal. Brain Res. 66, 185-208 (1974).

BARBUR, J.L. and NUNN, B.; A simple 8-channel data logger. Photobiol. Bulletin. 1, 40-50 (1978).

BARBUR, J.L.and RUDDOCK, K.H.; Spatial characteristics of movement detection mechanisms in human vision 1. Achromatic mechanisms. Biol. Cybernetics, 37, 77-92 (1980a).

BARBUR, J.L. and RUDDOCK, K.H.; Spatial characteristics of movement detection mechanisms in human vision 11. Chromatic mechanisms; Biol. Cybernetics, 37, 93-98 (1980b).

BARBUR, J.L., HOLLIDAY, I.E., RUDDOCK, K.H. and WATERFIELD, V.A.; Spatial characteristics of movement detection mechanisms in human vision 111. Subjects with abnormal visual pathways. Biol. Cybernetics, 37, 99-105 (1980).

BARBUR, J.L., HOLLIDAY, I.E. and RUDDOCK, K.H.; The spatial and temporal organisation of motion perception units in human vision. Acta Psychol. 48, 35-47 (1981).

BARLOW, H.B., FITZHUGH, R. and KUFFLER, S.W.; Change of organisation in the receptive fields of the cat's retina during dark adaptation. J. Physiol. 137, 338-354 (1957).

BARLOW, H.B. and LEVICK, W.R.; The mechanisms of directionally selective units in the Rabbit retina. J. Physiol. (Lond), 178, 477-504 (1965).

BERLUCCHI, G, GAZZANIGA, S. and RIZZOLATTI, G.; Microelectrode analysis of transfer of visual information by the corpus callosum. Arch. Biol. 105, 583-596 (1967).

BLAKEMORE, C.; Development of functional connexions in the mammalian visual system. Brit. Med. Bull. 30, 152-157 (1974).

BLAKEMORE, C. and CAMPBELL, F.W.; On the existance of neurones in the human visual system selectively sensitive to orientation and size of retinal images. J. Physiol., 203, 137-160 (1969).

BLAKEMORE, C. and COOPER, G.F.; Development of the brain depends on the visual environment. Nature, London. 228, 477-478 (1970).

BLAKEMORE, C. and EGGERS, H.; Animal models for human visual development. In: Frontiers in Visual Science (Ed. Cod and Smith) Spinger. New York (1977).

BLAKEMORE, C. and VAN SLUYTERS, R.G.; Experimental analysis of amblyopia and strabismus. Br. J. Ophthal. 58, 176-182 (1974).

BLOMMAERT, F.J.J. and ROUFS, J.A.J.; The foveal point spread function as a determinant of detailed vision. Vision Res. 21, 1223-1233 (1981).

BOYCOTT, B.B. and DOWLING, J.E.; Organisation of the primate retina: Light microscopy, Philos. Trans. Roy. Soc. B, 255, 109-184 (1969).

BRATTGARD, S.O.; The importance of adequate stimulation for the chemical composition of retinal ganglion cells during early post-natal development. Acta. Radiol. Suppl. 96, 1-80 (1952).

BREITMEYER, B. and JULESZ, B.; The role of on and off transients in determining the psychophysical spatial frequency response. Vision Res. 15, 411-415 (1975).

BREITMEYER, B., LEVI, D.M. and HARWERTH, R.S.; Flicker masking in spatial vision. Vision Res. 21, 1377-1385 (1981).

BURR, D.C.; Temporal summation of moving images by the human visual system. Proc. R. Soc. Lond. B211, 321-339 (1981).

BURTON, G., NAGSHINEH, S. and RUDDOCK, K.H.; Processing by the human visual system of the light and dark contrast components of the retinal image. Biol. Cybernetics, 27, 189-197 (1977).

CAMPBELL, F.W.; CLELAND, B.G.; COOPER, G.F. and ENROTH-CUGELL, C: The angular selectivity of the visual cortical cells to moving gratings. J. Physiol. 198, 237-250. (1968).

CAMPBELL, F.W. and ROBSON, J.G.: Application of Fourier analysis to the visibility of gratings. J. Physiol. (Lond.), 197, 551-566. (1968).

CHAVASSE, B.F.: Worth's Squint, 7th Edn. P. Blakistons, Philadelphia, (1939).

CHINO, Y.M.; SHANSKY, M.S. and HAMASAKI, D.I.: Development of receptive field properties of retinal ganglion cells in Kittens raised with a convergent squint. Exp. Brain. Res. 39, 313-320 (1980).

CHOUDHURY, B.P.; WHITTERIDGE, D. and WILSON, M.E.: The function of the callosal connections of the visual cortex. Quart. J. Exp. Physiol. 50, 214 219 (1965).

CLELAND, B.G.; DUBIN, M.W. and LEVICK, W.R.: Sustained and transient neurones in the Cat's retina and lateral geniculate nucleus. J. Physiol. 217, 473-496 (1971).

CLELAND, B.G.; MITCHELL, D.E.; GILLARD-CREWTHER, S. and CREWTHER, D.E.: Visual resolution of retinal ganglion cells in monocularly-deprived cats. Brain Res. 192, 261-266 (1980).

CLELAND, B.G.; CREWTHER, D.P.; GILLARD-CREWTHER, S. and MITCHELL, D.E.: Normality of spatial resolution of retinal ganglion cells in cats with strabismic amblyopia. J. Physiol. 326, 235-249 (1982).

CRAWFORD, M.L.J. and VAN NOORDEN, G.K.: The effects of short-term experimental strabismus on the visual system in Macacu Mulatta. Invest. Ophthal. 18, 496-505 (1979).

DAVSON, H.: The physiology of the eye. 3rd Edn. Churchill Livingstone. Edinburgh and London (1972).

De LANGE, H.: Research into the dynamic nature of human fovea-cortex systems with intermittent and modulated light 1. Attenuation characteristics with white and coloured light. J. Opt. Soc. Am. 48, 777-784 (1958).

De MONASTERIO, F.M.: Properties of concentrically organised X- and Y-ganglion cells of macaque retina. J. Neurophysiol. 41, 1394-1417 (1978a).

De MONASTERIO, F.M.: Properties of ganglion cells with a typical receptive field organisation in retina of macaques. J. Neurophysiol. 41, 1435-1449 (1978b).

DOTY, R.W.: Remarks on the optic-tectum. In the Visual System. Ed. Jurg and Komhuber, 215-217, Berlin: Springer (1961).

DOWLING, J.E. and BOYCOTT, B.B.: Organisation of the primate retina: Electron microscopy. Proc. Roy. Soc. Biol. 166, 80-111 (1966).

DREHER, B.; FUKADA, Y. and RODIECK, R.M.: Identification, classification and anatomical segregation of cells with X-like and Y-like properties in the lateral geniculate nucleus of old-world primates. J. Physiol. 258, 433-452 (1976).

DUKE-ELDER, S.: Textbook of opthalmology. Vol. IV; 3832. Pub. by Henry and Kimpton, London (1949).

EBNER, F.F. and MYERS, R.E.: Distribution of corpus callosum and anterior commissure in Cat and Raccoon. J. Comp. Neurol. 124, 353-365 (1965).

EGGERS, H. and BLAKEMORE, C.: The neurophysiological basis of anisometropic amblyopia. Science, N.Y. 201, 244-247 (1978).

ROTH-CUGELL, C. and ROBSON, J.G.; The contrast sensitivity of retinal ganglion cells of the Cat. J. Physiol, 187, 517-552 (1966).

FLOM, M.C.: Eccentric fixation in amblyopia;is reduced foveal acuity the cause ? Am. J. Opt. Physiol. Opt. 55, 139-143 (1978).

FLOM, M.C. and WEYMOUTH, F.W.: Centricity of Maxwell's spot in strabismus and amblyopia. Arch. Ophthal. N. Y. 66, 260-268 (1961).

FOX, P.C., CHOW, K.L. and KELLY, A. S.; Effects of monocular lid closure on development of receptive-field characteristics of neurons in Rabbit superior colliculus. J. Neurophysiol. 41, 1359-1372 (1978).

FREEMAN, D.N. and MARG, E.: Visual acuity development coincides with the sensitive period in kittens. Nature (Lond.) 254, 614-615 (1975).

GAREY, L.J.; Interrelationships of the visual cortex and superior collosus in the Cat. Nature 207, 1410-1411 (1965).

GILINSKY, A.S.: Orientation-specific effects of patterns of adapting light on visual acuity. J. Opt. Soc. Am. 58, 13-18 (1968).

GLEES, P. and Le GROS-CLARK,W.E.: The termination of optic fibres in the lateral geniculate body of the Monkey. J. Anat. 75, 295-308 (1941).

GLOW, P.H. and ROSE, S.: Effects of light and dark on acetyl-cholinesterase acuity of the retina. Nature. London. 202, 422-423 (1964).

GORDON, B. and GUMMOWS L.: Effects of extraocular muscle section on receptive fields in Cat superior colliculous. Visien Res. 15, 1011-1019 (1975).

GOURAS, P.: Antidromic responses of orthodramically identified ganglion cells in monkey retina. J. Phsiol. 204, 407-409 (1969).

GREEN,M.: Psychophysical relations among mechanisms sensitive to pattern motion and flicker. Vision Res. 21, 971-983, (1981).

GUILLARY, R.W.: Patterns of fibre degeneration in the dorsal lateral geniculate nucleus of the Cat following lesions in the visual cortex. J. Comp. Neurol. 130, 197-211 (1967).

HAMASAKI, D.I. and POLLACK, J.G.: Depression of the late receptor potential and the E.R.G. by light deprivation in cats. Vis. Res. 12, 835-842. (1972).

HARWERTH, R.S.; BOLTZ, R.L. and EARL SMITH, N.L.: Psychophysical evidence for sustained and transient channels in the Monkey visual system. Vision Res. 20, 15-22. (1980).

HARWERTH, R.S. and LEVI, D.M.: A sensory mechanism for amblyopia: psychophysical studies. Am. J. Optom. Physiol. Opt. 55, 151-161. (1978).

HESS, R.F.: On the relationship between strabismic amblyopia and anisometropic amblyopia. Br. J. Opthal. 61, 767-773. (1977).

HESS, R.F.: A preliminary investigation of neural function and disfunction in amblyopia - 1. Size selective channels. Vision Res. 20, 749-754. (1980).

HESS, R.F. and BRADLEY, A.: Contrast perception above threshold is minimally impaired in human amblyopia. Nature, London. 287, 463-464. (1980).

HESS, R.F.; BURR, D.C. and CAMPBELL, F.W.: A preliminary investigation of neural function and disfuction in amblyopia - 111. Co-operative activity of amblyopic channels. Vision Res. 20, 757-760. (1980a).

HESS, R.F. and CAMPBELL, F.W.: A preliminary investigation of the neural function and dysfunctionin amblyopia - 11. Activity within an amblyopic "channel". Vision Res. 20, 755-756. (1980).

HESS, R.F.; CAMPBELL, F.W. and ZIMMERN, R.: Differences in the neural basis of human amblyopias: the effect of mean luminance. Vision Res. 20, 295-305. (1980b).

HESS, R.F. and HOWELL, E.R.: The threshold contrast sensitivity function in strabismic amblyopia: evidence for a two-type classification. Vision Res. 17, 1049-1055. (1977).

HESS, R.F. and HOWELL, E.R.: The luminance dependent nature of the visual abnormality in strabismic amblyopia. Vision Res. 18, 931-936. (1978).

HESS, R.F.; HOWELL, E.R. and KITCHEN, J.E.: On the relationship between pattern and movement preception in strabismic amblyopia. Vision Res. 18, 369-374. (1978).

HOLLIDAY, I.E. Ph.D Thesis: Spatio-temporal filtering in the human visual system. (1982).

HOLLIDAY, I.E. and RUDDOCK, K.H.: Two spatio-temporal filters in human vision. 1. Temporal and spatial frequency response characteristics. Biol. Cybern. 47, 173-190. (1983).

HOLMES, G.: Organisation of the visual cortex in man. Proc. Roy. Soc. Biol. 132, 348-361. (1945).

HUBEL, D.H. and WIESEL, T.N.: Integrative action in the Cat's lateral geniculate body. J. Physiol. 155, 385-398. (1961).

HUBEL, D.H. and WIESEL, T.N.: Receptive fields, binocular interaction and functional architecture in Cat's visual cortex. J. Physiol. Lond. 160, 106-154. (1962).

HUBEL, D.M. and WIESEL, T.N.: Receptive fields of cells in striate cortex of very young, visually inexperienced Kittens. J. Neurophysiol. 26, 994-1002. (1963).

HUBEL, D.H. and WIESEL, T.N: Binocular interaction in striate cortex of Kittens reared with artificial squint. J. Neurophysiol. 28, 1041-1059. (1965).

HUBEL, D.H. and WIESEL, T.N.: Receptive fields and functional architecture in Monkey striate cortex. J. Physiol., London. 195, 215-243. (1968).

HUBEL, D.H. and WIESEL, T.N.: Anatomical demonstration of columns in the Monkey striate cortex. Nature, 221, 747-750, (1969).

HUBEL, D.H. and WIESEL, T.N.: The period of susceptibility to the physiological effects of unilateral eye closure in kittens. J. Physiol. 206, 419-436. (1970).

IKEDA, H.: Visual acuity, its development and amblyopia. The Edridge Green lecture, 1979. J. Roy. Soc. Med. 73, 546-554. (1980).

IKEDA, H.; PLANT, G.T. and TREMAIN, K.E.: Nasal field loss in Kittens reared with convergent squint: neurophysiological and morphological studies of the lateral geniculate nucleus. J. Physiol. 270, 345-366. (1977).

IKEDA, H. and TREMAIN, K.E.: Different causes for amblyopia and loss of binocularity in squinting Kittens. J. Physiol. (Lond.) 269, 26-27. (1977).

IKEDA, H. and TREMAIN, K.E.: Amblyopia resulting from penalisation - neurophysiological studies of Kittens reared with atropinisation of one or both eyes. Brit. J. Ophthalmol. 62, 21-28 (1978a).

IKEDA,H. and TREMAIN, K.E.: Development of spatial resolving power of lateral geniculate neurones in Kittens. Exp. Brain. Res. 31, 193-206. (1978b).

IKEDA, H. and TREMAIN, K.E.: Amblyopia occurs in retinal ganglion cells of Cats reared with convergent squint without alterating fixation. Exp. Brian. Res. 35, 559-582. (1979).

IKEDA, H.; TREMAIN, K.E. and EINON, G.: Loss of spatial resolution of lateral geniculate neurones in Kittens reared with convergent squint produced at different stages of development. Exp. Brain. Res. 31, 207-220. (1978).

IKEDA, H. and WRIGHT, M.J.: Differential effects of refractive errors and receptive field organisation of central and peripheral ganglion cells. Vision Res. 12, 1465-1476. (1972a).

IKEDA, H. and WRIGHT, M.J.: Evidence for sustained and transient neurones in the Cat's visual cortex. Vision Res. 14, 133-136. (1974a).

IKEDA, H. and WRIGHT, M.J.: Is amblyopia due to inappropriate stimulation of the "sustained" pathway during development ? Br. J. Ophthal. 58, 165-175. (1974b).

IKEDA, H. and WRIGHT, M.J.: A possible neurophysiological basis for amblyopia. Br. Orthop. J. 32, 2-13. (1975).

IKEDA, H. and WRIGHT, M.J.: Properties of L.G.N. cells in Kittens reared with convergent squint; a neurophysiological demonstration of amblyopia. Exp. Brain. Res. 25, 63-77. (1976).

JACOBSON, S.G. and IKEDA, H.: Behavioural studies of spatial vision in cats reared with convergent squint; is amblyopia due to arrest of development ? Exp. Brain. Res. 34, 11-26. (1979).

JULESZ, B. Foundations of cyclopean perception. Univ. Chicago Press. (1971).

KECK, M.J., PALLELA, T.D. and PANTLE, A.: Motion after effect as a function of the contrast of sinusoidal gratings. Vis. Res. 16, 187-191 (1976).

KING-SMITH, P.E. and KULIKOWSKI, J.J.: Detection of gratings by independant activation of line detectors. J. Physiol. Lond. 247, 237-271 (1975).

KIRSHEN, D.G. and FLOM, M.C.: Visual acuity at different retinal loci of eccentrically fixating functional amblyopes. Am. J. Optom. Physiol. Opt. 55, 144-150 (1978).

KOLB, H.: Organisation of the outer plexiform layer of the primate retina; electron microscopy of Golgi- impregnated cells. Phil. Trans. 258, 261-283. (1970).

KULIKOWSKI, J.J. and KING-SMITH, P.E.: Spatial arrangement of line, edge and grating detectors revealed by subthreshold summation. Vis. Res. 13, 1455-1478. (1973).

KULIKOWSKI, J.J. and TOLHURST, D.J.: Psychophysical evidence of for sustained and transient detectors in human vision. J. Physiol. 232, 149-162. (1973).

LAVERGNE, G.: Adaptation a l'obscuite' et frequence critique de fusion de l'oeil amblyope. Docum. Ophthal. 23, 210-227. (1967).

LEE, B.B., CLELAND, B.G. and LEVICK, W.R.: The retinal input to cells in area 17 of the Cat's cortex. Exp. Brain. Res. 30, 527-538. (1977).

LEGENDY, C.R.: Can the data of Campbell and Robson be explained without assuming fourier analysis ? Biol. Cybernetics. 17, 157-163. (1975).

LEGGE, G.E.: Sustained and transient mechanisms in human vision: temporal and spatial properties. Vis. Res. 18, 69-81. (1978).

LEVICK, W.R.: Development of ideas on the functional organisation of retinal ganglion cells. Proc. Int. Union Physiol. Science. 14. 28th Inter. Congress, Budapest. 197 (1980).

LEVI, D.M.; HARWERTH, R.S.; and SMITH, E.L.: Humans deprived of normal binocular vision have binocular interaction, tuned to size and orientation. Science 205, 852-854. (1979).

LIBERMAN, R.: Retinal cholinesterase and glycolysis in Rats raised in darkness. Science N.Y. 135, 372-373. (1962).

LYLE, T.K. and WYBAR, K.C.: Lyle and Jackson's. Practical orthoptics in the treatment of squint. Fifth Ed. H.K. Lewis and Co. Ltd. (1970).

MAFFEI, L.; CERVETTO, L. and FIORENTINI, A.: Transfer characteristics of excitation and inhibition in Cat retinal ganglion cells. J. Neurophysiol. 33, 276-284. (1970).

MAFFEI, L. and FIORENTINI, A.: How the retinal channels build up the geniculate receptive field. Proc. Int. Union of Physiol. Science. Chapter 9, 358. Munich Excerptie Medica. Foundation (1971).

MALLET, R.F.: Investigation and management of amblyopia. Ophthal. Optic. 9, 768-780. (1969).

MARAINI, G.; CARTA, F. and FRANGUELLI, R.: Metabolic changes in retina and the optic centres following monocular light deprivation in the new born Rat. Exp. Eye Res. 8, 55-89. (1968).

MARR, D. and HILDRETH, E.: Theory of edge detection. Proc. Roy. Soc. London 207, 187-217 (1980).

MITCHELL, D.F., GIFFIN, F. and TIMNEY, B.: A behavioural technique for the rapid assessment of the visual capabilities of Kitten. Perception 6, 181-193. (1977).

MITCHELL, D.E.; GIFFIN, F.; WILKINSON, F.; ANDERSON, P. and SMITH, M.L.: Visual resolution in young Kittens. Vision Res. 16, 363-366. (1976).

MOHLER, C.W. and WURTZ, R.H.: Role of striate cortex and superior colliculus in visual guidance of saccadic eye-movements in Monkeys. J. Neurophysiol. 40, 74-94. (1977).

MOUNTCASTLE, V.B.: Modality and topographic properties of single neurones of Cats' somatic sensory cortex. J. Neurophysiol. 20, 408-434. (1957).

MYERS, R.E.: Commissural connections between occipital lobes of the Monkey. J. Comp. Neurol. 118, 1-10. (1962).

PANTLE, A. and SEKULER, R.: Velocity sensitive mechanisms in human vision. Vision Res. 8, 445-450. (1968).

PASIK, T. and PASIK, P.: The visual world of Monkeys deprived of striate cortex; effective stimulus parameters and the importance of the accessory optic tract. Vision Res. (Suppl.3), 419-435. (1971).

PENMAN, G.G.: The representation of the areas of the retina in the lateral geniculate body: Trans. Ophthal. Soc. U.K., 54, 232-270. (1934).

PIRENNE, M.H.: Vision and the Eye. London; Chapman and Hall. (1967).

POLYAK, S.L.: The Retina. Chicago: University Press. (1941).

ROTH, A.: Le sens chromatique dans l'amblyope fonctionelle. Docum. Ophthal. 24, 113-200. (1968).

ROUFS, J.A. L. and BLOMMAERT, F.J.J. : Temporal impulse and step responses of the human eye obtained by means of drift correction perturbation technique. Vis. Res. 21, 1203-1221 (1981).

RUDDOCK, K.H.: Psychophysical studies on subjects with visual defects. J. Roy. Soc. Med. 75, 315-322. (1982).

SACHS, M.B.; NACHMIAS, J. and ROBSON, J.G.: Spatial frequency channels in human vision. J. Opt. Soc. Am. 61, 1176-1186. (1971).

SHAPERO, M.: Amblyopia. Chilton, Radnor, Pennsylvania.(1971).

STONE, J and HOFFMANN, K.P.: Conduction velocity as a parameter in the organisation of the afferent relay in cat's lateral geniculate nucleus. Brain Res. 32, 454-459. (1972).

STONE, J. and FUKUDA, Y.: Properties of cat retinal ganglion cells; a comparison of W-cells and with X- and Y-cells. J. Neurophysiol. 37, 722-748. (1974).

SPEAR, P.D. and BAUMAN, T.P.: Effects of visual cortex removal on receptive-field properties of neurons in lateral suprasylvian visual area of the Cat. J. Neurophysiol. 42, 31-56,(1979).

SPRAGUE, J.M.: Interaction of cortex and superior colliculus in mediation of visually guided behaviour in the Cat. Science. 153, 1544-1547. (1966).

SPRAGUE, J.M. and MEIKLE, T.H.: The role of the superior colliculus in visually guided behaviour. Exp. Neurol. 11, 115-146. (1965).

TOLHURST, D.J.: Separate channels for the analysis of shape and of the movement of a moving visual stimulus. J. Physiol. London. 231, 385-402. (1973).

TOLHURST. D.J.: Sustained and transient channels in human vision. Vision Res. 15, 1151-1155. (1975).

TSUMODO, T. and SUDA, K.: Evidence for excitatory connections from the deprived eye to the visual cortex in monocularly deprived Kittens. Brain Res. 153, 150-156 (1978).

Van BOLAN, and HENKES, : Attention and amblyopia, an electro-encephalographic approach to an ophthalmological problem. British J. Ophthalmol. 46, 12-20. (1962).

Von NOORDEN, G.K.: Histological studies of the visual system in Monkeys with experimental amblyopia. Invest. Ophthalmol. 12, 727-738, (1973).

Von NOORDEN, G.K.; DOWLING, J.E. and FERGUSON, D.C.: Experiments on amblyopia in Monkeys 1; behavioural studies of stimulus deprivation in amblyopia. In A.M.A. Archs. Ophthal. 84, 206-214, (1970).

VASTOLA, E.F.: Monocular inhibition in the lateral geniculate body. E.E.G. Clin. Neurophysiol. 12, 399-403. (1960).

WEISKRANTZ, L.: Sensory deprivation and the Cat's optic neurous system. Nature, London. 181, 1047-1050. (1958).

WEISKRANTZ, L.; WARRINGTON, E.K.; SANDERS, M.B. and MARSHALL, J.: Visual capacity in the hemianopic field following a restricted occipital ablation. Brain. 97, 709-718. (1974).

WEYMOUTH, F.W.: Visual sensory units and the minimum angle of resolution. Am. J. Ophtahl. 46, 102-113. (1958).

WICKELGREN-GORDON, B.: Some effects of visual deprivation on the Cat superior colliculus. Investive. Ophthal. 11, 460-467. (1972).

WIESEL, T.N. and HUBEL, D.H.: Single-cell response in striate cortex of Kittens deprived of vision in one eye. J. Neurophysiol. 26, 1003-1017. (1963).

WOLFF, E.: Anatomy of the eye and orbit; (revised by R.J. Last) London. pub. by H.K. Lewis. 1968.

WORTH, C.: Squint; its causes, pathology and treatment. 2nd edn. P. Blakiston's Philadelphia. (1903).

YINON, V.; AUERBACH, E.; BLANK, M. and FRIESENHAUSEN, J.: The ocular dominance of cortical neurons in Cats developed with divergent and convergent squint. Vision Res. 15, 1251-1256. (1976).

YOUNG, R.W.: The renewal of receptor cell outer segments. J. Cell. Biol. 33, 61-72. (1967).

ZEKI, S.M.: Functional organisation of the visual area in the posterior bank of the superior temporal sulcus of the Rhesus Monkey. J. Physiol. (Lond.). 236, 549-573. (1974a).

ZEKI, S.M.: Cells responding to changing image size and disparity in the posterior bank of the superior temporal sulcus of the Rhesus Monkey. J. Physiol. (Lond.) 242, 827-847. (1974b).

ZEKI, S.M.: Functional specialisation in the visual cortex of the Rhesus Monkey. Nature, 274, 423-427. (1978).

ADDITIONAL REFERENCES

BRINDLEY, G.S. and HAMASAKI, D.I.: Histological evidence against the view that the cat's optic nerve contains centrifugal fibres. J. Physiol. 184, 444 – 449. (1966).

ACKNOWLEDGEMENTS

Firstly, I should like to thank my Supervisor, Dr. K.H. Ruddock for much help and constructive criticism over the past few years which has resulted in the completion of this thesis.

I should also like to extend my thanks to my collegues who have contributed much to this work, in particular to Dr. I.E. Holliday.

Thanks is also due to the subjects who's many hours of patience has produced the results presented in this thesis.

I owe deep thanks to my Parents for encouragement, and for looking after my daughter Katie, thus enabling me to complete the written work.

Finally, I wish to thank Mrs. Jill Marshall for typing this thesis in such a presentable manner.

Biol. Cybern. 47, 191–201 (1983)

Biological Cybernetics

Two Spatio-Temporal Filters in Human Vision

2. Selective Modification in Amblyopia, Albinism, and Hemianopia

A. R. Grounds*, I. E. Holliday*, and K. H. Ruddock**

* Departments of Physics (Biophysics)
** Pure and Applied Biology, Imperial College of Science and Technology, London, England

Abstract. 1. We have used the psychophysical methods described in the first paper of this series (Holliday and Ruddock, 1983) to determine selected spatial and temporal response characteristics of the ST1 and ST2 filters for subjects suffering visual defects. Data are given for 19 amblyopes, an albino and a hemianope, and comparison data are also given for a number of subjects with normal vision. 2. The ST1 spatial responses for both the "normal" and "amblyopic" eyes of 12 convergent strabismic amblyopes are displaced to low spatial frequencies compared to the normal curve, which implies that there is a loss of fine spatial tuning. In all but one subject, the curve for the "amblyopic" eye peaks at a spatial frequency lower than that for the "normal" eye, thus the former deviates further from the normal pattern than the latter. 3. The ST1 spatial responses of 6 refractive amblyopes are also displaced to the low frequency side of the normal curve, although on average the shift is smaller than in the case of the strabismic amblyopes. For each subject, the response curve of the "amblyopic" eye peaks at a lower spatial frequency than does that for the "normal" eye. 4. ST1 spatial responses were measured for targets located up to 30° off-axis along the horizontal meridian and sample data are given for one strabismic and one refractive amblyope and for two normal subjects. It is concluded from these data that the changes in the spatial responses associated with amblyopia do not simply reflect eccentric fixation of the target. 5. The ST2 spatial response was measured for the "normal" and "amblyopic" eyes of 9 amblyopes (7 strabismic and 2 refractive). There is no significant difference between the average amblyopic response and that of normal subjects, and only in one case does the response for an "amblyopic" eye peak at a frequency lower than the peak frequency for normal vision. 6. The ST2 temporal response for 9 amblyopes shows no systematic deviations from the normal response. 7. For the albino, both the ST1 and ST2 spatial responses peak at around 0.3 cycles deg^{-1}, and both curves are displaced considerably to the low spatial frequency side of the normal ST2 spatial response. The albino's ST2 temporal response is essentially normal. 8. Measurements for the hemianope's "blind" hemifield under conditions appropriate to the isolation of the ST1 and ST2 spatial responses reveal no tuning curves. The ST2 temporal response for the "blind" hemifield, however, is of large amplitude, with a peak at 2 Hz, well below the normal frequency response peak. 9. It is argued that the loss of fine spatial tuning which occurs in the ST1, but not the ST2, spatial responses of the amblyopes is consistent with the sequential organisation of these two filter classes proposed by Holliday and Ruddock (1983). Further, for the only two subjects whose ST2 spatial response curves are displaced to abnormally low frequencies (the albino and a strabismic amblyope) the ST1 spatial response is shifted to low spatial frequencies compared to the normal ST2 curve. This is also consistent with Holliday and Ruddock's (1983) model.

Introduction

It has been shown that background field modulation produces well-defined changes in thresholds for detection of moving targets (Holliday and Ruddock, 1983) and response characteristics of two spatio-temporal filters were derived from measurement of target threshold over a range of background field modulation frequencies. The experimental data were represented by a network which provides a basis for the analysis of visual mechanisms revealed by background field modulation methods. In this paper, we examine the frequency response characteristics of the two filter classes in subjects suffering three kinds of visual defect, namely amblyopia, albinism and hemianopia.

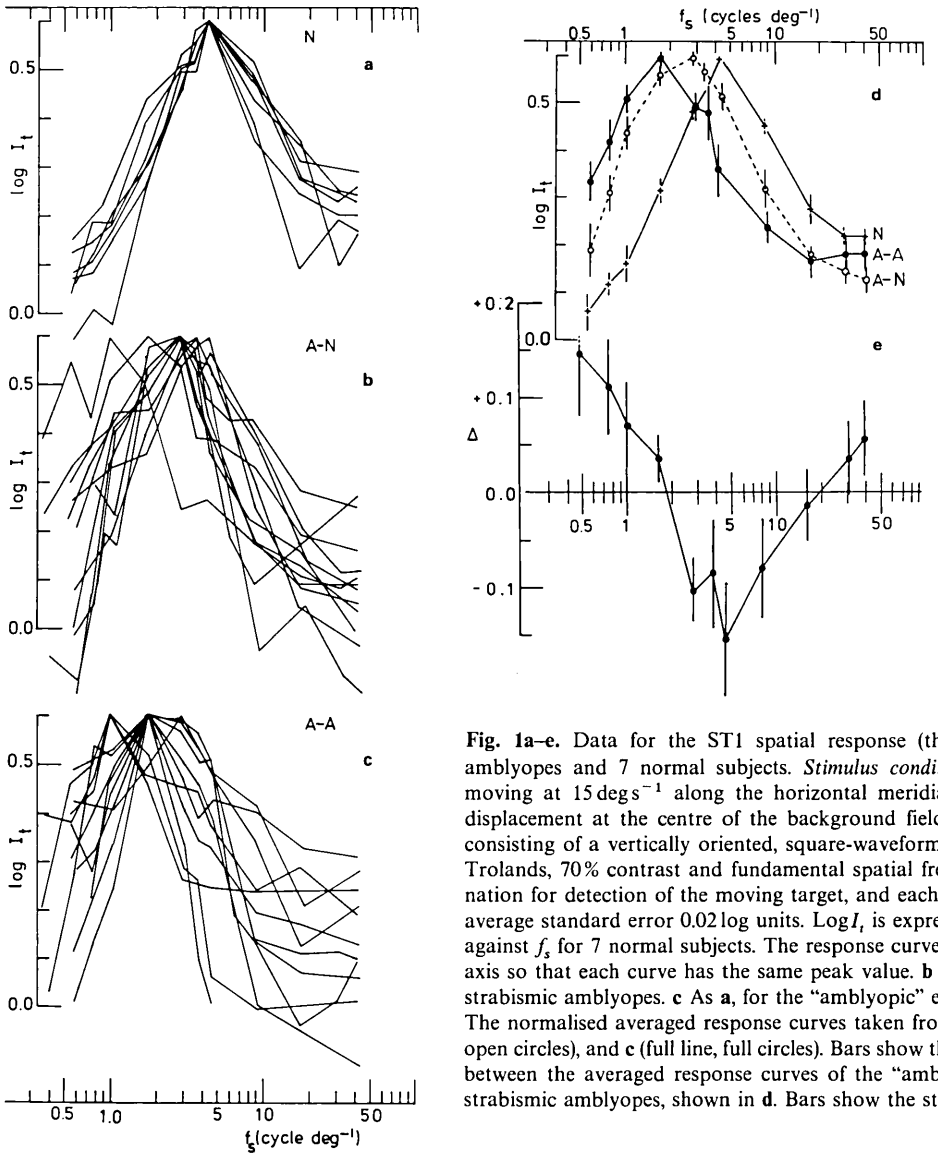

Fig. 1a–e. Data for the ST1 spatial response (the IMG function), for 12 strabismic amblyopes and 7 normal subjects. *Stimulus conditions: Circular target*, 3.5° diameter, moving at 15 deg s^{-1} along the horizontal meridian. Target movement covered an 8° displacement at the centre of the background field. *Circular background*, 17° diameter, consisting of a vertically oriented, square-waveform grating of mean illumination 1.4 log Trolands, 70% contrast and fundamental spatial frequency, f_s. I_t is the threshold illumination for detection of the moving target, and each point was measured four times, with average standard error 0.02 log units. LogI_t is expressed in relative units. **a** LogI_t plotted against f_s for 7 normal subjects. The response curves have been displaced along the logI_t axis so that each curve has the same peak value. **b** As **a**, for the "normal" eyes of the 12 strabismic amblyopes. **c** As **a**, for the "amblyopic" eyes of the 12 strabismic amblyopes. **d** The normalised averaged response curves taken from **a** (full line, crosses), **b** (broken line, open circles), and **c** (full line, full circles). Bars show the standard errors **e**. The difference, Δ, between the averaged response curves of the "amblyopic" and "normal" eyes of the 12 strabismic amblyopes, shown in **d**. Bars show the standard errors

Amblyopia is the term given to reduced spatial resolution exhibited by adults who, as children, suffered either strabismus (squint) or large refractive error in one eye. Such subjects tend, when young, to suppress visual images arising in the squinting or badly refracted eye and the consequent loss of spatial resolution in adulthood cannot be rectified by refractive correction. Amblyopia arises from abnormal development of the visual pathways due to modification of sensory input during childhood and there is, consequently, considerable interest in the underlying mechanisms.

In this paper, we show that for the amblyopes, including the albino who may be considered an extreme amblyope, there are selective changes in the spatial, but not in the temporal properties of the two filters. In the hemianope, however, visual responses in the "blind" hemifield are characterised by an abnormal temporal response pattern.

Methods

Using the background modulation methods described in the first paper of this series (Holliday and Ruddock, 1983) we have measured selected ST1 and ST2 filter responses in subjects displaying certain classes of visual abnormality. Thus threshold illumination, I_t, for detection of a target moving across a modulated background was determined as a function of the background parameters. The functions measured and the background modulation required for their investigation are summarised as follows:

1. The ST1 spatial response, for which the target moves across a spatially modulated background con-

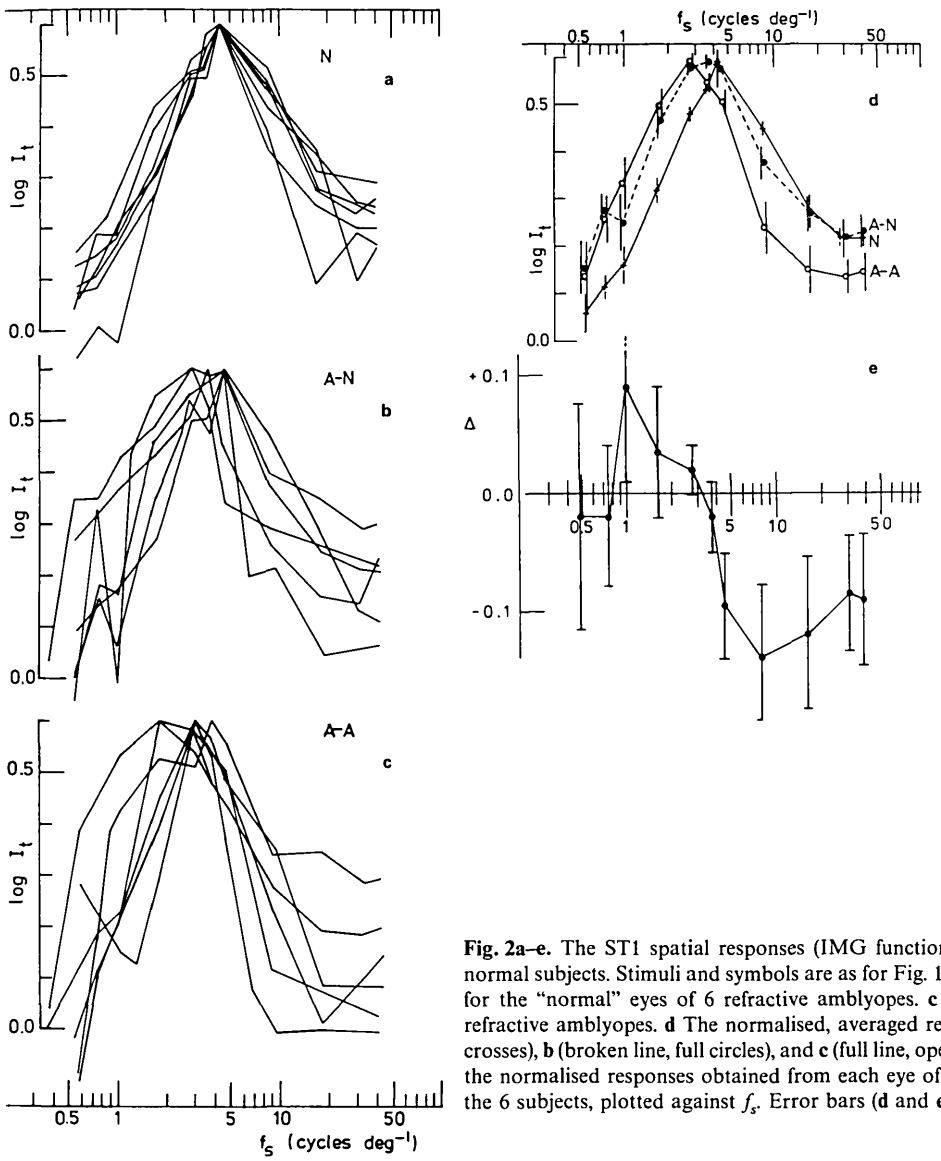

Fig. 2a–e. The ST1 spatial responses (IMG functions) for 6 retractive amblyopes and 7 normal subjects. Stimuli and symbols are as for Fig. 1. **a** Data for 7 normal subjects. **b** Data for the "normal" eyes of 6 refractive amblyopes. **c** Data for the "amblyopic" eyes of 6 refractive amblyopes. **d** The normalised, averaged response curves taken from **a** (full line, crosses), **b** (broken line, full circles), and **c** (full line, open circles). **e** The difference, Δ, between the normalised responses obtained from each eye of the amblyopic subjects, averaged for the 6 subjects, plotted against f_s. Error bars (**d** and **e**) denote standard errors

sisting of a square-waveform grating, of periodicity f_s, and I_t is determined as a function of f_s (Barbur and Ruddock, 1980). The ST1 spatial mechanism exhibits a relatively high pass band response suitable for fine spatial resolution.

2. The ST2 spatial response, for which the target moves across a spatio-temporally modulated background consisting of alternate steady and flickering bars (Holliday and Ruddock, 1983, Fig. 1). Threshold illumination, I_t, is determined as a function of the periodicity, f_s, of the background grating.

3. The ST2 temporal response, for which the target moves across a spatially uniform, temporally modulated background. Threshold illumination, I_t, is determined as a function of the temporal frequency, f_t, of the background modulation. The ST2 temporal response is pass band (i.e. transient) in nature, suitable for the detection of temporal changes in the light stimulus. The corresponding ST2 spatial response is relatively coarse and therefore does not provide high spatial resolution.

In the case of the amblyopes, visual acuity was measured for each eye, separately, with a Snellen test chart consisting of high contrast black letters on a white background. All amblyopes were examined ophthalmoscopically for eccentric fixation using a Linksz star graticule (Lyle and Wybar, 1967) and as far as possible, their ophthalmic history was collected. The albino, *D*, a 35 year old male, is classed as type tyrosinase negative, and exhibits pronounced nystagmus. The hemianope, *G*, a 23 year old male, has a homonymous right field hemianopia as a result of a deep laceration behind the left ear, suffered at age 8 years. He can none-the-less detect and locate moving

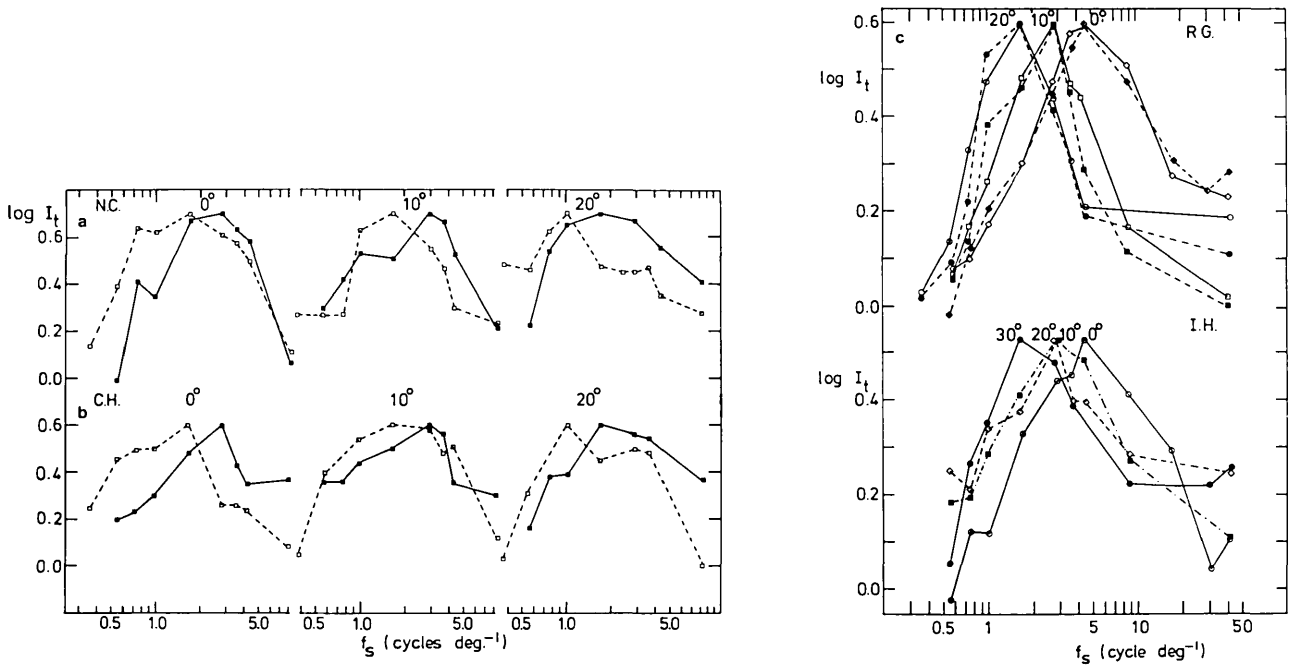

Fig. 3a–c. Normalized ST1 spatial responses (IMG functions) for four subjects, obtained for target movement centred at different points along the horizontal meridian, in the temporal retina. All stimulus parameters and symbols as in Fig. 1. **a** Data for the strabismic amblyope, NC, measured at the fovea (0°, and 20° off-axis. Full lines (full squares) refer to the "normal" eye and broken lines (open squares) refer to the "amblyopic" eye. Each point is the mean of 8 readings, with standard error 0.02 log units. **b** As **a**, but for the refractive amblyope CH. **c** Ax **a**, but for the normal subjects RG and IH. In the case of RG data are given for the right eye (full lines) and left eye (broken lines); all data for IH refer to the right eye

or flashed targets presented within his "blind" hemifield (Barbur et al., 1980).

The equipment and experimental procedures were the same as those described in previous papers (Holliday and Ruddock, 1983; Barbur and Ruddock, 1980). Except for the data of Figs. 3 and 7, all measurements were made under foveal viewing conditions. All stimuli were white light.

Results

Amblyopes

The spatial responses of the ST1 filter (the IMG spatial response) were measured for twelve convergent strabismic amblyopes and six refractive amblyopes. In normal vision, two ST1 spatial functions are found, one for background illuminations below 2 log Trolands, with peak response at about 4 cycles deg^{-1} and the other, for background illuminations above 2.2 log Trolands, with peak response at about 8 cycles deg^{-1} (Barbur and Ruddock, 1980). We measured ST1 spatial responses at background illuminations appropriate to the isolation of these two different responses, but for all but one amblyope and even for two normal subjects, we found only one response function, with peak response at or below 4.3 cycles deg^{-1}. Data are therefore given for only one background illumination, equal to 1.4 log Trolands. The reasons why we did not observe a second response function are peripheral to the present study and will be considered elsewhere.

Threshold illumination, I_t, for detection of a circular target (diameter 3.5°), moving at 15 deg s^{-1} across a background grating, was measured as a function of the grating spatial period. Under these experimental conditions, normal subjects exhibit a well-defined tuning curve, with $\log I_t$ peaking at a background fundamental spatial frequency, f_s, of about 4 cycles deg^{-1}. The data for seven normal subjects all exhibit this response pattern, with rather small scatter between the different subjects (Fig. 1a). Results for the "normal" (Fig. 1b) and "amblyopic" (Fig. 1c) eyes of twelve strabismic amblyopes display a marked deviation from the normal curves. In all but one of the normal eyes and in all the "amblyopic" eyes, the responses peak at a frequency below the normal value of 4.3 cycles deg^{-1}, and it can be seen by inspection that the variation between individual amblyopes is very much greater than that for the normal subjects. Plots of the normalised, averaged responses for the seven normal subjects and for each eye of the amblyopes (Fig. 1d) confirm that the spatial responses for the amblyopes are displaced to the low frequency side of the normal response, and that this effect is greater for the "amblyopic" than for the "normal" eyes. Comparison between the results for the two eyes of

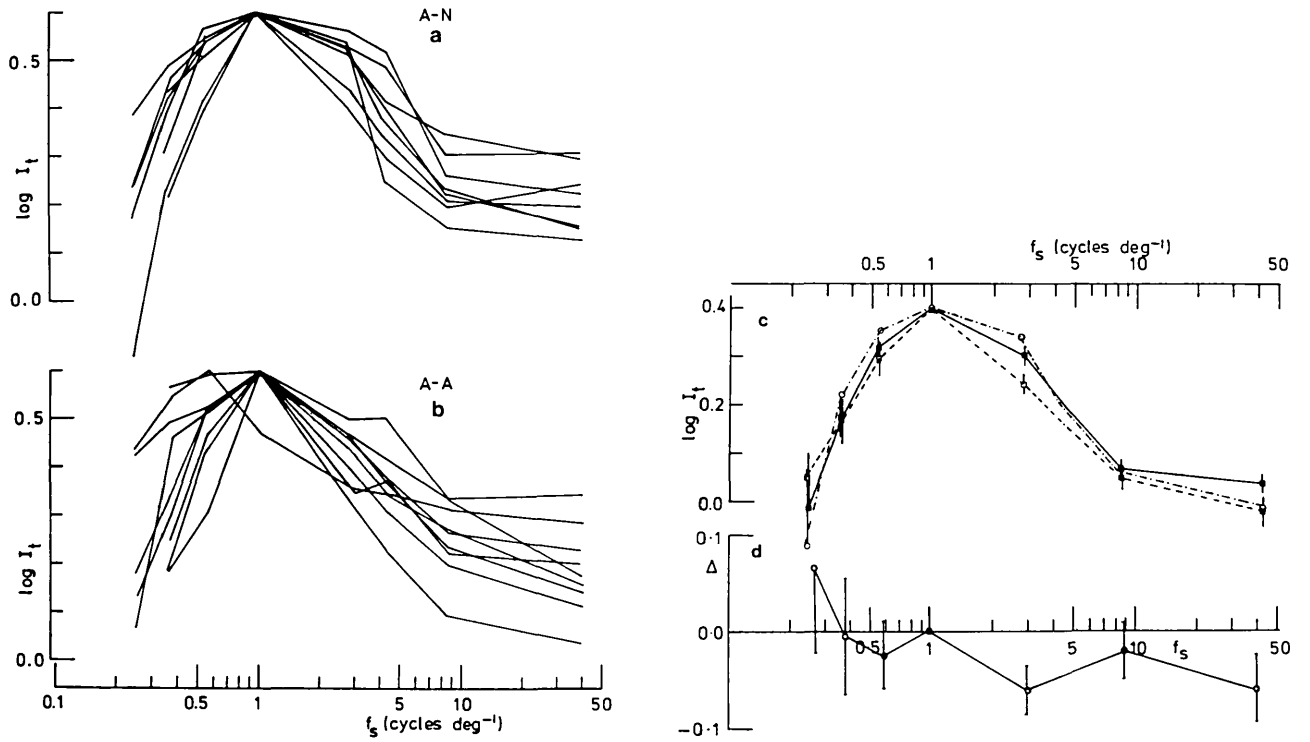

Fig. 4a–d. ST2 spatial responses for 9 amblyopes. *Stimulus conditions: Circular target*, 1.4° diameter, moving at 15 deg s^{-1} along the horizontal meridian. The target displacement covered 8° and was centred on the background field. *Circular background*, 17° diameter consisting of a vertical grating composed of alternate steady and flickering (20 Hz) bars. The mean illumination of the flickering bars was 2.7 log Trolands, equal to that of the steady bars. The flicker modulation was 100% and the fundamental spatial frequency of the grating is the parameter, f_s. I_t is the threshold illumination for detection of the target and each point was measured 8 times, with mean standard error 0.02 log units. Log I_t is expressed in relative units. **a** Log I_t plotted against f_s for the "normal" eyes of 8 of the 9 amblyopes. Each curve has been displaced along the log I_t axis so that all curves have the same peak value. **b** As **a**, but for the "abnormal" eyes of the 9 amblyopes. **c** The normalised average responses taken from **a** (full line, full squares) and **b** (broken line, open squares). The dot-dash line (open circles) is the mean value for 6 normal subjects (taken from Holliday and Ruddock, 1983, Fig. 8c). The bars represent the standard errors. **d** The difference, Δ, between the ST2 spatial responses recorded for each eye of the 9 amblyopes plotted against f_s

each amblyope reveals that the response for the "normal" eye peaks at a spatial frequency higher than that for the "amblyopic" eye, except in one case, for which both functions peak at 1 cycle deg^{-1}. The averaged differences, Δ, between the normalised log I_t values for each eye of the amblyopic subjects are plotted against f_s in Figs. 1e. This plot shows that the spatial frequency functions for the "amblyopic" eyes are displaced to the low frequency side of those for the "normal" eyes, the two converging to the same value for f_s equal to 40 cycles deg^{-1}, which is effectively a uniform background. Data similar to those for the convergent strabismic amblyopes were also obtained for six refractive amblyopes. These are plotted in Fig. 2 and the responses for the seven normal subjects are included for comparison purposes (Fig. 2a). The "normal" eyes of the refractive amblyopes show, on average, only small deviations from the normal data, whereas the "abnormal" eyes show larger deviations, with a significant increase in inter-subject variation (Fig. 2c). These observations are confirmed by the plot of the averaged spatial responses for the "normal" and "amblyopic" eyes of the six refractive amblyopes (Fig. 2d). The averaged differences, Δ, between log I_t values for the normalised response functions of the two eyes of the refractive amblyopes are plotted against f_s in Fig. 2e. The relationship between f_s and Δ differs from that found for the strabismic amblyopes (Fig. 1e), because at low non-zero spatial frequencies, Δ approaches zero for Fig. 2e, but increases to a large value in Fig. 1e. This may reflect a difference between the mechanisms of strabismic and refractive amblyopias, as has been suggested by some authors (Hess and Bradley, 1980; Hess et al., 1980). ST1 spatial response curves for a few amblyopic and normal subjects were measured with the moving target located at a number of different positions in the visual field. Data for one strabismic and one refractive amblyope, and also for two normal subjects, are given in Fig. 3. These data establish that for all subjects, the response functions shift to lower spatial frequencies as target eccentricity increases, but for the amblyopes, the functions for the "abnormal" eyes are displaced to lower spatial frequencies than those for the "normal" eyes, at all retinal locations

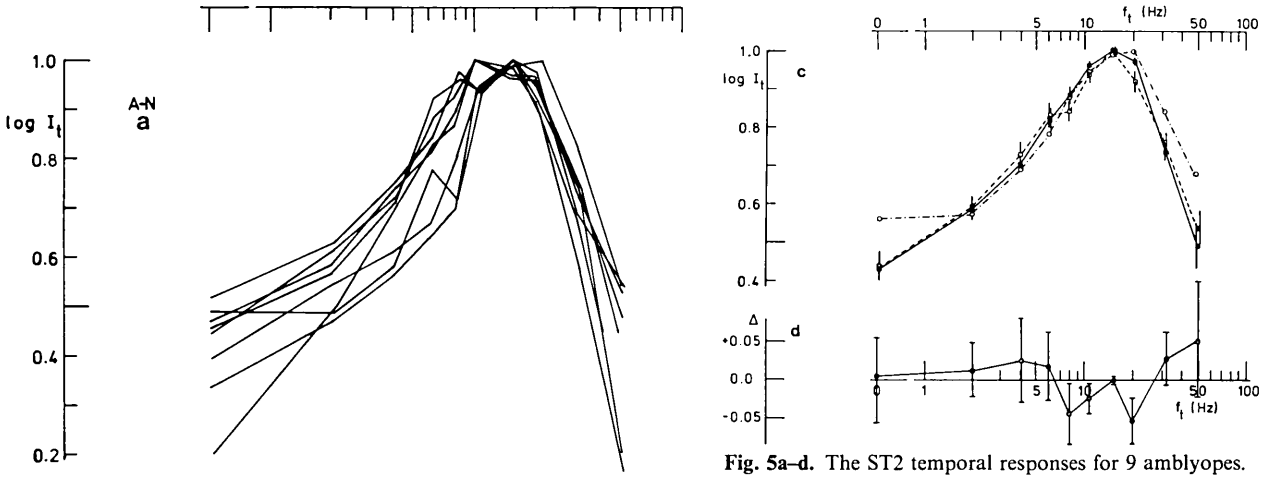

Fig. 5a–d. The ST2 temporal responses for 9 amblyopes. *Stimulus conditions: Circular target*, diameter 1.4° moving at 15 deg s^{-1} along the horizontal meridian. The target moved across 8° at the centre of the background field. *Circular background*, diameter 17°, spatially uniform and modulated temporally at f_t Hz. The mean background illumination was 2.7 log Trolands and the flicker modulation depth was 25%. I_t is the threshold illumination for detection of the moving target and each point was measured 8 times, giving an average standard error of 0.02 log units. Log I_t is expressed in relative units. **a** Log I_t plotted against f_t for the "normal" eyes of 8 of the 9 amblyopes. The response curves have been displaced along the log I_t axis so that each has the same peak value. **b** As **a**, but for the "amblyopic" eyes of the 9 amblyopes. **c** The normalised, averaged response curves taken from **a** (full line, full squares) and **b** (broken line, open squares). The dot-dash line (open circles) represents average data for 5 normal subjects. Bars represent standard errors. **d** The difference, Δ, between the log I_t values for the two eyes of each amblyopic subject, plotted against f_s and averaged for the 9 amblyopes

(Fig. 3a and b). In contrast, data for the normal subject RG (Fig. 3c) show close correlation between the IMG functions for each eye, at all retinal locations.

The spatial response of the ST2 filters was measured for 9 amblyopes (7 strabismic and 2 refractive) taken from the same group as those for which the ST1 spatial response was measured. The measurement was performed using the method described in the first paper of this series (Holliday and Ruddock, 1983, Figs. 1f and 8); thus, a circular target (1.4° diameter) moved at 15 deg s^{-1} across a background grating consisting of alternate steady and flickering (20 Hz) bars. The average illumination of the flickering bars, set at 2.7 log Trolands, was equal to that of the steady bars. Threshold, I_t, for detection of the moving target was measured as a function of the grating period; for normal subjects, log I_t peaks at a grating fundamental frequency, f_s, of 1 cycle deg^{-1} (Holliday and Ruddock, 1983, Fig. 8). The data for all the "normal" eyes and all but one of the "abnormal" eyes of the amblyopic subjects peak at 1 cycles deg^{-1} (Fig. 4a and b) and the averaged, normalised spatial frequency curves for the amblyopic and normal subjects are very similar, both in peak value and in overall shape (Fig. 4c). The averaged values of the differences, Δ, between the normalised log I_t values for the two eyes of the amblyopes are plotted against f_s in Fig. 4d, and this plot demonstrates the relatively small differences in response between the "normal" and "amblyopic" eyes. We conclude that in contrast to the ST1 spatial responses illustrated in Figs. 1 and 2, the ST2 spatial responses are little influenced by amblyopia.

In order to investigate the temporal responses of the amblyopic subjects, we measured the ST2 temporal response by the method described by Holliday and Ruddock (1983). Thus, threshold illumination, I_t, for detection of a circular target (1.4° diameter) moving at 15 deg s^{-1} across a spatially uniform, temporally flickering background, was measured as a function of background flicker frequency, f_t. The mean background illumination was 2.7 log Trolands, for which normal vision is characterised by a temporal response peaking at about 15 Hz (Holliday and Ruddock, 1983, Fig. 2). Data obtained with the 9 amblyopes for whom

the ST2 spatial response was recorded, are plotted in Fig. 5, those for the "normal" eyes being plotted in Fig. 5a and those for the "amblyopic" eyes in Fig. 5b. It is clear that both sets of response curves are similar in shape and in peak response frequency (15 Hz), although there is greater inter-subject variability for the "amblyopic" eyes. The averaged amblyopic responses are similar to the normal response (Fig. 5c) and the averaged difference values between the functions recorded for the two eyes of the amblyopes are of small amplitude (Fig. 5d). We conclude that the ST2 temporal response function is normal in amblyopic vision.

Albino Subject

The spatial and temporal frequency responses of the ST2 filter were measured for the albino subject, *D*, under experimental conditions identical to those employed in the study of amblyopia. The ST2 spatial response is plotted in Fig. 6a, together with *D*'s ST1 spatial response (Barbur et al., 1980, Fig. 3b) and the normal ST1 and ST2 spatial responses. *D*'s ST1 and ST2 spatial responses are similar to each other, peaking at around 0.3 cycles deg^{-1} compared with values for the normal ST1 and ST2 spatial responses of about 4 cycles deg^{-1} and 1 cycle deg^{-1} respectively. *D*'s ST2 temporal response is plotted in Fig. 6b, together with data for a normal subject and shows that despite his pronounced nystagmus, *D* has essentially normal temporal response.

Hemianope, G

Measurement of ST2 spatial and temporal frequency responses were made for target movement centred 20° off-axis, along the horizontal meridian, in the "blind" temporal hemifield of his right eye. Other experimental parameters were similar to those used in the measurements for amblyopic subjects. The plot of log threshold illumination, $\log I_t$, against spatial frequency, f_s, for the ST2 spatial response (Fig. 7a) reveals no tuning curve, although there is a general increase in threshold for all background fields which incorporate flickering bars, except the very coarse grating with f_s equal to 0.3 cycles deg^{-1}. In contrast, the ST2 temporal response shows a well-defined, pass-band response, peaking at about 2 Hz (Fig. 7b). Two sets of comparison data, recorded at the same retinal location for a subject with normal vision, are also plotted, one recorded with the same background illumination (2.2 log Trolands) for which *G*'s responses were measured and the other at a lower level (1.0 log Troland). The noteworthy features of *G*'s temporal responses are the large amplitude of the ST2 tuning curve and the low frequency for peak response.

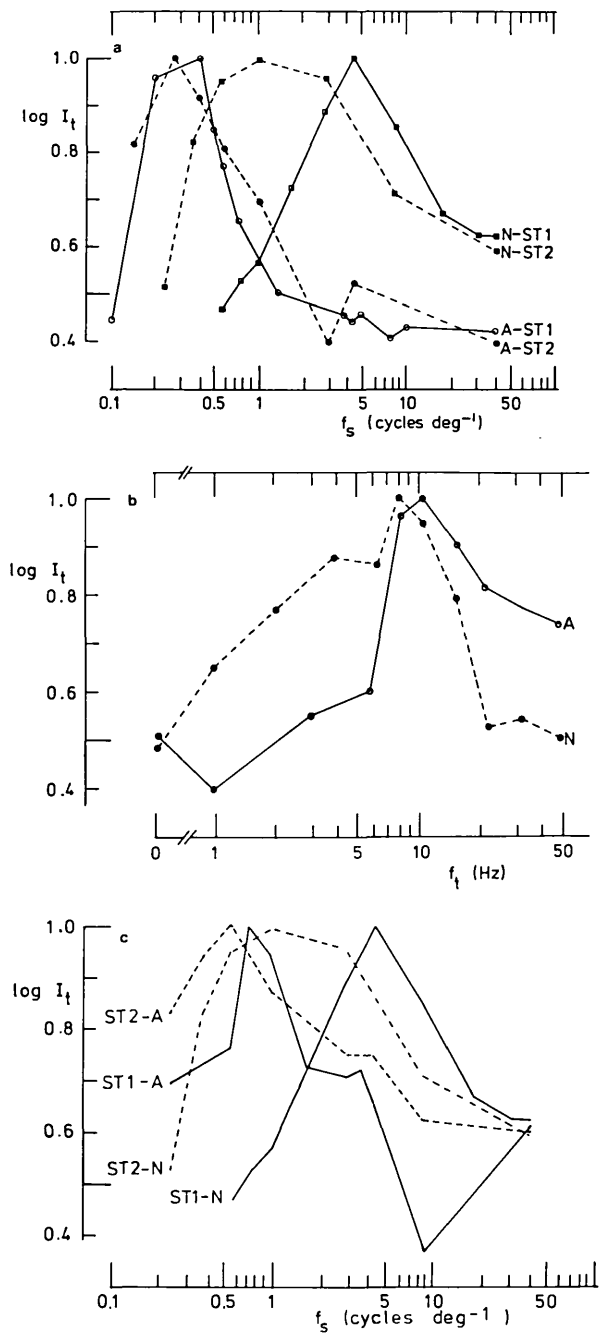

Fig. 6. **a** Normalised ST1 and ST2 spatial responses for the albino subject, *D*, denoted by *A*-, and the averaged normal curves, denoted *N*-, taken from Figs. 1a and 4c. Stimulus parameters for *A*- were as in Figs. 1 and 4 except that for both responses, the mean background illumination was 1.4 log Trolands. **b** Normalised ST2 temporal responses for the albino, *A*, and the normal subject IEH. Threshold illumination, I_t, was measured for detection of a 3.5° diameter circular target moving at 15 deg s^{-1} along the horizontal meridian. The 17° diameter background was spatially uniform and temporally modulated at f_t Hz. The background mean illumination was 1.4 log Trolands. Each point is the mean of 5 measurements and the average standard error was 0.03 log units. **c** Normalised ST1 and ST2 spatial responses for subject *K* denoted *A*, and the averaged normal data, denoted *N*, taken from Figs. 1a and 4c

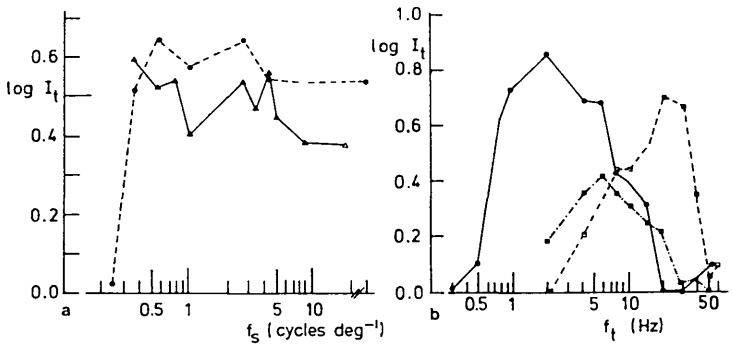

Fig. 7a and b. Data for the hemianopic subject, *G*, measured for stimuli centred 20° or 30° off-axis along the horizontal meridian, in the "blind" hemifield. **a** ST1 and ST2 spatial responses for subject *G*, represented by the full line (open triangles) and the broken line (full circles) respectively. The ST1 response is taken from Barbur et al. (1980), Fig. 5. The ST2 response was measured with a 5° diameter circular target, moving at 30 deg s^{-1} across a background grating consisting of alternate steady and flickering bars. The mean background illumination was 1.8 log Trolands and the flicker frequency was 2 Hz. Stimuli were centered 20° off-axis (data points are the mean of 5 readings with mean standard error of 0.05 log units). **b** ST2 temporal responses for subject *G* (full line, full circles) and the normal subject IEH, measured 20° off-axis. The 5° diameter, circular target moved at 30 deg s^{-1} along the horizontal meridian. The background was modulated at frequency f_t (100% modulation depth) and was of mean illumination 2.2 log Trolands (full circles and open squares) or 1.0 log Trolands (full squares). The half-field opposite to that viewing the stimuli was covered up to 7° from the foveal fixation point by a steady, uniform field illumination 2.6 log Trolands, in order to suppress effects of light scattered into *G*'s normal hemifield (data points for *G* are the mean of 5 readings, with standard errors in the range 0.04–0.07 log units)

Discussion

We examine, firstly, the temporal responses recorded for the different classes of abnormal vision. For the amblyopic and the albino subjects, the ST2 temporal response appears to be entirely normal (Figs. 5 and 6b) and as this response can be derived from the ST1 temporal response, it is probable that the latter is also normal. (We did not measure the ST1 function directly because the method for its determination was not discovered until we had virtually completed the study on amblyopia.) Our observations therefore support previous reports that amblyopes have normal sensitivity for detection of flicker (Miles, 1949). As noted, the albino subject's marked nystagmus has no significant effect on his ST2 temporal response. The results for the hemianope, *G*, show that his "blind" sight is characterised by high sensitivity to low temporal frequency. The very large amplitude of the threshold illumination increase which occurs at about 2 Hz (Fig. 7b) is quite different from the responses found in normal vision, although it correlates well with the low critical fusion frequencies of *G*'s "blindsight" reported by Barbur et al. (1980). These authors suggested that *G*'s "blindsight" is mediated by retinal projections to the superior colliculus and thence, via the pulvinar, to the cortex. The data of Fig. 7 establish that whichever pathway generates *G*'s "blind" field responses possesses low temporal frequency characteristics. Low critical fusion frequency is found in subjects with intracranial tumours (Phillips, 1933), and it has been noted (Wilson, 1967) that the visual integration time, which is closely related to the temporal frequency response, is constant except in subjects who suffer lesions of the central visual pathways. Subject *G* suffers such a lesion in his "blind" hemifield projections, and the associated abnormal temporal frequency response is consistent with Wilson's observation.

All abnormal subjects who took part in this investigation suffer visual abnormalities involving loss of spatial resolution, so it is not unexpected that the spatial, rather than the temporal, response functions exhibit abnormal responses. Before discussing the significance of these abnormal spatial responses, however, we firstly show that the eccentric fixation which occurs in some of the amblyopes is not a significant factor in the ST1 spatial responses. We note the following:

a) None of the refractive amblyopes have eccentric fixation, yet they all exhibit low frequency ST1 spatial functions in their amblyopic eyes (Fig. 2c).

b) The target used in this study traverses 8° of visual angle, thus for normal subjects, the responses are averaged over a corresponding retinal region. The strabismic amblyopes of this study fixate at maximum 3° eccentricity, which lies within the retinal range over which the normal responses are averaged, yet there are large differences between the normal and strabismic IMG functions (Fig. 1).

c) At 20° to 30° eccentricity, which far exceeds the 3° maximum fixation displacement observed in our amblyopic subjects, the ST1 spatial response functions of normal subjects peak at 1.5–3 cycles deg^{-1} (Fig. 3c and d), whereas for some of the amblyopes, they peak at 1 cycle deg^{-1} or below (Figs. 1c and 2c).

d) At eccentricities up to 20°, the ST1 spatial functions for the "abnormal" eyes of both the strabismic and refractive amblyopes are displaced to low frequencies compared to those for the "normal" eyes (Fig. 3a and b).

We conclude that the low frequency ST1 spatial functions observed in amblyopia do not simply represent non-foveal responses associated with eccentric fixation.

All the ST1 spatial responses measured for "amblyopic" eyes are displaced to low spatial frequencies relative to the normal response (Figs. 1c and 2c), which implies that these ST1 filters have larger spatial distributions than that associated with normal vision. Calculation of the ST1 "receptive field" using the method described by Barbur and Ruddock (1980, Appendix) shows that on average the ST1 receptive field centre for strabismic amblyopic eyes is of diameter 20′, compared with a value of 9′ for normal subjects (Fig. 8). A similar, although smaller effect, is also observed in the "normal" eyes of the amblyopes, particularly those of the strabismic subjects (Fig. 1b). In contrast to the results for the ST1 filter, the ST2 spatial responses of all but one of the amblyopes are essentially normal (Fig. 4). In the proposed network representation of the ST1 and ST2 spatial filters (Holliday and Ruddock, 1983, Fig. 17), ST2 filter responses are obtained by lateral interaction between ST1 filters. The ST2 spatial characteristics were attributed to the lateral spread of the ST2 input network, rather than to the intrinsic spread of the ST1 spatial filter. It was therefore predicted that an increase in size of the ST1 spatial distribution would cause an increase in the ST2 spatial response only if the spatial extent of the ST1 filter were to exceed that of the normal ST2 filter. Loss of fine spatial tuning in the ST1 filters combined with normal ST2 spatial responses is, therefore, consistent with the model. For two subjects, a divergent strabismic amblyope *K* and the albino subject *D*, the ST1 spatial responses are displaced to the low frequency side of the *normal* ST2 response curve (Fig. 6a and c) and for both subjects, the ST2 response curve is also shifted to lower frequencies, such that it coincides approximately with the ST1 frequency response. This result is consistent with sequential organisation of the ST1 and ST2 filters, as shown in the network representation of Holliday and Ruddock (1983). Failure to observe the ST2 spatial tuning curve for "blindsight" (Fig. 7a) confirms *G*'s lack of spatial discrimination in his "blind" hemifield (Barbur et al., 1980).

Amblyopia is associated with loss of visual resolving power, thus it is of considerable interest to establish whether there is direct correlation between visual resolution and the ST1 spatial responses recorded for

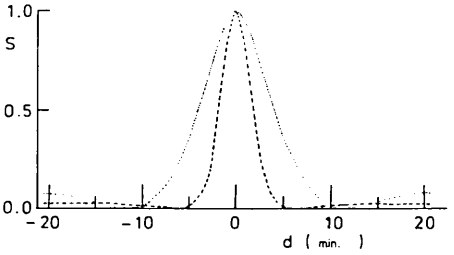

Fig. 8. Cross-sections through the receptive fields of the ST1 mechanism calculated for normal subjects (broken line) and for the average data of the "amblyopic" eyes of 12 strabismic subjects (dots, calculated taken from Fig. 1c and d). Relative response, *S*, is plotted against distance, *d*, from the centre of the receptive field. Note that the curves illustrate the shape of the receptive field, but do not define the positive and negative regions

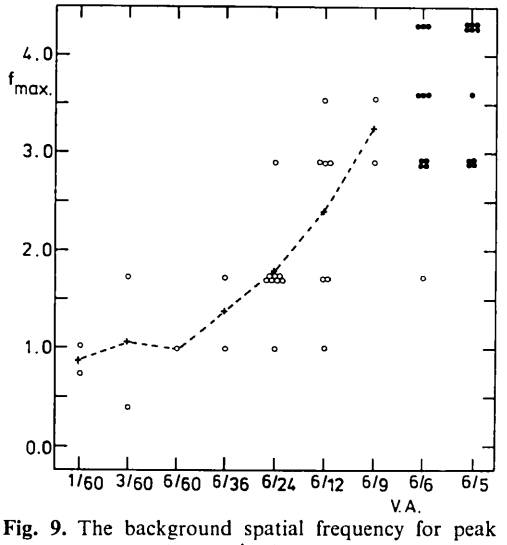

Fig. 9. The background spatial frequency for peak ST1 spatial response, f_{max} (cycles deg^{-1}) plotted against visual acuity, VA. Each open circle refers to the "amblyopic" eye of an ablyope and each full circle to the "normal" eye of an amblyope. The crosses denote the averaged values of f_{max} for each value of VA

the amblyopic subjects. We therefore measured visual acuity for each eye of all the amblyopes, using Snellen test charts, and the result are expressed as the fractional resolving power, e.g. 1/60, corresponding to resolution of an object placed 6 m from the eye, and subtending 1° at the eye. The background grating frequency, f_{max}, for peak response is taken as the measure of the ST1 spatial response and this is plotted against visual acuity (V.A.) in Fig. 9. As can be seen, there is considerable scatter in the individual data points for the "amblyopic" eyes (Fig. 9, open circles), although on average there is an increase in f_{max} as V.A. increases. The correlation is, however, weak and this is emphasised by the fact that for the "normal" eyes (Fig. 9, closed circles), there is a wide distribution of f_{max} values for a single, normal value of V.A. Two factors may contribute to the low correlation between the ST1 spatial response and the overall visual acuity. Firstly, amblyopes can significantly improve their

acuity if forced to use the "abnormal" eye in a training programme, thus their measured visual acuity values do not reflect absolute limits set by visual filter characteristics. Secondly, acuity losses in amblyopia, measured in terms of contrast threshold sensitivity, fall into two classes (Hess and Howell, 1977), but disappear for supra-threshold contrast stimuli of the kind employed in the Snellen chart (Hess and Bradley, 1980). The difficulty of correlating acuity with the spatial responses (receptive fields) of neurophysiological or psychophysical units which we meet in this study also occurs in normal vision, where the hyper-acuity of Vernier discrimination implies spatial resolution well below the receptive field size of single units in the visual pathways. Other factors which influence amblyopic resolving power, such as age of onset of amblyopia and the history of medical treatment, will be treated elsewhere (Grounds et al., in preparation).

As in the equivalent study on normal vision, it is possible to compare the findings on amblyopic subjects with the results of electrophysiological studies. The neural mechanisms of amblyopia have been examined in cats with surgically induced convergent strabismus and two contradictory patterns of response have been observed. In an extended and detailed study, Ikeda and Tremain (1979), see also Ikeda (1980), observed changes in the receptive fields of retinal ganglion cells in adult cats consequent upon the surgical induction of convergent strabismus at age 3 weeks. In particular, they show that the receptive fields of X-type ganglion cells in the "abnormal" or squinting eye of cats with convergent strabismus exhibit much coarser receptive field centres with weak inhibitory surround. A similar effect is observed in X-type cells of the LGN (Ikeda et al., 1978), and it was shown that the effect decreases as the age at which the squint is introduced increases from 3 weeks to 16 weeks. In normal kittens, the receptive field sizes of X-type ganglion cells decrease with age from birth up to about 16 weeks (Ikeda and Tremain, 1978), and the effect of the "induced" strabismus is, apparently, to arrest development of the receptive fields. Ikeda and her coworkers have, therefore, established a detailed case for the involvement of retinal ganglion cells in amblyopia. In contrast, the Y-type ganglion cells showed little change in receptive field properties as a consequence of the surgery. Selective loss of fine spatial tuning in X- rather than Y-type neurones is also seen in the ganglion cells of cats with "refractive" amblyopia, induced by use of atropine to dilate the pupil of one or both eyes, thereby blurring the retinal image (Ikeda, 1980). These findings were not confirmed by Cleland et al. (1982), whose study on six cats with surgically induced strabismic amblyopia failed to reveal any significant changes in the receptive fields of retinal ganglion cells, despite the fact that, behaviourally, the cats were amblyopic. To the extent that psychophysical studies can provide evidence about neural mechanisms, our data for amblyopia support Ikeda and Tremain's model. Thus changes in spatial responses are restricted, with the exception of two extreme cases, to the ST1 mechanism, whilst the ST2 mechanism remains unchanged. We have argued previously that the ST1 and ST2 mechanisms correspond respectively to the X- and Y-type neural mechanisms (Ruddock, 1982; Holliday and Ruddock, 1983), thus the selectivity of the changes observed psychophysically is the same as that described by Ikeda and Tremain. Although it is clearly not possible to identify the anatomical level at which psychophysical responses arise, we note that the spatial responses revealed by our methods possess circular symmetry and are monocularly controlled. They may well, therefore, reflect ganglion cell activity, although as is demonstrated in the case of the hemianope, they can be modified by central mechanisms (Fig. 7; see also Barbur et al., 1980).

Acknowledgements. We are grateful to all the subjects who took part in this investigation, but particularly to *D* and *G*, who undertook extensive measurements in our laboratory. A. G. acknowledges with thanks a grant awarded by the British Ophthalmic Association and I. H. a grant awarded by the Ministry of Defence.

References

Barbur, J.L., Ruddock, K.H.: Spatial characteristics of movement detection mechanisms in human vision. 1. Achromatic mechanisms. Biol. Cybern. **37**, 77–92 (1980)

Barbur, J.L., Ruddock, K.H., Waterfield, V.A.: Human visual responses in the absence of the geniculo-calcarine projection. Brain **103**, 905–928 (1980)

Barbur, J.L., Holliday, I.E., Ruddock, K.H., Waterfield, V.A.: Spatial characteristics of movement detection mechanisms in human vision. III. Subjects with abnormal visual pathways. Biol. Cybern. **37**, 99–105 (1980)

Cleland, B.E., Crewther, D.P., Crewther, S.G., Mitchell, D.E.: Normality of spatial resolution of retinal ganglion cells in cats with strabismic amblyopia. J. Physiol. (London) **326**, 235–249 (1982)

Hess, R.F., Howell, E.R.: The threshold contrast sensitivity function in strabismic amblyopia. Evidence for a two type classification. Vision Res. **17**, 1049–1055 (1977)

Hess, R.F., Bradley, A.: Contrast perception above threshold is only minimally impaired in human amblyopia. Nature **287**, 463–464 (1980)

Hess, R.F., Campbell, F.W., Zimmern, R.: Differences in the neural basis of amblyopias: the effect of mean luminance. Vision Res. **20**, 295–306 (1980)

Holliday, I.E., Ruddock, K.H.: Two spatio-temporal filters in human vision. 1. Temporal and spatial frequency response characteristics. Biol. Cybern. **47**, 173–190 (1983)

Ikeda, H.: Visual acuity – its development and amblyopia. Edridge-Green Lecture 1979. J. R. Soc. Med. **73**, 546–555 (1980)

Ikeda, H., Tremain, K.E.: Development of spatial resolving power of lateral geniculate neurones in kittens. Exp. Brain. Res. **31**, 193–206 (1978)

Ikeda, H., Tremain, K.E.: Amblyopia occurs in retinal ganglion cells of cats reared with convergent squint without alternating fixation. Exp. Brain Res. **35**, 559–582 (1979)

Ikeda, H., Tremain, K.E., Einion, O.: Loss of spatial resolution of lateral geniculate neurones in kittens reared with convergent squint produced at different stages of development. Exp. Brain Res. **31**, 207–220 (1978)

Lyle, T.K., Wybar, K.C.: Lyle and Jackson's practical orthoptics in the treatment of squint (and other anomalies of binocular vision) (5th edn.) H. K. Lewis, London, 1967

Miles, P.W.: Flicker fusion frequency in amblyopia ex anopsia. Am. J. Opthalnol. **32**, 225–231 (1949)

Phillips, G.: Perception of flicker in lesions of visual pathways. Brain **56**, 464–478 (1933)

Ruddock, K.H.: Psychophysical studies on subjects with visual defects. The Edridge-Green Lecture 1981. J. R. Soc. Med. **75**, 315–322 (1982)

Wilson, M.E.: Spatial and temporal summation in impaired regions of the visual field. J. Physiol. (London) **189**, 189–208 (1967)

Received: December 14, 1982

Dr. K. H. Ruddock
Imperial College of Science and Technology
The Blackett Laboratory
Prince Consort Road
London SW7 2BZ
England